THE BK VIRUS AND HIV-ASSOCIATED SALIVARY GLAND DISEASE:
CORROBORATING THE LINK

Raquel Burger-Calderon

A thesis submitted to the faculty of the University of North Carolina at Chapel Hill in partial fulfillment of the requirements for the degree of Doctor in Philosophy in the Department of Microbiology and Immunology in the School of Medicine.

Chapel Hill
2014

Approved by:

Jennifer Webster-Cyriaque

Nancy Raab-Traub

Kristina Abel

Volker Nickeleit

David Margolis

ABSTRACT

Raquel Burger-Calderon: *The BK virus and HIV-associated Salivary Gland Disease:*
Corroborating the Link
(Under the direction of J. Webster-Cyriaque, DDS/PhD)

BK polyomavirus (BKPyV) is the most common viral pathogen among allograft patients and is known to adversely affect immune suppressed individuals since the discovery of the virus in 1971. Increasing evidence links BKPyV to the human oral compartment and to HIV-associated salivary gland disease (HIVSGD). To date, few studies have analyzed oral-derived BKPyV. The studies described in this manuscript, aimed to characterize BKPyV isolated from throatwash (TW) samples of HIVSGD patients. The BKPyV non-coding control region (NCCR) is the main determinant of viral replication and rearranges readily *in vivo* and *in vitro*. Further, NCCR rearrangements have been associated with functional differences. This study analyzed 36 clinical samples, of which 29 were BKPyV positive. One hundred percent of TW samples from HIVSGD patients and urine samples from transplant patients yielded BKPyV NCCR sequences. Importantly, 94% of the BKPyV HIVSGD NCCRs carried the rearranged OPQPQQS block arrangement, suggesting a distinctive architecture among this sample set. Of interest, in the 22% of BKPyV positive oral samples from individuals without HIVSGD, the BKPyV substrains were distinct from OPQPQQS. The studies also assessed the replication potential and NCCR promoter strength of HIVSGD-derived clinical isolates *in vitro*. The majority of HIVSGD-derived BKPyV isolates underwent productive infection and had active promoters in an oral cell culture system.

Quantitation of infectious virus suggested that HIVSGD BKPyV had preferential tropism for salivary gland cells over kidney cells. Evidence of HIVSGD-derived BKPyV oral tropism and adept viral replication in human salivary gland cells corroborated the potential link between HIVSGD pathogenesis and BKPyV.

ACKNOWLEDGEMENTS

PREFACE

Chapter 2 is in revision and will be resubmitted to the Journal of Virology by the spring of 2014. Chapter 3 previously appeared as published article in the Journal of Virology. Permission to include it in this manuscript has been obtained from the journal. The original citation is as follows: Burger-Calderon, R. *et al.* "Replication of Oral BK Virus in Human Salivary Gland Cells", J. Virol. 2014, 88(1): 559. Appendix 1 is in revision and will be resubmitted to the Antiviral Research Journal. Appendix 2 previously appeared as published article in the Journal of Cancer Therapy. Permission to include it in this manuscript has been obtained from the journal. The original citation is as follows: Jeffers, LK *et al*. "Correlation of Transcription of MALAT-1, a Novel Noncoding RNA, with Deregulated Expression of Tumor Suppressor p53 in Small DNA Tumor Virus Models", Journal of Cancer Therapy, 2013, 4, 774-786.

TABLE OF CONTENTS

LIST OF TABLES

LIST OF FIGURES

LIST OF ABBREVIATIONS

A	Adenosine
AIDS	Acquired Immunodeficiency Syndrome
ATCC	American Type Culture Collection
BKPyV	BK Polyomavirus
BKN	BKPyV-associated Nephropathy
BKVN	BKPyV-associated Nephropathy
bp	Base Pair
C	Cytidine
CMV	Cytomegalovirus
CSF	Cerebrospinal Fluids
DAPI	4',6-diamidino-2-phenylindole
DILS	Diffuse Infiltrative Lymphocytic Syndrome
DMEM	Dulbecco's Minimal Essential Cell Culture Medium
DNA	Deoxyribonucleic Acid
EBV	Epstein Barr Virus
ER	Endoplasmic Reticulum
EtBr	Ethidium Bromide
FFU	Fluorescence-forming Units
FBS	Fetal Bovine Serum
HAART	Highly Active Antiretroviral Therapy
HHV	Human Herpes Virus
HIV	Human Immunodeficiency Virus

HIVSGD   HIV-associated Salivary Gland Disease

HPyV   Human Polyomavirus

HSG   Human Submandibular Salivary Gland Cells

HSY   Human Parotid Salivary Gland Cells

HSV   Herpes Simplex Virus

IRB   Institutional Review Board

IRIS   Immune Reconstitution Inflammatory Syndrome

JCPyV   JC Polyomavirus

kDa   Kilo Daltons

kb   Kilobase

Luc   Luciferase

Malat-1   Metastasis-associated Lung Adenocarcinoma-associated Transcript 1

MCPyV   Merkel Cell Polyomavirus

min   minute(s)

NCCR   Non-coding Control Region

P/S   Penicillin/Streptomycin

PyV   Polyomavirus

PCR   Polymerase Chain Reaction

pi   post-infection

pt   post-transfection

qPCR   Quantitative Polymerase Chain Reaction

RNA   Ribonucleic Acid

RFP   Red Fluorescent Protein

RPTE	Renal Proximal Tubular Epithelial Cells
RT-PCR	Real Time Polymerase Chain Reaction
SGD	Salivary Gland Disease
SV40	Simian Virus 40
T	Thymidine
Tag	Large T antigen
tag	Small T antigen
TEM	Transmission Electron Microscopy
TW	Throatwash
UNC	University of North Carolina
VP	Viral Protein
VL	Viral Load
wg	whole genome
wt	wildtype

CHAPTER 1: INTRODUCTION

<u>Opportunistic Infections - An HIV/AIDS Public Health Challenge</u>

HIV/AIDS has become one of the world's main public health challenges since its first reported case in 1981 (1). According to the UNAIDS Report 2013 an estimate of 35.3 (32.2– 38.8) million people were living with HIV globally in 2012. The report further quotes that an estimate of 1.6 million people died of AIDS in 2012 alone. AIDS-related deaths have declined in the past years (2), thanks to increased interdisciplinary humanitarian efforts. Opportunistic infections and cancer however are still the primary cause of death among HIV positive individuals. Despite AIDS-associated opportunistic pathogens being prevalent among AIDS patients, they remain poorly understood. Cytomegalovirus (CMV), herpes simplex virus (HSV) and paramyxovirus infections are reported frequently among AIDS patients, while the BK polyomavirus (BKPyV) has been emerging as a new opportunistic pathogen within that group, possibly carrying harmful implications (3).

<u>AIDS-related Salivary Lymphadenopathy</u>

AIDS-related salivary lymphadenopathy was first described in 1983, shortly after the initial AIDS case (4). The salivary gland lymph nodes often become the primary site of lymphadenopathy (disease affecting the lymph nodes) associated with HIV infection and opportunistic pathogens (5). Salivary glands are intimately associated with the lymph nodes in the oral cavity (5). Lymph nodes are embedded in the parotid gland and

found adjacent to the submaxillary gland (5). Salivary gland structures, such as acini and ducts are frequently present in oral cervical lymph nodes (5). One can therefore refer to this intertwined system as the salivary gland lymph nodes. Visually lymphadenopathy is commonly identified by enlarged lymph nodes and can lead to dry mouth or xerostomia. Histological analysis reveals frequent salivary gland duct obstruction and inflammation of saliva producing tissue (lymphadenitis).

Persistent lymphadenopathies were reported in homosexual men in New York and considered a possible early symptom of AIDS in 1987 (4). Only two years later, lymphadenopathies in the neck and head region were found to precede opportunistic infections and neoplasia in a similar patient cohort (6). Similar symptoms, salivary gland enlargement due lymphocytic infiltration, xerostomia and predisposition to lymphoma formation, are also known as Sjogren's Syndrome-like illness (4), AIDS-associated Persistent Generalized Lymphadenopathy (6) and Diffuse Infiltrative Lymphocytosis Syndrome (DILS) (7). The resemblance to Sjogren's syndrome was determined to be superficial from the start, since neither the clinical nor the pathologic criteria were satisfied. None of the AIDS-related salivary lymphadenopathy cases displayed autoimmune phenomena or tested positively for the presence of autoantibodies (8). Schiodt *et al.* were the first to coin the term HIV-associated salivary gland disease (HIVSGD) in 1989 (9), a disease encompassing clinical indicators described for all the AIDS-related salivary lymphadenopathies mentioned above. The group defined HIVSGD as disease encompassing symptoms linked to AIDS-related salivary lymphadenopathy such as, enlargement of the major salivary glands and/or xerostomia (dry mouth) and localized lymphocytic infiltration.

<u>HIV-associated Salivary Gland Disease</u>

Today, HIV-associated salivary gland disease (HIVSGD) is among the most common salivary gland presentations in HIV + individuals (10). Incidence is as high as 48% among HIV-infected patients in developing countries (11). HIVSGD is more commonly diagnosed among the pediatric population, considered AIDS-defining among children, but affects adults as well. Importantly, HIVSGD is considered a pre-malignant lesion and its diagnosis is associated with increased lymphoma incidence (5, 8, 12, 13).

HIVSGD presents itself superficially as unilateral or bilateral salivary gland enlargement due parotitis. Histologically, the oral disease is characterized by hyperplastic, intraparotid lymph nodes and/ or lymphatic CD8 + infiltrates (10). Parotid gland enlargements are greater and more disfiguring in children than in adults (13). HIVSGD also affects the minor salivary glands, with labial salivary glands demonstrating features of sialadenitis (13). Patients diagnosed with HIVSGD commonly have reduced salivary flow rates of the parotid, submandibular, and sublingual glands (10). Saliva composition may be affected as well as saliva contains increased sodium, chloride, lysozyme, peroxidase, lactoferrin, and immunoglobulin A levels (10).

Salivary gland disease impacts oral health. Maintenance of good oral health among HIV/AIDS patients is of outmost importance to protect the patients from secondary and opportunistic infections. Bacterial, viral and fungal infections that begin in the mouth may escalate to systemic infections and may in turn harm vital organs if left untreated (14). Moreover, the decline of oral health has shown to impact the patients quality of life by limiting career opportunities and social contact as result of facial appearance and odor (14). Poor oral health may also lead to complications with food intake, leading to general malnutrition and malabsorption of their medication (14). Poor oral health further predisposes the development of

oral diseases such as dry mouth (xerostomia). Xerostomia leads to dental decay, periodontal disease and increases the patients likelihood to be affected by pathogenic opportunistic infections (14). Xerostomia indicates a dysfunction of the salivary glands and is commonly associated with AIDS-related salivary lymphadenopathy.

HIVSGD Etiology

Interestingly, there has been an increase in HIVSGD prevalence of among HIV + patients in the highly active antiretroviral therapy (HAART) era at the UNC hospitals (Fig. 1.1. Adapted from J. Webster-Cyriaque) (15, 16). Taking a combination of three or more anti-retroviral drugs is termed HAART and its application dramatically increase the life expectancy of HIV+ patients. HIVSGD has risen from 1.8% to 5% among HIV-infected adults from 1995 to 1999, even though the overall presence of oral lesions has decreased (15). Patton's data implies that AIDS patients might be experiencing a higher risk of developing HIVSGD under HAART treatment. The group also determined that there has been a change in the occurrences of oral opportunistic infections in general from 1995/96, where the use of HIV protease inhibitor was less common, to 1999, a period of greater protease inhibitor use, indicating the importance of understanding opportunistic pathogens (15). HAART hinders AIDS progression by reducing HIV RNA levels and increasing CD4+ cell counts, but it has been shown that opportunistic infectious agents can take advantage of the newly reconstituted immune system.

Twenty-five to 35% of patients undergoing HAART develop a pathological inflammatory response called immune reconstitution inflammatory syndrome (IRIS) to previously treated or asymptomatic opportunistic infections. The majority of IRIS cases are reported within the first two months of HAART, even though IRIS development can take up to two years (17). Detecting

an increase in prevalence of HIVSGD among HIV + patients in the HAART era may therefore

hint towards persistence of an opportunistic infectious agent as the cause of HIVSGD.

Further evidence suggesting an infectious agent as HIVSGD etiological agent is data

suggesting antigen-driven HIVSGD pathogenesis. A prospective study analyzing epidemiology,

clinical presentation, and extra-glandular manifestations of HIVSGD suggests that this

lymphadenopathy is an antigen (viral)- driven response (18). Further, an antigen-driven MHC-

determined host immune response recorded by Itescu *et al.* based on the infiltrating lymphoid

cells characterizing HIVSGD, points to an antigen-driven response (19). Finding differential

rates of HIVSGD in children (20-47%) and adults (3-7.8%) (12) may also elude to a viral

infection as it indicates primary viral infection in children versus residual immunity in adults

(13). Trials are ongoing in our group to address these questions.

The reviewed literature suggests that the etiological agent of HIVSGD is an opportunistic

infectious agent. Additionally there is published evidence suggesting the etiological agent of

HIVSGD to be a virus.
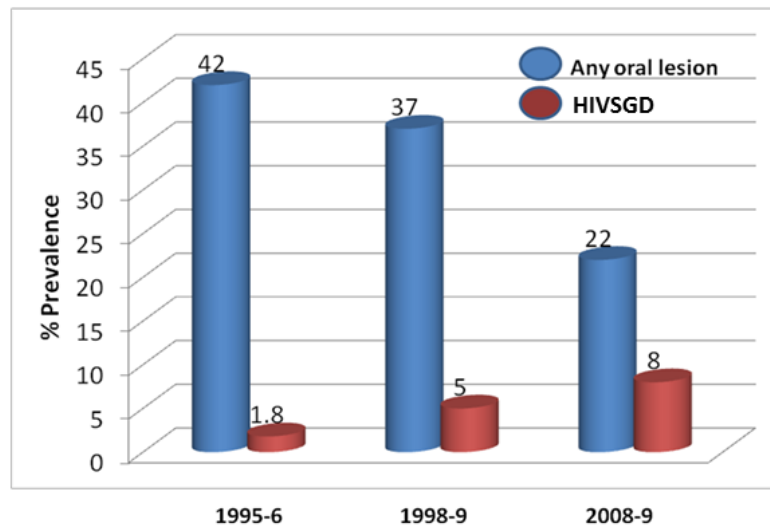
Figure 1.1. HIVSGD (red) has increased during the HAART era compared to all other

HIV-associated oral lesions (blue) at the UNC Hospitals from 1995 to 2009.

Viral Salivary Gland Infection and Pathology

AIDS-related salivary lymphadenopathy has previously been postulated to be caused by a viral agent (20). Furthermore, viral co-infections have been implicated in the pathogenesis of HIV-related salivary gland disease (SGD) (21) and opportunistic DNA viruses are often the etiologic agents of HIV-associated oral lesions. For example, Epstein-Barr virus (EBV) causes EBV-associated hairy leukoplakia, Human Herpesvirus 8 (HHV8) causes Kaposi's sarcoma and polyomaviruses cause salivary gland pathology. It is of evolutionary advantage to an infectious agent to infect and replicate within the oral compartment and subsequently spread by oral fluids or contaminated objects. Various viral agents are known to have evolved to infect and replicate efficiently within oral tissues. It is of no surprise that various salivary gland diseases are consequently associated with viral infections. Viruses well known to infect human salivary glands include Paramyxovirus, EBV, and cytomegalovirus (CMV) among many others (22). For a more comprehensive review see Jeffers et al. (13) where the link between viral infections and salivary gland pathology are further explored.

Mumps is the most prevalent virally induced salivary gland disease, despite its incidence being reduced significantly by the introduction of the mumps vaccine in 1967 (22). The mumps virus causes paramyxo-induced parotitis and symptoms are characterized by bilateral parotid swelling, although other salivary glands may be involved. Mumps is a highly infectious but self-limiting disease (22). It is caused by a single-stranded RNA virus, member of the paramyxovirus family and infects exclusively humans. Transmission commonly occurs via the upper respiratory tract by droplets, aerosol, direct contact, or fomites (23). Previous to vaccinations mumps lead to meningitis and encephalitis in up to 36% of reported cases in the United States (24).

EBV is a DNA virus, member of the herpesviridae family and establishes persistent latent infection with sporadic reactivation (25). EBV has been shown to infect salivary glands, and viral particles are exclusive shed by saliva (22). EBV causes infectious mononucleosis (better known as mono), nasopharyngeal carcinoma and Burkitt's lymphoma (26, 27). Rivera *et al.* analyzed biopsies of DILS patients and consistently detected EBV, but not CMV DNA (21). The connection between EBV and DILS pathogenesis could not further confirmed however.

CMV, as all members of the herpesviridae family, also establishes persistent latent infection with sporadic reactivation (28). It is a ubiquitous virus that rarely shows clinical symptoms in the healthy host but can cause mononucleosis similar to EBV-associated mononucleosis (28). CMV affects mostly the immunocompromised and is one of the most common, significant, and difficult opportunistic pathogens among HIV + and transplant patients (28).

Polyomavirus-induced Salivary Gland Pathology

Polyomavirus-induced salivary gland pathology in animals is well described. Polyomavirus (PyV) infections have been shown to cause salivary gland enlargements and tumors in animal models (13). In 1984 Ward *et al.* showed that athymic nude rats infected with PyV develop a wasting disease that is accompanied by parotid sialoadenitis with intranuclear inclusion bodies. Importantly, the intranuclear inclusions of the parotid epithelium were found to express PyV antigens (29). Transgenic mice expressing BKPyV develop hepatocellular carcinoma and renal tumors (30, 31). Another transgenic mouse study shows that mice expressing PyV T antigen (Tag) undergo salivary gland tumorigenesis as the animals developed submandibular gland adenocarcinomas of intercalated duct origin by 1 year of age (32). Similar studies further corroborate the transforming potential of Tag in mice and show that conditional

expression of PyV Tag in transgenic mice induces ductal hyperplasia (33, 34). Hence, there is substantial evidence establishing an association between PyV and salivary gland pathology and carcinogenesis in animals. The carcinogenic potential of PyV products may explain the risk of increased lymphoma formation among HIVSGD patients. Interestingly, animal models also reflect the characteristic lymphocyte infiltration detected in HIVSGD pathology. Murine and guinea pig animal models reflected HIVSGD on a histological level as mouse PyV-induced salivary epitheliomas in neonatal mice were infiltrated with T lymphocytes (35). Similar infiltrates were characterized in tumors growing from newborn guinea pigs infected with SE polyomavirus that also develop salivary gland enlargements (36).

Polyomavirus Family

BK polyomavirus (BKPyV), JC polyomavirus (JCPyV), Merkel cell polyomavirus (MCPyV) and Simian Virus 40 (SV40) are the most recognized members of the human polyomavirus family (37). However several new members have been discovered in the past years from which all have been suggested to be ubiquitous and of opportunistic nature. The human polyomaviruses KI (KIPyV) (38) and WU (WUPyV) (39) were isolated and characterized in 2007. Trichodysplasia spinulosa-associated polyomavirus (TSPyV) was discovered in skin lesions of immunosuppressed patients with Trichodysplasia spinulosa more recently (40). Human polyomavirus (HPyV) 6, 7, 9 and 10 were discovered most recently and are currently not associated with any disease. Wieland *et al.* evaluated cutaneous DNA prevalence and viral loads of the HPyV 6, 7, 9, 10 and TSPyV by real-time PCR in HIV + men and compared to healthy male controls. While they found HPyV6, HPyV7, TSPyV, and HPyV10 to be found more frequently among HIV + men as compared to HIV negative men (p < 0.05) they did not connect any of the viruses to a particular disease state (41).

Based on epidemiological, virological, and phylogenetic data it has been hypothesized that human polyomaviruses evolved with their hosts, leading to high prevalence, low morbidity and symptom-less latency (42). Yet, on a molecular level, the definition of latency is unclear among polyomavirus. It is not clear whether the virus maintains minimal replication levels or if the viruses undergo true latency. It is also unclear whether polyomavirus DNA is commonly integrated into the host genome. Human polyomaviruses tend to become latent post-primary infection and undergo reactivation among immune-compromised individuals. Their opportunistic nature and associated viral reactivation leads to serious complications, such as progressive multifocal leukoencephalopathy (PML), trichodysplasia spinulosa, Merkel cell carcinoma, and BKPyV-associated nephropathy (BKVN) (43). Individuals with suppressed or compromised immune systems include mainly HIV and organ transplant patients (43). Immunosuppressant conditions such as seen during pregnancy or chronic alcohol abuse may be sufficient however, to lead to polyomavirus reactivation (43). The specific factors of a dysfunctional host cellular immune system leading to reactivation however are yet to be defined. The identification of these factors is of increasing importance as the human polyomavirus family is rapidly expanding.

BK Polyomavirus (BKPyV)

BKPyV was first isolated from the urine of a British renal transplant patient in 1971 (44). BKPyV is a holoendemic member of the polyomavirus family and therefore found at high frequencies throughout most human populations. BKPyV transmission is not clear but thought to take place mainly via the respiratory route during infancy (45). Others have suggested BKPyV to be transmitted by a fecal-oral route (42), a urino-oral route (43) or vertically. Boldorini *et al.* analyzed blood and urine samples of 19 pregnant women and their newborns. Detected BKPyV DNA and seroprevalence suggested that BKPyV is likely to be transmitted during pregnancy or

soon after birth (46). While primary BKPyV infection commonly occurs without symptoms, in rare cases it can cause clinical complications such as urinary tract disease (47). Upon reactivation BKPyV is mainly associated with 3 major clinical syndromes: ureteral stenosis, hemorrhagic cystitis, and BKPyV-associated nephropathy (BKVN) (48).

BKPyV-associated Diseases

BKPyV has been studied mainly due the severe complications reactivation causes among transplant patient even though symptomatic BKPyV infection is also known to cause interstitial inflammations, renal tubular atrophy, pneumonia and meningoencephalitis in other settings (3, 49). Ten percent of renal transplant patients with increased BKPyV viremia and viruria, compared to healthy individuals, will develop BKPyV-associated nephropathy (BKVN), which leads to graft loss in 90% of the cases (50). BKVN has developed into a new epidemic, becoming the most important infectious complication affecting kidney transplants over the past eight years. The worldwide BKVN incidence rate lies within 1% and 9% (6.5% at the University of North Carolina in Chapel Hill) among children and adults and has been increasing due the development of potent immunosuppressive drugs (51). Yet, effective antiviral treatments are not available and BKVN often results in chronic allograft dysfunction and failure (52). Clearly, the deleterious implications of BKPyV on public health are significant (48), emphasizing the importance of elucidating the pathological process leading to BKPyV-associated disease. Our work done in chapter 3 adds to the knowledge of BKPyV-associated pathogenesis in that we characterized and compared viral replication levels and tropisms of clinical BKPyV isolates in human salivary gland and kidney cells that are likely to have caused HIVSGD *in vivo*. Our work presented in the appendix advances the anti-BKPyV treatment options in that we characterized

10

the antiviral effects several drugs have on clinical and laboratory-derived BKPyV isolates *in vitro*.

BKPyV Structure And Life Cycle

BKPyV consists of a naked icosahedral virion with a diameter of about 45 nm (28). The capsid is constituted of 72 capsomers, made of the major structural protein VP1 and one copy of a minor structural protein VP2 or VP3, which also link the genome to the capsid structure (53). The viral genome is a circular, double-stranded 5 kb DNA molecule and is divided into three functional regions (Fig. 1.2), the early region, the late region and the promoter, termed non-coding control region (NCCR). The early region encodes the regulatory proteins T antigen (Tag): large Tag (80.5 kDa), small tag (20.5 kDa) and the truncated Tag (17 kDa), which arise from three different mRNAs by alternative splicing of a single primary transcript (53). Polyomaviruses in general depend on the host cell for replication, as they do not encode for their own polymerase. Tag in particular carries numerous and indispensible functions and displays 76% sequence similarity to the well-studied SV40 Tag (54). Tag acts as major regulatory protein and interacts with pRb and p53 through its domains in order to overcome the host cell cycle control and disrupt host apoptosis. Furthermore, Tag carries DNA unwinding/helicase activity and regulates viral DNA replication and gene expression by interacting with host-cell transcription factors and the viral promoter region (NCCR) (42). The late region encodes the three structural proteins VP1 (40.1 kDa), VP2 (38.3 kDa) and VP3 (26.7 kDa) and the non-structural agnoprotein (7.4 kDa). Proteins VP2 and VP3 are translated from the same transcript and the agnoprotein and protein VP1 are translated from a different open reading frame (ORF) (53). The agnoprotein is a small, non-immunogenic lipid-associated cytoplasmic protein with elusive functional nature even thought it has been thought to be important for capsid assembly

and egress. The late BKPyV genome region contains additional ORFs, which are not well studied but may encode a protein similar to the VP4 protein of SV40 (55).
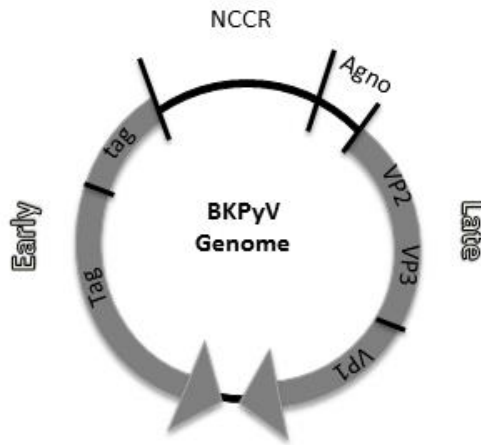
Figure 1.2. BKPyV Genome

BKPyV Promoter Region

The BKPyV promoter region, a.k.a. non-coding control region (NCCR), is of bidirectional nature and controls transcription of the early and late genes. The NCCR has been found to be the major determinant of *in vitro* replication (56, 57) and is divided into 5 block sequences. The O block contains 57 bp, the P block 68 bp, the Q block 39 bp, the R block 63 bp and the S block 63 bp. The O block contains the origin of DNA replication and each block carries a combination of transcription factor binding sites (TFBS) (28, 58). TFBS AP-1, CREB, NF-1, C/EBPβ, C/EBPδ, NF-kB, NF-kB1, p53, Sp1, Tag and p300 among others have been described within the polyomavirus NCCR (57, 59-62). The NCCR commonly undergoes block

deletions and/or duplications as compared to the archetype (Fig. 1.3). Promoter architectures that diverge from the original urine-derived archetypic OPQRS arrangement are referred to as rearranged (rr) and are readily detected *in vitro* and *in vivo* (63-70). It has been shown that NCCR block rearrangements bestow remarkable differences in transforming potential and host cell permissivity (57, 64, 69, 71-73). Clinical studies determined that the emergence of rr NCCR BKPyV variants in the plasma samples from immune suppressed kidney transplant recipients was correlated to increased replication efficiencies and pathogenesis (71). Furthermore, rearranged NCCRs have been reported to be more efficient replicators *in vitro* (56, 57, 66, 74, 75).

JCPyV, the closely related polyomavirus member mentioned above, has been studied in more detail than BKPyV. JCPyV exhibits tropism for oligodendrocytes in the brain and is the etiological agent of the neurodegenerative disease progressive multifocal leukoencephalopathy (PML) (76). Similar to BKPyV, the JCPyV promoter has been found to rearrange and rearrangements of following substrains isolated from brain, kidney, lymphocytes of PML patients, brain, cerebrospinal fluids (CSF), and lymphocytes of healthy individuals have been described (77-81). JCPyV promoter region includes binding sites for a variety of transcription factors, similar to the BKPyV NCCR. Interestingly, within JCPyV it is thought that these rearrangements lead to alterations of the TFBS and hence transcriptional patterns of the promoter, which are thought to increase the viral replication capacity in the brain and ultimately the viral disease potential (82). It is important to note that the correlation between promoter structure rearrangement and disease is not perfect in JCPyV as the same promoter architectures can be found within patients with extensive and patients without noticeable disease (45). It is known however that following TFBS Tst-1, NF-1, Sp1, GBPi, NF-kB, YB-1, Pura, and GF-1

determine the tropism of JCPyV to glial cells in the brain (45, 83-89). While host factors contribute to the viral pathogenic capacity and likely fluctuate between individuals and over time (45) both JCPyV and BKPyV promoter rearrangements are likely to drive viral replication and therefore pathogenicity *in vivo*.

Whether BKPyV rr NCCR variants are more efficient at *in vivo* disease development is debated (90, 91) but not unlikely since JCPyV promoter rearrangements have also been suggested to drive neural tropism and bestow increased virulence as discussed above (92). It is important to conclusively determine whether BKPyV promoter rearrangements truly endow higher replication levels and increased virulence in order to understand BKPyV pathogenesis and prevent disease development effectively. This may be facilitated by either using certain BKPyV NCCR architectures as biomarkers or treatment targets. We therefore aimed to characterize the BKPyV promoter region of clinical isolates from HIVSGD patients. We asked whether there was a specific promoter architecture detected among HIVSGD patients. We further determined whether the promoter architecture potentially affects viral tropism. The promoter architecture from following samples have been described: bladder, brain, cerebrospinal fluid, eye, heart, kidney, lung, muscle, nasopharyngeal aspirates, ovarium, monocytes, placenta, prostate, ureter, urine and sewage (73). To our knowledge our group is the first to characterize the NCCR from oral-derived HIVSGD BKPyV. The work described in Chapter 2 detected a unique OPQPQQS BKPyV NCCR promoter sequence among 18 out of 19 analyzed HIVSGD TW samples. Chapter 3 describes a study that corroborated the OPQPQQS promoter architecture in two clinical HIVSGD-derived BKPyV isolates (58).

Figure 1.3. BKPyV NCCR Block Architectures

BKPyV Tropism

Given the historic connection between BKPyV and the uroepithelial compartment and our novel connection between BKPyV and the oral malady we wanted to ensure that HIVSGD-derived BKPyV isolates displayed oral tropism. Indeed, the work presented in Chapter 3 shows that HIVSGD-derived BKPyV isolates replicated well within human salivary gland cells and provided evidence of preferred oral tropism as HIVSGD-derived BKPyV isolates replicated more efficiently in human salivary gland (HSG) cells than in kidney cells (58).

Interestingly, it is not clear which factors determine BKPyV tropism. Members of the polyomavirus family have a narrow species host range but infect a wide range of cell types within a host (48). BKPyV capsid proteins interact directly with the receptor molecules as infection is initiated, since it is a non-enveloped virus. This interaction is generally thought to be the major determinant of viral host and tissue tropism (93). BKPyV binds to cellular receptors

such as N-linked glycoproteins with a2,3-linked sialic acids and gangliosides GD1b and GT1b.

BKPyV is subsequently internalized via caveolae-mediated endocytosis, and is transported

towards the endoplasmic reticulum (ER) via the host cell cytoskeleton. Mutations in the major

capsid protein VP1 may lead to differential host cell receptor binding. Neu *et al. (94)* described

the structural requirements that underlie receptor switching and showed that the amino acid at

position 68 in VP1 is a determinant of receptor specificity. The *in vitro* experiments show that a

lysine to serine mutation of this residue switches the receptor specificity of BKPyV from GD3 to

GM1. These findings emphasize the plasticity of viral receptor binding sites and potential host

cell type retargeting mechanism.

How does BKPyV infect human salivary gland cells? Jeffers *et al.* infected human

parotid (HSY) and submandibular gland (HSG) cells with laboratory strain BKPyV (VR837),

emphasizing the capability of BKPyV to replicate in human oral tissue. The study illustrates

successful viral ganglioside-dependent entry, uncoating, gene expression, virion formation and

release (95). Interestingly, there is evidence that downstream events such as endocytosis, virus-

induced signaling, intracellular trafficking and transcriptional regulation contributes significantly

to viral tropism (93). We therefore wanted to ask what factors, beyond the initial receptor

interaction is likely to allow BKPyV to infect and replicate within the oral compartment and

subsequently cause HIVSGD? Could the promoter region be a major determinant, similar to

JCPyV described earlier?

During infection BKPyV undergoes uncoating once at the endoplasmic reticulum (ER)

and nuclear localization signals (found on the minor capsid proteins VP2 and/or VP3) further

direct viral genomes to the nucleus and are subsequently imported via the host's nuclear import

machinery (53). Maraldi et al. showed that this process may be completed within 12 hours (96).

Once in the nucleus, the early genes are expressed and the BKPyV genome is replicated before late gene expression starts and virions are assembled in the nucleus (42). Given the hypothesis that receptor interactions may be not be the only factors determining tropism and JCPyV tropism to be determined by its promoter, it may be important to consider the contribution of transactivating factors affecting BKPyV gene expression to tropism (57, 93). As mentioned earlier, the BKPyV NCCR promoter contains the origin of replication and the enhancer/promoter elements of the genome and is the main determinant of BKPyV replication *in vitro* (56). The NCCR is a hypervariable region and comparative studies have suggested that it may regulate host cell tropism mainly due to the rearrangement, duplication or deletion of TFBS (57, 93, 97). It is therefore plausible that the interplay of TFBS found within the NCCR sequence of a certain BKPyV substrain and transcription factors present within a certain cell type may allow for successful completion of a viral life cycle and therefore determine BKPyV tropism. We therefore analyzed the TFBS present within the signature OPQQPS NCCR architecture of the clinical HIVSGD BKPyV isolates in Chapter 2.

BKPyV *in vitro* Cultivation

In vitro cultivation of archetype BKPyV in kidney cells, a biologically relevant strain and cell culture model, is inefficient unless Tag is provided in trans by over-expression (74) and few studies have successfully cultivated clinical BKPyV isolates. Much of the BKPyV *in vitro* cultivation work has been done in cell types that do not represent the natural host, therefore unlikely to mimic natural infection. Archetypic BKPyV has been passaged and studied in skin fibroblasts (63), HT-1080 fibrosarcoma cell line (98), HeLa cervical cancer cells (60), HEL-299 human lung fibroblast (99) and WI-38 human embryonic fibroblasts (100). Similarly, the bulk of BKPyV *in vitro* studies were performed with laboratory BKPyV substrains, equally unsuited to

represent a natural infection. The following laboratory BKPyV substrains have been used to elucidate the BKPyV life cycle: Dunlop (101), TU (99), Proto-2 (98), Gardner strain, VR837 (100), MM (60). When the cell culture system was suited to represent natural infection, the focus was solely on kidney cells due the historic connection of BKPyV and the renal transplants. BKPyV infection and transfection experiments intended to represent the naturally infected renal compartment have been performed in human embryonic kidney cells (63), human primary renal proximal tubule epithelial cells RPTE cells (56, 98), Vero cells (75, 99), baby hamster kidney (BHK), newborn rat kidney (NRK) cells, monkey kidney (BSC and CV1) cells (101, 102) and primary human urothelial (HUCs) cells (103).

The lack of an *in vitro* system that adequately represents the oral *in vivo* compartment and a system that allows for efficient cultivation of clinical BKPyV isolates hinders the complete elucidation of the BKPyV life cycle, potential pathogenic mechanism within the oral compartment or testing of HIVSGD treatment options. My work described in Chapter 2 and Chapter 3 will address this gap. A cell culture system that allows studying oral BKPyV replication, potential pathogenesis and anti-viral treatment options was established. Our group previously cultivated laboratory strain BKPyV in human salivary gland cells (95), and in Chapter 2 and Chapter 3, for the first, time clinical BKPyV isolates were assessed in human salivary gland cells (58).

BK Polyomavirus - HIVSGD Association

BKPyV has been shown to display oral tropism *in vivo* and *in vitro.* BKPyV has been detected in tonsillar tissue from both pediatric and adult donors (45, 104, 105) and Jeffers *et al.* showed in 2009 that BKPyV is able to infect and reproduce in human salivary gland cells *in vitro* (95). Our group showed that laboratory strain BKPyV undergoes entry, transcribes, translates

and produces virions within human submandibular (HSG) and parotid (HSY) salivary gland cells. It is plausible therefore that the oral compartment represents an infectious reservoir in addition to the historically described renal/urinary compartment (51, 106). Previous studies have shown that the replication compartments of urine and plasma-derived BKPyV are distinct in vivo (71, 72), similarly, the salivary gland may embody a separate replication compartment in the HIVSGD setting (107).

The Koch's postulates, used as scientific standard since its publication over 100 years ago, established a guideline to identify a causal correlation between a microorganism and a disease. Fredricks and Relman re-formulated Koch's postulates in 1996 by integrating modern sequence-based identification of microbial pathogens (108). In short, sequences from a microorganism proposed to cause a disease need to be found in the majority of cases among diseased organisms, ideally at affected sites. Furthermore, fewer or no sequences from the microorganisms must be found within negative controls. Based on the re-formulated postulates we were able to corroborate that BKPyV contributes to HIVSGD. Jeffers *et al.* detected, for the first time, significantly higher BKPyV viral loads (VLs) in the saliva of patients diagnosed with HIVSGD as compared to HIV negative patients (95). The oral BKPyV VLs of HIVSGD patients (n=11) ranged from 10^1 to 10^4 copies/ml whereas the HIV negative control cohort (n=7) VLs ranged from 0 to 10^2 copies/ml. Our group confirmed the high BKPyV levels shed in a HIVSGD cohort two years later (13). The study found highest BKPyV VLs in patients diagnosed with HIVSGD (n=11) as compared to patients who are HIV + without HIVSGD (n=46) and HIV negative individuals (n=12). Furthermore, our group found BKPyV products, but not herpesviral DNA, via PCR and immunofluorescence in HIVSGD patient salivary gland biopsies but not in biopsies from patients without HIVSGD (109). Hence, BKPyV sequences were detected among

most HIVSGD TW samples and biopsies. Furthermore, significantly lower BKPyV levels were detected among HIVSGD negative TW samples and no BKPyV sequence were found among biopsies from patients without HIVSGD. In summary, based on Fredricks and Relman's postulates, we have provided evidence that BKPyV may be involved in HIVSGD pathogenesis. To further strengthen these assertions, Chapter 2 and Chapter 3 of this thesis will characterize *in vitro* replication and the promoter region and activity of HIVSGD-derived BKPyV and compared to those detected in transplant patients with BKPyV infection. We established a salivary gland cell culture system that allows the cultivation and study of clinical BKPyV isolates which is important because HIVSGD is associated with significant morbidity. Furthermore, Appendix 1 describes how the salivary gland cell culture system was used to test antiviral treatment options potentially alleviating general BKPyV-associated ailments.

Increased lymphoma incidence among HIVSGD patients is one of the most significant morbidities. In light of potential treatment options it is important to define whether the BKPyV DNA tumorvirus is the potential cause of it. As mentioned earlier, HIVSGD is considered a pre-malignant lesion and its diagnosis is associated with increased lymphoma incidence (5, 8, 12, 13). While evidence of BKPyV causing cancer in humans is less conclusive than in animal models (discussed earlier), there are numerous cases where BKPyV sequences were found in human tumors, including brain, pancreas, rhabdomyosarcoma, lung, liver, Kaposi's sarcoma, and urinary tract neoplasms (45, 110-119). The most definite evidence linking BKPyV to cancer focused on the urinary tract. Monini *et al.* PCR-amplified BKPyV sequences from both normal and tumor urinary tract tissue and found BKPyV in almost all samples, as would be expected due the holoendemic and renal/urinary tract-tropic nature of BKPyV (117). By Southern Blot analysis however they detected integrated BKPyV in tumor samples only. Moreover they found

the NCCR architecture of the tumor-derived BKPyV to be homologous (although not sequence homologous), rearranged and to represent a novel substrain they termed URO1. It is remarkable that the group found a novel and conserved BKPyV substrain, similar to our study described in Chapter 2, where we analyze the NCCR region of HIVSGD-derived patients and find a uniform OPQPQQS architecture in 18 out of 19 samples (see Chapter 2).

BKPyV tumorigenic capability in experimental models, as mentioned above, is accredited to the presence of the oncoprotein Tag (101). Tag is a nuclear phosphoprotein that wields its transforming abilities by interacting and suppressing cellular tumor suppressor proteins p53 and members of the pRb family, which leads to unrestrained host cell proliferation (120). It transforms rodent cells and immortalizes human cell lines *in vitro*. The viral protein immortalizes human cell lines independently or in the presence of other oncogenes including ras, myc and adenovirus E1A (reviewed in (120)). Understanding the complete life cycle of the virus and the role Tag plays during infection will be critical in the development of possible therapeutic interventions of lymphoma formation during HIVSGD pathogenesis. Towards that goal we have completed a study analyzing the possible connection between the metastasis-associated lung adenocarcinoma-associated transcript 1 (MALAT-1) and PyV Tag described in Appendix 2.

My Scientific Contributions To The Field

As suggested by the reviewed literature, there is likely a connection between BKPyV and HIVSGD development. My first goal was to corroborate the BKPyV-HIVSGD connection by confirming elevated BKPyV VL levels in oral samples from HIVSGD patients (Chapter 2). Secondly, I aimed to characterize the BKPyV promoter region of the HIVSGD isolates due the importance of the NCCR for the viral life cycle and potentially its pathogenic potential and

tropism (Chapter 2). I aimed to study the *in vitro* replication levels and tropism of clinical

HIVSGD-derived isolates in order to elucidate the role BKPyV may play during HIVSGD

pathogenesis and to determine whether the virus could be inhibited in this system (Chapter 3,

Appendix 1). Further, I aimed to determine downstream cellular effects associated with BKPyV

salivary gland infection (Appendix 2). We have therefore pursued and completed following

AIMS:

AIM1: To determine BKPyV viral loads in HIVSGD throatwash (TW) *in vivo,* we screened TW

samples from HIVSGD positive and negative patients for BKPyV. Concomitantly, we

characterized the BKPyV promoter from HIVSGD positive and HIVSGD negative TW samples

and urine samples from transplant patients (Chapter 2).

AIM2: To determine BKPyV viral fitness in the human oral cavity, we explored the tropism and

in vitro replication efficiency of HIVSGD TW-derived BKPyV in human salivary gland and

kidney cells *in vitro (*Chapter 3).

REFERENCES

1.   1981. Pneumocystis pneumonia--Los Angeles. MMWR. Morbidity and mortality weekly report **30:**250-2.

2.   UNAIDS Global Report 2013. [Online.]

3.   **Cubukcu-Dimopulo, O., A. Greco, A. Kumar, D. Karluk, K. Mittal, and J. Jagirdar.** 2000. BK virus infection in AIDS. The American journal of surgical pathology **24:**145-9.

4.   **Ulirsch, R. C., and E. S. Jaffe.** 1987. Sjogren's syndrome-like illness associated with the acquired immunodeficiency syndrome-related complex. Human pathology **18:**1063-8.

5.   **Ioachim, H. L., J. R. Ryan, and S. M. Blaugrund.** 1988. Salivary gland lymph nodes. The site of lymphadenopathies and lymphomas associated with human immunodeficiency virus infection. Archives of pathology & laboratory medicine **112:**1224-8.

6.   **Ryan, J. R., H. L. Ioachim, J. Marmer, and J. M. Loubeau.** 1985. Acquired immune deficiency syndrome--related lymphadenopathies presenting in the salivary gland lymph nodes. Archives of otolaryngology **111:**554-6.

7.   **Itescu, S.** 1991. Diffuse infiltrative lymphocytosis syndrome in human immunodeficiency virus infection--a Sjogren's-like disease. Rheumatic diseases clinics of North America **17:**99-115.

8.   **Ioachim, H. L., and J. R. Ryan.** 1988. Salivary gland lymphadenopathies associated with AIDS. Human pathology **19:**616-7.

9.   **Schiodt, M., D. Greenspan, J. A. Levy, J. A. Nelson, D. Chernoff, H. Hollander, and J. S. Greenspan.** 1989. Does HIV cause salivary gland disease? AIDS **3:**819-22.

10.   **Shanti, R. M., and S. R. Aziz.** 2009. HIV-associated salivary gland disease. Oral and maxillofacial surgery clinics of North America **21:**339-43.

11. **McArthur, C. P., A. Subtil-DeOliveira, D. Palmer, R. M. Fiorella, S. Gustafson, D. Tira, and R. N. Miranda.** 2000. Characteristics of salivary diffuse infiltrative lymphocytosis syndrome in West Africa. Archives of pathology & laboratory medicine **124:**1773-9.

12. **DiGiuseppe, J. A., R. L. Corio, and W. H. Westra.** 1996. Lymphoid infiltrates of the salivary glands: pathology, biology and clinical significance. Curr Opin Oncol **8:**232-7.

13. **Jeffers, L., and J. Y. Webster-Cyriaque.** 2011. Viruses and salivary gland disease (SGD): lessons from HIV SGD. Adv Dent Res **23:**79-83.

14. **Program, R. W. H.**, posting date. Oral Health Release. [Online.]

15. **Patton, L. L., R. McKaig, R. Strauss, D. Rogers, and J. J. Eron, Jr.** 2000. Changing prevalence of oral manifestations of human immuno-deficiency virus in the era of protease inhibitor therapy. Oral surgery, oral medicine, oral pathology, oral radiology, and endodontics **89:**299-304.

16. **Greenspan, D., A. J. Canchola, L. A. MacPhail, B. Cheikh, and J. S. Greenspan.** 2001. Effect of highly active antiretroviral therapy on frequency of oral warts. Lancet **357:**1411-2.

17. **Shelburne, S. A., F. Visnegarwala, J. Darcourt, E. A. Graviss, T. P. Giordano, A. C. White, Jr., and R. J. Hamill.** 2005. Incidence and risk factors for immune reconstitution inflammatory syndrome during highly active antiretroviral therapy. AIDS **19:**399-406.

18. **Basu, D., F. M. Williams, C. W. Ahn, and J. D. Reveille.** 2006. Changing spectrum of the diffuse infiltrative lymphocytosis syndrome. Arthritis and rheumatism **55:**466-72.

19. **Itescu, S., L. J. Brancato, and R. Winchester.** 1989. A sicca syndrome in HIV infection: association with HLA-DR5 and CD8 lymphocytosis. Lancet **2:**466-8.
20. **Scully, C.** 1988. Viruses and salivary gland disease: are there associations? Oral surgery, oral medicine, and oral pathology **66:**179-83.

21. **Rivera, H., N. G. Nikitakis, S. Castillo, H. Siavash, J. C. Papadimitriou, and J. J. Sauk.** 2003. Histopathological analysis and demonstration of EBV and HIV p-24 antigen but not CMV expression in labial minor salivary glands of HIV patients affected by

diffuse infiltrative lymphocytosis syndrome. Journal of oral pathology & medicine : official publication of the International Association of Oral Pathologists and the American Academy of Oral Pathology **32:**431-7.

22. **Schreiber, A., and G. Hershman.** 2009. Non-HIV viral infections of the salivary glands. Oral and maxillofacial surgery clinics of North America **21:**331-8.

23. **Takahashi, M., T. Nakayama, Y. Kashiwagi, T. Takami, S. Sonoda, T. Yamanaka, H. Ochiai, T. Ihara, and T. Tajima.** 2000. Single genotype of measles virus is dominant whereas several genotypes of mumps virus are co-circulating. Journal of medical virology **62:**278-85.

24. **Peltola, H.** 1993. Mumps vaccination and meningitis. Lancet **341:**994-5.

25. **Purtilo, D. T.** 1987. Epstein-Barr virus: the spectrum of its manifestations in human beings. Southern medical journal **80:**943-7.

26. **Kimura, H.** 2011. [Chronic active Epstein-Barr virus infection]. Uirusu **61:**163-73.

27. **Raab-Traub, N., P. Rajadurai, K. Flynn, and A. P. Lanier.** 1991. Epstein-Barr virus infection in carcinoma of the salivary gland. Journal of virology **65:**7032-6.

28. 2007. Fields' Virology. *In* P. M. H. David M. Knipe (ed.), 5th ed. Wolters Kluwer Health/Lippincott Williams & Wilkins, Philadelphia.

29. **Ward, J. M., A. Lock, M. J. Collins, Jr., M. A. Gonda, and C. W. Reynolds.** 1984. Papovaviral sialoadenitis in athymic nude rats. Laboratory animals **18:**84-9.

30. **Small, J. A., G. Khoury, G. Jay, P. M. Howley, and G. A. Scangos.** 1986. Early regions of JC virus and BK virus induce distinct and tissue-specific tumors in transgenic mice. Proceedings of the National Academy of Sciences of the United States of America **83:**8288-92.

31. **Dalrymple, S. A., and K. L. Beemon.** 1990. BK virus T antigens induce kidney carcinomas and thymoproliferative disorders in transgenic mice. Journal of virology **64:**1182-91.

32.   **Dardick, I., J. Ho, M. Paulus, P. L. Mellon, and L. Mirels.** 2000. Submandibular gland adenocarcinoma of intercalated duct origin in Smgb-Tag mice. Laboratory investigation; a journal of technical methods and pathology **80:**1657-70.

33.   **Breuer, M.** 1991. The use of transgenic mice in unraveling the multistep process of tumorigenesis. Radiation and environmental biophysics **30:**181-3.

34.   **Furth, P. A., M. Li, and L. Hennighausen.** 1998. Studying development of disease through temporally controlled gene expression in the salivary gland. Annals of the New York Academy of Sciences **842:**181-7.

35.   **Harrod, F. A., and J. R. Kettman.** 1990. Transplantable polyoma virus-induced epitheliomas harbor immature T lymphocytes. Cellular immunology **125:**29-41.

36.   **Eddy, B. E., G. S. Borman, R. L. Kirschstein, and R. H. Touchette.** 1960. Neoplasms in guinea pigs infected with SE polyoma virus. The Journal of infectious diseases **107:**361-8.

37.   **Bialasiewicz, S., D. M. Whiley, S. B. Lambert, M. D. Nissen, and T. P. Sloots.** 2009. Detection of BK, JC, WU, or KI polyomaviruses in faecal, urine, blood, cerebrospinal fluid and respiratory samples. J Clin Virol **45:**249-54.

38.   **Allander, T., K. Andreasson, S. Gupta, A. Bjerkner, G. Bogdanovic, M. A. Persson, T. Dalianis, T. Ramqvist, and B. Andersson.** 2007. Identification of a third human polyomavirus. Journal of virology **81:**4130-6.

39.   **Gaynor, A. M., M. D. Nissen, D. M. Whiley, I. M. Mackay, S. B. Lambert, G. Wu, D. C. Brennan, G. A. Storch, T. P. Sloots, and D. Wang.** 2007. Identification of a novel polyomavirus from patients with acute respiratory tract infections. PLoS pathogens **3:**e64.

40.   **Kazem, S., E. van der Meijden, and M. C. Feltkamp.** 2013. The trichodysplasia spinulosa-associated polyomavirus: virological background and clinical implications. APMIS : acta pathologica, microbiologica, et immunologica Scandinavica **121:**770-82.

41. **Wieland, U., S. Silling, M. Hellmich, A. Potthoff, H. Pfister, and A. Kreuter.** 2014. Human polyomaviruses 6, 7, 9, 10 and Trichodysplasia spinulosa-associated polyomavirus in HIV-infected men. The Journal of general virology.

42. **Hirsch, H. H., and J. Steiger.** 2003. Polyomavirus BK. Lancet Infect Dis **3:**611-23.

43. **Wiedinger, K., C. Bitsaktsis, and S. Chang.** 2014. Reactivation of human polyomaviruses in immunocompromised states. Journal of neurovirology.

44. **Gardner, S. D., A. M. Field, D. V. Coleman, and B. Hulme.** 1971. New human papovavirus (B.K.) isolated from urine after renal transplantation. Lancet **1:**1253-7.

45. **Imperiale, M. J.** 2000. The human polyomaviruses, BKV and JCV: molecular pathogenesis of acute disease and potential role in cancer. Virology **267:**1-7.

46. **Boldorini, R., S. Allegrini, U. Miglio, A. Paganotti, N. Cocca, M. Zaffaroni, F. Riboni, G. Monga, and R. Viscidi.** 2011. Serological evidence of vertical transmission of JC and BK polyomaviruses in humans. The Journal of general virology **92:**1044-50.

47. **Hashida, Y., P. C. Gaffney, and E. J. Yunis.** 1976. Acute hemorrhagic cystitis of childhood and papovavirus-like particles. The Journal of pediatrics **89:**85-7.

48. **Weinberg, G. A., and A. N. Mian.** 2010. BK virus nephropathy and other polyoma virus infections. The Pediatric infectious disease journal **29:**257-60.

49. **Vidal, J. E., M. C. Fink, F. Cedeno-Laurent, S. Delbue, P. Ferrante, R. F. Dauar, F. B. Filho, R. S. Nogueira, E. E. Calore, C. S. Pannuti, J. R. Trujillo, and A. C. de Oliveira.** 2007. BK virus associated meningoencephalitis in an AIDS patient treated with HAART. AIDS research and therapy **4:**13.

50. **Jiang, M., J. R. Abend, S. F. Johnson, and M. J. Imperiale.** 2009. The role of polyomaviruses in human disease. Virology **384:**266-73.

51. **Nickeleit, V., and M. J. Mihatsch.** 2006. Polyomavirus nephropathy in native kidneys and renal allografts: an update on an escalating threat. Transpl Int **19:**960-73.

52.   **Nickeleit, V.** 2006. Animal models of polyomavirus nephropathy: hope and reality. Am J Transplant **6:**1507-9.

53.   **Rinaldo, C. H., G. D. Tylden, and B. N. Sharma.** 2013. The human polyomavirus BK (BKPyV): virological background and clinical implications. APMIS : acta pathologica, microbiologica, et immunologica Scandinavica **121:**728-45.

54.   **Pipas, J. M.** 1992. Common and unique features of T antigens encoded by the polyomavirus group. Journal of virology **66:**3979-85.

55.   **Daniels, R., D. Sadowicz, and D. N. Hebert.** 2007. A very late viral protein triggers the lytic release of SV40. PLoS pathogens **3:**e98.

56.   **Broekema, N. M., J. R. Abend, S. M. Bennett, J. S. Butel, J. A. Vanchiere, and M. J. Imperiale.** 2010. A system for the analysis of BKV non-coding control regions: application to clinical isolates from an HIV/AIDS patient. Virology **407:**368-73.

57.   **Johnsen, J. I., O. M. Seternes, T. Johansen, U. Moens, R. Mantyjarvi, and T. Traavik.** 1995. Subpopulations of non-coding control region variants within a cell culture-passaged stock of BK virus: sequence comparisons and biological characteristics. J Gen Virol **76 (Pt 7):**1571-81.

58.   **Burger-Calderon, R., V. Madden, R. A. Hallett, A. D. Gingerich, V. Nickeleit, and J. Webster-Cyriaque.** 2013. Replication of oral BK virus in human salivary gland cells. J Virol.

59.   **Gorrill, T. S., and K. Khalili.** 2005. Cooperative interaction of p65 and C/EBPbeta modulates transcription of BKV early promoter. Virology **335:**1-9.
60.   **Markowitz, R. B., and W. S. Dynan.** 1988. Binding of cellular proteins to the regulatory region of BK virus DNA. J Virol **62:**3388-98.

61.   **Cho, S., Y. Tian, and T. L. Benjamin.** 2001. Binding of p300/CBP co-activators by polyoma large T antigen. J Biol Chem **276:**33533-9.

62.   **Poulin, D. L., A. L. Kung, and J. A. DeCaprio.** 2004. p53 targets simian virus 40 large T antigen for acetylation by CBP. J Virol **78:**8245-53.

63.   **Rubinstein, R., B. C. Schoonakker, and E. H. Harley.** 1991. Recurring theme of changes in the transcriptional control region of BK virus during adaptation to cell culture. J Virol **65:**1600-4.

64.   **Sundsfjord, A., T. Johansen, T. Flaegstad, U. Moens, P. Villand, S. Subramani, and T. Traavik.** 1990. At least two types of control regions can be found among naturally occurring BK virus strains. J Virol **64:**3864-71.

65.   **Sundsfjord, A., T. Flaegstad, R. Flo, A. R. Spein, M. Pedersen, H. Permin, J. Julsrud, and T. Traavik.** 1994. BK and JC viruses in human immunodeficiency virus type 1-infected persons: prevalence, excretion, viremia, and viral regulatory regions. J Infect Dis **169:**485-90.

66.   **Hanssen Rinaldo, C., H. Hansen, and T. Traavik.** 2005. Human endothelial cells allow passage of an archetypal BK virus (BKV) strain--a tool for cultivation and functional studies of natural BKV strains. Arch Virol **150:**1449-58.

67.   **Bennett, S. M., N. M. Broekema, and M. J. Imperiale.** 2012. BK polyomavirus: emerging pathogen. Microbes Infect **14:**672-83.

68.   **Chatterjee, M., T. B. Weyandt, and R. J. Frisque.** 2000. Identification of archetype and rearranged forms of BK virus in leukocytes from healthy individuals. J Med Virol **60:**353-62.

69.   **Olsen, G. H., P. A. Andresen, H. T. Hilmarsen, O. Bjorang, H. Scott, K. Midtvedt, and C. H. Rinaldo.** 2006. Genetic variability in BK Virus regulatory regions in urine and kidney biopsies from renal-transplant patients. J Med Virol **78:**384-93.

70.   **Perets, T. T., I. Silberstein, J. Rubinov, R. Sarid, E. Mendelson, and L. M. Shulman.** 2009. High frequency and diversity of rearrangements in polyomavirus bk noncoding regulatory regions cloned from urine and plasma of Israeli renal transplant patients and evidence for a new genetic subtype. J Clin Microbiol **47:**1402-11.

71.   **Gosert, R., C. H. Rinaldo, G. A. Funk, A. Egli, E. Ramos, C. B. Drachenberg, and H. H. Hirsch.** 2008. Polyomavirus BK with rearranged noncoding control region emerge in vivo in renal transplant patients and increase viral replication and cytopathology. J Exp Med **205:**841-52.

72.	**Funk, G. A., R. Gosert, and H. H. Hirsch.** 2007. Viral dynamics in transplant patients: implications for disease. Lancet Infect Dis **7:**460-72.

73.	**Moens, U., and M. Van Ghelue.** 2005. Polymorphism in the genome of non-passaged human polyomavirus BK: implications for cell tropism and the pathological role of the virus. Virology **331:**209-31.

74.	**Broekema, N. M., and M. J. Imperiale.** 2012. Efficient propagation of archetype BK and JC polyomaviruses. Virology **422:**235-41.

75.	**Olsen, G. H., H. H. Hirsch, and C. H. Rinaldo.** 2009. Functional analysis of polyomavirus BK non-coding control region quasispecies from kidney transplant recipients. J Med Virol **81:**1959-67.

76.	**Weber, T., and E. O. Major.** 1997. Progressive multifocal leukoencephalopathy: molecular biology, pathogenesis and clinical impact. Intervirology **40:**98-111.

77.	**Martin, J. D., D. M. King, J. M. Slauch, and R. J. Frisque.** 1985. Differences in regulatory sequences of naturally occurring JC virus variants. Journal of virology **53:**306-11.

78.	**White, F. A., 3rd, M. Ishaq, G. L. Stoner, and R. J. Frisque.** 1992. JC virus DNA is present in many human brain samples from patients without progressive multifocal leukoencephalopathy. Journal of virology **66:**5726-34.

79.	**Kato, K., J. Guo, F. Taguchi, O. Daimaru, M. Tajima, H. Haibara, J. Matsuda, M. Sumiya, and Y. Yogo.** 1994. Phylogenetic comparison between archetypal and disease-associated JC virus isolates in Japan. Japanese journal of medical science & biology **47:**167-78.

80.	**Ciappi, S., A. Azzi, R. De Santis, F. Leoncini, G. Sterrantino, F. Mazzotta, and L. Mecocci.** 1999. Archetypal and rearranged sequences of human polyomavirus JC transcription control region in peripheral blood leukocytes and in cerebrospinal fluid. The Journal of general virology **80 (Pt 4):**1017-23.

81.	**Newman, J. T., and R. J. Frisque.** 1999. Identification of JC virus variants in multiple tissues of pediatric and adult PML patients. Journal of medical virology **58:**79-86.

82. **Daniel, A. M., J. J. Swenson, R. P. Mayreddy, K. Khalili, and R. J. Frisque.** 1996. Sequences within the early and late promoters of archetype JC virus restrict viral DNA replication and infectivity. Virology **216:**90-101.

83. **Tamura, T., T. Inoue, K. Nagata, and K. Mikoshiba.** 1988. Enhancer of human polyoma JC virus contains nuclear factor I-binding sequences; analysis using mouse brain nuclear extracts. Biochemical and biophysical research communications **157:**419-25.

84. **Khalili, K., J. Rappaport, and G. Khoury.** 1988. Nuclear factors in human brain cells bind specifically to the JCV regulatory region. The EMBO journal **7:**1205-10.

85. **Feigenbaum, L., S. H. Hinrichs, and G. Jay.** 1992. JC virus and simian virus 40 enhancers and transforming proteins: role in determining tissue specificity and pathogenicity in transgenic mice. Journal of virology **66:**1176-82.

86. **Kerr, D., C. F. Chang, N. Chen, G. Gallia, G. Raj, B. Schwartz, and K. Khalili.** 1994. Transcription of a human neurotropic virus promoter in glial cells: effect of YB-1 on expression of the JC virus late gene. Journal of virology **68:**7637-43.

87. **Chen, N. N., and K. Khalili.** 1995. Transcriptional regulation of human JC polyomavirus promoters by cellular proteins YB-1 and Pur alpha in glial cells. Journal of virology **69:**5843-8.

88. **Chen, N. N., C. F. Chang, G. L. Gallia, D. A. Kerr, E. M. Johnson, C. P. Krachmarov, S. M. Barr, R. J. Frisque, B. Bollag, and K. Khalili.** 1995. Cooperative action of cellular proteins YB-1 and Pur alpha with the tumor antigen of the human JC polyomavirus determines their interaction with the viral lytic control element. Proceedings of the National Academy of Sciences of the United States of America **92:**1087-91.

89. **Safak, M., G. L. Gallia, and K. Khalili.** 1999. A 23-bp sequence element from human neurotropic JC virus is responsive to NF-kappa B subunits. Virology **262:**178-89.

90. **Sharma, P. M., G. Gupta, A. Vats, R. Shapiro, and P. S. Randhawa.** 2007. Polyomavirus BK non-coding control region rearrangements in health and disease. J Med Virol **79:**1199-207.

91.   **Boldorini, R., C. Veggiani, E. Turello, D. Barco, and G. Monga.** 2005. Are sequence variations in the BK virus control region essential for the development of polyomavirus nephropathy? Am J Clin Pathol **124:**303-12.

92.   **Elsner, C., and K. Dorries.** 1998. Human polyomavirus JC control region variants in persistently infected CNS and kidney tissue. J Gen Virol **79 (Pt 4):**789-99.

93.   **Ashok, A., and W. J. Atwood.** 2006. Virus receptors and tropism. Advances in Experimental Medicine and Biology **577:**60-72.

94.   **Neu, U., S. A. Allen, B. S. Blaum, Y. Liu, M. Frank, A. S. Palma, L. J. Stroh, T. Feizi, T. Peters, W. J. Atwood, and T. Stehle.** 2013. A structure-guided mutation in the major capsid protein retargets BK polyomavirus. PLoS pathogens **9:**e1003688.

95.   **Jeffers, L. K., V. Madden, and J. Webster-Cyriaque.** 2009. BK virus has tropism for human salivary gland cells in vitro: implications for transmission. Virology **394:**183-93.

96.   **Maraldi, N. M., G. Barbanti-Brodano, M. Portolani, and M. La Placa.** 1975. Ultrastructural aspects of BK virus uptake and replication in human fibroblasts. The Journal of general virology **27:**71-80.

97.   **Moens, U., T. Johansen, J. I. Johnsen, O. M. Seternes, and T. Traavik.** 1995. Noncoding control region of naturally occurring BK virus variants: sequence comparison and functional analysis. Virus genes **10:**261-75.

98.   **Abend, J. R., and M. J. Imperiale.** 2008. Transforming growth factor-beta-mediated regulation of BK virus gene expression. Virology **378:**6-12.

99.   **Seamone, M. E., W. Wang, P. Acott, P. L. Beck, L. A. Tibbles, and D. A. Muruve.** 2010. MAP kinase activation increases BK polyomavirus replication and facilitates viral propagation in vitro. Journal of virological methods **170:**21-9.

100.   **Randhawa, P., N. A. Farasati, and Y. Huang.** 2007. BK Virus replication in vitro: limited effect of drugs interfering with viral uptake and intracellular transport. Antimicrobial agents and chemotherapy **51:**4492-4.

101. **Abend, J. R., A. E. Joseph, D. Das, D. B. Campbell-Cecen, and M. J. Imperiale.** 2009. A truncated T antigen expressed from an alternatively spliced BK virus early mRNA. J Gen Virol **90:**1238-45.

102. **Deyerle, K. L., and S. Subramani.** 1989. Human papovavirus BK early gene regulation in nonpermissive cells. Virology **169:**385-96.

103. **Li, R., B. N. Sharma, S. Linder, T. J. Gutteberg, H. H. Hirsch, and C. H. Rinaldo.** 2013. Characteristics of polyomavirus BK (BKPyV) infection in primary human urothelial cells. Virology **440:**41-50.

104. **Goudsmit, J., M. L. Baak, K. W. Sleterus, and J. Van der Noordaa.** 1981. Human papovavirus isolated from urine of a child with acute tonsillitis. British medical journal **283:**1363-4.

105. **Goudsmit, J., P. Wertheim-van Dillen, A. van Strien, and J. van der Noordaa.** 1982. The role of BK virus in acute respiratory tract disease and the presence of BKV DNA in tonsils. Journal of medical virology **10:**91-9.

106. **Nickeleit, V., H. H. Hirsch, I. F. Binet, F. Gudat, O. Prince, P. Dalquen, G. Thiel, and M. J. Mihatsch.** 1999. Polyomavirus infection of renal allograft recipients: from latent infection to manifest disease. J Am Soc Nephrol **10:**1080-9.

107. **Robaina, T. F., G. S. Mendes, F. J. Benati, G. A. Pena, R. C. Silva, M. A. Montes, M. E. Janini, F. P. Camara, and N. Santos.** 2013. Shedding of polyomavirus in the saliva of immunocompetent individuals. J Med Virol **85:**144-8.

108. **Fredericks, D. N., and D. A. Relman.** 1996. Sequence-based identification of microbial pathogens: a reconsideration of Koch's postulates. Clinical microbiology reviews **9:**18-33.

109. **Dovigi, D. A.** 2005. HIV Salivary Gland Disease: A Role For Viral Infection. University of North Carolina at Chapel Hill, Chapel Hill, NC.

110. **Fiori, M., and G. Di Mayorca.** 1976. Occurrence of BK virus DNA in DNA obtained from certain human tumors. Proceedings of the National Academy of Sciences of the United States of America **73:**4662-6.

111. **Caputo, A., A. Corallini, M. P. Grossi, L. Carra, P. G. Balboni, M. Negrini, G. Milanesi, G. Federspil, and G. Barbanti-Brodano.** 1983. Episomal DNA of a BK virus variant in a human insulinoma. Journal of medical virology **12:**37-49.

112. **Dorries, K., G. Loeber, and J. Meixensberger.** 1987. Association of polyomaviruses JC, SV40, and BK with human brain tumors. Virology **160:**268-70.

113. **Barbanti-Brodano, G., M. Pagnani, P. Viadana, E. Beth-Giraldo, G. Giraldo, and A. Corallini.** 1987. BK virus DNA in Kaposi's sarcoma. Antibiotics and chemotherapy **38:**113-20.

114. **Corallini, A., M. Pagnani, P. Viadana, E. Silini, M. Mottes, G. Milanesi, G. Gerna, R. Vettor, G. Trapella, V. Silvani, and et al.** 1987. Association of BK virus with human brain tumors and tumors of pancreatic islets. International journal of cancer. Journal international du cancer **39:**60-7.

115. **Negrini, M., P. Rimessi, C. Mantovani, S. Sabbioni, A. Corallini, M. A. Gerosa, and G. Barbanti-Brodano.** 1990. Characterization of BK virus variants rescued from human tumours and tumour cell lines. The Journal of general virology **71 (Pt 11):**2731-6.

116. **De Mattei, M., F. Martini, A. Corallini, M. Gerosa, K. Scotlandi, P. Carinci, G. Barbanti-Brodano, and M. Tognon.** 1995. High incidence of BK virus large-T-antigen-coding sequences in normal human tissues and tumors of different histotypes. International journal of cancer. Journal international du cancer **61:**756-60.

117. **Monini, P., A. Rotola, D. Di Luca, L. De Lellis, E. Chiari, A. Corallini, and E. Cassai.** 1995. DNA rearrangements impairing BK virus productive infection in urinary tract tumors. Virology **214:**273-9.

118. **Flaegstad, T., P. A. Andresen, J. I. Johnsen, S. K. Asomani, G. E. Jorgensen, S. Vignarajan, A. Kjuul, P. Kogner, and T. Traavik.** 1999. A possible contributory role of BK virus infection in neuroblastoma development. Cancer research **59:**1160-3.

119. **Monini, P., L. de Lellis, A. Rotola, D. Di Luca, T. Ravaioli, B. Bigoni, and E. Cassai.** 1995. Chimeric BK virus DNA episomes in a papillary urothelial bladder carcinoma. Intervirology **38:**304-8.

120. **Abend, J. R., M. Jiang, and M. J. Imperiale.** 2009. BK virus and human cancer: innocent until proven guilty. Seminars in cancer biology **19:**252-60.

CHAPTER 2:

DISTINCT BK VIRUS NON-CODING CONTROL REGION (NCCR) VARIANTS IN ORAL FLUIDS OF HIV- ASSOCIATED SALIVARY GLAND DISEASE PATIENTS

Overview

BK polyomavirus (BKPyV) has been recognized as human pathogen, affecting immune suppressed individuals, since its discovery in 1971. Our group has recently linked the small DNA tumorvirus BKPyV to HIV-associated salivary gland disease (HIVSGD), a disease persisting throughout the era of highly active antiretroviral therapy (HAART). The BKPyV non-coding control region (NCCR) is the main determinant of viral replication and rearranges readily *in vivo* and *in vitro*. Further, NCCR rearrangements have been associated with functional differences. This study analyzed 36 clinical samples for BKPyV, of which 29 were BKPyV positive. One hundred percent of throatwash (TW) samples from HIVSGD patients and urine samples from transplant patients yielded BKPyV NCCR sequences. Importantly, 94% of the BKPyV HIVSGD NCCRs carried the rearranged OPQPQQS block arrangement, suggesting a distinctive architecture among this sample set. These findings confirm the HIVSGD-derived BKPyV NCCR architecture previously described by our group. Only 22% of TW samples from HIV positive individuals without HIVSGD were BKPyV positive and resulted in NCCR sequences distinct from OPQPQQS. Despite the block homology in HIVSGD NCCRs, analysis of the underlying nucleotide sequences revealed substantial polymorphisms. The NCCR nucleotide polymorphisms predicted differential sets of transcription factor binding sites (TFBS).

TFBS C/EBPβ in particular, was significantly associated with differences in the detected viral loads. Finally, cloned HIVSGD BKPyV isolates displayed active promoters and efficient replication capability in human salivary gland cells *in vitro.* The unique HIVSGD NCCR architecture may define a new BKPyV substrain that is of significance for HIVSGD and for oral BKPyV pathogenesis.

Introduction

HIV-associated Salivary Gland Disease (HIVSGD) has persisted through the era of highly active antiretroviral therapy (HAART) and is associated with salivary gland enlargement, irreversible salivary gland damage, xerostomia (1-4) and increased risk of lymphoma development (5). HIVSGD is among the most commonly diagnosed salivary gland-associated complications in HIV positive individuals (6). Still, current treatment options are few due to the lack of insight into disease etiology and progression. Our group has previously established a link between HIVSGD and BK polyomavirus (BKPyV) (7-9). BKPyV is commonly detected in the adult population (10, 11) where it is thought to undergo latency in the uroepithelium and reactivate upon immune-suppression. BKPyV is the major driver of renal dysfunction among kidney transplant patients where reactivation of BKPyV, marked by increased viremia and viruria, is linked to polyomavirus-associated nephropathy (BKVN) (12-17). BKPyV, a member of the small DNA tumorvirus family, carries a circular double-stranded 5 kb genome, which consists of three major elements: the bidirectional viral promoter, known as the non-coding control region (NCCR), the early and the late regions (18). The early region encodes for non-structural viral proteins large, small and mini T antigen (Tag), which are associated with the

transforming ability of BKPyV. The late region encodes for the agnoprotein and the structural

proteins VP1, VP2 and VP3 (18).

Broekema *et al*. (19) determined that the BKPyV NCCR not only controls gene

expression but is also the main driver of *in vitro* replication. The NCCR consists of five block

sequences: O (142 bp), P (68 bp), Q (39 bp), R (63 bp) and S (63 bp) (20, 21), which contain the

origin of DNA replication and transcription factor binding sites (TFBS) (22, 23). Archetypic

BKPyV carries the originally described NCCR architecture OPQRS (24). TFBS AP-1, CREB,

NF-1, C/EBPβ, C/EBPδ, NF-kB, NF-kB1, p53, Sp1, Tag and p300 among others have been

described within the polyomavirus NCCR (20, 23, 25-27). According to mathematical models,

95% of archetypic urine BKPyV result from urothelial replication (11, 28, 29), and are excreted

in the urine. Hence, the archetypic NCCR may be considered as kidney-tropic substrain. The

NCCR is a hyper variable region and commonly undergoes block deletions and/or duplications

as compared to the archetype. NCCR architectures that differ from the archetypic OPQRS

arrangement are referred to as rearranged (rr) and have been found *in vitro* and *in vivo* (24, 30-

36). Importantly, NCCR block rearrangements confer remarkable differences in transforming

potential and host cell permissivity (24, 25, 28, 31, 37, 38). BKPyV carrying rr NCCRs are more

efficient replicators both *in vitro* (19, 25, 33, 39, 40) and *in vivo* compared to the archetype (37).

Gosert *et al.* determined that the emergence of rr NCCR BKPyV variants in the plasma samples

from immune suppressed kidney transplant recipients *in vivo* was correlated to increased

replication potential and pathogenesis (37). A connection between enhanced promoter efficiency

of rr NCCR variants and *in vivo* disease development is debated (29, 41). Of interest, this

rearrangement ability is conserved among the polyomaviruses. JC polyomavirus (JCPyV) is a

closely related member of the polyomavirus family and an opportunistic pathogen that also

affects HIV positive individuals (18). Similar to the JCPyV promoter, BKPyV promoter reformation may be the main driver of tropism and increased virulence (42).

The BKPyV NCCR architecture of a wide range of human samples has been analyzed, including bladder, brain, cerebrospinal fluid, eye, heart, kidney, lung, muscle, nasopharyngeal aspirates, ovarium, monocytes, placenta, prostate, ureter, urine and sewage (38). A recent study from our group analyzed the BKPyV NCCR architecture and replication potential of two clinical HIVSGD-derived BKPyV isolates (9). The study detected an OPQPQQS NCCR architecture among HIVSGD-derived BKPyV isolates and showed evidence of both HIVSGD-derived BKPyV oral tropism and adept viral replication in human salivary gland (HSG) cells. The present study screened an additional 17 HIVSGD TW samples for HIVSGD-derived BKPyV. To our knowledge, the present study is the first to characterize the NCCR of a comprehensive set of orally-derived BKPyV substrains.

BKPyV NCCR block arrangement and activity were analyzed, along with the underlying sequence variations in the context of transcription factor binding sites (TFBS). We found that the majority of HIVSGD TW BKPyV carried the distinct OPQPQQS NCCR architecture, found in the previous study, suggesting that the analyzed HIVSGD patient cohort sheds a common BKPyV substrain. Furthermore, we found that nucleotide polymorphism underlying the NCCR block homology influenced predicted TFBS. Finally, *in vitro* viral replication capacities and promoter activity of the clinical isolates were assessed.

Materials and Methods

Patient Information and Sample Collection

Patient-derived samples described in this study were retrieved retrospectively from studies conducted at UNC Chapel Hill enrolling North Carolina residents. HIV positive individuals from the UNC Chapel Hill Hospital Dental Clinics and Infectious Disease Clinic were screened for HIVSGD and chosen for throat-wash (TW) collection under IRB approved studies (informed consent HRSA IRB study #: 07-1431). HIV + patients were part of a yearlong longitudinal study, where participants were screened for HIVSGD-defining lesions and symptoms at baseline, at 6 months and at 12 months. A patient diagnosed with HIVSGD at any of the three time points during the 12 months study was considered HIVSGD positive (Table 1). Throatwash (TW) samples from 28 HIV + individuals were collected at baseline, and BKPyV viral loads (VLs) and NCCR architecture was determined. 19 of these individuals had HIV-associated Salivary Gland Disease (Table 1) and 9 were HIVSGD negative (Table 2). TW samples and clinical information pertaining to the patients HIV status was recorded at entry (1st time point) and for 5 HIVSGD patients at the end of the study (12 months, 2nd time point; not shown). Demographic information (age, gender and county of residency) and clinical information pertaining to the patients HIV status (HIV VLs and CD4 counts) were collected and are reflected in each table. Of the 8 transplant patient-derived samples, 5 were isolated from individuals diagnosed with BKPyV-associated nephropathy (BKVN). Each gathered sample corresponded to a single patient and time point of collection with the exception of samples T4-1 and T4-2, which belonged to the same transplant patient and were collected one year apart. 10 ml TW samples (saline solution washes) were collected, centrifuged and DNA was isolated via the QIAamp DNA Blood Mini Kit as described by manufacturer (Qiagen). Patient samples T1,

HIVSGD19 and HIVSGD21 were collected and analyzed in a previous study under the identifications U1, HIVSGD-1 and HIVSGD-2 respectively (9). The samples were renamed and included in this study in order to expand on previous results. Eight urine samples from UNC Chapel Hill Hospital kidney transplant patients were collected and kindly donated by Dr. V. Nickeleit. Urine samples were centrifuged and the DNA isolated via Qiagen DNeasy kit as done for the TW samples (Qiagen).

Whole Genome BKPyV Cloning and Transfection

BKPyV whole genomes were cloned from clinical samples via the naturally occurring BamH1 restriction site as described in (9). Whole genome clones HIVSGD19 and HIVSGD21 were available from the previous study. Human submandibular salivary gland epithelial cells (HSG cells) were transfected with re-ligated BKPyV episomes or NCCR constructs as described in (9). Supernatant from transfected cells was collected over 15 days, DNA isolated and BKPyV VLs determined.

BKPyV Viral Load Measurements

Encapsidated BKPyV genomes contained in clinical samples and supernatant of BKPyV transfected HSG cells were quantified via quantitative real-time PCR (qPCR) analysis: Roche Light Cycler 480 Syber Green I Master Mix in the Roche Light Cycler 480 (9). A BKPyV plasmid, kindly donated by Dr. V. Nickeleit, was used to establish a standard curve.

BKPyV NCCR Sequencing

Clinical and laboratory strain BKPyV NCCR was genotyped by PCR amplification with Vent polymerase and primers BKPyVTT1F and BKPyVTT1R (9, 31). PCR products were purified with the QIAquick PCR Purification Kit by Qiagen (according to manufacturer) and sequenced by Genewiz (www.genewiz.com). PCR amplification and sequencing was repeated a

minimum of three times per patient sample. Resulting NCCR nucleotide sequences were analyzed and aligned by the Vector NTI Advance program. Vector NTI identified the BKPyV NCCR block motifs with minimum similarity of 70% to original block sequences (20, 21). A Vector NTI Guide Tree, which resembles a phylogenetic tree, was built using the Neighbor Joining method (NJ) of Saitou and Nei (43). The Guide Tree Pane was built based on matrix distance values (in parenthesis following the molecule name displayed on the tree) which relate to the degree of divergence between sequences (44).

NCCR Promoter Activity

Reporter constructs were used to perform the dual luciferase (luc) assay as previously described (9). HIVSGD19 and HIVSGD21 NCCR luc clones used were available from the previous study, while all the others were cloned for this study. Briefly, HSG cells were transfected with NCCR-pGL3 constructs, pGL3 Basic and pGL3 Control. Each of these plasmids were co-transfected with RFP plasmid DNA, for transfection efficiency which was consistently detected at over 50%, and with pGL3 control (SV40 promoter), which demonstrated activity 4 times higher than the NCCR constructs. Resulting luciferase activity was normalized to pGL3 Basic activity and reported as relative luciferase units (RLU).

Transcription Factor Binding Site Analysis

Transcription factor binding sites (TFBS) were predicted via ALGGEN PROMO (http://alggen.lsi.upc.es/cgi-bin/promo_v3/promo/promoinit.cgi?dirDB=TF_8.3.) with a similarity margin of greater than or equal to 95%. PROMO predicts putative eukaryotic TFBS from the TRANSFAC® database, which is based on experimentally proven binding sites and consensus binding sequences (positional weight matrices). Eleven human TFBS, previously described in the context of the BKPyV NCCR (21, 31, 45-47), were selected along with non-

human T-Ag in order to analyze the NCCR O blocks of BKPyV HIVSGD and MM: AP-1 [T00029], CREB [T00163], NF-1 [T00539], C/EBPβ [T00581], C/EBPδ [T00583], NF-kB [T00590], NF-kB(-like) [T00591], NF-kB1 [T00593], p53 [T00671], Sp1 [T00759], T-Ag [T00788], p300 [T01427]. For the TFBS analysis of the entire NCCR, the similarity margin was greater than or equal to 85% and the following TFBS were included: AP-1 [T00029], C/EBPα [T00105], c-Fos [T00123], c-Jun [T00133], CREB [T00163], NF-1 [T00539], NF-AT1 [T00550], C/EBPβ [T00581], C/EBPδ [T00583], NF-kB [T00590], NF-kB(-like) [T00591], NF-kB1 [T00593], p53 [T00671], Sp1 [T00759], T-Ag [T00788], p300 [T01427), STAT1α [T01492], STAT3 [T01493], STAT1β [T01573], STAT4 [T01577], NF-AT2 [T01945], NF-AT4 [T01946], NF-AT1 [T01948], IRF-3 [T04673], IRF-7A [T04674], STAT5A [T04683], STAT5B [T04684], STAT1 [T04759], STAT1:STAT1 [T05692].

Statistical Analysis

The correlation between orally shed BKPyV VLs (from TW) and HIV VL, CD4 count and age was determined by calculating the correlation coefficient. The correlation between orally shed BKPyV VLs (TW) and HAART was determined by Wilcoxon rank sum test. The BKPyV VLs in HIVSGD TW, control TW, and urine were compared using the Kruskal-Wallis test with pairwise comparisons using Dunn's multiple comparison test. Samples were grouped by source (either HIVSGD TW or urine) and by NCCR architecture (OPQPQQS or any other architecture). Differences in viral load between the groups were assessed using two-way ANOVA. Samples were also grouped by TFBS and replication efficiency. Low efficiency replicators were defined as those with BKPyV VLs $< 10^4$ copies/mL, while high efficiency replicators had VL at or above this threshold. Differences between these groups were assessed by two-way ANOVA and a significant interaction was detected between replication efficiency and TFBS, with certain TFBS

being significant in Bonferroni posttests. Multiple BKPyV VLs thresholds were assessed. The

choice of thresholds had little effect on the outcome. For example, C/EBPβ was significant at all

thresholds tested: 10^2, 10^3, 10^4, 10^5, and 10^6. C/EBPα was also significant at the 10^4 and 10^5

thresholds and p300 at 10^5.

The NCCRs with 10 predicted TFBS all had the same combination of TFBS: the

consensus sites three C/EBPβ sites and one p300 site (CC3C). The viral loads of samples with 10

TFBS predicted in the NCCR were compared to viral loads of samples with any other

combination of predicted TFBS using the two-tailed Mann-Whitney U test. The significance

level for all analyses was set at p=0.05. All significance tests were performed in GraphPad Prism

5.01. Hierarchical clustering was performed on the number of each TFBS predicted in the full-

length HIVSGD TW NCCRs in R, using the hclust function with heatmap.2 in the gplots

package. The distance metric used was Euclidean distance.

Results

<u>BKPyV VLs among patient-derived samples</u>

HIV + patients were part of a yearlong longitudinal study, where participants were

screened for HIVSGD-defining lesions and symptoms at baseline, at 6 months and at 12 months.

Throatwash (TW) samples from 28 HIV + individuals were collected at baseline, BKPyV viral

loads (VLs) and NCCR architecture was determined and clinical information was collected.

Nineteen of the HIV + individuals had clinically diagnosed HIV-associated Salivary Gland

Disease (HIVSGD; Table 2.1.) and 9 were HIVSGD negative (Table 2.2.).

Sample	HIV Status	Clinical Status	Sample[a]	Age[b]	Gender[c]	NCCR[d]	BKPyV VL[e]	HAART[f]	HIV VL[e]	CD4[g]
HIVSGD1	HIV +	HIVSGD	TW	53	M	OPQPQQS	3.24E+1	Y	U	513
HIVSGD2	HIV +	HIVSGD	TW	50	M	OPQPQQS	2.48E+8	Y	90	505
HIVSGD3	HIV +	HIVSGD	TW	52	F	OPQPQQS	2.93E+0	Y	5100	18
HIVSGD4	HIV +	HIVSGD	TW	48	M	OPQPQQ	9.04E+1	N	10000	303
HIVSGD5	HIV +	HIVSGD	TW	29	F	OPQPQQS	2.44E+3	Y	283	644
HIVSGD6	HIV +	HIVSGD	TW	30	M	OPQPQQS	8.51E+7	Y	60	730
HIVSGD7	HIV +	HIVSGD	TW	34	M	OPQPQQS	9.30E+2	Y	52	230
HIVSGD9	HIV +	HIVSGD	TW	47	M	OPQPQQS	1.36E+4	Y	U	336
HIVSGD10	HIV +	HIVSGD	TW	42	M	OPQPQQS	7.10E+6	Y	5891	478
HIVSGD11	HIV +	HIVSGD	TW	48	M	OPQPQQS	3.64E+3	Y	16000	490
HIVSGD12	HIV +	HIVSGD	TW	54	M	OPQPQQS	3.85E+0	Y	U	1033
HIVSGD13	HIV +	HIVSGD	TW	38	M	OPQPQQS	5.80E+4	Y	U	550
HIVSGD14	HIV +	HIVSGD	TW	DA	M	OPQPQQS	DA	Y	2280	387
HIVSGD15	HIV +	HIVSGD	TW	47	M	OPQPQQS	2.87E+6	Y	10785	455
HIVSGD16	HIV +	HIVSGD	TW	45	M	OPQPQQS	DA	Y	U	118
HIVSGD17	HIV +	HIVSGD	TW	DA	M	OPQPQQS	DA	Y	66455	48
HIVSGD18	HIV +	HIVSGD	TW	DA	DA	OPQPQQS	2.00E+5	N	DA	DA
HIVSGD19	HIV +	HIVSGD	TW	47	M	OPQPQQS	1.76E+5	Y	1001	628
HIVSGD21	HIV +	HIVSGD	TW	60	M	OPQPQQS	2.57E+5	Y	1544	366

Table 2.1. **HIVSGD patient-derived BKPyV NCCR block arrangement and viral load variation, demographics and HIV-specific clinical information at baseline.** This table summarizes clinical and BKPyV-specific information collected from 19 patients diagnosed with HIVSGD at baseline (study entry). DNA from all throatwash (TW) samples was isolated, BKPyV viral loads (VLs) determined and the BKPyV NCCR sequenced and analyzed as described in materials and methods. [a]Throatwash. [b]Patient age at time point of sample collection (yrs). [c]Male/Female. [d]Non-coding control region. [e]Viral load (copies/ml). [f]Highly Active Antiretroviral Therapy, yes/no. [g]CD4 T cell counts (cells/mm^3). U; undetectable. DA; data not available.

Patient ID	HIV Status	Clinical Status	Sample	Age[a]	Gender[b]	NCCR[c]	BKPyV VL[d]	HAART[e]	HIV VL[d]	CD4[f]
C1	HIV +	HIVSGD negative	TW[g]	54	M	OPPQRS	U	Y	91713	540
C2	HIV +	HIVSGD negative	TW[g]	52	M	OPPQRS	U	Y	132	653
T1	HIV --	BKVN, lung transplant	Urine	31	M	OPQ	1.79E+09			
T2	HIV --	BKVN, kidney transplant	Urine	49	M	OPQRS	3.75E+08			
T3	HIV --	BKVN, kidney transplant	Urine	17	M	OPQRS	3.93E+09			
T4-1	HIV --	Kidney transplant	Urine 1	19	M	PQRS	1.22E+07			
T4-2	HIV --	Kidney transplant	Urine 2	20	M	OPQPQQS	9.10E+08			
T5	HIV --	BKVN, kidney transplant	Urine	49	M	OPQRS	2.07E+09			
T6	HIV --	Kidney transplant	Urine	13	M	OPQPQQS	1.68E+08			
T7	HIV --	BKVN, kidney transplant	Urine	37	M	OPQRS	1.91E+07			

Table 2.2. **Non-HIVSGD patient-derived BKPyV NCCR block arrangement and viral load variation, demographics and clinical information at baseline.** This table summarizes clinical and BKPyV-specific information collected from 2 HIV + patients without HIVSGD (C) at baseline (study entry) and 7 HIV negative renal transplant patients (T). Samples from HIV + patients without HIVSGD that did not yield BKPyV were not listed in this table. DNA from all clinical samples was isolated, BKPyV viral loads (VLs) determined and the BKPyV NCCR sequenced and analyzed as described in materials and methods. [a]Patient age at time point of sample collection (yrs). [b]Male/Female. [c]Non-coding control region. [d]Viral load (copies/ml). [e]Highly Active Antiretroviral Therapy, yes/no. [f]CD4 counts (cells/mm^3). [g]Throatwash. U; undetectable.

Demographic information and data pertaining to the HIV status of the patient were collected from the HIVSGD patient cohort at study entry. The average HIV VLs and CD4 counts were $9x10^3$ copies/ml (range: undetectable – $6x10^4$ copies/ml) and $4x10^2$ cells/mm^3 (range: 18-$1x10^3$) respectively. At study entry (baseline) the HIVSGD patients were mostly male (16 males, 2 females, 1 undetermined), were on average 45 years old (range: 29-60 years) and the majority were on HAART (17 on HAART, 2 not on HAART).

BKPyV VLs in TW samples from HIV + patients without HIVSGD (negative controls) and urine samples from HIV naive transplant patients (positive controls) were assessed (Table 2.2.). Based on previous findings, HIV + patients without HIVSGD were expected to shed little or no BKPyV via TW (7, 8). Transplant patients, diagnosed with BKPyV-associated nephropathy (BKVN), are known to shed high BKPyV VLs in the urine, ranging from 10^4 to 10^{10} BKPyV copies/ml (28, 48, 49). Baseline HIVSGD TW BKPyV VLs ranged from 2.9 to $2.4x10^8$ copies/ml, with a mean of $2x10^7$ copies/ml. This analysis excluded samples HIVSGD14, HIVSGD16 and HIVSGD17 from which the available DNA volume was limited and BKPyV VL determination was not possible (DA, Table 2.1.). The BKPyV VLs in HIVSGD negative TW samples (n=9) were consistently below the linear range of qPCR detection. BKPyV VLs among transplant patient urine samples ranged from $1x10^7$ to $3x10^9$ copies/ml (Fig. 2.1.). There was a significant difference between BKPyV VLs of transplant patient urine samples (n=8) compared to HIVSGD negative TW samples (n=9) (p<0.001). More importantly, HIVSGD TW VL (n=16) and HIVSGD negative TW VL (n=9) were significantly different at baseline (p<0.01), highlighting the striking differences in oral BKPyV VLs detected among HIV + patients with and without HIVSGD. A potential association between orally shed BKPyV levels and factors reflecting the patients HIV status were assessed, including HIV VLs, CD4 counts and HAART

treatment. None of these factors had a statistically significant correlation with oral BKPyV VLs

(correlation value ≥ 0.2). Furthermore, no correlation between orally shed BKPyV levels and

geographical residential location (by counties) was found. The HIV patient cohort resides in

North Carolina (NC) counties spanning a 300 mile radius. Since the majority of patients were

male (26/28), the association between orally shed BKPyV VLs and gender was not tested.
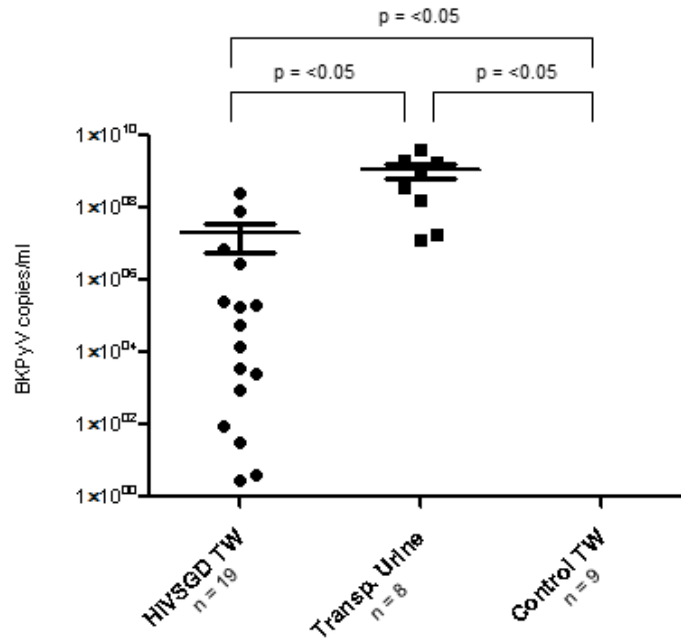
Fig. 2.1. **BKPyV VL comparison between patient cohorts.** This graph visualizes HIVSGD

TW, control TW and transplant urine sample BKPyV VLs measured via qPCR at baseline. The

"Control TW" cohort represents the negative control and is formed by HIV + patients without

HIVGSD. HIVSGD TW VLs were significantly higher than control TW VLs. Transplant urine

VLs were significantly higher than HIVSGD and control TW VLs. P values were assessed via

non-parametric one way ANOVA (Kruskal Wallis) test. Depicted are each data point with the

mean and the standard errors of the mean (SEM).

In order to monitor BKPyV longitudinally, DNA was isolated from 5 HIVSGD patient-derived TW samples at a second time point (1 year). Despite the relatively high BKPyV VLs among HIVSGD TW samples at baseline, none of the TW samples collected past baseline had BKPyV VLs above the detection level (not shown). Further, no BKPyV NCCR sequences could be PCR amplified from the samples past baseline. Hence, they were considered BKPyV negative.

BKPyV detection and NCCR block alignment analysis of patient-derived samples

All DNA samples were subject to BKPyV NCCR amplification. Samples yielding consistent NCCR products via PCR, were subsequently sequenced off-site and were considered BKPyV positive. PCR amplification likely detects the most prevalent NCCR species. Hence, there may be additional BKPyV subspecies undetected by PCR that may be identified by cloning. All 19 HIVSGD samples (100%), all 8 transplant urine samples (100%) and 2 HIV positive HIVSGD negative control samples (22%) were BKPyV NCCR positive (Table 2.3.). Resulting NCCR sequences were analyzed for block architecture using Vector NTI. The BKPyV NCCR architecture is traditionally based on the following system:

TTTGCAAAAATTGCAAAGAATAGGGATTTCCCCAAATAGTTTTGCTAGGCC
TCAGAAAAAGCCTCCACACCCTTACTACTTGAGAGAAAGGGTGGAGGCAGAGGCGG
CCTCGGCCTCTTATATATTATAAAAAAAAAGGC - O block sequence,
CACAGGGAGGAGCTGCTTACCCATGGAATGCAGCCAAACCATGACCTCAGGAAGGA
AAGTGCATGACTG – P block sequence,
GGCAGCCAGCCAGTGGCAGTTAATAGTGAAACCCCGCC – Q block sequence,
GGCAGCCAGCCAGTGGCAGTTAATAGTGAAACCCCGCCA – R block sequence and

GACAGACATGTTTTGCGAGCCTAGGAATCTTGGCCTTGTCCCCAGTTAAACTGGACA

AAGGCC – S block sequence (20, 21). Greater than or equal to 70% sequence similarity to these

block sequences was required for NCCR block identification using Vector NTI. The NCCR

architecture of three previously described BKPyV laboratory strain sequences (MM, Dunlop and

VR837) was confirmed as a control measure (9). Archetypic OPQRS NCCRs were detected in 4

out of 8 transplant urine-derived samples. Rearranged NCCR block sequences, that differed from

the archetypic NCCR architecture, were detected in 25/29 (86%) of the clinical samples. A

common rr NCCR OPQPQQS alignment was recovered from 18/19 HIVSGD TW samples

(94.7%, Table 2.1.). The only HIVSGD sample (HIVSGD4) that did not carry this common

alignment had an OPQPQQ NCCR alignment, which differed from the signature alignment only

in that it lacked the final S block. HIVSGD negative oral samples did not carry the signature

alignment; the block alignment OPPQRS was detected in two HIV + HIVSGD negative-derived

TW control sequences (C1, C2). Three distinct block alignments were detected in transplant

urine samples including: OPQRS (T2, T3, T5, T7), OPQPQQS (T4-2, T6), OPQ (T1) and PQRS

(T4-1) (Table 2.3.). Compared to the transplant urine-derived NCCR architectures, the HIVSGD

NCCR OPQPQQS architectures were highly homologous (Table 2.2.). This rr NCCR OPQPQQS

alignment was also detected in 2 transplant urine samples (T4-2 and T6) and 1 laboratory strain

MM BKPyV. The Fisher's Exact Test was used to determine whether HIVSGD-derived BKPyV

was more likely to contain the OPQPQQS architecture than HIV + HIVSGD negative-derived or

transplant patient-derived BKPyV. Indeed, HIVSGD patient-derived substrains were 72 times

more likely to have the OPQPQQS block arrangement than the other substrains (OR:72, 95% CI:

5.67-914.3).

Source	OPQPQQS	OPPQRS	OPQPQQ	OPQPQS	OPQRS[a]	OPQ	PQRS	OPPPS	BKPyV +/Total[b]
HIV+ SGD+ (TW)	**18**		1						19/19
HIV+ HIVSGD- (TW)		2							2/9
HIV- Transplant (Urine)	2				4	1	1		8/8
Lab. strain[c]	1 (MM)			1 (VR837)				1 (Dunlop)	3/3

Table 2.3**. NCCR architectures among clinical samples at baseline.** This table depicts all BKPyV NCCR block architectures found among the analyzed clinical samples. The NCCR of 94.7% HIVSGD throatwash (TW)-derived BKPyV resulted in a matching NCCR block sequence (bold, signature alignment). Patients diagnosed with HIVSGD at any time point over the one year study are considered HIVSGD positive. [a]Archteype BKPyV NCCR. [b]BKPyV positive samples over total number of samples. [c]Laboratory strain BKPyV.

HIVSGD BKPyV NCCR nucleotide polymorphisms

To further analyze the clinical BKPyV promoters, the degree of divergence among the underlying nucleotide NCCR sequences was determined. Distance values (displayed in parenthesis) between clinical NCCR nucleotide sequences were calculated using the neighbor joining algorithm and visualized by a Guide Tree (Fig. 2.2A). Cluster I contained NCCR sequences from HIVSGD negative transplant patient urine (T) and HIV + HIVSGD negative TW (C) samples. Cluster II contained NCCR sequences from following HIVSGD patients: 3, 4, 5, 7, 9, 10, 11, 12 and 13. Cluster III contained a second group of NCCRs from HIVSGD patients: 2, 6, 14, 15, 16, 17, 18, 19 and 21. The following HIVSGD NCCR sequences within Cluster III

were identical: 6, 14, 15, 16, 17 and 18. Interestingly, HIVSGD1 did not aggregate within the three clusters. The three clusters visually emphasize the differences between HIVSGD-derived NCCR sequences as compared to the control groups. Importantly, the clusters highlight the significant sequence similarity detected among HIVSGD-derived NCCR structures as compared to the other clinical isolates. Most interestingly, despite the block homology, underlying nucleotide polymorphisms were detected among the OPQPQQS HIVSGD NCCRs. NCCR nucleotide sequence alignment analysis (including all HIVSGD NCCRs and laboratory BKPyV strain MM NCCR) revealed identical P and Q blocks (not shown). Most sequence variation was detected within the O block (Fig. 2.2B) and minor polymorphisms were detected in the S block (Fig. 2.2C). The first 50 bp of the O block contained the majority of differences with only 4 conserved regions: O_{16} (1), O_{27} (2), O_{33-34} (3) and O_{45} (4) (Fig. 2.2B). Only HIVSGD2 and HIVSGD4 displayed additional nucleotide differences outside of this 50 bp region; HIVSGD2: cytidine insertion (C) at O_{89} and adenosine (A) insertion at O_{94} and HIVSGD4: A-guanosine (G) transition at O_{61}. Within the NCCR S block, the following polymorphisms were detected: G-A transitions at S_{441} for HIVSGD7 and HIVSGD10 and a thymidine (T)-C mutation at S_{451} for HIVSGD2 (Fig. 2.2C).
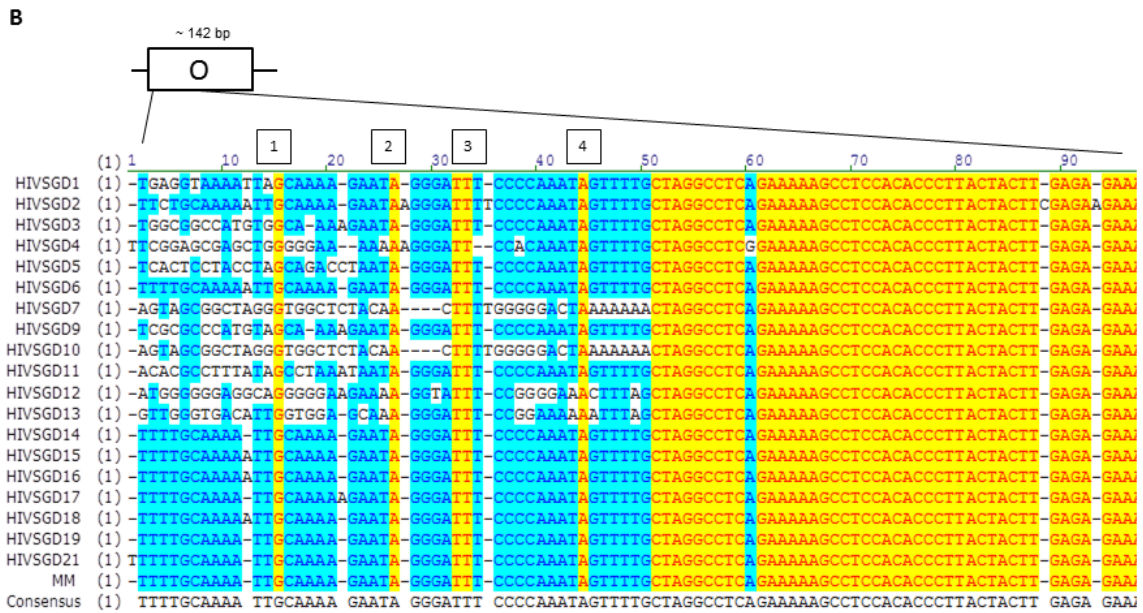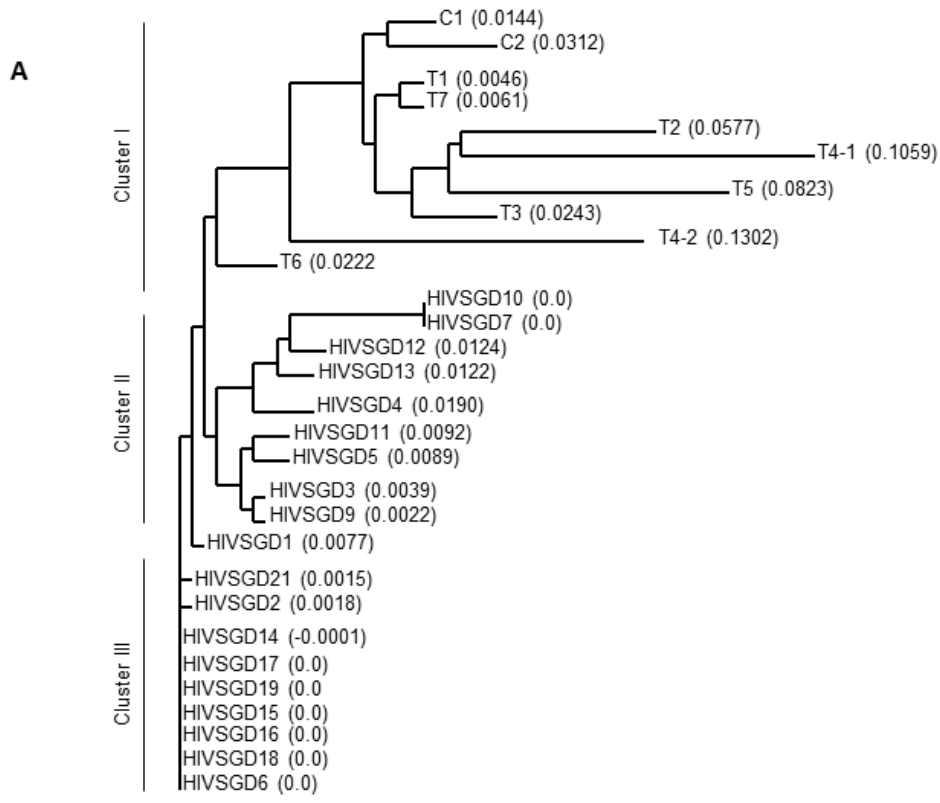
C
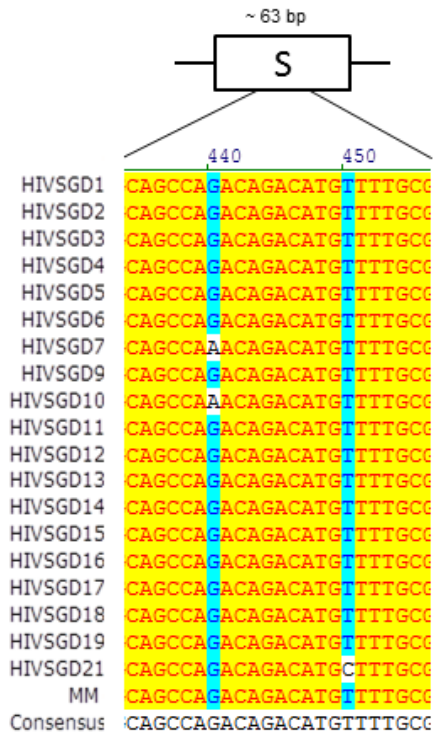
Fig. 2.2. **Nucleotide polymorphism underlying the OPQPQQS NCCR block**

homology. A. This graph depicts the Guide Tree built based on NCCR sequences retrieved from

clinical samples. NCCR nucleotide sequences were aligned by Vector NTI. Distance values (in

parenthesis) designated relative degrees of divergence among the sequences. The Guide Tree

NCCR analysis aggregated clinical BKPyV in 3 clusters (excluding HIVSGD1). Cluster I

contained the NCCRs of HIVSGD negative urine- and TW-derived BKPyV strains. Clusters II

and III contained exclusively HIVSGD BKPyV NCCR sequences. **B./C.** NCCR nucleotide

sequence alignment of HIVSGD patient-derived BKPyV bearing the OPQPQQS signature

alignment along with MM exposed underlying nucleotide sequence that were present despite

NCCR block homology. The O (B.) and S block (C.) carried the majority of the sequence

variety, while the P and Q blocks were sequence identical (not shown).

Full-length NCCR TFBS

To determine whether the detected polymorphisms potentially influenced viral transcription, TFBS were predicted for all 19 HIVSGD BKPyV NCCRs, laboratory strains MM, Dunlop, VR837 and transplant urine-derived T1. The ALGGEN PROMO prediction analysis included two previously characterized NCCRs (HIVSGD19 and HIVGSD21) (9). Table 2.4. describes the predicted TFBS types (first column) for each BKPyV NCCR substrain (top row). TFBS abbreviations are listed on the legend (Table 2.4., left). To determine whether the presence or combination of specific TFBS was correlated with increased *in vivo* replication efficiency a multiple linear regression analysis was performed (not shown). None of the predicted TFBS coefficients and (increased or decreased) *in vivo* BKPyV VL associations were statistically significant. Next, *in vivo* BKPyV VLs and TFBS were grouped via hierarchical clustering to determine whether specific TFBS groups may cluster with increased or decreased VLs (not shown). The analysis yielded clusters that grouped members of the same signaling pathway but did not identify significant associations with increased or decreased VLs despite a detected trend between NCCR TFBS CCAAT/enhancer binding factor (C/EBP)β and higher BKPyV replication efficiency. Grouped were different members of the C/EBP family, as were different members of the NF-AT family and members of the STAT family.

Abrᵃ	TFBS
A	AP-1
C1	C/EBPα
cF	c-Fos
cJ	c-Jun
NF1	NF-1
NA1	NF-AT1
C	C/EBPβ
N	NFkB
Nk	NFkB(-like)
Nk1	NF-kB1
p53	p53
Sp1	Sp1
T	Tag
3	p300
S3	STAT3
S1	STAT1β
S4	STAT4
NT2	NF-AT2
NT4	NF-AT4
NT1	NF-AT1b
I3	IRF-3
S5	STAT5A

TFBS	HIVSGD																			Lab. Strain			BKN
	1	2	3	4	5	6	7	9	10	11	12	13	14	15	16	17	18	19	21	MM	Dun	VR	T1
A	3	3	3	3	3	3	3	3	3	7	3	3	3	3	3	3	3	3	3	3	2	2	1
C1	3	4	3	2	2	4	1	3	1	2	1	2	4	4	4	4	4	3	4	3	4	4	4
cF	6	6	5	6	6	6	5	6	5	6	6	7	6	6	6	6	6	6	6	6	6	4	2
cJ	6	6	6	6	6	6	6	6	6	6	6	7	6	6	6	6	6	6	6	6	6	4	2
NF1	4	4	4	4	4	4	5	4	5	0	4	4	4	4	4	4	4	4	4	4	4	3	2
NA1	5	5	5	6	5	5	4	5	4	5	6	6	5	5	5	5	5	5	5	5	4	4	4
C	3	5	3	2	2	6	1	3	1	2	1	2	6	6	6	6	6	4	6	4	6	6	6
N	4	4	4	4	4	4	3	4	3	4	4	4	4	4	4	4	4	4	4	4	4	3	2
Nk	0	1	0	0	0	0	0	0	0	0	0	0	0	0	0	0	0	0	0	0	0	0	0
Nk1	0	1	1	0	1	1	0	1	0	1	0	0	1	1	1	1	1	1	1	1	1	1	1
p53	4	4	4	4	4	4	4	5	4	4	4	4	4	4	4	4	4	4	4	4	0	3	2
Sp1	2	2	2	2	2	2	2	2	2	2	2	2	2	2	2	2	2	2	2	2	1	2	2
T	6	6	6	6	6	6	6	6	6	6	7	6	6	6	6	6	6	6	6	6	6	6	6
3	18	18	18	21	19	18	17	18	17	18	20	20	18	18	18	18	18	18	18	18	20	16	16
S3	0	0	0	0	0	0	0	0	0	0	1	2	0	0	0	0	0	0	0	0	0	0	0
S1	5	5	5	6	5	5	4	5	4	5	6	6	5	5	5	5	5	5	5	5	4	4	4
S4	11	11	11	13	11	11	10	11	10	11	13	12	11	11	11	11	11	11	11	11	11	9	8
NT2	5	5	5	6	5	5	4	5	4	5	6	6	5	5	5	5	5	5	5	5	4	4	4
NT4	0	1	0	1	0	0	0	0	0	0	0	1	0	0	0	0	0	0	0	0	0	0	0
NT1	5	5	5	6	5	5	4	5	4	5	6	6	5	5	5	5	5	5	5	5	4	4	4
I3	5	5	5	6	5	5	4	5	4	5	6	6	5	5	5	5	5	5	5	5	4	4	4
S5	11	11	11	13	11	11	10	11	10	11	13	12	11	11	11	11	11	11	11	11	11	9	8
Total	106	112	106	117	106	111	93	108	93	105	115	118	111	111	111	111	111	108	111	108	102	92	82

Table 2.4. **Predicted TFBS for full-length NCCR via ALGGEN PROMO.** Visualized are the types of predicted TFBS (first column) for each BKPyV NCCR substrain (top row). The top row lists the name of analyzed full-length NCCR sequences, which included 19 HIVSGD BKPyV, 3 laboratory strains and 1 urine-derived strain isolated from a patient diagnosed with BKPyV-associated nephropathy (BKVN). TFBS included for the PROMO TFBS prediction program are listed in the materials and methods section. TFBS abbreviations are listed on the legend (left). ᵃTFBS Abbreviation.

To further analyze the potential association between the frequency of certain predicted TFBS or TFBS combinations and high or low BKPyV *in vivo* shedders, HIVSGD TW samples were categorized as high or low replicators based on an oral VL threshold of 10^4 BKPyV copies/ml (Fig. 2.3.). TFBS predicted for each full-length HIVSGD BKPyV NCCR within these groups were compared by two way ANOVA. C/EBPα and C/EBPβ, were significantly different and more abundant within the higher replicators ($p<0.05$, $p<0.001$). Interestingly, the threshold choice of 10^4 BKPyV copies/ml had little effect on the outcome, as C/EBPβ was associated with significantly higher VLs at all tested thresholds (10^2, 10^3, 10^4, 10^5, and 10^6 copies/ml). C/EBPα was significant at both the 10^4 and 10^5 copies/ml thresholds and p300 at the 10^5 copies/ml threshold ($p<0.05$). Interestingly, a potential association between NCCR TFBS C/EBPβ and higher BKPyV replication efficiency was also observed in the hierarchical clustering analysis of TFBS predicted for the full-length BKPyV NCCR despite it not being statistically significant (mentioned earlier, not shown).
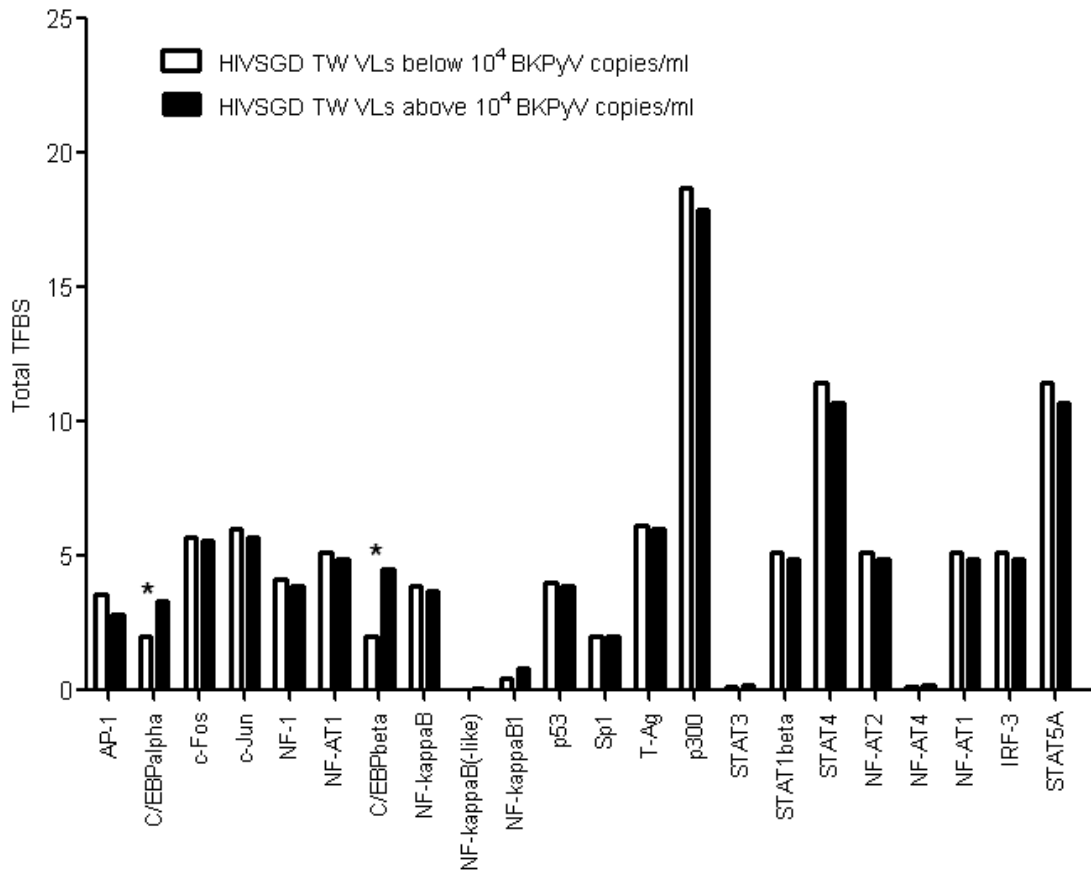
Fig. 2.3. **TFBS divergence based on BKPyV VL threshold.** This graph depicts varying numbers of TFBS per threshold group. HIVSGD TW samples were grouped according to a threshold of 10^4 BKPyV copies/ml, and respective TFBS predicted for full-length HIVSGD BKPyV NCCRs were compared via a two way ANOVA. The analysis allowed determining whether the frequency of a certain predicted TFBS may be significantly different among higher or lower BKPyV replicators. C/EBPα and C/EBPβ (see *) were significantly different and more abundant within the higher replicators. The threshold choice had little effect on the outcome as C/EBPβ was significant at all thresholds tested: 10^2, 10^3, 10^4, 10^5, and 10^6 copies/ml. C/EBPα was significant at the 10^4 and 10^5 copies/ml thresholds and p300 at 10^5 copies/ml.

O Block NCCR TFBS

The NCCR O block is critical to the viral life cycle since contains the start codon for the early BKPyV gene expression, a palindrome of two inverted repeat sequences, a 20-bp A/T region (45). Given the considerable sequence variation detected within this block (Fig. 2.2B) TFBS predicted exclusively for the O block were analyzed. TFBS C/EBPβ (C), Tag (T), p300 (3) and NF-kB (N) were predicted within the HIVSGD BKPyV NCCRs and were assigned to nucleotide stretches (Table 2.5.). Interestingly, all of the included HIVSGD BKPyV NCCR O blocks carried six common TFBS; resulting in six consensus binding sites: four Tag and two p300 binding sites (not shown). Based on total number of TFBS, five NCCR O block groups were formed containing 7, 8, 9, 10 or 11 total TFBS. The group with a total number of 10 TFBS carried a TFBS combination of "CC3C" unique to this group and contained the highest number of C/EBPβ and p300 TFBS (group 11 was excluded for statistical analysis because it only contained a single NCCR).

Abbreviation	TFBS
C	C/EBPβ
T	T-Ag
3	p300
N	NF-kB

Nucleotide	10	20	30	40	50	Total # of TFBS
HIVSGD 7				3		7
HIVSGD 10				3		7
HIVSGD 12	3					7
HIVSGD 11			3		C	8
HIVSGD 1		C	3		C	9
HIVSGD 3		C	3		C	9
HIVSGD 4	3		3		C	9
HIVSGD 5	3		3		C	9
HIVSGD 9		C	3		C	9
HIVSGD 13		3/C	3			9
HIVSGD 6	C	C	3		C	10
HIVSGD 14	C	C	3		C	10
HIVSGD 15	C	C	3		C	10
HIVSGD 16	C	C	3		C	10
HIVSGD 17	C	C	3		C	10
HIVSGD 18	C	C	3		C	10
HIVSGD 19	C	C	3		C	10
HIVSGD 21	C	C	3		C	10
HIVSGD 2	C	C	N/3		C	11

Table 2.5. **Predicted TFBS for the NCCR O block.** A. TFBS AP-1, CREB, NF-1, C/EBPβ, C/EBPδ, NF-kB, NF-kB1, p53, Sp1, Tag and p300 were included for the O block ALGGEN PROMO analysis (see materials and methods). TFBS C/EBPβ, Tag, p300 and NF-kB were predicted. Each substrain contained two p300 and four Tag predicted TFBS, which were termed consensus sites (not shown). Shown are the TFBS predicted in addition to the consensus sites and the total number of TFBS for each substrain (last row/grey). Based on total number of TFBS 5 groups of NCCR O blocks were formed (7, 8, 9, 10 and 11 total TFBS).

Comparing *in vivo* VLs from HIVSGD BKPyV NCCRs carrying highest predicted number of C/EBPβ and p300 in the O block ("CC3C" group) to all others ("Other" group) yielded a statistically significant difference ($p = 0.0414$, Fig. 2.4A). TFBS group medians and

respective VL plots detected a positive trend. Increased VLs were associated with an increased number of predicted C/EBPβ or p300 (Fig. 2.4B). These results suggest that the presence of the TFBS combination C/EBP-p300 within the HIVSGD BKPyV NCCR may enhance BKPyV *in vivo* replication efficiencies.

A

B
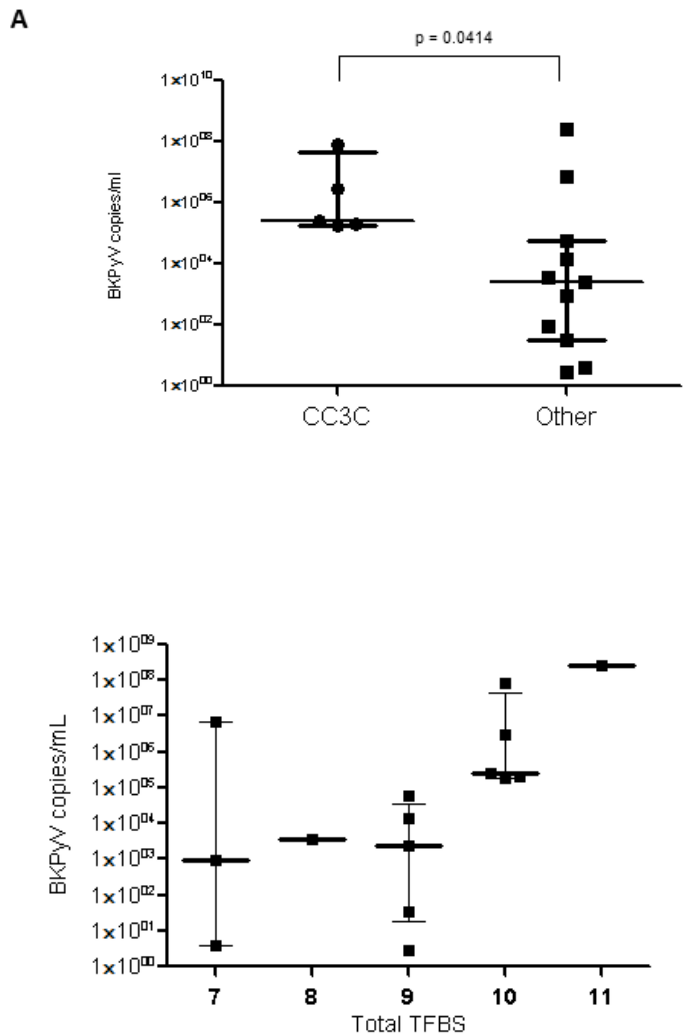
Fig. 2.4. **O block TFBS analysis.** A. The graph shown compares clinical BKPyV VL (y-axis) based on predicted TFBS (x-axis). Two groups were formed. The "CC3C" group included clinical BKPyV predicted to have TFBS combination C/EBPβ, C/EBPβ, p300, C/EBPβ within

the O block (10 total TFBS). The "Other" group designated BKPyV O blocks differing from that TFBS combination. Depicted are the median and the interquartile range of each group. A statistically significant difference (p = 0.0414) between VLs from the CC3C (10 TFBS group) group and "other" was determined via a Mann-Whitney U test. The "CC3C" group contained higher VLs than "others" not containing that specific combination of TFBS, potentially suggesting that the presence of this combination or frequency of TFBS may be endowing higher *in vivo* replication efficiencies. **B.** Since increased total number of TFBS correlated with increased C/EBPβ TFBS, NCCR O block groups with equal number of total TFBS were correlated to VL (BKPyV copies/ml). Plotting the median of each total TFBS group and respective VLs resulted in a positive trend, associating increasing sample VL with increasing number of predicted C/EBPβ TFBS (see Table 6 for detailed listing of TFBS). Black squares represent single data point, the thick black bars represent the median of measured BKPyV VLs and the thin black error bars represent interquartile range.

NCCR promoter activity and *in vitro* replication efficiency

HIVSGD BKPyV NCCR promoter activity and *in vitro* replication efficiency were assessed in human salivary gland cells, mimicking the *in vivo* oral compartment. The BKPyV NCCR promoter of HIVSGD substrains (HIVSGD1, HIVSGD2, HIVSGD3, HIVSGD11), MM and Dunlop were cloned into luciferase (luc) reporter constructs, to test promoter induction in human salivary gland (HSG) cells. Cloned reporter constructs were transfected and promoter activity measured via a luciferase assay 48hrs post-transfection. Relative light unit (RLU) measurements, normalized to pBasic, allowed the comparison and ranking of promoter activities. Ranked from highest to lowest were HIVSGD11, HIVSGD3, HIVSGD2, HIVSGD19, HIVSGD1, MM, HIVSGD21, and Dunlop (Fig. 2.5A). All but one HIVSGD promoter (83%)

was more readily induced than laboratory strains, suggesting basal promoter activity of HIVSGD

NCCR BKPyV was stronger than laboratory strains MM and Dunlop in HSG cells. Higher

promoter activity may be associated with the signature NCCR block sequence OPQPQQS as the

lowest activity was recorded by Dunlop which carries an OPPPS NCCR architecture. All the

cloned NCCRs had the same number of predicted p300 TFBS (18). Hence, we were unable to

confirm p300 as driver for differences in promoter activity. Increased predicted C/EBP binding

sites did not correlate with augmented promoter activity *in vitro* either. HIVSGD21, the least

active HIVSGD promoter, had the highest number of predicted C/EBPβ sites (6) compared to the

other HIVSGD clones. HIVSGD11, containing the least C/EBPβ (2) compared to the other

HIVSGD clones, exhibited the most active promoter (Table 2.5., Fig. 2.5A). However,

HIVSGD11 BKPyV NCCR had the most AP-1 (A) and the least NF-1 (NF1) TFBS compared to

predicted sites from clones HIVSGD and laboratory strains MM and Dunlop. Overall, a

predicted increase in NCCR C/EBP and p300 TFBS among more readily induced BKPyV

promoters was not confirmed *in vitro*, but it was determined that all but one HIVSGD promoter

(83%) was more readily induced than laboratory strains in HSG cells.

 In vitro replication efficiency was assessed by the transfection of HIVSGD BKPyV

whole genomes. Whole genome BKPyVs were cloned for the following substrains: HIVSGD2,

HIVSGD15, HIVSGD17, HIVSGD18, MM, VR837, Dunlop and transplant urine-derived T1.

Cloned genomes were excised from their backbones, religated and transfected into HSG cells.

Media from these cells was collected daily for 15 days and BKPyV VLs (copies/ml) quantified

to monitor viral replication efficiency (Fig. 2.5B). All HIVSGD BKPyV substrains replicated

well within HSG cells, consistently yielding BKPyV VLs above 10^4 copies/ml and up to 10^8

copies/ml. HIVSGD15 and Dunlop BKPyV were the least efficient replicators and yielded VLs

ranging from 10^2 to the 10^5 copies/ml over the 15-day time span. Based on average VLs over 15 days the *in vitro* replication efficiencies ranked from highest to lowest: HIVSGD19, HIVSGD18, MM, T1, VR837, HIVSGD17, HIVSGD21, HIVSGD15 and Dunlop (Fig. 2.5B). All but one cloned HIVSGD substrain (HIVSGD15) replicated more efficiently than laboratory strain Dunlop in HSG cells. Predicted C/EBP and p300 sites within the full-length HIVSGD BKPyV NCCR did not correlate with increased *in vitro* replication efficiency of whole genome HIVSGD BKPyV in HSG cells. Dunlop, for example, consistently carried lowest VLs and yet had the highest number of predicted C/EBPβ (6) and p300 (20) sites compared to other NCCRs. HIVSGD19, containing fewer C/EBPβ (4) and the same number of p300 (18) sites as compared to other whole genome HIVSGD BKPyVs clones, yielded the highest VLs (Table 2.5, Fig. 2.5B). While the relationship between viral replication and the predicted increase in NCCR C/EBP and p300 TFBS was not confirmed *in vitro*, it was determined that all HIVSGD strains replicate readily in HSG cells. The HIVSGD NCCR architecture may lend to this replication ability. High VLs were recorded for the laboratory strain MM, which like HIVSGD BKPyV contains the OPQPQQS architecture. Urine-derived T1 (OPQ) and laboratory strain VR837 (OPQPQS) however replicated efficiently as well, despite not carrying the HIVSGD architecture OPQPQQS. The laboratory strain Dunlop (OPPS), that lacked any Q blocks and did not carry the OPQPQQS architecture, was the least efficient *in vitro* replicator and had the weakest promoter (Fig. 2.5).
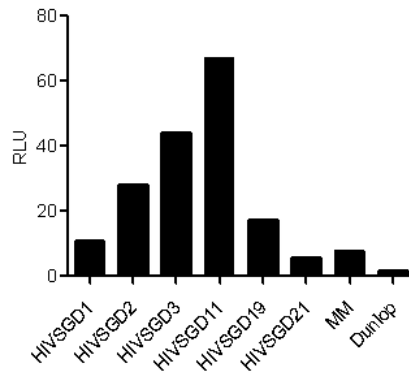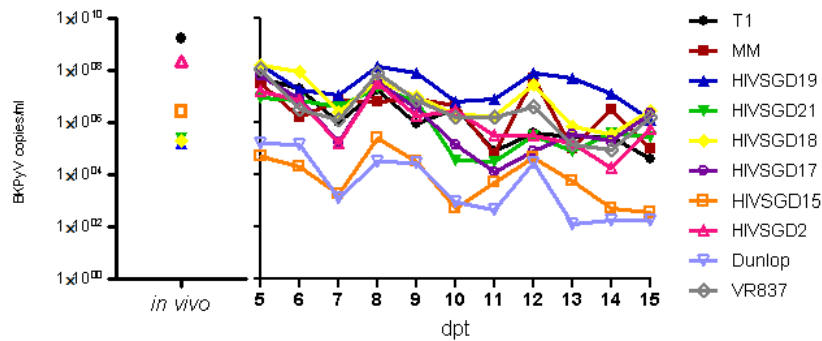
Fig. 2.5. *In vitro* **BKPyV promoter activity and replication efficiency**. **A.** The schematic is a representative result of BKPyV promoter activity within human salivary gland (HSG) cells. BKPyV promoter activity of 6 HIVSGD-derived and three laboratory strain-derived reporter constructs (in the early direction) were recorded via a luciferase (luc) assay 48 hours post-transfection. All but one HIVSGD strain (HIVSGD21) were more readily induced than laboratory strains MM and Dunlop. **B.** The schematic is a representative result of BKPyV VLs quantified over 15 days after transfection of human salivary gland (HSG) cells with cloned HIVSGD and laboratory strain BKPyV. All HIVSGD isolates replicated readily in HSG cells and all but one (HIVSGD15) replicated more efficiently than laboratory strain Dunlop. *In vitro*

65

replication efficiencies of HIVSGD BKPyV were determined post-whole genome BKPyV transfection and graphed along with *in vivo* BKPyV VLs.

Discussion

HIV-associated Salivary Gland Disease (HIVSGD), a commonly diagnosed salivary gland-associated complication in HIV + individuals, has been linked to the BK polyomavirus (BKPyV) (7, 8). The BKPyV non-coding control region (NCCR) is the main determinant of viral replication *in vitro* (19) and archetypic BKPyV NCCR rearrangements occur readily *in vitro* and *in vivo* (11, 29, 30, 35-37, 41). The shift from archetype to rr NCCR has been linked to overall functional differences in BKPyV viral fitness, including higher replication capacity, higher plasma viral loads and increased cell damage (24, 25, 31, 37, 38). Determining whether HIVSGD BKPyV promoter rearrangements endow higher replication levels and increased virulence may facilitate elucidation of BKPyV pathogenesis and potentially allow for NCCR architectures to serve as biomarkers or treatment targets. A previous study detected a conserved OPQPQQS NCCR architecture in two HIVSGD-derived BKPyV isolates and showed evidence of oral tropism and adept viral replication in human salivary gland (HSG) cells (9). The present study screened additional 17 clinical HIVSGD throatwash (TW) samples for BKPyV and characterized the NCCR promoter region. Here we described the first comprehensive assessment of oral BKPyV NCCR block arrangement and activity, along with underlying sequence variations in the context of transcription factor binding sites (TFBS). Finally, we determined *in vitro* NCCR promoter activity and viral replication capacities of the oral clinical isolates in HSG cells.

The BKPyV NCCR architecture and viral loads (VLs) from a cohort of 36 immuno-suppressed individuals were assessed including 19 HIVSGD TW samples, 9 HIV + HIVSGD negative TW samples and 8 urine samples from HIVSGD negative transplant patients (Table 2.1.). First, we aimed to confirm previously published data showing that HIVSGD patients shed increased BKPyV VLs orally, corroborating a potential link between HIVSGD and BKPyV (7, 8). The BKPyV VLs in HIVSGD negative TW samples (n=9) were consistently below the qPCR detection level and significantly lower than HIVSGD positive TW (n=16) (p<0.01) and transplant urine samples (n=8) (p<0.001). Interestingly, the mean BKPyV VL of both HIVSGD positive TW samples ($2x10^7$ copies/ml) and the urine samples ($1x10^9$ copies/ml) were comparable and reflected BKPyV VLs previously reported in the urine (mean; $2x10^8$ copies/ml) and plasma (mean: $2x10^7$ copies/ml) of patients suffering from BKPyV-associated nephropathy (BKVN) (48), implying that the salivary glands may be a potential compartment suitable for BKPyV replication, pathogenesis and potential salivary transmission. High levels of orally shed virus may potentially incite a pathogenic response by inducing direct cytolytic effects on the salivary gland cells or by activating the immune system. Detection of HIVSGD TW VLs up to 10^8 copies/ml (Table 2.1.) suggested that HIVSGD BKPyV were efficient *in vivo* replicators under conditions provided at study entry.

Notably, 94.7% of the HIVSGD TW samples carried a common rearranged (rr) BKPyV NCCR block alignment OPQPQQS (Table 2.4.)(9). A single HIVSGD-derived BKPyV did not carry the distinct NCCR alignment (HIVSGD4) and revealed an OPQPQQ block combination, differing from the signature alignment by the lack of the S block. The OPQPQQS architecture was not simply associated with HIV as the two HIV + individuals that did not have HIVSGD had a distinct block arrangement. However, the OPQPQQS NCCR block combination was also

detected in two of the eight urine samples from transplant patients, which corroborated the substrain's potential biological significance. Detection of expected NCCR structures in urine samples (archetypic) and laboratory strains (previously published) and overall detection of eight distinct NCCR block alignment groups (Table 2.3.) confirmed the validity of our NCCR sequence results. Interestingly, HIVSGD NCCR block architectures were more homologous than urine-derived BKPyV NCCRs which displayed a range of NCCR arrangements (OPQPQQS, OPQRS, OPQ and PQRS; Table 2.3.).

The phylogenetic analysis emphasized the NCCR architecture homology among HIVSGD BKPyV but also reflected underlying nucleotide polymorphisms (Fig. 2.2A). These results were similar to a study published by Drew *et al.,* where urine-derived clinical isolates were described (50) that carried overall block similarities but differed by single nucleotide polymorphisms. The sequence analysis revealed that most polymorphisms were found with the O and the S blocks (Fig. 2.2.). Importantly, there was a relationship between the HIVSGD block sequence OPQPQQS and enhanced promoter activity and replication potential (Fig. 2.5.). Five out of six (83%) of the HIVSGD NCCR promoters were more active than laboratory strain promoters in HSG cells (Fig. 2.5A) and all HIVSGD strains replicated readily in salivary gland cells *in vitro* (Fig. 2.5B). Interestingly, all but one HIVSGD substrain replicated more efficiently than laboratory strain Dunlop in HSG cells over a 15-day time span (Fig. 2.5B).

Based on the significance of the BKPyV promoter to the viral life cycle (19) and the link between rearranged promoters and higher replication capacities and increased cell damage (24, 25, 31, 37, 38), it appeared that the HIVSGD OPQPQQS rearrangement may have endowed facilitated replication relative to laboratory strains. P block repetitions within the NCCR have been shown to result in greater promoter activity (51-53). P and S block preservations and R

block deletions seem to be selected for in clinically isolated BKPyV in past publications (38, 41). It is likely that P block duplications and R block deletions, as compared to archetype, may provide *in vitro* and *in vivo* replication advantages. The P and the S block were conserved, the R block deleted and additional 2 Q blocks added in HIVSGD NCCR compared to archetype BKPyV, which is known to replicate with great difficulty *in vitro*. Three Q blocks were added and 1 P block was removed compared to Dunlop BKPyV, which did not replicate well in salivary gland cells. Clearly, future work will have to elucidate the potential driving force of each block in the BKPyV NCCR context. JCPyV the closely related polyomavirus member mentioned above has been studied in more detail than BKPyV. JCPyV exhibits tropism for oligodendrocytes in the brain and is the etiological agent of the neurodegenerative disease progressive multifocal leukoencephalopathy (PML) (54). Similar to BKPyV, the JCPyV promoter has been found to contain TFBS and rearrange readily *in vivo* (55-59). It is known that JCPyV promoter rearrangements lead to alterations of TFBS which affect the transcriptional pattern of the promoter and increase the viral replication capacity in the brain and ultimately the viral disease potential (60). TFBS Tst-1, NF-1, Sp1, GBPi, NF-kB, YB-1, Pura, and GF-1 specifically determine the tropism of JCPyV to glial cells in the brain (61-68). While host factors contribute to the viral pathogenic capacity and likely fluctuate between individuals and over time (61) both JCPyV and BKPyV promoter rearrangements may drive viral replication and therefore pathogenicity *in vivo*.

While BKPyV NCCR TFBS in clinical samples (21, 29, 38, 69-71) and the relationship between TFBS and promoter activity or *in vitro* replication have been studied (22, 25, 30, 72) little published work assesses the correlation of NCCR TFBS and clinical VLs. Priftakis *et al.* attempted to correlate a C/G mutation in the NCCR Sp1 site with increased BKPyV VLs in

patients with hemorrhagic cystitis (HC) but could not confirm it (73, 74). We predicted TFBS for

the clinical and laboratory strain full-length (Table 2.4.) and O block (Table 2.5.) BKPyV

promoters and analyzed a potential correlation between *in vivo* VLs and sets of TFBS. A

potential association between NCCR TFBS C/EBPβ and p300 and higher *in vivo* BKPyV

replication efficiency was detected by *in silico* analysis (Fig. 2.3. and Fig. 2.4.). Previous studies

predicted C/EBPβ binding within the BKPyV NCCR and determined that C/EBPβ and p65

(subunit of NF-kB) stimulated NCCR transcription in the early direction in transfection

experiments, in CV-1 monkey kidney cells), suggesting C/EBPβ was important for early

promoter induction (23, 75). However, despite the long-held hypothesis that there is a link

between NCCR TFBSs and BKPyV replication efficiency (16, 21, 53), subsequent *in vitro*

experiments performed in this study did not confirm a correlation between TFBS C/EBPβ and

p300 and promoter activity (Fig. 2.5A) or viral replication levels (Fig. 2.5B). Factors other than

C/EBP and p300, such as AP-1, are thought to increase archetypic BKPyV promoter

transcriptional activity (76), and NF-1, is thought to be a repressor of the BKPyV promoter (77).

These factors may override the potential C/EBP and p300 effect *in vitro*. Alternatively, basal

levels of C/EBP in salivary gland cells may be different *in vitro* than *in vivo*. Similar to the

clinical BKPyV study performed by Gosert *et al.* (37), early clinical rr BKPyV NCCR promoters

displayed strong gene expression but no conclusive TFBS alterations could be identified as

directing promoter activity and replication efficiency. Furthermore, overall NCCR promoter

activity, *in vivo* and *in vitro* BKPyV VLs did not consistently reflect each other. The *in vivo* and

in vitro differences may have been associated with endogenous factors present in *in vivo* that

were not present *in vitro.* Promoter activity and *in vivo* or *in vitro* replication levels may also be

associated with BKPyV genome aberrations outside of the NCCR that could dramatically affect

the viral life cycle (9). Clearly, further work is required to determine the importance of TFBS in the multifaceted organization of BKPyV NCCR-mediated gene expression.

In summary, HIVSGD patients shed relatively high BKPyV VLs via the oral cavity and a highly homologous OPQPQQS NCCR block architecture sequence was detected among 19 HIVSGD BKPyV NCCR oral isolates (Table 2.3.). While it is unclear whether the OPQPQQS NCCR signature may be an adaptive response or may promote salivary gland cell tropism, this study determined that cloned HIVSGD BKPyV isolates displayed active promoter activity and efficient replication capability in human salivary gland cells *in vitro*. Overall, the high frequency of a viable OPQPQQS BKPyV substrain among HIVSGD TW samples corroborated the presence of a stable, biologically significant and potentially pathogenic substrain that may be linked to HIVSGD pathogenesis.

REFERENCES

1. **Terry, J. H., T. R. Loree, M. D. Thomas, and J. R. Marti.** 1991. Major salivary gland lymphoepithelial lesions and the acquired immunodeficiency syndrome. Am J Surg **162:**324-9.

2. **DiGiuseppe, J. A., R. L. Corio, and W. H. Westra.** 1996. Lymphoid infiltrates of the salivary glands: pathology, biology and clinical significance. Curr Opin Oncol **8:**232-7.

3. **Ioachim, H. L., and J. R. Ryan.** 1988. Salivary gland lymphadenopathies associated with AIDS. Hum Pathol **19:**616-7.

4. **Schiodt, M., C. L. Dodd, D. Greenspan, T. E. Daniels, D. Chernoff, H. Hollander, D. Wara, and J. S. Greenspan.** 1992. Natural history of HIV-associated salivary gland disease. Oral Surg Oral Med Oral Pathol **74:**326-31.

5. **Islam, N. M., I. Bhattacharyya, and D. M. Cohen.** 2012. Salivary gland pathology in HIV patients. Diagnostic Histopathology **18:**366-372.

6. **Shanti, R. M., and S. R. Aziz.** 2009. HIV-associated salivary gland disease. Oral Maxillofac Surg Clin North Am **21:**339-43.

7. **Jeffers, L. K., V. Madden, and J. Webster-Cyriaque.** 2009. BK virus has tropism for human salivary gland cells in vitro: implications for transmission. Virology **394:**183-93.

8. **Jeffers, L., and J. Y. Webster-Cyriaque.** 2011. Viruses and salivary gland disease (SGD): lessons from HIV SGD. Adv Dent Res **23:**79-83.

9. **Burger-Calderon, R., V. Madden, R. A. Hallett, A. D. Gingerich, V. Nickeleit, and J. Webster-Cyriaque.** 2013. Replication of oral BK virus in human salivary gland cells. J Virol.

10. **Kean, J. M., S. Rao, M. Wang, and R. L. Garcea.** 2009. Seroepidemiology of human polyomaviruses. PLoS Pathog **5:**e1000363.

11. **Knowles, W. A.** 2006. Discovery and epidemiology of the human polyomaviruses BK virus (BKV) and JC virus (JCV). Adv Exp Med Biol **577:**19-45.

12.   **Egli, A., S. Binggeli, S. Bodaghi, A. Dumoulin, G. A. Funk, N. Khanna, D. Leuenberger, R. Gosert, and H. H. Hirsch.** 2007. Cytomegalovirus and polyomavirus BK posttransplant. Nephrol Dial Transplant **22 Suppl 8:**viii72-viii82.

13.   **Nickeleit, V., and M. J. Mihatsch.** 2006. Polyomavirus nephropathy in native kidneys and renal allografts: an update on an escalating threat. Transpl Int **19:**960-73.

14.   **Nickeleit, V., H. H. Hirsch, I. F. Binet, F. Gudat, O. Prince, P. Dalquen, G. Thiel, and M. J. Mihatsch.** 1999. Polyomavirus infection of renal allograft recipients: from latent infection to manifest disease. J Am Soc Nephrol **10:**1080-9.

15.   **Ramos, E., C. B. Drachenberg, M. Portocarrero, R. Wali, D. K. Klassen, J. C. Fink, A. Farney, H. Hirsch, J. C. Papadimitriou, C. B. Cangro, M. R. Weir, and S. T. Bartlett.** 2002. BK virus nephropathy diagnosis and treatment: experience at the University of Maryland Renal Transplant Program. Clin Transpl**:**143-53.

16.   **Hirsch, H. H., and J. Steiger.** 2003. Polyomavirus BK. Lancet Infect Dis **3:**611-23.

17.   **Randhawa, P. S., S. Finkelstein, V. Scantlebury, R. Shapiro, C. Vivas, M. Jordan, M. M. Picken, and A. J. Demetris.** 1999. Human polyoma virus-associated interstitial nephritis in the allograft kidney. Transplantation **67:**103-9.

18.   2007. Fields' Virology. *In* P. M. H. David M. Knipe (ed.), 5th ed. Wolters Kluwer Health/Lippincott Williams & Wilkins, Philadelphia.

19.   **Broekema, N. M., J. R. Abend, S. M. Bennett, J. S. Butel, J. A. Vanchiere, and M. J. Imperiale.** 2010. A system for the analysis of BKV non-coding control regions: application to clinical isolates from an HIV/AIDS patient. Virology **407:**368-73.

20.   **Markowitz, R. B., and W. S. Dynan.** 1988. Binding of cellular proteins to the regulatory region of BK virus DNA. J Virol **62:**3388-98.

21.   **Moens, U., T. Johansen, J. I. Johnsen, O. M. Seternes, and T. Traavik.** 1995. Noncoding control region of naturally occurring BK virus variants: sequence comparison and functional analysis. Virus genes **10:**261-75.

22. **Jordan, J. A., K. Manley, A. S. Dugan, B. A. O'Hara, and W. J. Atwood.** 2010. Transcriptional regulation of BK virus by nuclear factor of activated T cells. J Virol **84:**1722-30.

23. **Gorrill, T. S., and K. Khalili.** 2005. Cooperative interaction of p65 and C/EBPbeta modulates transcription of BKV early promoter. Virology **335:**1-9.

24. **Olsen, G. H., P. A. Andresen, H. T. Hilmarsen, O. Bjorang, H. Scott, K. Midtvedt, and C. H. Rinaldo.** 2006. Genetic variability in BK Virus regulatory regions in urine and kidney biopsies from renal-transplant patients. J Med Virol **78:**384-93.

25. **Johnsen, J. I., O. M. Seternes, T. Johansen, U. Moens, R. Mantyjarvi, and T. Traavik.** 1995. Subpopulations of non-coding control region variants within a cell culture-passaged stock of BK virus: sequence comparisons and biological characteristics. J Gen Virol **76 (Pt 7):**1571-81.

26. **Cho, S., Y. Tian, and T. L. Benjamin.** 2001. Binding of p300/CBP co-activators by polyoma large T antigen. J Biol Chem **276:**33533-9.

27. **Poulin, D. L., A. L. Kung, and J. A. DeCaprio.** 2004. p53 targets simian virus 40 large T antigen for acetylation by CBP. J Virol **78:**8245-53.

28. **Funk, G. A., R. Gosert, and H. H. Hirsch.** 2007. Viral dynamics in transplant patients: implications for disease. Lancet Infect Dis **7:**460-72.

29. **Boldorini, R., C. Veggiani, E. Turello, D. Barco, and G. Monga.** 2005. Are sequence variations in the BK virus control region essential for the development of polyomavirus nephropathy? Am J Clin Pathol **124:**303-12.

30. **Rubinstein, R., B. C. Schoonakker, and E. H. Harley.** 1991. Recurring theme of changes in the transcriptional control region of BK virus during adaptation to cell culture. J Virol **65:**1600-4.

31. **Sundsfjord, A., T. Johansen, T. Flaegstad, U. Moens, P. Villand, S. Subramani, and T. Traavik.** 1990. At least two types of control regions can be found among naturally occurring BK virus strains. J Virol **64:**3864-71.

32. **Sundsfjord, A., T. Flaegstad, R. Flo, A. R. Spein, M. Pedersen, H. Permin, J. Julsrud, and T. Traavik.** 1994. BK and JC viruses in human immunodeficiency virus

type 1-infected persons: prevalence, excretion, viremia, and viral regulatory regions. J Infect Dis **169:**485-90.

33. **Hanssen Rinaldo, C., H. Hansen, and T. Traavik.** 2005. Human endothelial cells allow passage of an archetypal BK virus (BKV) strain--a tool for cultivation and functional studies of natural BKV strains. Arch Virol **150:**1449-58.

34. **Bennett, S. M., N. M. Broekema, and M. J. Imperiale.** 2012. BK polyomavirus: emerging pathogen. Microbes Infect **14:**672-83.

35. **Chatterjee, M., T. B. Weyandt, and R. J. Frisque.** 2000. Identification of archetype and rearranged forms of BK virus in leukocytes from healthy individuals. J Med Virol **60:**353-62.

36. **Perets, T. T., I. Silberstein, J. Rubinov, R. Sarid, E. Mendelson, and L. M. Shulman.** 2009. High frequency and diversity of rearrangements in polyomavirus bk noncoding regulatory regions cloned from urine and plasma of Israeli renal transplant patients and evidence for a new genetic subtype. J Clin Microbiol **47:**1402-11.

37. **Gosert, R., C. H. Rinaldo, G. A. Funk, A. Egli, E. Ramos, C. B. Drachenberg, and H. H. Hirsch.** 2008. Polyomavirus BK with rearranged noncoding control region emerge in vivo in renal transplant patients and increase viral replication and cytopathology. J Exp Med **205:**841-52.

38. **Moens, U., and M. Van Ghelue.** 2005. Polymorphism in the genome of non-passaged human polyomavirus BK: implications for cell tropism and the pathological role of the virus. Virology **331:**209-31.

39. **Broekema, N. M., and M. J. Imperiale.** 2012. Efficient propagation of archetype BK and JC polyomaviruses. Virology **422:**235-41.

40. **Olsen, G. H., H. H. Hirsch, and C. H. Rinaldo.** 2009. Functional analysis of polyomavirus BK non-coding control region quasispecies from kidney transplant recipients. J Med Virol **81:**1959-67.

41. **Sharma, P. M., G. Gupta, A. Vats, R. Shapiro, and P. S. Randhawa.** 2007. Polyomavirus BK non-coding control region rearrangements in health and disease. J Med Virol **79:**1199-207.

42. **Elsner, C., and K. Dorries.** 1998. Human polyomavirus JC control region variants in persistently infected CNS and kidney tissue. J Gen Virol **79 (Pt 4):**789-99.

43. **Saitou, N., and M. Nei.** 1987. The neighbor-joining method: a new method for reconstructing phylogenetic trees. Mol Biol Evol **4:**406-25.

44. **Shi, L., and W. Zhang.** 2004. Comparative analysis of eukaryotic-type protein phosphatases in two streptomycete genomes. Microbiology **150:**2247-56.

45. **Jordan, J. A., K. Manley, A. S. Dugan, B. A. O'Hara, and W. J. Atwood.** 2010. Transcriptional regulation of BK virus by nuclear factor of activated T cells. Journal of virology **84:**1722-30.

46. **Liang, B., I. Tikhanovich, H. P. Nasheuer, and W. R. Folk.** 2012. Stimulation of BK virus DNA replication by NFI family transcription factors. Journal of virology **86:**3264-75.

47. **Macian, F.** 2005. NFAT proteins: key regulators of T-cell development and function. Nature reviews. Immunology **5:**472-84.

48. **Drachenberg, C. B., J. C. Papadimitriou, H. H. Hirsch, R. Wali, C. Crowder, J. Nogueira, C. B. Cangro, S. Mendley, A. Mian, and E. Ramos.** 2004. Histological patterns of polyomavirus nephropathy: correlation with graft outcome and viral load. Am J Transplant **4:**2082-92.

49. **Bressollette-Bodin, C., M. Coste-Burel, M. Hourmant, V. Sebille, E. Andre-Garnier, and B. M. Imbert-Marcille.** 2005. A prospective longitudinal study of BK virus infection in 104 renal transplant recipients. American journal of transplantation : official journal of the American Society of Transplantation and the American Society of Transplant Surgeons **5:**1926-33.

50. **Drew, R. J., A. Walsh, B. N. Laoi, and B. Crowley.** 2012. Phylogenetic analysis of the complete genome of 11 BKV isolates obtained from allogenic stem cell transplant recipients in Ireland. J Med Virol **84:**1037-48.

51. **Chakraborty, T., and G. C. Das.** 1989. Identification of HeLa cell nuclear factors that bind to and activate the early promoter of human polyomavirus BK in vitro. Mol Cell Biol **9:**3821-8.

52. **Deyerle, K. L., and S. Subramani.** 1988. Linker scan analysis of the early regulatory region of human papovavirus BK. J Virol **62:**3378-87.

53. **Markowitz, R. B., S. Tolbert, and W. S. Dynan.** 1990. Promoter evolution in BK virus: functional elements are created at sequence junctions. J Virol **64:**2411-5.

54. **Weber, T., and E. O. Major.** 1997. Progressive multifocal leukoencephalopathy: molecular biology, pathogenesis and clinical impact. Intervirology **40:**98-111.

55. **Martin, J. D., D. M. King, J. M. Slauch, and R. J. Frisque.** 1985. Differences in regulatory sequences of naturally occurring JC virus variants. Journal of virology **53:**306-11.

56. **White, F. A., 3rd, M. Ishaq, G. L. Stoner, and R. J. Frisque.** 1992. JC virus DNA is present in many human brain samples from patients without progressive multifocal leukoencephalopathy. Journal of virology **66:**5726-34.

57. **Kato, K., J. Guo, F. Taguchi, O. Daimaru, M. Tajima, H. Haibara, J. Matsuda, M. Sumiya, and Y. Yogo.** 1994. Phylogenetic comparison between archetypal and disease-associated JC virus isolates in Japan. Japanese journal of medical science & biology **47:**167-78.

58. **Ciappi, S., A. Azzi, R. De Santis, F. Leoncini, G. Sterrantino, F. Mazzotta, and L. Mecocci.** 1999. Archetypal and rearranged sequences of human polyomavirus JC transcription control region in peripheral blood leukocytes and in cerebrospinal fluid. The Journal of general virology **80 (Pt 4):**1017-23.

59. **Newman, J. T., and R. J. Frisque.** 1999. Identification of JC virus variants in multiple tissues of pediatric and adult PML patients. Journal of medical virology **58:**79-86.

60. **Daniel, A. M., J. J. Swenson, R. P. Mayreddy, K. Khalili, and R. J. Frisque.** 1996. Sequences within the early and late promoters of archetype JC virus restrict viral DNA replication and infectivity. Virology **216:**90-101.

61. **Imperiale, M. J.** 2000. The human polyomaviruses, BKV and JCV: molecular pathogenesis of acute disease and potential role in cancer. Virology **267:**1-7.

62.   **Tamura, T., T. Inoue, K. Nagata, and K. Mikoshiba.** 1988. Enhancer of human polyoma JC virus contains nuclear factor I-binding sequences; analysis using mouse brain nuclear extracts. Biochemical and biophysical research communications **157:**419-25.

63.   **Khalili, K., J. Rappaport, and G. Khoury.** 1988. Nuclear factors in human brain cells bind specifically to the JCV regulatory region. The EMBO journal **7:**1205-10.

64.   **Feigenbaum, L., S. H. Hinrichs, and G. Jay.** 1992. JC virus and simian virus 40 enhancers and transforming proteins: role in determining tissue specificity and pathogenicity in transgenic mice. Journal of virology **66:**1176-82.

65.   **Kerr, D., C. F. Chang, N. Chen, G. Gallia, G. Raj, B. Schwartz, and K. Khalili.** 1994. Transcription of a human neurotropic virus promoter in glial cells: effect of YB-1 on expression of the JC virus late gene. Journal of virology **68:**7637-43.

66.   **Chen, N. N., and K. Khalili.** 1995. Transcriptional regulation of human JC polyomavirus promoters by cellular proteins YB-1 and Pur alpha in glial cells. Journal of virology **69:**5843-8.

67.   **Chen, N. N., C. F. Chang, G. L. Gallia, D. A. Kerr, E. M. Johnson, C. P. Krachmarov, S. M. Barr, R. J. Frisque, B. Bollag, and K. Khalili.** 1995. Cooperative action of cellular proteins YB-1 and Pur alpha with the tumor antigen of the human JC polyomavirus determines their interaction with the viral lytic control element. Proceedings of the National Academy of Sciences of the United States of America **92:**1087-91.

68.   **Safak, M., G. L. Gallia, and K. Khalili.** 1999. A 23-bp sequence element from human neurotropic JC virus is responsive to NF-kappa B subunits. Virology **262:**178-89.

69.   **Randhawa, P., D. Zygmunt, R. Shapiro, A. Vats, K. Weck, P. Swalsky, and S. Finkelstein.** 2003. Viral regulatory region sequence variations in kidney tissue obtained from patients with BK virus nephropathy. Kidney Int **64:**743-7.

70.   **Barcena-Panero, A., J. E. Echevarria, M. Van Ghelue, G. Fedele, E. Royuela, N. Gerits, and U. Moens.** 2012. BK polyomavirus with archetypal and rearranged non-coding control regions is present in cerebrospinal fluids from patients with neurological complications. J Gen Virol **93:**1780-94.

71.   **Carr, M. J., G. P. McCormack, K. J. Mutton, and B. Crowley.** 2006. Unique BK virus non-coding control region (NCCR) variants in hematopoietic stem cell transplant recipients with and without hemorrhagic cystitis. J Med Virol **78:**485-93.

72.   **Moens, U., M. Van Ghelue, B. Johansen, and O. M. Seternes.** 1999. Concerted expression of BK virus large T- and small t-antigens strongly enhances oestrogen receptor-mediated transcription. J Gen Virol **80 (Pt 3):**585-94.

73.   **Priftakis, P., G. Bogdanovic, M. Kalantari, and T. Dalianis.** 2001. Overrepresentation of point mutations in the Sp1 site of the non-coding control region of BK virus in bone marrow transplanted patients with haemorrhagic cystitis. J Clin Virol **21:**1-7.

74.   **Priftakis, P., G. Bogdanovic, P. Kokhaei, H. Mellstedt, and T. Dalianis.** 2003. BK virus (BKV) quantification in urine samples of bone marrow transplanted patients is helpful for diagnosis of hemorrhagic cystitis, although wide individual variations exist. J Clin Virol **26:**71-7.

75.   **White, M. K., M. Safak, and K. Khalili.** 2009. Regulation of gene expression in primate polyomaviruses. Journal of virology **83:**10846-56.

76.   **Markowitz, R. B., S. Tolbert, and W. S. Dynan.** 1990. Promoter evolution in BK virus: functional elements are created at sequence junctions. Journal of virology **64:**2411-5.

77.   **Kraus, R. J., L. Shadley, and J. E. Mertz.** 2001. Nuclear factor 1 family members mediate repression of the BK virus late promoter. Virology **287:**89-104.

CHAPTER 3:

REPLICATION OF ORAL BK VIRUS IN HUMAN SALIVARY GLAND CELLS[1]

Overview

BK polyomavirus (BKPyV) is the most common viral pathogen among allograft patients. Increasing evidence links BKPyV to the human oral compartment and to HIV-associated salivary gland disease (HIVSGD). To date, few studies have analyzed oral-derived BKPyV. This study aimed to characterize BKPyV isolated from throatwash (TW) samples of HIVSGD patients. The replication potential of HIVSGD-derived clinical isolates HIVSGD-1 and HIVSGD-2, both containing the non-coding control region (NCCR) architecture OPQPQQS, were assessed and compared to urine-derived virus. The BKPyV isolates displayed significant variation in replication potential. Whole genome alignment of the two isolates revealed three nucleotide differences that were analyzed for a potential effect on the viral life cycle. Analysis revealed a negligible difference in NCCR promoter activity despite sequence variation and emphasized the importance of functional Tag for efficient replication. HIVSGD-1 encoded for full-length Tag, underwent productive infection in both human salivary gland cells and kidney cells and expressed viral DNA and Tag protein. Additionally, HIVSGD-1 generated DNAse resistant particles and by far surpassed the replication potential of the kidney-derived isolate in HSG cells. HIVSGD-2 encoded a truncated form of Tag and replicated much less efficiently. Quantitation of infectious virus, via the fluorescent forming unit assay, suggested that HIVSGD BKPyV had

---

[1] This chapter previously appeared as an article in the Journal of Virology. The original citation is as follows: Burger-Calderon, R. *et al.* "Replication of Oral BK Virus in Human Salivary Gland Cells", J. Virol. 2014, 88(1): 559.

preferential tropism for salivary gland cells over kidney cells. Similarly, results suggested that kidney-derived virus had preferential tropism for kidney cells over salivary gland cells. Evidence of HIVSGD-derived BKPyV oral tropism and adept viral replication in human salivary gland cells corroborated the potential link between HIVSGD pathogenesis and BKPyV.

Introduction

BK polyomavirus (BKPyV) was first isolated from the urine of a renal allograft recipient in 1971 and was subsequently identified as a member of the small DNA tumorvirus family (1). BKPyV infection is ubiquitous and seroconversion of up to 90% of the world's population by the age of 10 suggests that BKPyV transmission takes place during early childhood (2, 3). BKPyV primary infection is asymptomatic and persists latently in the kidney of immunocompetent individuals (4). Reactivation occurs under immune-suppressed conditions, such as those experienced by patients receiving organ transplants and patients infected with HIV (5). BKPyV reactivation among kidney transplant patients has been associated with BKPyV nephropathy (BKN), which is by far the most significant complication among renal transplant patients (6-8).

The BKPyV genome (5 kb) is divided into three major components: the early region, the late region and the bidirectional viral promoter, also known as non-coding control region (NCCR). The NCCR is the major determinant of *in vitro* replication (9) and is arbitrarily divided into five block sequences: O (142 bp), P (68 bp), Q (39 bp), R (63 bp) and S (63 bp). The blocks contain the origin of DNA replication and an array of transcription factor binding sites (TFBS) (10-13). The late region encodes the agnoprotein and the structural proteins VP1, VP2 and VP3 (4, 14). The early BKPyV genome region encodes the non-structural viral proteins: large, small and mini T antigen (Tag). Large Tag is critical for the viral lifecycle and drives the host cell into

the S phase (4, 15-17). Viral DNA synthesis is initiated by Tag's helicase activity, which unwinds the origin of replication within the viral NCCR promoter (4) and subsequently recruits DNA synthetic machinery (5). As the major BKPyV transforming viral oncoprotein, Tag interacts with both pRb and p53, instigating deregulated cell growth. The Tag transformation potential is linked to the p53-binding domain located near the carboxy- terminus of the protein (18). Upon initiation of DNA replication, Tag induces late viral gene expression, and represses early gene expression (19).

Given its historic link to renal pathogenesis, BKPyV has been considered a kidney-tropic virus. Data however suggest a connection between BKPyV and the oral compartment. Both respiratory (5) and fecal-oral (20) routes have been suggested as likely transmission pathways. BKPyV DNA has been detected in tonsillar biopsies from immunocompetent children (21-23) and nasopharyngeal aspirates of immunocompromised and immunocompetent individuals (children and adults) (24). Finally, our group has suggested a potential link between BKPyV and the oral malady HIV-associated Salivary Gland Disease (HIVSGD) (25, 26).

HIVSGD is among the most important HIV/AIDS-associated lesions (27). HIVSGD pathogenesis is not well understood and present treatment strategies focus solely on symptom alleviation (25). HIVSGD is characterized by salivary gland enlargement and damage that incites xerostomia (28-31). HIVSGD diagnosis has been tied to an increased risk of lymphoma development in HIV-infected individuals (32). Finally, affected patients may suffer stigma as HIVSGD's outward appearance suggests HIV infection. As for HIVSGD etiology, molecular evidence has previously established an association between polyomaviruses (PyV) and salivary gland pathology. Rodent models demonstrated that PyV injection resulted in salivary gland tumors in mice (33). *In vivo*, HIVSGD patients shed twenty-fold higher levels of BKPyV in

throatwash (TW) and plasma (viremia) compared to HIV positive patients without HIVSGD and compared to HIV negative individuals (25). Moreover, our group has demonstrated successful replication of a BKPyV laboratory strain in human salivary gland cell lines (HSG and HSY) *in vitro* (26). While contemporary advances have allowed efficient *in vitro* cultivation of archetype BKPyV in kidney cells (providing Tag in trans (34)), studies analyzing clinical BKPyV isolates have been limited, kidney-focused and have not assessed salivary gland infection (9, 35-38). Molecular evidence demonstrates that the *in vivo* replication compartments of urine and plasma-derived BKPyV are distinct (39, 40). Similarly, the salivary gland may provide an additional BKPyV replication compartment in HIVSGD (41).

In the current study HIVSGD-derived BKPyV underwent successful replication in human salivary gland (HSG) cells, providing proof of concept that salivary glands of HIVSGD patients may be replication competent. We further compared the replication potential of TW-derived BKPyV clinical isolates to urine- and laboratory-derived BKPyV in human salivary gland (HSG) cells and in kidney cells (Vero). The replication potential of the clinical isolates HIVSGD-1 and HIVSGD-2 differed greatly despite the two isolates bearing the same NCCR architecture (OPQPQQS) and their genomes differing by only three nucleotides. The replication inefficiency of HIVSGD-2 was likely caused by the introduction of a stop codon that produced a truncated Tag mutant. Interestingly, HIVSGD-1 BKPyV encoded full-length Tag, replicated efficiently, and displayed preferential tropism for salivary gland cells over kidney cells, as suggested by quantitation of infectious virus.

Materials and Methods

Patient Information and Sample Collection

      HIVSGD positive individuals from the UNC hospital dental clinic were selected for

throatwash (TW) collection under IRB approved studies. Urine samples from HIV negative

patients were kindly donated and collected under the supervision of Dr. Nickeleit at UNC

hospitals. Patient samples were centrifuged, DNAse treated and DNA isolated via Qiagen

DNeasy kit as described by the manufacturer.

BKPyV NCCR Sequencing

      The BKPyV NCCR was PCR amplified (Vent polymerase, New England BioLabs Inc.)

with primers BKPyVTU1F and BKPyVTU1R (37) from patient sample DNA and products

subsequently sequenced by Genewiz (www.genewiz.com). NCCR amplification and sequencing

was repeated a minimum of three times per patient sample. Resulting NCCR nucleotide sequence

was analyzed and aligned by the Vector NTI program. Vector NTI identified the block motifs

with minimum similarity of 70% to original block sequences (10).

Whole Genome BKPyV Cloning

      Whole genome (wg) BKPyVs, including the naturally occurring BamH1 restriction

fragment recognition sites, were PCR amplified from clinical samples with primers BKPyVWGF

(VP1 Forward: 5'-GCGGGATCCAGATGAAAACCTTAGG-3') and BKPyVWGR (Reverse:

5'- GCGGGATCCCCCATTTCTGG-3'), using the Expand Long Range dNTPack (Roche) as

described by manufacturer. Amplified wg BKPyV products were purified by QIAquick PCR

Purification Kit (QIAGEN) as described by manufacturer. Purified HIVSGD-2 and U1 wg

BKPyV DNA was cloned via the TOPO TA Cloning Kit (Invitrogen) as described by

manufacturer. Purified HIVSGD-1 DNA and pUC18 vector (2.6 kb) from Stratagene were

digested separately with restriction endonuclease BamH1, isolated, ligated via T4 DNA Ligase (BioLabs). DH5 alpha bacterial cells (Invitrogen) were transformed with the HIVSGD-1, HIVSGD-2 and MM ligation products. All bacterial-derived constructs were isolated via QIAfilter Plasmid Midi Kit (QIAGEN) post-24hrs incubation at 37 °C.

Virus, Transfection and Infection Conditions

Clinical BKPyV cloned by us: HIVSGD-1, HIVSGD-2 and U1.

Commercially available infectious BKPyV: VR837 (ATCC)

Laboratory-derived Dunlop BKPyV clone, kindly donated by Dr. Michael J. Imperiale

Laboratory-derived MM (ATCC 45026) BKPyV clone (42) is commercially available. Interestingly, MM BKPyV NCCR and Tag sequencing results obtained in this study (BankIt1648707 KF445133 and BankIt1648650 and KF445132 respectively) were not homologous with previously published sequence (GenBank V01109).

BKPyV Transfection: Cloned BKPyV was cut out of its respective backbones by over night (37°C) BamH1 endonuclease digestion; HIVSGD-1 (pUC18), HIVGD-2 (pCR2.1), U1 (pCR2.1) and MM (ATCC 45026, pBR322). Wg BKPyV cloned into pCR2.1 were digested with endonuclease Taq1a for an additional 3hrs at 65°C. Wg BKPyV cloned into pBR322 was digested with endonuclease BsAa1 for an additional 3 hrs at 37°C. All digested samples were run on a 2% EtBr agarose gel and 5kb bands isolated in order to obtain wg BKPyV. Wg BKPyV DNA was purified via QIAquick Gel Extraction Kit (Qiagen) as instructed by manufacturer and re-ligated via T4 DNA Ligase (BioLabs), over night at 16°C. Episomal viral DNA was subsequently purified via phenol-chloroform. Single layers of HSG and Vero cells were passaged by trypsinizing (~15 mins) and resuspended in 2% FBS and 1% penicillin–streptomycin culture medium and subsequently seeded at ~30% confluency. Episomal BKPyV

was introduced into the cells via lipid-mediated gene delivery, using *Trans*IT®-LU1 (Mirus) according to the manufacturer's protocol. Media was changed 48 hrs pt. Media and cells were collected at different time points for further analysis.

Infection: Equal amounts of infectious clinical and laboratory strain BKPyV (determined via FFA) were used for infection of HSG and Vero cells: Part 2 of the *in vitro* model (Fig. 4). Supernatant of transfected HSG cells carrying infectious BKPyV were passed through 0.45μm filters and added to fresh HSG and Vero cells.

Cell Culture

Human submandibular salivary gland epithelial cells, a.k.a. HSG cells, from adenocarcinoma. (43) were obtained from Dr. B. Baum (NIH) and maintained in McCoy's 5A medium (Sigma), supplemented with 10% fetal bovine serum (FBS; Sigma), and 1% penicillin– streptomycin (P/S; Gibco). African green monkey kidney epithelial cells, a.k.a. Vero cells, were obtained from the American Type Culture Collection (ATCC), maintained in Dulbecco's minimal essential medium (DMEM; Sigma), supplemented with 10% FBS and 1% P/S. Both cell lines were incubated in humidified atmosphere at 37°C and 5% CO_2.

Reporter Construct Formation

Primers BKPyVTU1F and BKPyVTU1R (37) were used to amplify the BKPyV NCCR with flanking Sac1 restriction fragment recognition sites via PCR (Vent polymerase, New England BioLabs Inc.). Amplified DNA products were purified by QIAquick PCR Purification Kit (QIAGEN) as described by manufacturer. Purified DNA and pGL3-Basic vector (5 kb) from Promega were digested separately with restriction endonuclease Sac1, isolated and ligated via T4 DNA Ligase (BioLabs). DH5 alpha bacterial cells (Invitrogen) were transformed with products

and constructs were isolated via QIAfilter Plasmid Midi Kit (QIAGEN) after 24hrs incubation at 37°C.

BKPyV NCCR Promoter Activity

HIVSGD-1 and HIVSGD-2 BKPyV NCCR promoter activity was measured with and without the presence of wild-type large Tag in HSG cells via the luciferase (luc) reporter assay (pGL3 vectors, Promega). Cloned reporter constructs (1 µg) were transfected into HSG cells via lipid-mediated gene delivery, using *Trans*IT®-LU1 (Mirus) according to manufacturer's protocol. pCDNA RFP was co-transfected along with and without Tag (0.5 μg) expression plasmid (in pCMV myc; kindly provided by Dr. L. Jeffers). The Tag expression plasmid encoded for VR837 BKPyV-derived full-length wild-type large Tag. Cells were collected from each treatment according to the Luciferase Assay protocol (Promega) at 48 hrs. Luc activity of HIVSGD clones, pGL3 control vector (positive control, not shown) and pGL3 basic vector (negative control) were measured in a microplate format by the LMAX luminometer (Molecular Devices). HIVSGD luc activity was normalized to pGL3 basic.

Fluorescent Focus Assay (FFA)

Vero cells (50% confluency) were infected with varying volumes of filtered (0.45µm) supernatant from transfected HSG cells and incubated over four days. Where low levels of virus were present, higher volumes were utilized in order to attain infection. These differences in volumes used for Vero cell infection are accounted for in fluorescent forming units (FFU)/µl calculations (44). Vero cells were fixed in 50:50 Methanol/Acetone, air-dried and stored at -80 °C over night 4dpi. Cells were rehydrated with phosphate buffered saline (PBS) the next day and incubated with anti-JC/BK polyomavirus primary antibody NCL JCBK (Novocastra, Leica; 1:10 dilution in PBS for 30 mins at 37 °C and 30 mins at room temperature (RT). The secondary

antibody goat anti-mouse Alexa Flour 488 (Life Technologies; 1:100 dilution in PBS) was added

for 1hr at RT after washing the cells with PBS twice. Cells were washed with PBS prior to

DAPI/DNA stain addition (1:10,000) and fluorescent microscopy analysis (Olympus IX81).

BKPyV infected cells were counted at 20X magnification for a minimum of 10 fields per dish

and FFUs were calculated as described in (44). FFU values were graphed for each treatment and

depicted as FFU/μl or FFU/ μl +1 in order to transform the zero values for the log10-based y-

axis.

BKPyV DNA detection via Southern Blot hybridization

BKPyV episomes were transfected (see above for BKPyV DNA and transfection details)

into HSG cells at the following concentrations 0.39 μg Dunlop, 0.45 μg U1, 0.72 μg HIVSGD-1,

0.9 μg MM and 0.9 μg pcDNA3 DNA. Differential amounts of DNA were transfected for the

Dpn1 resistance assay. Hence, this assay was not intended to compare BKPyV replication levels.

All succeeding experiments were intended to evaluate relative viral replication levels and

transfections were done with equal amounts of BKPyV DNA. Low molecular weight DNA was

isolated from HSG cells 6dpt by a previously described (45) modified Hirt Method, digested by

endonucleases Sau3a and Dpn1, electrophoresed on a 7% agarose gel and transferred onto a SPC

membrane by the Whatman Nytran SPC Turbo Blotter (General Electric), as described by the

manufacturer. Membrane-associated BKPyV DNA was detected by hybridization to randomly

primed wg MM BKPyV (ATCC 45026) ^{32}P-labeled DNA probe and exposed to film (Kodak).

Expected MM BKPyV DNA band sizes according to mapped Dpn1/Sau3a cut sites: 1522, 681,

529, 451, 432, 346, 294, 230, 216, 129, and 116 bp.

<u>Encapsidated viral DNA isolation and qPCR amplification</u>

Transfected and infected HSG and Vero cell supernatant was passed through 0.45μm filters and DNAse treated (Promega), removing debris/cells and non-encapsulated viral DNA respectively. DNA was isolated using QIAamp DNA Blood Mini Kit (QIAGEN) as instructed by the manufacturer. Viral load (VL) was quantified via quantitative real-time PCR (qPCR) analysis using Roche LightCycler 480 Syber Green I Master Mix as a detector in the Roche Light Cycler 480 by using previously published primers for VP1 (46). BKPyV plasmid, kindly donated by Dr. Nickeleit, was used to establish a standard curve and for subsequent quantification of encapsidated viral genomes present in the cellular supernatant.

<u>Transmission Electron Microscopy (TEM)</u>

Three-milliliters of transfected, infected or control HSG and Vero cell supernatant was spun at 13,000 rpm for 30 mins at 4°C in order to remove cellular debris and then at 290,000 rpm for 1hr at 4°C by ultracentrifugation in order to concentrate BKPyV and decrease the suspension volume. Metal grids were subjected to purified supernatant and treated with 2% uralic acetate for negative staining. Virus was subsequently visualized via EM910 transmission electron microscopy (Zeiss) utilizing a Gatan SC1000 camera.

<u>Immunoblotting</u>

Episomal BKPyV DNA (0.3 μg) was transfected into HSG cells and whole cell lysates harvested with 1% SDS lysis buffer 4 days post-transfection. Protein was quantified using the BioRad protein assay, and equal amounts electrophoresed on a 10% Bis–Tris polyacrylamide minigel (Invitrogen). Tag antibody PAb416 (Genetex; 1:200) in 5% non-fat dry milk in 0.1% Tween-20 PBS (PBS-T) was used to detect Tag expression post wg BKPyV transfection of HSG cells. cMyc-tagged Tag expression was detected via anti c-Myc antibody (Santa Cruz; 1:1000)

post-reporter construct transfection of HSG cells. Actin expression was detected via the (C-11)-R

sc-1615-R antibody (Santa Cruz Biotechnology; 1:1000) in 5% non-fat dry milk (as above).

Blots were washed in PBS-T three times for 10 mins at RT and probed with a horseradish

peroxidase-conjugated secondary antibody (Promega 1:10,000), exposed to SuperSignal West

Pico Chemiluminescent substrate (Thermo scientific) and exposed to film (Kodak). Band

intensity was measured via densitometry. Relative band density was determined by normalizing

Tag to actin expression via Gene Tools from Syngene.

Results

HIVSGD-1 and HIVSGD-2 BKPyV isolation and sequence analysis

Throatwash (TW) samples were collected from two HIV positive subjects with diagnosed

HIVSGD. To obtain kidney-derived BKPyV, urine was collected from an HIV negative lung

transplant patient with diagnosed BKPyV nephropathy (BKN). Patient demographic data (HIV

status, other clinical status, age and sex) was collected and BKPyV viral load (VL) was

determined. Whole genome BKPyVs were cloned from each sample and the viral NCCR

promoters were sequenced (Table 1). All three clinical samples had high VLs ranging from

$1.7x10^5$ to $1.7x10^9$ copies/ml. Similar to the laboratory strain MM, both of the HIVSGD-derived

BKPyV isolates had OPQPQQS NCCR block alignments. The transplant urine sample carried

BKPyV with a OPQ NCCR block alignment. The NCCR architecture of previously studied

laboratory strains MM, Dunlop and VR837 BKPyV were sequenced as a control measure and

recovered correctly (Table 3.1). Alignment of the whole genome nucleotide sequences of

HIVSGD-1 and HIVSGD-2 BKPyV detected 99.9% whole genome similarity. The three single

nucleotide differences were: (1) a single bp thymidine (T) deletion between sequences that

90

encoded agnoprotein and VP2, (2) a thymidine/cytidine transition (T/C) within the NCCR and

(3) a single bp adenosine (A) deletion within the Tag coding sequence (Fig. 3.1A). All three

mutations were analyzed for potential biological significance. The T deletion located between

the genes encoding for agnoprotein and VP2 was assumed to be least important since this

mutation did not affect either of the adjacent open reading frames, VP2 and agnoprotein (Fig.

3.1B).

Patient-derived	HIV Status	Clinical Status	Source	Age[a]	Gender	VL[b]	NCCR[c]
HIVSGD-1	HIV +	HIVSGD[d]	TW[e]	47	M[f]	1.76×10^5	OPQPQQS
HIVSGD-2	HIV +	HIVSGD[d]	TW[e]	60	M[f]	2.57×10^5	OPQPQQS
U1	HIV -	BKN[g], lung transplant	urine	31	M[f]	1.79×10^9	OPQ
Laboratory-derived		Origin					NCCR
Dunlop		laboratory-derived clone					OPPPS
VR837		ATCC, infectious virus					OPQPQS
MM		ATCC, clone					OPQPQQS

Table 3.1. Demographics and viral characterization of clinical BKPyV isolates. Clinical

whole genome BKPyV was cloned from two HIVSGD TW samples (HIVSGD-1 and HIVSGD-

2) and one transplant patient urine sample (U1) for *in vitro* analysis. Laboratory strains Dunlop,

VR837 and MM served as laboratory control strains. [a]Patient age at time point of sample

collection (yrs). [b]BKPyV viral load (copies/ml). [c]Non-coding control region. [d]HIV-associated

Salivary Gland Disease. [e]Throatwash. [f]Male. [g]BKPyV nephropathy.

VP2 protein   **M G A A L A L**

HIVSGD-1 GACTCTGTAAAAGACTCCTAGGTAAGTAATCCCTTTTTT`TTTGTAT`TTCCAGGTTCATGGGTGCTGCTCTAGCACTT

HIVSGD-2 GACTCTGTAAAAGACTCCTAGGTAAGTAATCCCTTTTTT`TT–GTAT`TTCCAGGTTCATGGGTGCTGCTCTAGCACTT

Agnoprotein **D S V K D S .**

A

B

Figure. 3.1. Whole genome sequence comparison between HIVSGD BKPyV isolates

revealed three polymorphisms. A. Schematic shows linearized BKPyV genome and encoded

viral proteins. Black bars and numbers denote the three single base pair polymorphisms (1-3)

differentiating whole genomes HIVSGD-1 and HIVSGD-2: 1. Thymidine deletion between the

open reading frames (ORFs) encoding for agnoprotein and VP2. 2. Thymidine to cytidine

transition within the non-coding control region (NCCR). 3. Adenosine deletion within the ORF

encoding for Tag. B. The depicted DNA stretches show the thymidine deletion between the

ORFs encoding for agnoprotein and VP2 found within HIVSGD-2 but not HIVSGD-1.

The HIVSGD-1 and HIVSGD-2 NCCRs differed by a T/C transition located within the S

block of the viral promoter. To assess the potential biological significance of this nucleotide

transition, putative human transcription factor binding sites (TFBS) were predicted within this

region of the NCCR. Identical TFBS (Smad3, Smad4, C/EBPα, AP-2αA and E47) were

predicted for both HIVSGD-1 and HIVSGD-2 (Fig. 3.2A). Next, *in vitro* promoter activity was assessed to determine whether the transition led to differential promoter activity despite homologous TFBS. HIVSGD-1 and HIVSGD-2 NCCR-pGL3 reporter constructs were generated in the early and in the late directions. NCCR reporter and pGL3 basic control constructs were co-transfected with (black bar) and without (white bar) full-length VR837-derived Tag in HSG cells (Fig. 3.2B and 3.2C). Promoter activity was determined as fold luciferase (luc) induction over pGL3 basic. Tag protein expression was confirmed by immunoblot analysis. Similar promoter activity levels were achieved for both HIVSGD-1 and HIVSGD-2 in the early direction, independent of Tag presence or absence: 2.7 vs. 2.4 fold and 12 vs.11.4 fold induction respectively (Fig. 3.2B). HIVSGD-2 promoter activity was higher than HIVSGD-1in the late direction independent of Tag presence or absence: 54 vs. 31 fold and 7 vs. 2 fold induction respectively (Fig. 3.2C). Overall, NCCR activity differences between HIVSGD -1 and HIVSGD-2 were nominal. Functional Tag is known to suppress the BKPyV NCCR in the early and induce in the late direction (4). Hence, the observations made here suggested that the cloned HIVSGD NCCRs were functional within the reporter constructs.

A
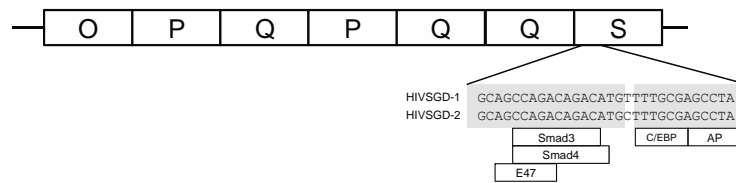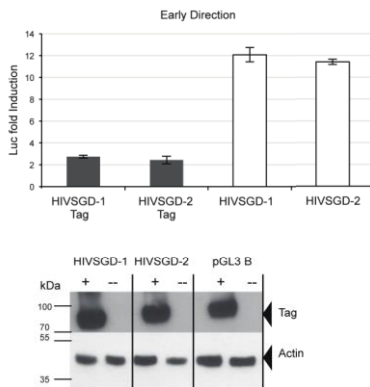
B   C
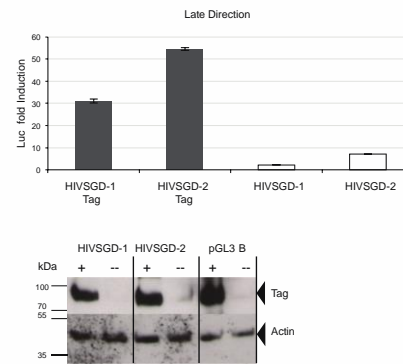
Figure. 3.2. Similar trends in promoter activity were detected for HIVSGD-1 and

HIVSGD-2 BKPyV. A. Schematic represents HIVSGD BKPyV NCCR block architecture and

thymidine/cytidine transition within the S block. Identical human putative transcription factor

binding sites (TFBS) were predicted for HIVSGD-1 and HIVSGD-2 despite the transition: E47,

Smad3, Smad4, C/EBPα (C/EBP) and AP-2αA (AP). B./C. Graphs show NCCR luciferase (luc)

activity in the presence and absence of wild-type Tag for the early (B.) and the late (C.) promoter

direction. Luc activity was depicted as fold induction relative to pGL3 basic (pGL3 B) and error

bars represent standard deviations. Tag (Myc-tagged Tag ~82kDa) and actin (~45kDa) protein

expression were visualized by immunoblotting.

The adenosine (A) deletion detected within the Tag nucleotide sequence of HIVSGD-2 but not within HIVSGD-1 was analyzed for potential biological significance (Fig. 3.3A). ClustalW (47) based Tag amino acid sequence alignment of HIVSGD-1, HIVSGD-2 and the SV40 pRb binding domain (1GH6:ChainA) located the deletion distal to the pRb binding site of the Tag viral protein and detected 82.5% sequence identity between SV40 and HIVSGD-1 full-length Tag. The deletion was predicted to introduce an early stop codon that truncated the original Tag nuclear translocation signal from PKKKRKV to PKKKER (Fig. 3.3B). HIVSGD-2 Tag, that carried the early stop codon, was calculated to express a Tag mutant of 15.6 kDa instead of the 80.5 kDa full length Tag expressed by BKPyV HIVSGD-1 (Fig. 3.3C). A schematic model of full-length HIVSGD-1 and truncated HIVSGD-2 Tag was created using the HHPred and MODELLER structural prediction tools (48). This truncating deletion was likely the most significant of the three nucleotide mutations due to the importance of Tag for the viral life cycle.

Assessment of HIVSGD BKPyV replication *in vitro*: post-transfection

The post-transfection replication potential of HIVSGD-1 and HIVSGD-2 BKPyV was assessed within human salivary gland and kidney cells (Fig. 3.4). BKPyV clones of throatwash-derived HIVSGD-1 and HIVSGD-2, kidney-derived U1 and laboratory strains MM and Dunlop were used for *in vitro* analysis (Table 3.1). Laboratory strain VR837 was used as infectious BKPyV positive control.

The capacity for *de novo* BKPyV DNA synthesis post-salivary gland cell (HSG)-transfection was determined. HSG cells were transfected with HIVSGD-1 (encoding full-length Tag), U1, MM and Dunlop BKPyV episomes and evaluated using a restriction enzyme resistance assay. The Dpn1/Sau3a enzyme resistance assay allowed discernment between transfected

BKPyV genomes (methylated bacterial plasmid DNA) and BKPyV genomes made *de novo* (non-methylated eukaryotic DNA). DNA was isolated six days post-transfection (dpt), digested with Dpn1 and Sau3a and visualized by Southern blot (Fig. 3.5). Dpn1 and Sau3a cleaved the same restriction sites, but Dpn1 digested exclusively bacterial and not eukaryotic methylation patterns, while Sau3a digestion was methylation pattern-independent (9, 49). While multiple bands were detected post Sau3a digestion, clear differences in the banding pattern are detected upon comparison to Dpn1 digestion for both HIVSGD-1 and of MM BKPyV DNA. The detection of HIVSGD-1 (Fig. 3.5B; lane 5 vs. lane 6) and MM (Fig. 3.5A; lane 7 vs. lane 8) DNA bands post-Sau3a, but not post-Dpn1 digestion, in the range of 100bp to 1600bp, suggested that the detected BKPyV DNA was of eukaryotic origin and therefore HIVSGD-1 and MM BKPyV underwent whole genome replication in HSG cells. While not all bands are distinct, they corresponded to mapped MM BKPyV (GenBank V01109.1) Dpn1/Sau3a cut sites resulting in fragments ranging from 1kb to 1.6kp. BKPyV DNA bands between 1.6kb and 5kb and are likely due incomplete digestion and prominent bands at ~5kb (Fig. 3.5A, lane 7) correspond to whole genome BKPyV as previously reported (9). In summary, the enzyme resistance assay suggested that both HIVSGD-1 and MM BKPyV DNA were made *de novo* in transfected HSG cells. The intention of this assay was not to compare BKPyV replication levels, but to firmly establish that HIVSGD-1 BKPyV could replicate its DNA in human salivary gland cells. Faint kidney-derived U1 BKPyV DNA bands were visualized upon long exposure, suggesting potential replication (Fig. 3.5A, lane 3 and lane 4).

Figure. 3.3. HIVSGD BKPyV Tag sequence analysis revealed a premature stop codon in HIVSGD-2. A. The depicted BKPyV DNA sequences show the Tag adenosine (A) deletion found within HIVSGD-2 but not HIVSGD-1. B. Alignment of the Tag amino acid sequences of HIVSGD-1, HIVSGD-2 and the SV40 pRb binding domain (1GH6:chainA) via ClustalW localized the deletion distal to the pRb binding domain. The deletion was predicted to alter the original PKKKRKV nuclear translocation signal found within HIVSGD-1 into PKKKER (see square) in HIVSGD-2. C. The deletion was further predicted to introduce an early stop codon

(see square) and subsequently truncate HIVSGD-2 Tag. Schematic models of full-length

HIVSGD-1 Tag (wildtype, 80.5 kDa protein) and truncated HIVSGD-2 Tag (15.6 kDa protein)

were created using the HHPred and MODELLER structural prediction servers (sequence and

model coloring coincide). Left depicting full-length and right truncated sequence and schematic

models respectively.
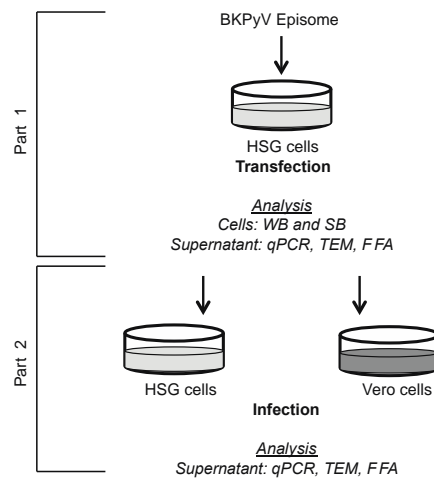
Figure. 3.4. Multi-step salivary gland cell *in vitro* system for viral fitness assessment. The

diagram shows the two parts of the *in vitro* model: Part 1: human salivary gland cell (HSG)

transfection with episomal BKPyV. Part 2: HSG and Vero cell infection with transfection-

derived BKPyV.
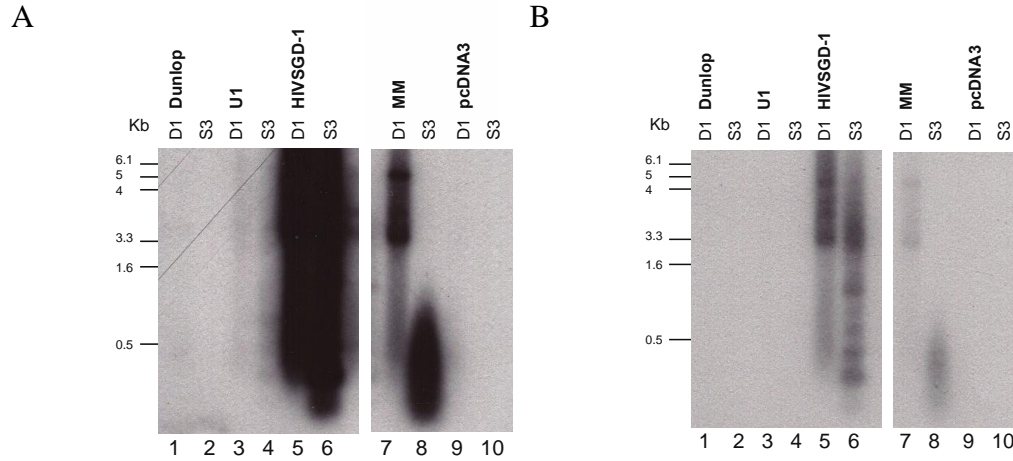
Figure. 3.5. HIVSGD-1 and MM BKPyV DNA were made *de novo* in human salivary gland cells. Panel A and panel B show the same blot at different exposures (A. 15 min and B. 1 min exposure). Low molecular weight DNA was isolated 6 days post-HSG cell transfection with Dunlop, MM, U1 and HIVSGD-1 BKPyV DNA. pcDNA3 DNA transfection served as negative control. Isolated DNA was digested with endonucleases Dpn1 (D1) and Sau3a (S3) and visualized via Southern blot. Dpn1 and Sau3a cut the same sites, but Dpn1 recognizes exclusively bacterial and not eukaryotic methylation patterns. DpnI resistance assay allows differentiation of BKPyV DNA that was transfected (of bacterial origin) and BKPyV DNA that was made *de novo* by HSG cells (of eukaryotic origin). Detection of stronger DNA bands (at expected size) post-Sau3a digestion vs. post-Dpn1 digestion as seen for BKPyV HIVSGD-1 and MM DNA (lane 5 vs. lane 6 and lane 7 vs. lane 8) suggested that BKPyV DNA was made *de novo* by transfected HSG cells. No Dunlop BKPyV DNA (lanes 1 and 2) and faint U1 (lanes 3 and 4) bands were found.

Tag protein expression reflects successful transition through the early BKPyV life cycle. The consequence of the HIVSGD-2 Tag mutation on its protein expression was assessed. Levels of Tag protein expression were determined five days post-HSG transfection and compared

among clinical isolates HIVSGD-1, HIVSGD-2, U1 and laboratory strain MM BKPyV by Western Blot (Fig. 3.6A). The laboratory strain Dunlop BKPyV was not further assessed as HSG cells were unable to support DNA replication (Fig. 3.5). The harvest time point was selected based on previous studies that detected Tag protein expression 4 dpt (26, 34). Tag was normalized to beta-actin expression, a loading control (Fig. 3.6B). Highest Tag expression was detected for HIVSGD-1 (full-length, ~80kDa), followed by MM and U1 BKPyV (Fig. 6B). Both full-length and truncated (~15 kDa, not shown) forms of Tag protein were below the level of immunoblot detection for HIVSGD-2. No Tag protein was detected in mock infected negative controls.

To further evaluate the replication potential of each isolate, encapsulated BKPyV virions, released from transfected HSG cells were quantified. At 6 dpt, BKPyV viral loads (VLs) of filtered and DNAse treated media from transfected HSG cells were determined by quantitative real time PCR (qPCR). The supernatant of all BKPyV transfected HSG cells carried encapsulated BKPyV DNA. MM and HIVSGD-1 transfected HSG cells supported similarly high VLs, with 3.5×10^7 and 2.4×10^7 copies/μl respectively. U1 and HIVSGD-2 VLs were significantly lower than HIVSGD-1, with VLs of 1.4×10^3 and 2.6×10^2 copies/μl respectively (Fig. 3.7A). Differences between HIVSGD-2 and U1 VLs each compared to HIVSGD-1 were highly statistically significant (p=0.0001). HIVSGD-1 was the most efficient replicator, followed by MM, U1 and HIVSGD-2. Interestingly, low levels of HIVSGD-2 virions were detected, despite the Tag mutation and lack of Tag expression, described above. To confirm the presence of BKPyV virions, HSG supernatant (6 dpt) was analyzed by transmission electron microscopy (TEM). BKPyV particles were detected by TEM for HIVSGD-1 and MM but were not detected for lower replicators U1 or HIVSGD-2 BKPyV (Fig. 3.7B). Morphological features of HIVSGD-

1 and MM BKPyV were reminiscent of icosahedral (T=7) symmetrical BKPyV particles with a diameter of 45nm (4) that have been visualized in *in vitro*-derived supernatants (34) and patient-derived fluids (50).

The titer of infectious HSG transfection-derived BKPyV virions was determined via the fluorescent focus assay (FFA). FFA provided antibody based detection of intracellular PyV proteins post-infection (44). Vero cells were exposed to HSG cell supernatant containing BKPyV, incubated for 4 days and infected cells were quantified. Intracellular PyV structural proteins (VP1, VP2, VP3; green) were detected for HIVSGD-1, HIVSGD-2 and laboratory strain MM, but not for U1 BKPyV or mock infection (Fig. 3.8). As in previous studies (44), PyV proteins were detected exclusively in the nucleus (DAPI/blue) of infected Vero cells (Fig. 3.8C). Infectious BKPyV VR837, which has been shown to replicate permissively in HSG and Vero cells (26) served as positive control. HIVSGD-1, MM and HIVSGD-2 scored 80, 50 and 1 FFU/µl respectively. HIVSGD-1 infected significantly more cells than laboratory strain MM (p=0.01) and HIVSGD-2 (p=0.0001, Fig. 3.8B). Despite detectable U1 VLs by qPCR , U1 BKPyV intracellular proteins were not detected by FFA.
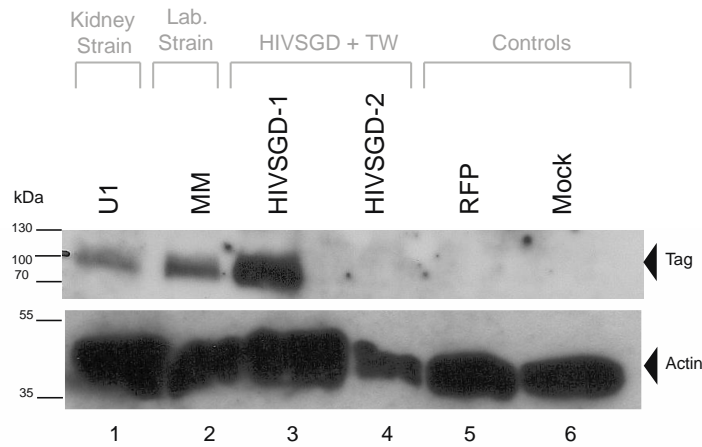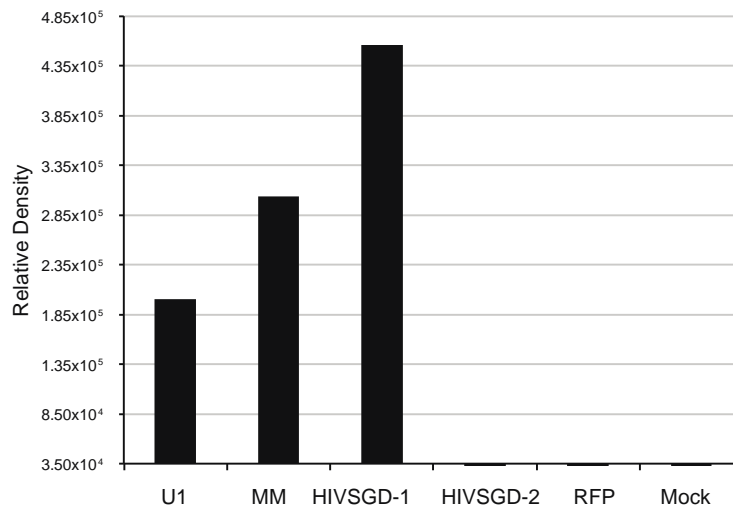
Figure 3.6. HIVSGD-1 but not HIVSGD-2 expressed BKPyV Tag protein post-HSG cell transfection. A. Panel shows protein bands visualized via Western Blotting (WB). Total cell lysates were harvested 5 dpt and proteins analyzed by WB, probing for viral Tag (~82kDa) and cellular β–actin (~45kDa, loading control). Tag expression levels ranked (high to low): HIVSGD-1, MM and U1 BKPyV. No HIVSGD-2 Tag protein was detected. B. The chart shows relative protein band density, measured by densitometry and normalized to actin.

A
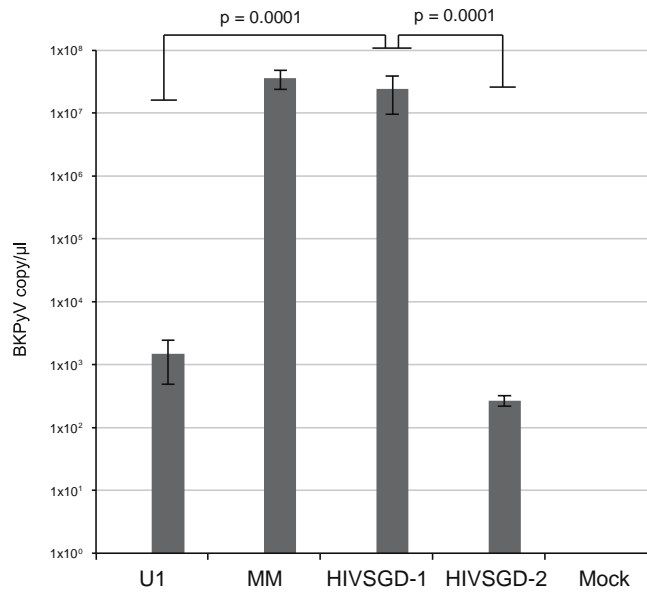
B
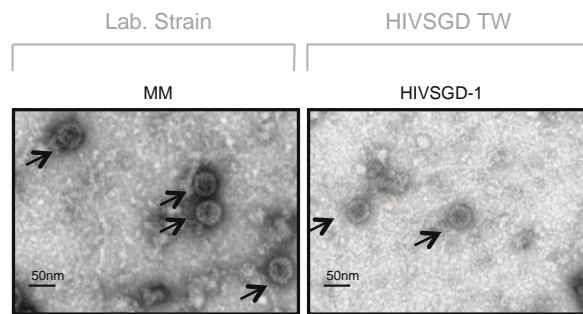
Figure 3.7. Significantly higher viral loads were detected for HIVSGD-1 than for HIVSGD-2 BKPyV post-HSG cell transfection. A. The chart shows viral loads (VL) measured from the supernatant of HSG cells transfected with BKPyV genomes. HSG cell supernatant was harvested 6 dpt, filtered, DNAse treated, BKPyV quantified via qPCR and depicted as BKPyV copy/µl. VL levels ranked (high to low): MM, HIVSGD-1, U1 and HIVSGD-2 BKPyV. The p values were determined via One-way ANOVA and error bars represent standard deviations. B. Representative images visualizing HIVSGD-1 and MM BKPyV virions from HSG cell supernatant via transmission electron microscopy (TEM) 6 dpt (see black arrows).
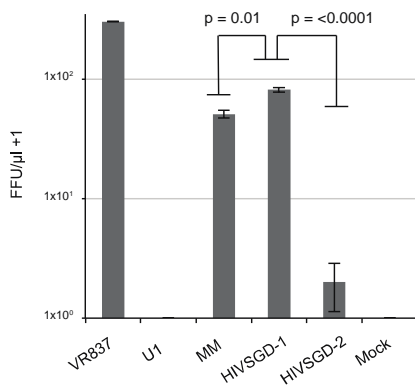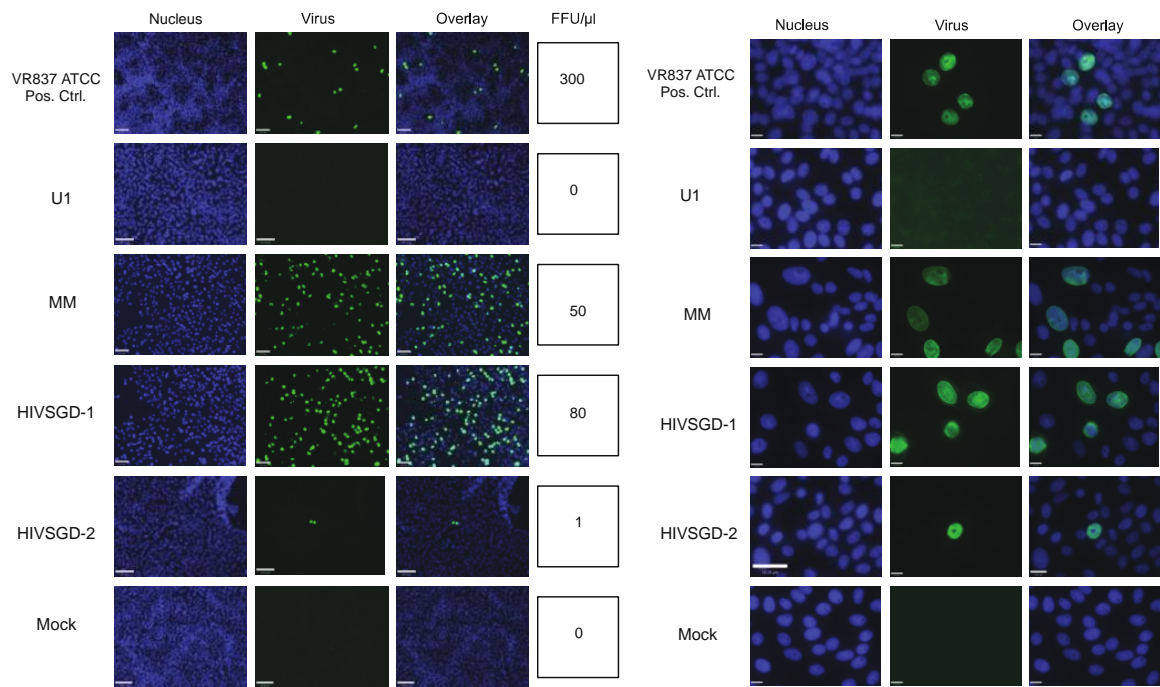
Figure 3.8. Infectious HIVSGD-1, HIVSGD-2 and MM BKPyV progeny were detected post-HSG cell transfection. A. Representative images showing HIVSGD-1, HIVSGD-2, MM and VR837 BKPyV infected Vero cells. Transfected HSG cell supernatant was transferred onto Vero cells and BKPyV infected cells visualized via FFA. BKPyV protein (green) was detected in the nucleus (DAPI/blue). VR837 infection served as positive control. The number of infected cells was counted for each treatment in a minimum of 10 fields at 20X magnification and FFU/µl values were calculated. B. FFU values were graphed for each treatment and depicted as FFU/µl+1. The error bars represent the standard deviation and the p values were assessed via One-way ANOVA. C. Representative images at higher magnification: IFA, 60X, oil immersion.

Clinical and laboratory strain BKPyV: post-infection

Infections were performed to assess cell-type dependent reproduction of HSG-derived BKPyV (Part 2, Fig. 3.4). HSG and Vero cells were simultaneously infected with equal amounts of BKPyV that originated from HSG cell transfections; an equivalent of 200 FFU for each viral substrain (Part 1, Fig. 3.4). Encapsulated BKPyV virions released from infected HSG and Vero cells were quantified by qPCR at 2, 4, 6 and 8 days post-infection (dpi). HIVSGD-1 and MM BKPyV VLs increased by 4 and 3 orders of magnitude, respectively, in HSG cells over 8 dpi. In Vero cells, HIVSGD-1 and MM BKPyV VLs increased by 5 and 4 orders of magnitude respectively over 8 dpi (Fig 3.9A). These results indicated that HSG cell transfection-derived HIVSGD-1 and MM BKPyV were infectious and underwent replication in both HSG and Vero cells. Encapsulated HIVSGD-2 and U1 BKPyV DNA were not detected from either cell type. Interestingly, VL kinetics of BKPyV in Vero and HSG cells were similar upon infection, suggesting that virion production was equally efficient in both HSG and Vero cells post-infection. TEM confirmed BKPyV virion presence and morphology via (8 dpi). Visualized particles were classified as BKPyV based on capsid morphology and diameter. BKPyV particles were detected in the media of HSG cells infected with HIVSGD-1 and in Vero cells infected with HIVSGD-1 and MM BKPyV (Fig. 3.9B). U1 and HIVSGD-2 virions were not identified upon inspection. MM BKPyV infected HSG cell media was not analyzed by TEM.

The infectivity of HSG and Vero derived BKPyV progeny was assessed by FFA (Fig. 3.10). Vero cells were infected with HSG and Vero cell media 8 dpi and incubated over 4 days. PyV structural proteins (VP1, VP2, VP3; green) were detected at 289 FFU/µl for VR837 (positive control) and no viral proteins were detected in mock infections (Fig. 3.10A). HSG cell infection-derived MM and HIVSGD-1 BKPyV both scored 48 FFU/µl whereas U1 scored 5

FFU/µl (9.6 fold less). No infectious HIVSGD-2 BKPyV was detected (Fig. 3.10B).

Interestingly, much lower FFUs were detected in <u>Vero cell</u> infection-derived MM and HIVSGD-1 BKPyV (10 FFU/µl and 19 FFU/µl respectively) as compared to these viruses of HSG-cell origin (48 FFU/µl). These results indicated that HIVSGD-1 and MM BKPyV were more infectious originating from HSG (salivary gland) cells than Vero (kidney) cells (Fig. 3.10C and 3.10D) despite the detection of similar VLs in both cell types (Fig. 3.9). Most strikingly, among Vero cell-derived BKPyV, the kidney-derived virus U1 (58 FFU/µl), was most infectious and displayed 5.8 fold higher FFU/µl than MM and 3 fold higher FFU/µl than HIVSGD-1 BKPyV. Despite the lack of detectable VLs (Fig. 3.9) U1 (kidney-derived) BKPyV scored higher FFUs originating from kidney (Vero) cells than salivary gland (HSG) cells (Fig. 3.10C and 3.10D). As expected, the lack of measurable HIVSGD-2 BKPyV VL was associated with an inability to detect infected cells, whether Vero or HSG cell-derived.

Discussion

HIV-associated salivary gland disease (HIVSGD) is among the most significant HIV/AIDS-associated oral lesions (25). Previously published data by our group suggested a correlation between HIVSGD and BKPyV (25, 26). To our knowledge, we are the first to analyze HIVSGD BKPyV and to establish a fully permissive salivary gland cell culture model supporting productive replication of clinical BKPyV isolates. The present study assessed replication differences in genomically similar HIVSGD isolates and compared a kidney-derived clinical isolate to HIVSGD clinical isolates. We assessed the non-coding control region (NCCR) of these isolates and determined in *vitro* replication capabilities in both salivary gland and kidney

cells. Importantly, this study provides evidence for differences in cell tropism based on the cell origin of BKPyV.

Three clinical BKPyV isolates were characterized and compared: HIVSGD-1 and HIVSGD-2 were isolated from the throatwash (TW) samples of HIVSGD positive patients and U1 was isolated from the urine sample of a HIVSGD negative transplant patient (kidney-associated isolate). BKPyV viral loads (VLs) from all three clinical samples were high and ranged from 1.7×10^5 to 1.7×10^9 copies/ml, likely reflecting immunosuppression in each instance. We previously established that VLs in healthy individuals and in HIV positive patients without HIVSGD were 3 to 4 logs lower than the VLs detected in HIVSGD positive individuals (25). Comparable VLs in the HIVSGD-associated oral fluid samples and in the urine sample of a transplant patient diagnosed with BKN suggested a significant increase in shed virus, perhaps at pathogenic levels.

Whole genome sequence alignment of the two HIVSGD clones (HIVSGD-1 and HIVSGD-2) determined 99.9% similarity, despite three point mutations (Fig. 3.1A). A thymidine deletion was detected between the open reading frames (ORFs) that encoded agnoprotein and VP2 (Fig. 3.1A, 1). The deletion was outside of the respective ORFs and was therefore unlikely to affect replication. Nevertheless, it was possible that the mutation could have interfered with VP2 gene expression via disruption of a potential internal ribosome entry site (IRES) that was present in this region of the BKV genome. However, the affected nucleotide stretch did not contain a known IRES (Fig. 3.1B).

The BKPyV NCCR is the main determinant of *in vitro* replication (9) and rearrangements confer significant differences in replication capacity, transforming potential, host cell permissivity and tropism (12, 37, 39, 40, 51-53). NCCR rearrangements are defined as changes

in the NCCR block sequences as compared to the archetype. The archetypic BKPyV substrain, defined by carrying the OPQRS NCCR architecture, is commonly shed in urine (5). We sequenced the BKPyV NCCR of the three clinical isolates and detected a common signature OPQPQQS block alignment among the HIVSGD TW samples. NCCR block divergence from archetype into rearranged (rr) variants, as detected in this study, have been previously recorded both *in vivo* (16, 51, 54, 55) and *in vitro* (16, 35, 37, 38, 56). Prior studies among transplant recipients with prolonged viremia illustrated, that rearranged architectures eventually became dominant over the archetype (39). The rr NCCR OPQPQQS may reflect the dominant architecture within these HIVSGD patients and may represent a stable and biologically significant variant. Despite VP1-based classification of BKPyV genotypes (57), BKPyV variants are categorized by NCCR block sequence (58). The OPQPQQS NCCR block alignment was previously described in laboratory strain MM, however, to our knowledge, other clinical isolates carrying this architecture have not been reported. Importantly, underlying nucleotide differences distinguished the HIVSGD clinical isolates from MM. Inclusion of well-described BKPyV laboratory strains during NCCR genotyping corroborated the authenticity of our results.

HIVSGD-1 and MM BKPyV shared NCCR OPQPQQS block architecture, and exhibited similar levels of Tag expression, virion production and infectivity. Similar replication efficiency between HIVSGD-1 and MM may be explained by the analogous NCCR architecture. HIVSGD-2, however, consistently lacked signs of efficient *in vitro* replication. While HIVSGD-2 shared the overall NCCR architecture with HIVSGD-1 and MM, the HIVSGD-2 NCCR S block contained a thymidine (T)/cytidine (C) transition (Fig. 3.1A, 2). This NCCR transition did not lead to differential prediction of putative human TFBS (Fig. 3.2A) or to differences in the early promoter activity in the presence or absence of full-length Tag (Fig. 3.2B), thus was an unlikely

contributor to differences in replication efficiency. Interestingly, the HIVSGD-2 promoter in the late direction was induced more readily, in the presence or absence of full-length Tag, than the high replicator HIVSGD-1 (Fig. 3.2C). Based on *in vitro* results that characterized HIVSGD-2 as an inefficient replicator, higher HIVSGD-2 promoter activity in the late direction was unlikely to affect its viral fitness. Despite the well-documented importance of the NCCR for BKPyV replication, the S block point mutation appeared unlikely to affect viral fitness.

Inefficient HIVSGD-2 replication was likely associated with the adenosine deletion distal to the Tag pRb binding domain. This point mutation was predicted to introduce an early stop codon and modify the nuclear translocation signal (Fig. 3.3A and 3.3B). This resulted in the expression of a truncated form of Tag that decreased the predicted Tag protein size from 80.5 kDa to 15.6 kDa. The mutant form of Tag lost the origin-binding domain (OBD), p53 site and ATP/helicase domain (Fig. 3.3C) and carried a modified version of the nuclear translocation signal (Fig. 3.3A and 3.3B). Tag is central to genome replication and PyV life cycle completion (59-61). Insufficient Tag expression has been shown to impede archetypic BKPyV replication *in vitro* (34). It is therefore likely that insufficient Tag expression dramatically inhibited HIVSGD-2 replication. Remarkably, the isolation of HIVSGD-2 BKPyV from the TW sample and generation of progeny virus served as evidence of minimal HIVSGD-2 replication both *in vivo* and *in vitro*. HIVSGD-2 virus was detected at low levels post-transfection as determined by qPCR (VL measurement, Fig. 7) and was infectious as measured by FFA (Fig. 3.8). Two potential mechanisms that may have allowed for low levels of HIVSGD-2 replication: 1) *in vivo* - Provision of Tag in trans by other BKPyV substrains. Broekema *et al*. demonstrated that provision of overexpressed Tag allowed the cultivation of archetype BKPyV, a typically low *in vitro* replicator (34). 2) *in vitro* and *in vivo* - Low levels of full-length Tag could be produced by

ribosomal frame shifting. Ribosomal frame shifting commonly takes place in retroviruses facilitated by a slippery A/T-rich heptanucleotide sequence that allows for low protein expression despite the presence of a stop codon (62). The A/T rich stretch within HIVSGD-2 BKPyV Tag located 5' to the stop codon may allow for frame shifting in the context of BKPyV. Moreover, premature truncations of Tag have been detected in other PyVs. Merkel Cell polyomavirus (MCV) mutations that prematurely truncated Tag, were found in human tumor-derived but not in benign sources, and have been postulated to render MCV more malignant (60). Likewise, there is the potential that truncation of HIVSGD BKPyV Tag may not only decrease replication efficiency but may also be associated with increased *in vivo* transformation potential.

HIVSGD BKPyV *in vitro* viability was assessed by transfection (Part 1, Fig. 3.4) and infection (Part 2, Fig. 3.4) of salivary gland cells and kidney cells. Kidney cells represented the historically described replication niche. HIVSGD BKPyV fitness was compared to both kidney-derived substrain U1 and laboratory strain MM (Table 3.1). We hypothesized that shed HIVSGD isolates were likely to replicate in salivary gland cells *in vivo* and by extension these isolates would replicate efficiently within HSG cells *in vitro*. Indeed, HIVSGD-1 consistently exhibited high replication competence in salivary gland cells. HIVSGD-1 and MM demonstrated highest post-transfection replication efficiency compared to HIVSGD-2 and kidney-derived U1, as determined by viral protein concentrations (Fig. 3.6), VLs (Fig. 3.7) and significant levels infectious BKPyV progeny (Fig. 3.8). Furthermore, the high replication capability of HIVSGD-1 was consistent during infection of HSG and Vero cells (Fig. 3.4, Part 2) with high levels of HSG cell-released progeny virus (Fig. 3.9). HIVSGD-1, MM and U1 but not HIVSGD-2 completed a full life cycle upon secondary viral passage.

HIVSGD-1 and MM VL measurements suggested equally efficient virion production upon infection of HSG and Vero cells, as replication kinetics were very similar (Fig. 3.9). Differences in scored infectious units however, suggested that while replication kinetics and progeny output were consistent for HIVSGD-1 and MM, subsequent infectivity was distinct depending on cell type and virus origin comparing HIVSGD-1/MM vs. kidney-derived U1 (Fig. 3.10D). When HIVSGD-1 and MM BKPyV originated from HSG cells rather than Vero cells higher FFUs were scored. Likewise, when kidney-derived U1 BKPyV originated from Vero cells rather than HSG cells higher FFUs were scored. Differential infectivity suggested HIVSGD BKPyV displayed preferential tropism for salivary gland cells over kidney cells. Similarly, U1 displayed preferential tropism for kidney cells over salivary gland cells. Additionally, we recorded a dramatic increase in viral progeny production for Vero cell-derived U1 during the 4 day Vero cell incubation for the FFA (Fig. 3.10). This was interesting since U1 VLs were below the level of detection for qPCR quantification at 8 dpi (Fig. 3.9), and suggested that kidney-derived U1 BKPyV was able to produce infectious progeny more efficiently in kidney cells (58 FFU/μl) than HSG cells (5 FFU/μl, Fig. 3.10). Overall, differential infectivity depending on cell origin suggested that U1 displayed kidney tropism and HIVSGD BKPyV displayed salivary gland tropism, consistent with their respective *in vivo* kidney and salivary gland origins. Interestingly, previous studies comparing laboratory strain BKPyV replication among a wide range of different cell lines detected few differences in replication potential and did not indicate specific cellular tropisms (63, 64). These studies assessed over 60 cell types among them were lung-, colon-, CNS-, ovary-, renal- and bladder-derived cell lines; salivary gland cells were not assessed.

BKPyV isolated from the TW of HIVSGD patients is likely relevant to disease in the *in vivo* setting and has now undergone initial *in vitro* characterization. High BKPyV VLs were detected in the oral fluids of two individuals diagnosed with HIVSGD. We identified a common NCCR block architecture among HIVSGD-derived BKPyV isolates and successfully cultured clinical HIVSGD-derived BKPyV in human salivary gland cells and in kidney cells. Our assessment of a high and a low replicating clinical isolate suggested that a single point mutation in Tag brought about the stark differences in the *in vitro* replication potential. The high replicator (HIVSGD-1) surpassed the replication potential of the kidney-derived isolate (U1) in human salivary gland cells, replicated efficiently in human salivary gland and kidney cells and displayed signs of salivary gland tropism.

Our results are significant, as they corroborate a potential connection between BKPyV and HIVSGD and provide an important initial understanding of BKV replication in the oral compartment. Our data suggest that HIVSGD TW-derived BKPyV displays preferential tropism for salivary gland cells and we have now proven that wild type oral-clinical BKV isolates undergo permissive replication in salivary gland cells *in vitro*. Permissive replication of wild type clinical BKV isolates previously thought to occur predominately in renal- and uro-epithelium may be ongoing at other sites as well. Saliva serves as a transmission vehicle for many microorganisms and our data corroborate previous data showing that the oral compartment and saliva may function as a transmission vehicle for BKPyV *in vivo as* well. The small number of characterized HIVSGD isolates is a clear limitation of this current study and thus may not be representative of all HIVSGD variants. A study encompassing a larger number of isolates, would be more representative and needs to be performed. Importantly, this study provides a system for

the study of clinical oral BKPyV infection and these observations provide insights to future

BKPyV pathogenesis, transmission and disease-association studies.

A
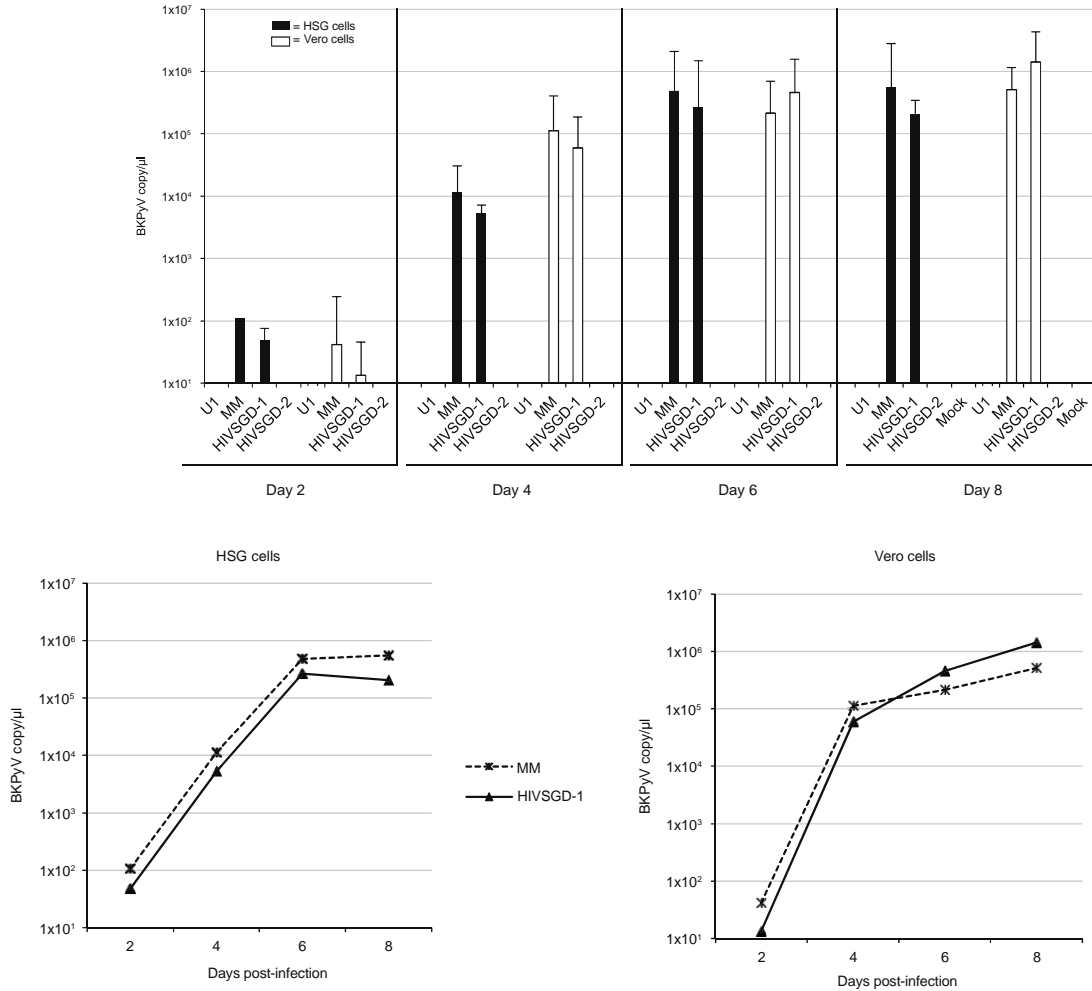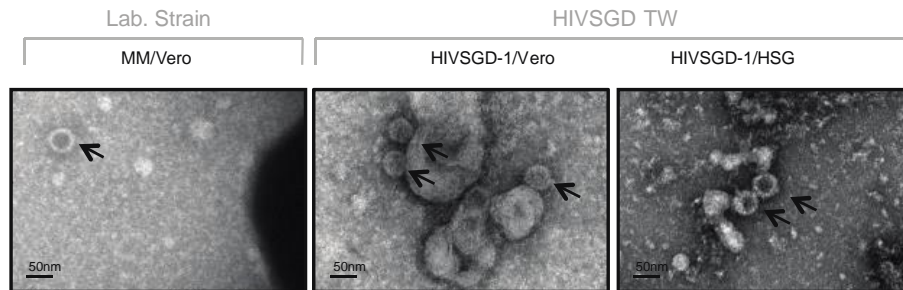
Figure 3.9. HIVSGD-1 and MM BKPyV exhibited similar replication kinetics in HSG and

Vero cells with increasing viral loads post-infection. A. The chart shows viral loads (VLs) in

BKPyV copy/μl, measured from the supernatant of infected HSG and Vero cells, 2, 4, 6 and 8

dpi. Filtered supernatant from transfected HSG cells was used to infect HSG (black) and Vero

(white) cells at equal viral loads. Supernatant from infected cells was harvested, filtered, DNAse

treated and BKPyV VL quantified via qPCR. BKPyV HIVSGD-1 VLs increased over 6 orders of

magnitude and MM over 5 orders of magnitude during the 8 dpi. Encapsulated HIVSGD-2 and

U1 BKPyV DNA were not detected. Error bars represent standard deviations. Graphed VLs from

infected HSG cells and Vero cells show similar growth kinetics for BKPyV HIVSGD-1 and

MM. B. HIVSGD-1 (Vero- and HSG cell-derived) and MM (Vero cell-derived) BK virions were

detected under TEM 8 dpi. MM BKPyV infected HSG supernatant was not analyzed. No virions

were detected for HIVSGD-2, U1 and mock infection in HSG or Vero cells (data not shown).

Mock infections were accomplished by using supernatant from mock transfected cells.
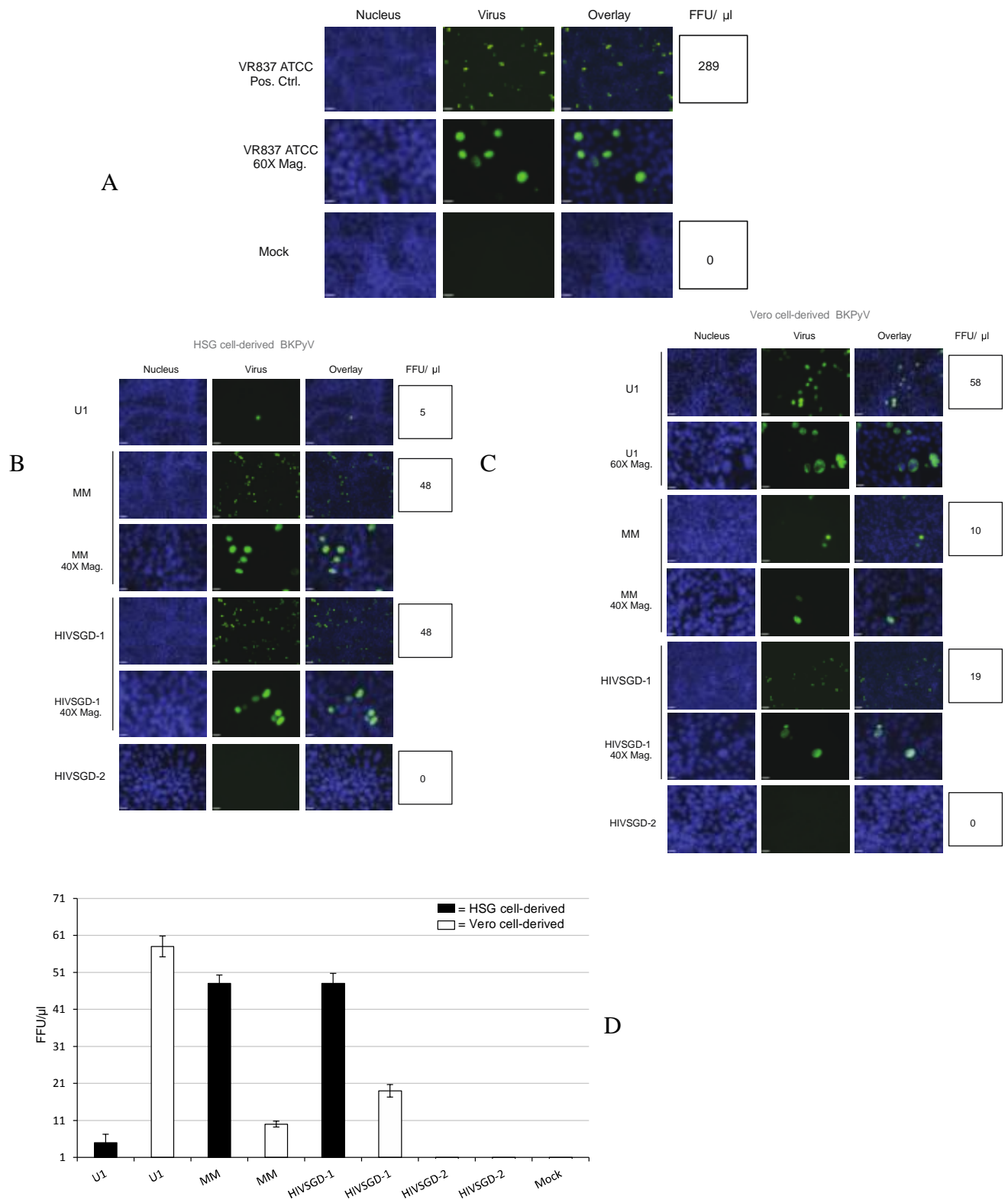
Figure 3.10. Cell type-dependent differential infection was detected based on viral origin.

A. Representative images of FFA controls: positive (VR837 BKPyV infection; 289 FFU/µl) and

negative (Mock infection; no virus detected). Infected cells (green) and nuclei (blue) were quantified and FFU/µl values calculated. B. Representative images of HIVSGD-1, U1 and MM BKPyV infected cells are shown. Supernatant of infected <u>HSG cells</u> (8dpi) was filtered and transferred onto Vero cells. HIVSGD-1 and MM and yielded 48 FFU/µl. U1 yielded 5 FFU/µl. No infected cells were detected for the HIVSGD-2 treatment. C. Representative images of HIVSGD-1, U1 and MM BKPyV infected cells are shown. Supernatant of infected <u>Vero cells</u> (8 dpi) was filtered and transferred onto Vero cells. Infected cells were visualized via FFA (green), quantified and FFU values calculated. HIVSGD-1 yielded 19 FFU/µl, MM yielded 10 FFU/µl and U1 yielded 58 FFU/µl. No infected cells were detected for the HIVSGD-2 treatment. D. The chart shows FFU values for each treatment, depicted as FFU/µl: HSG cell infection-derived BKPyV, (black bar), Vero cell infection-derived BKPyV (white bar). Error bars represent standard deviations

REFERENCES

1. **Gardner, S. D., A. M. Field, D. V. Coleman, and B. Hulme.** 1971. New human papovavirus (B.K.) isolated from urine after renal transplantation. Lancet **1:**1253-7.

2. **Kean, J. M., S. Rao, M. Wang, and R. L. Garcea.** 2009. Seroepidemiology of human polyomaviruses. PLoS Pathog **5:**e1000363.

3. **Knowles, W. A.** 2006. Discovery and epidemiology of the human polyomaviruses BK virus (BKV) and JC virus (JCV). Adv Exp Med Biol **577:**19-45.

4. 2007. Fields' Virology. *In* P. M. H. David M. Knipe (ed.), 5th ed. Wolters Kluwer Health/Lippincott Williams & Wilkins, Philadelphia.

5. **Reploeg, M. D., G. A. Storch, and D. B. Clifford.** 2001. Bk virus: a clinical review. Clin Infect Dis **33:**191-202.

6. **Egli, A., S. Binggeli, S. Bodaghi, A. Dumoulin, G. A. Funk, N. Khanna, D. Leuenberger, R. Gosert, and H. H. Hirsch.** 2007. Cytomegalovirus and polyomavirus BK posttransplant. Nephrol Dial Transplant **22 Suppl 8:**viii72-viii82.

7. **Nickeleit, V., and M. J. Mihatsch.** 2006. Polyomavirus nephropathy in native kidneys and renal allografts: an update on an escalating threat. Transpl Int **19:**960-73.

8. **Bohl, D. L., and D. C. Brennan.** 2007. BK virus nephropathy and kidney transplantation. Clin J Am Soc Nephrol **2 Suppl 1:**S36-46.

9. **Broekema, N. M., J. R. Abend, S. M. Bennett, J. S. Butel, J. A. Vanchiere, and M. J. Imperiale.** 2010. A system for the analysis of BKV non-coding control regions: application to clinical isolates from an HIV/AIDS patient. Virology **407:**368-73.

10. **Markowitz, R. B., and W. S. Dynan.** 1988. Binding of cellular proteins to the regulatory region of BK virus DNA. J Virol **62:**3388-98.

11.   **Gorrill, T. S., and K. Khalili.** 2005. Cooperative interaction of p65 and C/EBPbeta modulates transcription of BKV early promoter. Virology **335:**1-9.

12.   **Johnsen, J. I., O. M. Seternes, T. Johansen, U. Moens, R. Mantyjarvi, and T. Traavik.** 1995. Subpopulations of non-coding control region variants within a cell culture-passaged stock of BK virus: sequence comparisons and biological characteristics. J Gen Virol **76 (Pt 7):**1571-81.

13.   **Cho, S., Y. Tian, and T. L. Benjamin.** 2001. Binding of p300/CBP co-activators by polyoma large T antigen. J Biol Chem **276:**33533-9.

14.   **Abend, J. R., A. E. Joseph, D. Das, D. B. Campbell-Cecen, and M. J. Imperiale.** 2009. A truncated T antigen expressed from an alternatively spliced BK virus early mRNA. J Gen Virol **90:**1238-45.

15.   **Tognon, M., A. Corallini, F. Martini, M. Negrini, and G. Barbanti-Brodano.** 2003. Oncogenic transformation by BK virus and association with human tumors. Oncogene **22:**5192-200.

16.   **Bennett, S. M., N. M. Broekema, and M. J. Imperiale.** 2012. BK polyomavirus: emerging pathogen. Microbes Infect **14:**672-83.

17.   **White, M. K., M. Safak, and K. Khalili.** 2009. Regulation of gene expression in primate polyomaviruses. Journal of virology **83:**10846-56.

18.   **Khalili, K., and G. L. Stoner.** 2001. Human polyomaviruses : molecular and clinical perspectives, vol. Wiley, New York.

19.   2008, posting date. Number of U.S. Transplants Per Year, 1988 - 2008. Pearson Education. Inc. . [Online.]

20.   **Vanchiere, J. A., S. Abudayyeh, C. M. Copeland, L. B. Lu, D. Y. Graham, and J. S. Butel.** 2009. Polyomavirus shedding in the stool of healthy adults. Journal of clinical microbiology **47:**2388-91

21.   **Comar, M., N. Zanotta, M. Bovenzi, and C. Campello.** 2010. JCV/BKV and SV40 viral load in lymphoid tissues of young immunocompetent children from an area of north-east Italy. J Med Virol **82:**1236-40.

22.   **Comar, M., N. Zanotta, T. Rossi, G. Pelos, and P. D'Agaro.** 2011. Secondary lymphoid tissue as an important site for WU polyomavirus infection in immunocompetent children. J Med Virol **83:**1446-50.

23.   **Babakir-Mina, M., M. Ciccozzi, E. Trento, C. F. Perno, and M. Ciotti.** 2009. KI and WU polyomaviruses in patients infected with HIV-1, Italy. Emerg Infect Dis **15:**1323-5.

24.   **Bialasiewicz, S., D. M. Whiley, S. B. Lambert, M. D. Nissen, and T. P. Sloots.** 2009. Detection of BK, JC, WU, or KI polyomaviruses in faecal, urine, blood, cerebrospinal fluid and respiratory samples. J Clin Virol **45:**249-54.

25.   **Jeffers, L., and J. Y. Webster-Cyriaque.** 2011. Viruses and salivary gland disease (SGD): lessons from HIV SGD. Adv Dent Res **23:**79-83.

26.   **Jeffers, L. K., V. Madden, and J. Webster-Cyriaque.** 2009. BK virus has tropism for human salivary gland cells in vitro: implications for transmission. Virology **394:**183-93.

27.   **Shanti, R. M., and S. R. Aziz.** 2009. HIV-associated salivary gland disease. Oral and maxillofacial surgery clinics of North America **21:**339-43.

28.   **Terry, J. H., T. R. Loree, M. D. Thomas, and J. R. Marti.** 1991. Major salivary gland lymphoepithelial lesions and the acquired immunodeficiency syndrome. Am J Surg **162:**324-9.

29.   **DiGiuseppe, J. A., R. L. Corio, and W. H. Westra.** 1996. Lymphoid infiltrates of the salivary glands: pathology, biology and clinical significance. Curr Opin Oncol **8:**232-7.

30.   **Ioachim, H. L., and J. R. Ryan.** 1988. Salivary gland lymphadenopathies associated with AIDS. Hum Pathol **19:**616-7.

31.   **Schiodt, M., C. L. Dodd, D. Greenspan, T. E. Daniels, D. Chernoff, H. Hollander, D. Wara, and J. S. Greenspan.** 1992. Natural history of HIV-associated salivary gland disease. Oral Surg Oral Med Oral Pathol **74:**326-31.

32.   **Islam, N. M., I. Bhattacharyya, and D. M. Cohen.** 2012. Salivary gland pathology in HIV patients. Diagnostic Histopathology **18:**366-372.

33.   **Gollard, R. P., H. C. Slavkin, and M. L. Snead.** 1992. Polyoma virus-induced murine odontogenic tumors. Oral Surg Oral Med Oral Pathol **74:**761-7.

34.   **Broekema, N. M., and M. J. Imperiale.** 2012. Efficient propagation of archetype BK and JC polyomaviruses. Virology **422:**235-41.

35.   **Rubinstein, R., B. C. Schoonakker, and E. H. Harley.** 1991. Recurring theme of changes in the transcriptional control region of BK virus during adaptation to cell culture. J Virol **65:**1600-4.

36.   **Olsen, G. H., H. H. Hirsch, and C. H. Rinaldo.** 2009. Functional analysis of polyomavirus BK non-coding control region quasispecies from kidney transplant recipients. J Med Virol **81:**1959-67.

37.   **Sundsfjord, A., T. Johansen, T. Flaegstad, U. Moens, P. Villand, S. Subramani, and T. Traavik.** 1990. At least two types of control regions can be found among naturally occurring BK virus strains. J Virol **64:**3864-71.

38.   **Hanssen Rinaldo, C., H. Hansen, and T. Traavik.** 2005. Human endothelial cells allow passage of an archetypal BK virus (BKV) strain--a tool for cultivation and functional studies of natural BKV strains. Arch Virol **150:**1449-58.

39.   **Gosert, R., C. H. Rinaldo, G. A. Funk, A. Egli, E. Ramos, C. B. Drachenberg, and H. H. Hirsch.** 2008. Polyomavirus BK with rearranged noncoding control region emerge in vivo in renal transplant patients and increase viral replication and cytopathology. J Exp Med **205:**841-52.

40.   **Funk, G. A., R. Gosert, and H. H. Hirsch.** 2007. Viral dynamics in transplant patients: implications for disease. Lancet Infect Dis **7:**460-72.

41.   **Robaina, T. F., G. S. Mendes, F. J. Benati, G. A. Pena, R. C. Silva, M. A. Montes, M. E. Janini, F. P. Camara, and N. Santos.** 2013. Shedding of polyomavirus in the saliva of immunocompetent individuals. J Med Virol **85:**144-8.

42.   **Yang, R. C., and R. Wu.** 1979. BK virus DNA: complete nucleotide sequence of a human tumor virus. Science **206:**456-62.

43. **Shirasuna, K., M. Sato, and T. Miyazaki.** 1981. A neoplastic epithelial duct cell line established from an irradiated human salivary gland. Cancer **48:**745-52.

44. **Moriyama, T., and A. Sorokin.** 2009. BK virus (BKV): infection, propagation, quantitation, purification, labeling, and analysis of cell entry. Curr Protoc Cell Biol **Chapter 26:**Unit 26 2.

45. **Ziegler, K., T. Bui, R. J. Frisque, A. Grandinetti, and V. R. Nerurkar.** 2004. A rapid in vitro polyomavirus DNA replication assay. J Virol Methods **122:**123-7.

46. **Ding, R., M. Medeiros, D. Dadhania, T. Muthukumar, D. Kracker, J. M. Kong, S. R. Epstein, V. K. Sharma, S. V. Seshan, B. Li, and M. Suthanthiran.** 2002. Noninvasive diagnosis of BK virus nephritis by measurement of messenger RNA for BK virus VP1 in urine. Transplantation **74:**987-94.

47. **Larkin, M. A., G. Blackshields, N. P. Brown, R. Chenna, P. A. McGettigan, H. McWilliam, F. Valentin, I. M. Wallace, A. Wilm, R. Lopez, J. D. Thompson, T. J. Gibson, and D. G. Higgins.** 2007. Clustal W and Clustal X version 2.0. Bioinformatics **23:**2947-8.

48. **Soding, J., A. Biegert, and A. N. Lupas.** 2005. The HHpred interactive server for protein homology detection and structure prediction. Nucleic Acids Res **33:**W244-8.

49. **Pipas, J. M., K. W. Peden, and D. Nathans.** 1983. Mutational analysis of simian virus 40 T antigen: isolation and characterization of mutants with deletions in the T-antigen gene. Molecular and cellular biology **3:**203-13.

50. **Singh, H. K., V. Madden, Y. J. Shen, B. D. Thompson, and V. Nickeleit.** 2006. Negative-staining electron microscopy of the urine for the detection of polyomavirus infections. Ultrastruct Pathol **30:**329-38.

51. **Olsen, G. H., P. A. Andresen, H. T. Hilmarsen, O. Bjorang, H. Scott, K. Midtvedt, and C. H. Rinaldo.** 2006. Genetic variability in BK Virus regulatory regions in urine and kidney biopsies from renal-transplant patients. J Med Virol **78:**384-93.

52.   **Moens, U., and M. Van Ghelue.** 2005. Polymorphism in the genome of non-passaged human polyomavirus BK: implications for cell tropism and the pathological role of the virus. Virology **331:**209-31.

53.   **Barcena-Panero, A., J. E. Echevarria, M. Van Ghelue, G. Fedele, E. Royuela, N. Gerits, and U. Moens.** 2012. BK polyomavirus with archetypal and rearranged non-coding control regions is present in cerebrospinal fluids from patients with neurological complications. The Journal of general virology **93:**1780-94.

54.   **Chatterjee, M., T. B. Weyandt, and R. J. Frisque.** 2000. Identification of archetype and rearranged forms of BK virus in leukocytes from healthy individuals. J Med Virol **60:**353-62.

55.   **Perets, T. T., I. Silberstein, J. Rubinov, R. Sarid, E. Mendelson, and L. M. Shulman.** 2009. High frequency and diversity of rearrangements in polyomavirus bk noncoding regulatory regions cloned from urine and plasma of Israeli renal transplant patients and evidence for a new genetic subtype. J Clin Microbiol **47:**1402-11.

56.   **Sundsfjord, A., T. Flaegstad, R. Flo, A. R. Spein, M. Pedersen, H. Permin, J. Julsrud, and T. Traavik.** 1994. BK and JC viruses in human immunodeficiency virus type 1-infected persons: prevalence, excretion, viremia, and viral regulatory regions. J Infect Dis **169:**485-90.

57.   **Luo, C., M. Bueno, J. Kant, J. Martinson, and P. Randhawa.** 2009. Genotyping schemes for polyomavirus BK, using gene-specific phylogenetic trees and single nucleotide polymorphism analysis. Journal of virology **83:**2285-97.

58.   **Memon, I. A., B. A. Parikh, M. Gaudreault-Keener, R. Skelton, G. A. Storch, and D. C. Brennan.** 2012. Progression from Sustained BK Viruria to Sustained BK Viremia with Immunosuppression Reduction Is Not Associated with Changes in the Noncoding Control Region of the BK Virus Genome. Journal of transplantation **2012:**761283.

59.   **Feng, H., M. Shuda, Y. Chang, and P. S. Moore.** 2008. Clonal integration of a polyomavirus in human Merkel cell carcinoma. Science **319:**1096-100.

60.   **Shuda, M., H. Feng, H. J. Kwun, S. T. Rosen, O. Gjoerup, P. S. Moore, and Y. Chang.** 2008. T antigen mutations are a human tumor-specific signature for Merkel cell polyomavirus. Proc Natl Acad Sci U S A **105:**16272-7.

61.	**Campbell, K. S., K. P. Mullane, I. A. Aksoy, H. Stubdal, J. Zalvide, J. M. Pipas, P. A. Silver, T. M. Roberts, B. S. Schaffhausen, and J. A. DeCaprio.** 1997. DnaJ/hsp40 chaperone domain of SV40 large T antigen promotes efficient viral DNA replication. Genes Dev **11:**1098-110.

62.	**Reil, H., H. Kollmus, U. H. Weidle, and H. Hauser.** 1993. A heptanucleotide sequence mediates ribosomal frameshifting in mammalian cells. J Virol **67:**5579-84.

63.	**Li, R., B. N. Sharma, S. Linder, T. J. Gutteberg, H. H. Hirsch, and C. H. Rinaldo.** 2013. Characteristics of polyomavirus BK (BKPyV) infection in primary human urothelial cells. Virology **440:**41-50.

64.	**Schowalter, R. M., W. C. Reinhold, and C. B. Buck.** 2012. Entry tropism of BK and Merkel cell polyomaviruses in cell culture. PLoS One **7:**e42181.

CHAPTER 4: GENERAL CONCLUSIONS

HIV/AIDS has become one of the world's main public health challenges since its first reported case in 1981 (1) and opportunistic infections are among the leading causes of death among HIV positive individuals. BK polyomavirus (BKPyV) has been emerging as a new opportunistic pathogen within that group, possibly carrying harmful implications (2).

Our work and studies published by other groups suggest that the opportunistic infectious agent BKPyV may be the etiological agent of HIV-associated Salivary Gland Disease (HIVSGD), an HIV-associated oral malady.

Today, HIVSGD is among the most common salivary gland presentations among HIV + individuals (3) and it is considered a pre-malignant lesion as its diagnosis is associated with increased lymphoma incidence (4-7). HIVSGD presents itself as salivary gland enlargement with (8) reduced salivary flow rates of the parotid, submandibular, and sublingual glands (3). Histologically, the oral disease is characterized by hyperplastic, intraparotid lymph nodes and/ or lymphatic CD8 + infiltrates (3). Importantly, common HIVSGD treatment is palliative and there are no effective treatment options, mainly due the lack of determined HIVSGD etiology.

Data suggests that HIVSGD pathogenesis is antigen-driven (9, 10) and members of the polyomavirus (PyV) family have been shown to be important etiological agents in salivary gland pathology in experimental animal models. Athymic nude rats infected with PyV develop a wasting disease that is accompanied by parotid sialoadenitis with intranuclear inclusion bodies (11). Another transgenic mouse study shows that mice expressing PyV T antigen (Tag) undergo salivary gland tumorigenesis as the animals developed submandibular

124

gland adenocarcinomas (12). Murine and guinea pig animal models reflected HIVSGD on a histological level as mouse PyV-induced salivary epitheliomas in neonatal mice were infiltrated with T lymphocytes (13). Similar infiltrates were characterized in tumors growing from newborn guinea pigs infected with SE polyomavirus that also develop salivary gland enlargements (14). The carcinogenic potential of PyV products may explain the risk of increased lymphoma formation among HIVSGD patients.

BKPyV in particular has been shown to display oral tropism *in vivo* and *in vitro.* BKPyV products has been detected in patient tonsillar tissue (15-17) and Jeffers *et al.* showed that BKPyV is able to infect and reproduce in human salivary gland cells *in vitro* (18). Based on the re-formulated Fredricks and Relman's postulates (19) our group corroborated that BKPyV contributes to HIVSGD, as we detected significantly higher BKPyV viral loads (VLs) in the saliva of patients diagnosed with HIVSGD as compared to HIV negative patients (7, 18). Furthermore, our group found BKPyV products, but not herpesviral DNA, via PCR and immunofluorescence in HIVSGD patient salivary gland biopsies but not in biopsies from patients without HIVSGD (20). Hence, there is striking evidence linking HIVSGD to BKPyV.

BKPyV is known foremost as the etiological agent of BKPyV-associated nephropathy (BKVN), which developed into a new epidemic, becoming the most important infectious complication affecting kidney transplants. Yet, effective anti-BKPyV treatments are not available and BKVN often results in chronic allograft dysfunction and failure (21). Clearly, the deleterious implications of BKPyV on public health are significant (22), emphasizing the importance of elucidating the pathological process leading to BKPyV-associated disease and anti-BKPyV treatments.

Clearly there is a lack of HIVSGD treatment options and this gap would be addressed once the etiological is determined. We attempted to narrow this gap by further analyzing the connection between HIVSGD and BKPyV. Furthermore, the role BKPyV plays during HIVSGD pathogenesis needs to be analyzed in order to provide specific treatment targets once BKPyV would be unquestionably confirmed as the etiological agent of HIVSGD. We therefore characterized HIVSGD-derived BKPyV (Chapter 2), studied BKPyV replication in human salivary gland cells (Chapter 3) and analyzed potential mechanisms involved (Appendix 2). Finally, general anti-BKPyV drugs need to be explored in tandem in the near future as they are not well defined. We therefore tested antiviral drugs in vitro (Appendix 1).

Our work described in **CHAPTER 2** (AIM1) was designed to confirm BKPyV as the etiological agent of HIVSGD by determining BKPyV viral loads (VLs) in HIVSGD throatwash (TW) samples *in vivo.* We screened TW samples from HIVSGD positive and negative patients for BKPyV. Concomitantly, we aimed to characterize HIVSGD-derived BKPyV and determined the BKPyV promoter architecture of HIVSGD positive and HIVSGD negative TW-derived isolates and transplant patient urine-derived isolates.

The BKPyV NCCR promoter region was of special interest because it controls viral gene transcription and has been found to be the major determinant of *in vitro* replication (23, 24). The NCCR commonly undergoes block deletions and/or duplications and block rearrangements bestow remarkable differences in transforming potential and host cell permissivity (24-29). Furthermore, rearranged NCCRs have been reported to be more efficient replicators both *in vitro* and *in vivo* (23, 24, 30-32) 43). We therefore aimed to characterize the NCCR of HIVSGD-derived BKPyV and order to determine whether there was a prevalent architecture BKPyV that

could serve as potential biomarker and to discern whether there was evidence that promoter rearrangements endow higher replication levels or tropism. There is evidence that downstream events such as transcriptional regulation contributes significantly to viral tropism (24, 33). As mentioned earlier, the BKPyV NCCR promoter contains the origin of replication and the enhancer/promoter elements of the genome and is the main determinant of BKPyV replication *in vitro* (23). The NCCR is a hypervariable region and comparative studies have suggested that it may regulate host cell tropism. These changes have been attributed mainly to the rearrangement, duplication or deletion transcription factor binding sites (TFBS) (24, 33-36). It is therefore plausible that the interplay of TFBS found within the NCCR sequence of a certain BKPyV substrain and transcription factors present within a certain cell type may allow for successful completion of a viral life cycle and therefore determine BKPyV tropism. We therefore also aimed to predict TFBS present within the BKPyV NCCR architecture of the clinical HIVSGD BKPyV isolates.

Indeed, the study detected a conserved OPQPQQS NCCR architecture among 94.7% HIVSGD-derived BKPyV isolates which were confirmed in a study described in chapter 3. The BKPyV NCCR architecture and VLs from 36 immuno-suppressed individuals were assessed including 19 HIVSGD TW samples, 9 HIV positive/HIVSGD negative TW samples and 8 urine samples from HIVSGD negative transplant patients. First, we confirmed previously published data showing that HIVSGD patients shed increased BKPyV VLs orally, corroborating a potential link between HIVSGD and BKPyV (7, 18) and implying that the salivary glands may be a potential compartment suitable for BKPyV replication and pathogenesis. In order to rule out the patients HIV status as a co-factor driving BKPyV VLs, the correlation between HIV VLs, CD4 counts and HAART treatment were tested and were not statistically significant. Furthermore,

there was no significant correlation between orally shed BKPyV levels, age, gender and geographical residential location. Interestingly, not all patients were BKPyV positive when diagnosed with HIVSGD. Patient HIVSGD9, for example, shed BKPyV VLs of $1x10^4$ upon entry, despite being HIVSGD negative at that time point. The patient was diagnosed with HIVSGD 6 months later however. It is possible that BKPyV reactivates and flares up right before the development of HIVSGD symptoms. Additional studies were recently initiated in order to further analyze the connection between BKPyV and HIVSGD in the future. A controlled longitudinal epidemiologic prospective cohort study was designed to further dissect whether BKPyV is the driver rather than a passenger HIVSGD and results will be available before the end of the year. The study consists of 3 patient cohorts HIV+ HIVSGD+, HIV+ HIVSGD(-), HIV(-) healthy and HIV(-) kidney transplant patients (N=62 >80% power). BKPyV VLs in saliva, urine, blood and antibody status will be analyzed and salivary function/protein secretion will be correlated with BKPyV titers.

Given that NCCR changes have been attributed mainly to the rearrangement, duplication or deletion of transcription factor binding sites (TFBS), we predicted TFBS among the isolated clinical BKPyV promoters. Phylogenetic analysis of the detected BKPyV NCCRs displayed nucleotide differences among underlying the block homology. We predicted TFBS for the clinical and laboratory strain full-length and O block promoters and analyzed a potential correlation between *in vivo* VLs and sets of TFBS. We found a potential association between NCCR TFBS C/EBPβ and p300 with higher *in vivo* BKPyV replication efficiency by statistical analysis. Previous studies predicted C/EBPβ binding within the BKPyV NCCR and showed that C/EBPβ and p65 stimulated NCCR transcription in the early direction in transfection experiments both suggesting C/EBPβ to be crucial for early promoter induction (37, 38).

However, we could not confirm a correlation between TFBS C/EBPβ and p300 and promoter activity or *in vitro* replication levels. Hence, despite the long-held hypothesis that there is a link between NCCR TFBSs and BKPyV replication efficiency (36, 39, 40), we could not find common TFBS alterations that could be linked to promoter activity.

Most importantly however, this study classified 19 HIVSGD BKPyV NCCR isolates using block sequence, phylogenetic and TFBS analysis, detecting a highly homologous OPQPQQS NCCR among HIVSGD TW samples. Hence, our data show that HIVSGD patients orally shed considerable BKPyV VLs that carry highly homologous NCCR architectures. Since NCCR changes determine host cell tropism (24, 41), this new NCCR architecture may be an adaptive response to a switch of host cell type and allow BKPyV replication in the oral cavity. This was supported by our data that found all but one HIVSGD promoter (83%) to be more readily induced than a laboratory strain in HSG cells, all HIVSGD strains to replicate readily in HSG cells and all but one HIVSGD substrain to replicate more efficiently than laboratory strain Dunlop in HSG cells over a 15-day time span. Hence, while it is unclear whether this signature OPQPQQS NCCR may be an adaptive response to salivary gland cells and/or promote salivary gland cell tropism, our study showed that cloned HIVSGD BKPyV isolates displayed active promoter activity and efficient replication capabilities in human salivary gland cells *in vitro*. Overall, the high frequency of a viable BKPyV substrain among HIVSGD TW samples suggests a stable and potentially pathogenic and biologically significant BKPyV substrain that may be linked to HIVSGD pathogenesis. In the future, more comprehensive clinical studies will have to be conducted in order to: 1. Confirm BKPyV and the etiological agent of HIVSGD. 2. Confirm the characteristic OPQPQQS NCCR architecture among HIVSGD patients and potential

biomarker. 3. Define whether BKPyV NCCR rearrangements truly drive increased virulence *in vivo*.

Our work described in **CHAPTER 3** (AIM2) was designed to establish an oral cell culture system to characterize and compare viral replication levels and tropisms of clinical BKPyV isolates in human salivary gland and kidney cells that are likely to have caused HIVSGD *in vivo*.

In vitro cultivation of biologically relevant BKPyV strains has been inefficient unless Tag is provided in trans by over-expression (30) and few studies have successfully cultivated clinical BKPyV isolates. The lack of an *in vitro* system that allows for efficient cultivation of clinical BKPyV isolates hinders the complete elucidation of the BKPyV life cycle and pathogenic mechanism. The lack of an established cell culture system that adequately represents the oral *in vivo* compartment and that allows for infection with clinical isolates hinders the systematic elucidation of BKPyV pathogenesis in the oral compartment and testing of HIVSGD treatment options. Our group therefore established, to our knowledge for the first time, an oral cell culture system that allows studying clinical BKPyV isolates, potential pathogenesis and anti-viral treatment options. We aimed to corroborate the hypothesis that BKPyV may be the etiological agent of HIVSGD by determining whether the clinical isolates replicate within human salivary gland cells and whether there is display of oral tropism.

Three clinical BKPyV isolates were described and compared: HIVSGD-1 and HIVSGD-2 were isolated from the throatwash (TW) samples of HIVSGD patients and U1 was isolated from the urine sample of a HIVSGD negative transplant patient. BKPyV viral loads (VLs) from all three clinical samples were high and ranged from 1.7×10^5 to 1.7×10^9 copies/ml, likely

reflecting the previously established correlation between HIVSGD and BKPyV and BKVN and BKPyV. Most interestingly, both HIVSGD-derived BKPyV substrains shared the NCCR architecture previously described - OPQPQQS. HIVSGD-1 turned out to be a high *in vitro* replicator in human salivary gland cells as compared to HIVSGD-2 or the urine-derived isolate. HIVSGD-2 consistently lacked signs of overall *in vitro* replication.

Whole genome sequence alignment of the two HIVSGD whole genomes determined 99% similarity, despite three point mutations. 1. A thymidine deletion was detected between the open reading frames (ORFs) that encoded agnoprotein and VP2. The deletion was outside of the respective ORFs and is therefore unlikely to affect the viral life cycle. 2. A thymidine/cytidine transition was detected despite overall NCCR block architecture homology. The transition did not lead to differential prediction of putative human TFBS, nor to differences in the early promoter activity in the presence or absence of full-length Tag. The transition was thus equally unlikely contributor to differences in replication efficiency. 3. An adenosine deletion was detected distal to the Tag pRb binding domain and was likely the cause of inefficient HIVSGD-2 replication due Tag's central function to genome replication and PyV life cycle completion (42-44). Furthermore, insufficient Tag expression has been shown to obstruct BKPyV replication *in vitro* (30). The deletion predicted to introduce an early stop codon, modify the nuclear translocation signal and result in the expression of a truncated form of Tag. The mutant Tag was predicted to lose the origin-binding domain, p53 site and ATP/helicase domain. It is therefore likely that insufficient Tag expression dramatically inhibited HIVSGD-2 replication.

In summary, overall high BKPyV VLs were detected among HIVSGD TW samples, corroborating the connection between BKPyV and HIVSGD. A common OPQPQQS NCCR block architecture was found among BKPyV isolates from the oral fluids of two individuals

diagnosed with HIVSGD. Furthermore, clinical HIVSGD-derived BKPyV was successfully

cultured in human salivary gland cells and in kidney cells. Our assessments suggested that a

single point mutation in Tag, causing truncation, lead to a stark difference in the *in vitro*

replication potential. Furthermore, the high HIVSGD-derived replicator surpassed the replication

potential of the kidney-derived isolate in human salivary gland cells and displayed signs of

salivary gland tropism.

Permissive replication of wild type clinical BKV isolates is generally thought to happen

chiefly in renal- and uro-epithelium but the presented data suggested the oral compartment to be

a likely *in vivo* replication site as well. The main drawback of the study was the small number of

characterized HIVSGD isolates and may not be representative of all HIVSGD variants. In the

future, a study encompassing a larger number of isolates, would be more representative and

would give a more accurate picture of HIVSGD-derived BKPyV replication kinetics. Still, the

presented system allows studying clinical oral BKPyV infection and these observations provide

insights to future BKPyV pathogenesis, transmission and disease-association studies. In the

future, the oral BKPyV cell culture system may allow determining whether BKPyV infection

affects cell signaling and homeostasis and may mirror salivary gland dysfunctions *in vivo*. The

system may therefore lead to hints towards why HIVSGD patients have reduced saliva

production and may ultimately contribute to treatment options alleviating HIVSGD patients from

xerostomia and its deleterious consequences.

Our work described in **Appendix 1** describes how the salivary gland cell culture system

was used to test antiviral treatment options potentially alleviating general BKPyV-associated

ailments in patients. Antiviral effects of several drugs on clinical BKPyV isolates were

characterized *in vitro*, since there is currently no FDA approved antiviral drug to treat BKPyV infection. Previous studies have analyzed the anti-BKPyV effects of following drugs: cidofovir, CMX001, leflunomide, ciprofloxacin, and lactoferrin(45-51). However the results were mostly ambivalent (48, 49, 52, 53) and all of the listed drugs are likely to have non-specific effects since they are approved to treat other DNA virus infections, including hepadnaviruses, herpesviruses, adenovirus, papillomavirus, polyoma and poxviruses (54-58). The study presented in appendix 1 tested three drugs, ciprofloxacin, cidofovir and leflunomide on BKPyV replication in salivary gland cells, using the previously described BKV-infected salivary gland *in vitro* system and HIVSGD-derived BKPyV isolates. BKPyV replication was decreased by all three drug types in human salivary gland cells, while ciprofloxacin was the most effective. The anti-BKPyV mechanisms of each drug are currently unclear and present a future are of interest. It was proposed, however that BKPyV inhibition in salivary gland cells may be due to inhibition of a host intracellular signaling pathway important for viral replication, such as the Akt or mTOR pathway (Jeffers, LK, unpublished). Future clinical studies will have to be done to determine which antiviral drug is most effective to treat BKPyV infection in HIVSGD patients, but our study suggest ciprofloxacin to be the most efficacious.

Our work described in **<u>Appendix 2</u>** describes a study analyzing the possible connection between the metastatis-associated lung adenocarcinoma-associated transcript 1 (MALAT-1) and PyV Tag. MALAT-1 was found to be up-regulated in RNA extracted from HIVSGD biopsies versus biopsies from patients without HIVSGD and has previously been shown to be up-regulated in a variety of epithelial carcinomas.

BKPyV is a small DNA tumorvirus and its tumorigenic capability in experimental models is accredited to the presence of the oncoprotein Tag (59). Tag is a nuclear

phosphoprotein that wields its transforming abilities by interacting and suppressing cellular tumor suppressor proteins p53 and members of the pRb family, which leads to unrestrained host cell proliferation (60). Understanding the complete life cycle of the virus and the role Tag plays during infection will be critical in the development of possible therapeutic interventions of lymphoma formation during HIVSGD pathogenesis.

We found that Malat-1 regulation was associated with p53 dysfunction and may therefore serve as a biomarker for p53-specific transformation. Furthermore, these results suggest Malat-1 may be a potential biomarker for Tag transformed tissue, such as seen in HIVSGD, since PyV Tag suppresses p53 functions.

REFERENCES

1.   1981. Pneumocystis pneumonia--Los Angeles. MMWR. Morbidity and mortality weekly report **30:**250-2.

2.   **Cubukcu-Dimopulo, O., A. Greco, A. Kumar, D. Karluk, K. Mittal, and J. Jagirdar.** 2000. BK virus infection in AIDS. The American journal of surgical pathology **24:**145-9.

3.   **Shanti, R. M., and S. R. Aziz.** 2009. HIV-associated salivary gland disease. Oral and maxillofacial surgery clinics of North America **21:**339-43.

4.   **Ioachim, H. L., and J. R. Ryan.** 1988. Salivary gland lymphadenopathies associated with AIDS. Human pathology **19:**616-7.

5.   **Ioachim, H. L., J. R. Ryan, and S. M. Blaugrund.** 1988. Salivary gland lymph nodes. The site of lymphadenopathies and lymphomas associated with human immunodeficiency virus infection. Archives of pathology & laboratory medicine **112:**1224-8.

6.   **DiGiuseppe, J. A., R. L. Corio, and W. H. Westra.** 1996. Lymphoid infiltrates of the salivary glands: pathology, biology and clinical significance. Curr Opin Oncol **8:**232-7.

7.   **Jeffers, L., and J. Y. Webster-Cyriaque.** 2011. Viruses and salivary gland disease (SGD): lessons from HIV SGD. Adv Dent Res **23:**79-83.

8.   **Jeffers, L. K., K. Duan, L. G. Ellies, W. T. Seaman, R. A. Burger-Calderon, L. B. Diatchenko, and J. Webster-Cyriaque.** 2013. Correlation of transcription of MALAT-1, a novel noncoding RNA, with deregulated expression of tumor suppressor p53 in small DNA tumor virus models. Journal of cancer therapy **4**.

9.   **Basu, D., F. M. Williams, C. W. Ahn, and J. D. Reveille.** 2006. Changing spectrum of the diffuse infiltrative lymphocytosis syndrome. Arthritis and rheumatism **55:**466-72.

10.   **Itescu, S., L. J. Brancato, and R. Winchester.** 1989. A sicca syndrome in HIV infection: association with HLA-DR5 and CD8 lymphocytosis. Lancet **2:**466-8.

11.   **Ward, J. M., A. Lock, M. J. Collins, Jr., M. A. Gonda, and C. W. Reynolds.** 1984. Papovaviral sialoadenitis in athymic nude rats. Laboratory animals **18:**84-9.

12.   **Dardick, I., J. Ho, M. Paulus, P. L. Mellon, and L. Mirels.** 2000. Submandibular gland adenocarcinoma of intercalated duct origin in Smgb-Tag mice. Laboratory investigation; a journal of technical methods and pathology **80:**1657-70.

13.   **Harrod, F. A., and J. R. Kettman.** 1990. Transplantable polyoma virus-induced epitheliomas harbor immature T lymphocytes. Cellular immunology **125:**29-41.

14.   **Eddy, B. E., G. S. Borman, R. L. Kirschstein, and R. H. Touchette.** 1960. Neoplasms in guinea pigs infected with SE polyoma virus. The Journal of infectious diseases **107:**361-8.

15.   **Imperiale, M. J.** 2000. The human polyomaviruses, BKV and JCV: molecular pathogenesis of acute disease and potential role in cancer. Virology **267:**1-7.

16.   **Goudsmit, J., M. L. Baak, K. W. Sleterus, and J. Van der Noordaa.** 1981. Human papovavirus isolated from urine of a child with acute tonsillitis. British medical journal **283:**1363-4.

17.   **Goudsmit, J., P. Wertheim-van Dillen, A. van Strien, and J. van der Noordaa.** 1982. The role of BK virus in acute respiratory tract disease and the presence of BKV DNA in tonsils. Journal of medical virology **10:**91-9.

18.   **Jeffers, L. K., V. Madden, and J. Webster-Cyriaque.** 2009. BK virus has tropism for human salivary gland cells in vitro: implications for transmission. Virology **394:**183-93.

19.   **Fredericks, D. N., and D. A. Relman.** 1996. Sequence-based identification of microbial pathogens: a reconsideration of Koch's postulates. Clinical microbiology reviews **9:**18-33.

20.   **Dovigi, D. A.** 2005. HIV Salivary Gland Disease: A Role For Viral Infection. University of North Carolina at Chapel Hill, Chapel Hill, NC.

21.   **Nickeleit, V.** 2006. Animal models of polyomavirus nephropathy: hope and reality. Am J Transplant **6:**1507-9.

22.   **Weinberg, G. A., and A. N. Mian.** 2010. BK virus nephropathy and other polyoma virus infections. The Pediatric infectious disease journal **29:**257-60.

23.   **Broekema, N. M., J. R. Abend, S. M. Bennett, J. S. Butel, J. A. Vanchiere, and M. J. Imperiale.** 2010. A system for the analysis of BKV non-coding control regions: application to clinical isolates from an HIV/AIDS patient. Virology **407:**368-73.

24.   **Johnsen, J. I., O. M. Seternes, T. Johansen, U. Moens, R. Mantyjarvi, and T. Traavik.** 1995. Subpopulations of non-coding control region variants within a cell culture-passaged stock of BK virus: sequence comparisons and biological characteristics. J Gen Virol **76 (Pt 7):**1571-81.

25.   **Gosert, R., C. H. Rinaldo, G. A. Funk, A. Egli, E. Ramos, C. B. Drachenberg, and H. H. Hirsch.** 2008. Polyomavirus BK with rearranged noncoding control region emerge in vivo in renal transplant patients and increase viral replication and cytopathology. J Exp Med **205:**841-52.

26.   **Funk, G. A., R. Gosert, and H. H. Hirsch.** 2007. Viral dynamics in transplant patients: implications for disease. Lancet Infect Dis **7:**460-72.

27.   **Olsen, G. H., P. A. Andresen, H. T. Hilmarsen, O. Bjorang, H. Scott, K. Midtvedt, and C. H. Rinaldo.** 2006. Genetic variability in BK Virus regulatory regions in urine and kidney biopsies from renal-transplant patients. J Med Virol **78:**384-93.

28.   **Sundsfjord, A., T. Johansen, T. Flaegstad, U. Moens, P. Villand, S. Subramani, and T. Traavik.** 1990. At least two types of control regions can be found among naturally occurring BK virus strains. J Virol **64:**3864-71.

29.   **Moens, U., and M. Van Ghelue.** 2005. Polymorphism in the genome of non-passaged human polyomavirus BK: implications for cell tropism and the pathological role of the virus. Virology **331:**209-31.

30.   **Broekema, N. M., and M. J. Imperiale.** 2012. Efficient propagation of archetype BK and JC polyomaviruses. Virology **422:**235-41.

31.   **Hanssen Rinaldo, C., H. Hansen, and T. Traavik.** 2005. Human endothelial cells allow passage of an archetypal BK virus (BKV) strain--a tool for cultivation and functional studies of natural BKV strains. Arch Virol **150:**1449-58.

32.   **Olsen, G. H., H. H. Hirsch, and C. H. Rinaldo.** 2009. Functional analysis of polyomavirus BK non-coding control region quasispecies from kidney transplant recipients. J Med Virol **81:**1959-67.

33.   **Ashok, A., and W. J. Atwood.** 2006. Virus receptors and tropism. Advances in Experimental Medicine and Biology **577:**60-72.

34.   **Burger-Calderon, R., V. Madden, R. A. Hallett, A. D. Gingerich, V. Nickeleit, and J. Webster-Cyriaque.** 2013. Replication of oral BK virus in human salivary gland cells. J Virol.

35.   2007. Fields' Virology. *In* P. M. H. David M. Knipe (ed.), 5th ed. Wolters Kluwer Health/Lippincott Williams & Wilkins, Philadelphia.

36.   **Moens, U., T. Johansen, J. I. Johnsen, O. M. Seternes, and T. Traavik.** 1995. Noncoding control region of naturally occurring BK virus variants: sequence comparison and functional analysis. Virus genes **10:**261-75.

37.   **Gorrill, T. S., and K. Khalili.** 2005. Cooperative interaction of p65 and C/EBPbeta modulates transcription of BKV early promoter. Virology **335:**1-9.

38.   **White, M. K., M. Safak, and K. Khalili.** 2009. Regulation of gene expression in primate polyomaviruses. Journal of virology **83:**10846-56.

39.   **Markowitz, R. B., S. Tolbert, and W. S. Dynan.** 1990. Promoter evolution in BK virus: functional elements are created at sequence junctions. J Virol **64:**2411-5.

40.   **Hirsch, H. H., and J. Steiger.** 2003. Polyomavirus BK. Lancet Infect Dis **3:**611-23.

41.   **Barcena-Panero, A., J. E. Echevarria, M. Van Ghelue, G. Fedele, E. Royuela, N. Gerits, and U. Moens.** 2012. BK polyomavirus with archetypal and rearranged non-

coding control regions is present in cerebrospinal fluids from patients with neurological complications. J Gen Virol **93:**1780-94.

42. **Feng, H., M. Shuda, Y. Chang, and P. S. Moore.** 2008. Clonal integration of a polyomavirus in human Merkel cell carcinoma. Science **319:**1096-100.

43. **Shuda, M., H. Feng, H. J. Kwun, S. T. Rosen, O. Gjoerup, P. S. Moore, and Y. Chang.** 2008. T antigen mutations are a human tumor-specific signature for Merkel cell polyomavirus. Proc Natl Acad Sci U S A **105:**16272-7.

44. **Campbell, K. S., K. P. Mullane, I. A. Aksoy, H. Stubdal, J. Zalvide, J. M. Pipas, P. A. Silver, T. M. Roberts, B. S. Schaffhausen, and J. A. DeCaprio.** 1997. DnaJ/hsp40 chaperone domain of SV40 large T antigen promotes efficient viral DNA replication. Genes Dev **11:**1098-110.

45. **Longhi, G., V. Pietropaolo, M. Mischitelli, C. Longhi, M. P. Conte, M. Marchetti, A. Tinari, P. Valenti, A. M. Degener, L. Seganti, and F. Superti.** 2006. Lactoferrin inhibits early steps of human BK polyomavirus infection. Antiviral Res **72:**145-52.

46. **Rinaldo, C. H., R. Gosert, E. Bernhoff, S. Finstad, and H. H. Hirsch.** 2010. 1-O-hexadecyloxypropyl cidofovir (CMX001) effectively inhibits polyomavirus BK replication in primary human renal tubular epithelial cells. Antimicrob Agents Chemother **54:**4714-22.

47. **Farasati, N. A., R. Shapiro, A. Vats, and P. Randhawa.** 2005. Effect of leflunomide and cidofovir on replication of BK virus in an in vitro culture system. Transplantation **79:**116-8.

48. **Bernhoff, E., G. D. Tylden, L. J. Kjerpeseth, T. J. Gutteberg, H. H. Hirsch, and C. H. Rinaldo.** 2010. Leflunomide inhibition of BK virus replication in renal tubular epithelial cells. J Virol **84:**2150-6.

49. **Bernhoff, E., T. J. Gutteberg, K. Sandvik, H. H. Hirsch, and C. H. Rinaldo.** 2008. Cidofovir inhibits polyomavirus BK replication in human renal tubular cells downstream of viral early gene expression. Am J Transplant **8:**1413-22.

50. **Leung, A. Y., M. T. Chan, K. Y. Yuen, V. C. Cheng, K. H. Chan, C. L. Wong, R. Liang, A. K. Lie, and Y. L. Kwong.** 2005. Ciprofloxacin decreased polyoma BK virus load in patients who underwent allogeneic hematopoietic stem cell

transplantation. Clin Infect Dis **40:**528-37.

51.   **Gabardi, S., S. S. Waikar, S. Martin, K. Roberts, J. Chen, L. Borgi, H. Sheashaa, C. Dyer, S. K. Malek, S. G. Tullius, N. Vadivel, M. Grafals, R. Abdi, N. Najafian, E. Milford, and A. Chandraker.** 2010. Evaluation of fluoroquinolones for the prevention of BK viremia after renal transplantation. Clin J Am Soc Nephrol **5:**1298-304.

52.   **Rinaldo, C. H., and H. H. Hirsch.** 2007. Antivirals for the treatment of polyomavirus BK replication. Expert Rev Anti Infect Ther **5:**105-15.

53.   **Sharma, B. N., R. Li, E. Bernhoff, T. J. Gutteberg, and C. H. Rinaldo.** 2011. Fluoroquinolones inhibit human polyomavirus BK (BKV) replication in primary human kidney cells. Antiviral Res **92:**115-23.

54.   **Dropulic, L. K., and R. J. Jones.** 2008. Polyomavirus BK infection in blood and marrow transplant recipients. Bone Marrow Transplant **41:**11-8.

55.   **Hasegawa, K., W. Motsuchi, S. Tanaka, and S. Dosako.** 1994. Inhibition with lactoferrin of in vitro infection with human herpes virus. Jpn J Med Sci Biol **47:**73-85.

56.   **Hara, K., M. Ikeda, S. Saito, S. Matsumoto, K. Numata, N. Kato, K. Tanaka, and H. Sekihara.** 2002. Lactoferrin inhibits hepatitis B virus infection in cultured human hepatocytes. Hepatol Res **24:**228.

57.   **Evers, D. L., X. Wang, S. M. Huong, K. A. Andreoni, and E. S. Huang.** 2005. Inhibition of human cytomegalovirus signaling and replication by the immunosuppressant FK778. Antiviral Res **65:**1-12.

58.   **Ali, S. H., A. Chandraker, and J. A. DeCaprio.** 2007. Inhibition of Simian virus 40 large T antigen helicase activity by fluoroquinolones. Antivir Ther **12:**1-6.

59.   **Abend, J. R., A. E. Joseph, D. Das, D. B. Campbell-Cecen, and M. J. Imperiale.** 2009. A truncated T antigen expressed from an alternatively spliced BK virus early mRNA. J Gen Virol **90:**1238-45.

60.   **Abend, J. R., M. Jiang, and M. J. Imperiale.** 2009. BK virus and human cancer: innocent until proven guilty. Seminars in cancer biology **19:**252-60.

EFFECT OF LEFLUNOMIDE, CIDOFOVIR AND CIPROFLOXACIN ON REPLICATION OF BK VIRUS IN A SALIVARY GLAND IN VITRO CULTURE SYSTEM

Introduction

BK virus (BKV) belongs to the polyomavirus family and is ubiquitous in the human population (1). BKV infection typically occurs during childhood, without specific symptoms, followed by a state of non-replicative infection in various tissues, with the urogenital tract as the principal site (2). In the setting of relative or absolute cell-mediated immunosuppression, dramatic increase in BK viral replication occurs, resulting in the lytic destruction of infected uroepithelial cells, which in turn induces the influx of inflammatory immune cells(3). Destruction of kidney cells most often occurs in 5-8% of kidney transplants resulting in organ loss in half of these cases and is termed BKV-associated nephropathy (BKVN) (4) (5-7). BKV is also the cause of BKV-associated hemorrhagic cystitis which occurs in more than 10% of bone marrow transplant recipients (8, 9). BKV-associated disease incidence is increasing as a result of the growing number of immunocompromised patients, including transplant and HIV, and development of better immunosuppressive drugs.

Currently there is no FDA approved antiviral drug licensed to treat BKV infections despite its importance in transplant and immunocompromised patients. Several in vitro and in vivo studies however, have been performed to test for their efficacy against BKV including cidofovir, CMX001, leflunomide, ciprofloxacin, and lactoferrin(10-16). All of these drugs are effective against other DNA viruses including hepadnaviruses, herpesviruses, adenovirus, papillomavirus, polyoma and poxviruses (9, 17-20) but have shown mixed results against BKV, both in vitro and in vivo in kidney cells (13, 14, 21, 22). Ciprofloxacin (CPRO) is a synthetic antibiotic of the fluoroquinolone drug class. Ciprofloxacin's antibacterial activity functions by

inhibiting type II topoisomerases and has been shown to inhibit T antigen helicase activity (20). Cidofovir (CDV) is a nucleoside analog that inhibits viral DNA polymerase activity, however BKV does not encode for a DNA polymerase. CDV has been shown to inhibit BKV activity in vitro in human embryonic lung fibroblast cells (WI-38) (12) and in primary human renal proximal tubular epithelial cells (RPTECs)(14). In RPTECs, CDV inhibited BKV replication but also decreased host cellular DNA replication and metabolic activity (14). Although CDV has shown in vitro activity against BKV, there are conflicting reports of in vivo activity (23, 24). In addition, CDV has been shown to be nephrotoxic and must be given intravenously, therefore patients need to be hospitalized for drug administration. Most recently, CMX001, a hexadecyloxypropyl lipid conjugate of CDV has been shown to inhibit polyomaviruses JCV and BKV in human kidney and brain progenitor-derived astrocytes (11, 25). Leflunomide (LEF) is an anti-inflammatory drug known to inhibit dihydroorotate dehydrogenase, tyrosine kinase and pyrimidine synthesis(12). LEF has been approved to treat rheumatoid arthritis and has shown activity against cytomegalovirus and herpesvirus with conflicting reports against BKV(13, 26, 27).

We have previously shown that BKV DNA can be detected at high levels in the saliva of HIV patients diagnosed with salivary gland disease compared to patients without the disease (28, 29). HIV-associated salivary gland disease (HIV-SGD) has been universally established as among the most important AIDS-associated oral lesions. Oral lesions are important clinical indicators of HIV/AIDS by suggesting HIV infection in the undiagnosed individual, indicating clinical disease progression and predicting development of AIDS (30). In developing countries the incidence of HIV-SGD has been reported to be as high as 48% of HIV-1 infected patients(31). Also, HIV-SGD is of particular interest because in 1-2% of patients, malignant

lymphomas have been described in association with glandular lesions making this disease a premalignant lesion(32, 33). In addition, we have shown that BKV can productively infect salivary gland cells in an in vitro model described by Jeffers et al (28).

All assays to test anti-BKV drugs have been performed in kidney or lung cells (12, 34, 35). Therefore, an in vitro drug screen against BKV replication in human salivary gland cells would be useful to identify new viral targets for drug treatment. The aim of this study was to investigate the effect of three drugs, ciprofloxacin, cidofovir and leflunomide on BKV replication in salivary gland cells, using the previously described BKV-infected salivary gland in vitro culture system, the primary target cells in HIV-associated salivary gland disease.

Materials and Methods

Subjects, sample collection and cell culture

HIVSGD patients were recruited from UNC hospitals dental clinic to participate in the IRB approved study, where throat wash was collected from patients for viral detection and isolation. Urine from a lung transplant patient was kindly donated by Dr. Volker Nickeleit for viral detection and isolation. HSG cells, an epithelial cell line from human submandibular salivary gland (36), were obtained as a gift from Dr. B. Baum (NIH) and cultured in McCoy's 5A medium (Sigma). African kidney monkey cells or Vero cells (American Type Culture Collection [ATCC]) were also cultured in DMEM (Sigma). All cell types were grown in medium supplemented with 10% fetal bovine serum (FBS) (Sigma), unless otherwise stated and 1% penicillin-streptomycin (pen/strep) (Gibco) and maintained in a humidified 37^0C CO_2 chamber. BKV Gardner strain was obtained from ATCC (VR-837).

<u>Whole Genome BKV Cloning</u>

BKV VP1 gene forward (BKVWGF; 5'-GCGGGATCCAGATGAAAACCTTAGG-3')
and reverse primers (BKVWGR; 5'- GCGGGATCCCCCATTTCTGG-3') including the
naturally occurring BamH1 restriction fragment recognition sites were used to amplify the whole
genome (wg) of BKV via PCR from throatwash of HIVSGD patients, and the urine of a lung
transplant patient using the Expand Long Range dNTPack (Roche) as described by
manufacturer. Amplified wg BKV products were purified by QIAquick PCR Purification Kit
(QIAGEN) as described by manufacturer. Purified wg BKV DNA was cloned via the TOPO TA
Cloning Kit (Invitrogen) as described by manufacturer. Constructs were isolated via QIAfilter
Plasmid Midi Kit (QIAGEN) post-24hrs incubation of bacterial cells for clone DNA
amplification at 37 °C.

<u>Infection and Drug Treatment</u>

Ciprofloxacin (Sigma), Leflunomide/A771726 (Calbiochem) and Cidofovir (Gilead)
were dissolved to 150ug/ml, 20ug/ml and 40ug/ml, respectively in McCoy's 5A medium. HSG
cells were infected at about 50% confluence with 64 HAUs of BKV as described by Jeffers et al.
(28). As previously described by Jeffers et al, HSG cells were infected with BK virus for 24h for
optimal viral entry(28). At 24h post infection virus was removed from the culture medium,
washed with 1X PBS and replaced with fresh medium with or without drug. At various times
post infection the cell monolayers or supernatant were further processed for IFA, protein, RNA
or DNA isolation, as described below.

<u>Cell viability and cell proliferation assay</u>

The mitochondrial metabolic activity was monitored by the colorimetric WST-1 assay
(Roche), measuring the reduction of the tetrazolium salt WST-1 by mitochondrial

dehydrogenases. DNA synthesis was quantified by the colorimetric measurement of bromodeoxyuridine (BrdU) incorporation into DNA using the cell proliferation enzyme-linked immunosorbent assay (ELISA) BrdU kits (Roche). Both tests were performed in fresh medium with or without BKV Gardner in the presence or absence of drug at 3, 4 and 5 dpi.

RNA isolation and real-time RT-PCR amplification

Total RNA was extracted using TRizol (Invitrogen) as described by the manufacturer. Contaminating DNAs were removed by use of RQ1 DNase kit (Promega) as described by the manufacturer. cDNA was generated using 20µg RNA, random primers and the SuperScript[TM] II Reverse Transcriptase (RT) Kit (Invitrogen) as described by the manufacturer. A non-RT enzyme reaction was performed for each sample as a negative control for cDNA synthesis. cDNA was then subjected to real-time PCR analysis using Roche LightCycler 480 Syber Green I Master Mix as a detector in the Roche Light Cycler 480. Primers for T Ag and VP1 were previously described in Dana et al (37) and Ding (38) et al, respectively. Gene expression values were normalized to the levels of β-actin transcripts, using the $2^{-\Delta\Delta C(T)}$ method, and are presented as the changes (*n*-fold) in T Ag and VP1 transcript levels, with the levels in BKV only (no drug) samples arbitrarily set to 1.

Indirect immunofluorescence (IFA)

At stated times post-infection, cells were fixed for 10 min with 50% methanol/50% acetone, dried at RT then incubated at -20^0C overnight for antigen retrieval. Fixed cells were then thawed at RT, rehydrated with 1XPBS and incubated with PAb416 (Genetex) antibody (1:30), specific for SV40 LT-ag and cross reacts with BKV LT-ag for 1 hr at 37^0C followed by a fluorescencein-conjugated anti-mouse (Sigma) antibody (1:20). DAPI (Invitrogen) (1:10,000) was used to stain the nucleus. At least ten random fields of positively stained cells were counted

to determine percent infection. Nikon FXA with Q camera or Olympus IMT2 fluorescent microscopes were used to photograph cells.

Immunoblotting

Total cell protein was extracted using RIPA buffer. Protein concentration was determined using the BioRad protein assay, and equal amounts of protein were electrophoresed on a 4-12% Bis-Tris polyacrylamide minigel (Invitrogen). PAb416 (1:200) (Genetex) in 5% NFDM/PBS-T was used to detect T Ag expression and Actin (C-11)-R sc-1615-R (1:1000)(Santa Cruz Biotechnology) in 1%BSA/TBS-T for actin expression. After washing in PBS/TBS-T, blots were probed with a horseradish peroxidase-conjugated secondary antibody (1:10,000) (Promega). Antibody complexes were detected using SuperSignal West Pico Chemiluminescent substrate (Thermo scientific) and exposed to film (Kodak).

Detection of DNase resistant particles

The detection of infectious virus being released from HSG cells were performed by collecting HSG cell supernatant at stated times post infection. To degrade free DNA not encapsidated within virions, supernatant was treated with 250U DNase (Promega) or PBS for 15 min at 56^{0}C, followed by enzyme inactivation at 65^{0}C for 10 min. To release viral DNA (vDNA) from capsids, proteinase K was used as described in the blood and body fluid spin protocol of the QIAamp DNA blood minikit (QIAGEN). DNA was eluted in 200 µl of sterile water. Levels of viral DNA was determined using primers for T Ag and/or VP1 in quantitative real time PCR as described above. A plasmid, pBKV containing the entire genome of BKV, a gift from Volker Nickeleit (UNC-CH) was used to derive standard curves for viral DNA quantitation.

Data for the extracellular BKV DNA load and BrdU incorporation in the presence of increasing drug concentrations were expressed as percent inhibition for both uninfected and infected HSG cells. Graphs were generated by applying the best-fitting curve using GraphPad Prism to calculate the EC50 and CC50. The respective selectivity index (SI) was obtained by determining the CC50/EC50 ratios.

Results

Effect of Cidofovir, Ciprofloxacin and Leflunomide on BKV early gene expression in salivary gland cells and in Vero cells

To investigate the effect of cidofovir (CDV), ciprofloxacin (CPRO) and leflunomide (LEF) on BKV early gene expression, we measured T Ag RNA in triplicate at days 3 and 4 pi with VR-837 BKV (ATCC) by qRTPCR in 3 separate experiments (each symbol represents a distinct experiment) (Figure 1). The results were normalized to the levels of β-actin using the $2^{-\Delta\Delta C(T)}$ method, and are presented as the changes (n-fold) in T Ag transcript levels relative to untreated BKV-infected cells at each time point. Compared to salivary glands cells infected with BKV only, a consistent decrease in mean T Ag expression was observed in the presence of CPRO and CDV. No significant change was detected in mean BKV levels with LEF at day 3, but a significant decrease with LEF treatment was detected at day 4. Effect on gene expression was determined beginning on day 3 post infection because we have previously shown that BKV replication is delayed in salivary gland cells, such that a significant increase in extracellular viral load occurs at 3 dpi (28) compare to kidney (RPTE) cells which occurs after 2 dpi (28, 39) (Figure 1 supplemental).

In Vero cells, T Ag expression was measured in triplicate at 3, 4 and 5 days pi and post

drug treatment by qRTPCR. RNA levels were compared to BKV only. With CDV treatment a

variable trend of high T Ag expression was detected on day 3 pi followed by a decrease on day 4

and a rebound on day 5. LEF treatment resulted in low T Ag expression on day 3, followed by

an increase on day 4 and a decrease on day 5. CPRO treatment however was consistently low at

all time points post infection.

Effect of Cidofovir, Ciprofloxacin and Leflunomide on BKV late gene transcription in salivary

gland cells and in Vero cells

To investigate the effect of cidofovir, ciprofloxacin and leflunomide on BKV late gene

expression, VP1 RNA was measured by qRTPCR in triplicate at 3, 4 and 5 days pi and post

treatment. Four separate experiments were performed for days 3 and 4 and two separate

experiments for day 5 (Each symbol denotes a separate experiment) (Figure 2). The results were

normalized to the levels of β-actin using the $2^{-\Delta\Delta C(T)}$ method, and are presented as the changes

(n-fold) in VP1 transcript levels relative to untreated BKV-infected cells at each time point. A

consistent increase in mean VP1 expression was detected in the presence of CDV at days 3, 4

and 5. This increase was also observed with LEF at days 3 and 4, with a decrease at day 5. A

consistent decrease in mean VP1 expression was detected with CPRO treatment during each time

point post infection.

Similarly in Vero cells, VP1 RNA was measured in triplicate at 3, 4 and 5 days pi/post

drug treatment by qRTPCR. These studies were performed three times, Figure 2B is a

representative experiment. A decrease in mean VP1 expression was observed in the presence of

CDV at days 3 and 4pi but an increase in VP1 expression was detected on day 5 pi. LEF

treatment on day 4pi resulted in a slight decrease in VP1 expression compared to day 3 followed

by a significant increase on day 5pi. CPRO treatment showed consistently low levels of VP1 expression at each time point post infection.

Effect of Cidofovir, Ciprofloxacin and Leflunomide on protein expression in salivary gland cells

To investigate the effect of cidofovir, ciprofloxacin and leflunomide on BKV T Ag protein expression, T Ag protein was measured at 3, 4 and 5 days pi/post drug treatment by immonoblot (Figure 3A). The results were normalized to the levels of β-actin using densitometry (Figure 3B), and are presented as T Ag protein relative to untreated BKV-infected cells at each time point. A consistent decrease in T Ag protein expression was detected in the presence of all three drugs at days 3, 4 and 5. Interestingly, by day 5 LEF exhibited the most inhibition. Treatment with LEF may have had some effect on the infected cells as beta actin levels continued to decrease over the 3 day period. Similar to what was seen by immunoblot, immunofloresence also detected the most profound decrease in T Ag protein expression with CPRO treatment. T Ag expression was diminished by approximately the same amount in LEF and CDV treated cells. A representative panel is shown in Figure 3C. Similar results were detected for VP1 protein expression (data not shown).

Effect of Cidofovir, Ciprofloxacin and Leflunomide on BKV genome replication in salivary gland cells

To investigate whether BKV genome replication in salivary gland cells were affected by drug treatment, BKV DNA loads were measured at 3, 4 and 5 dpi/post drug treatment by qPCR (Figure 4). A standard curve was constructed using a plasmid encoding for the BKV genome to determine BKV copy number. The largest decrease of BKV genome replication occurred with CPRO-treated cells over the three day period 2.5-4 log decrease compared to untreated. LEF decreased BKV genome replication 0.5-1 log while CDV showed an intermediate phenotype

with a 2-3 log decrease over the three day period. Primers targeted toward both T Ag (Figure 4) and VP1 (supplemental Figure 4) regions of the genome provided similar results.

Effect of Cidofovir, Ciprofloxacin and Leflunomide on encapsidated BK viral progeny release in salivary gland cells and in Vero cells

To investigate how these treatments affected the release of encapsidated BK virions into the supernatant of HSG and Vero cells, DNase resistant particles were quantified by qPCR and BKV DNA loads measured at 3, 4 and 5 dpi/post drug treatment (Figure 5A). A standard curve was constructed using a plasmid encoding for BKV genome to determine BKV copy number. Amplification was performed with both T Ag (Figure 5A and 5C) and VP1 (5A suppl and 5C suppl) primer sets, both providing similar results. In media from both BKV only cell types, the virion release continued to increase from day 3 to day 5. In HSG media, treatment with all of the agents resulted in decrease of 1-1.5 logs at day 3 and 2-3 logs decrease at day 5 (Figure 5A). In Vero media, treatment with both CPRO and CDV resulted in 1.5-2 logs decrease while LEF showed an increase in encapsidated virion release over the 3 to 5 day post infection period (Figure 5C and 5C suppl).

The efficacy of these agents on the treatment of wild type clinical isolate-derived virus was also assessed 5 days pi of HSG cells. Across treatments a 0.5 to 1 log decrease was detected in two HIVSGD patient viruses (HIV SGD 18 and 19) and urine derived archetype virus (Lung transplant WW) while 0.5 log decrease was detected with treatment of the laboratory adapted strain (MM) at 5 days post treatment (Figure 5B). Amplification was performed with both T Ag (Figure 5B) and VP1 (5B suppl) primer sets, both providing similar results.

Effect of Cidofovir, Ciprofloxacin and Leflunomide on salivary gland cell proliferation and viability

To investigate metabolic activity of drug-treated HSG cells with or without BKV infection, WST-1 assays were used over 3 to 5 day period. Compared to uninfected untreated HSGs, BKV infection increased cellular metabolic activity at all time points, with the greatest increase occurring at 5 days pi to 105%. With the exception of CPRO at day 3, all drug-treated cells with BKV infection displayed increased metabolic activity compared to uninfected cells with drug at each time point (Figure 6A). The most significant increase occurred at day 4 pi, to 103% for CPRO+BKV, CDV+BKV and LEF+BKV. Compared to uninfected untreated HSG cells, drug treatment only did not significantly change metabolic activity at any time point investigated. To investigate host cell DNA replication and metabolic activity with increasing concentrations of drug treatment both BrdU incorporation and WST-1 assays were used. Each drug reduced host cell DNA replication in a concentration-dependent manner (Figure 6B).
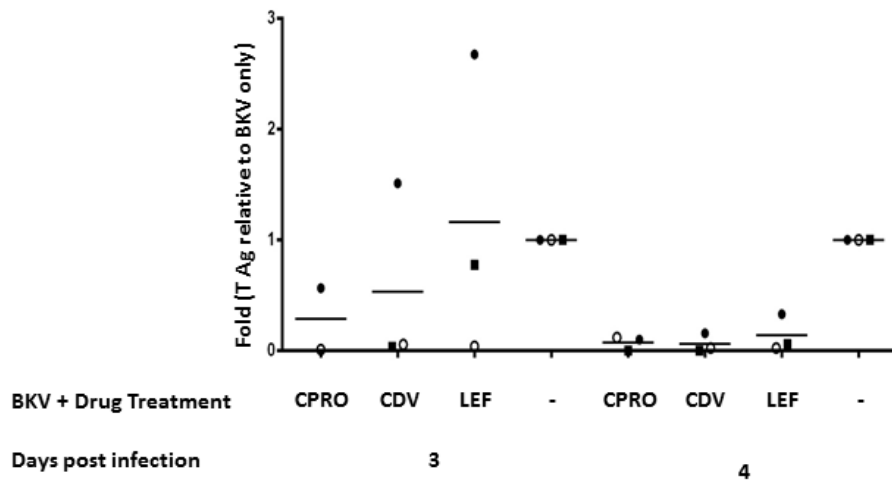
Figure 1A. Effect of drug treatment on early BK viral gene expression in human salivary gland cells. HSG cells were infected with BKV for 24h then treated with drug as described in

the materials and methods. At stated times post infection cells were collected, RNA isolated,

cDNA generated and qRTPCR performed for T Ag viral transcripts. Gene expression values

were normalized to the levels of β-actin transcripts, using $2^{-DDC(T)}$ method and are represented as

the changes (n-fold) in VP1transcript levels with the levels in non-drug treated (BKV only)

samples arbitrarily set to 1. Each symbol represents a different experiment.
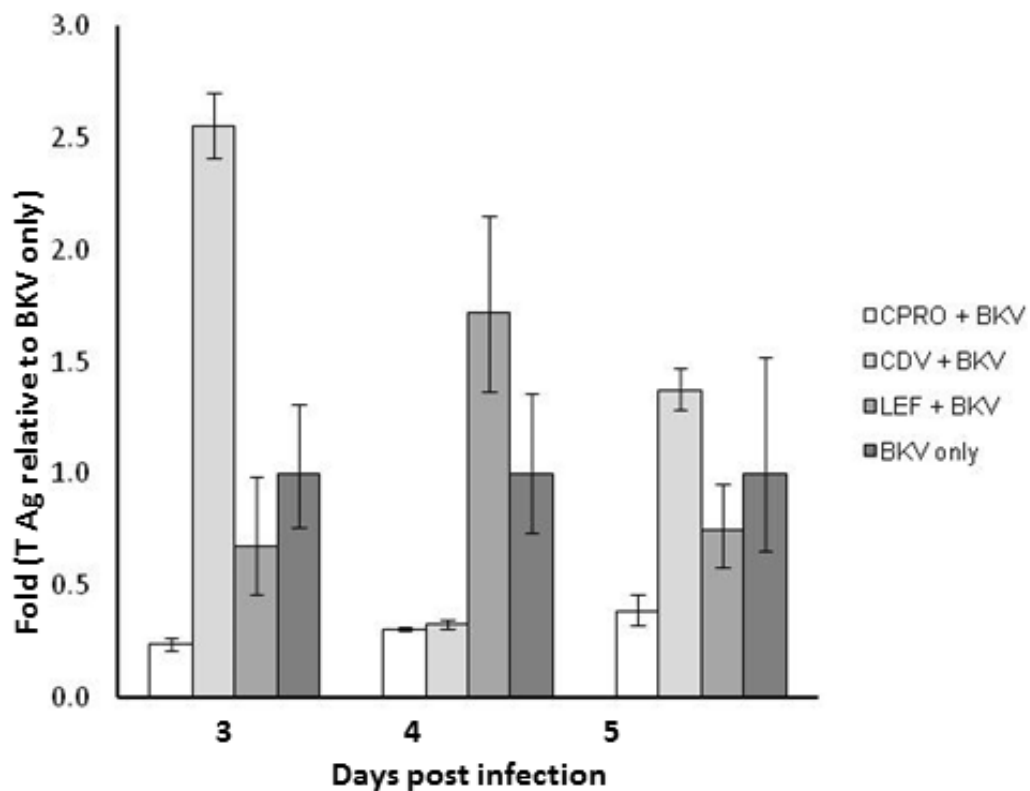
Figure 1B. Effect of drug treatment on early BK viral gene expression in Vero cells. Vero

cells were infected with BKV for 24h then treated with drug as described in the materials and

methods. At stated times post infection cells were collected, RNA isolated, cDNA generated and

qRTPCR performed for Tag viral transcripts. Gene expression values were normalized to the

levels of β-actin transcripts, using $2^{-DDC(T)}$ method and are represented as the changes (n-fold) in Tag transcript levels with the levels in non-drug treated (BKV only) samples arbitrarily set to 1.
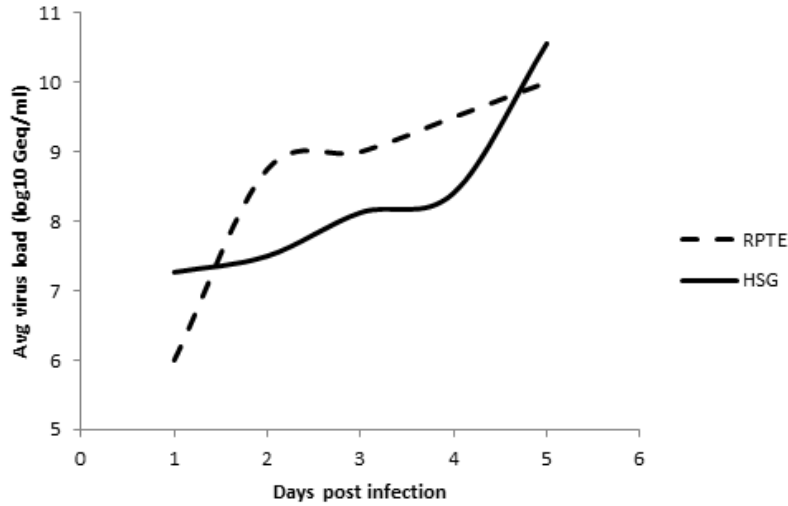
Figure 1 supplemental. Comparison of BKV replication trend over time in human kidney(RPTE) versus salivary gland (HSG) cells. HSG cells show a significant increase in extracellular BKV load at 3dpi compared to RPTE cells which occurs earlier at 2dpi. RPTE trend was extracted from work performed by Li et al(47).
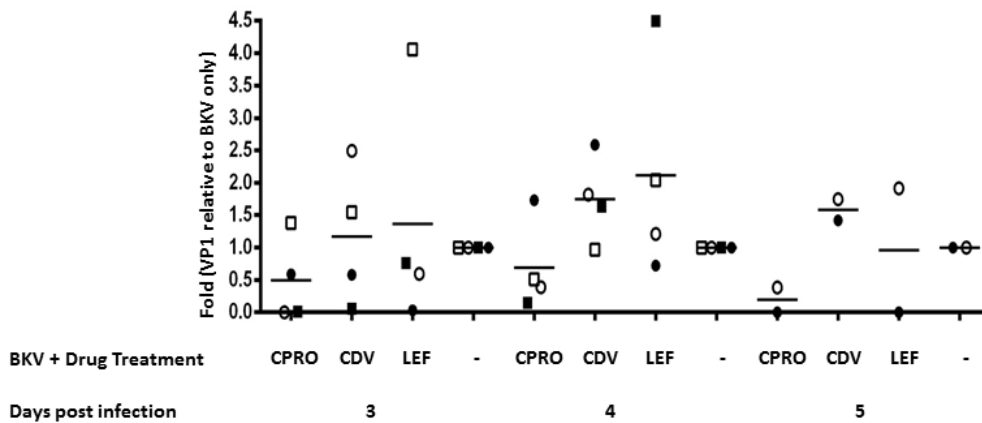
Figure 2A. Effect of drug treatment on late BK viral gene expression in human salivary gland cells. HSG cells were infected with BKV for 24h then treated with drug as described in the

materials and methods. At stated times post infection cells were collected, RNA isolated, cDNA generated and qRTPCR performed for VP1 viral transcripts. Gene expression values were normalized to the levels of β-actin transcripts, using $2^{-DDC(T)}$ method and are represented as the changes (n-fold) in VP1 transcript levels with the levels in non-drug treated (BKV only (-)) samples arbitrarily set to 1. Each dot represents a different experiment.
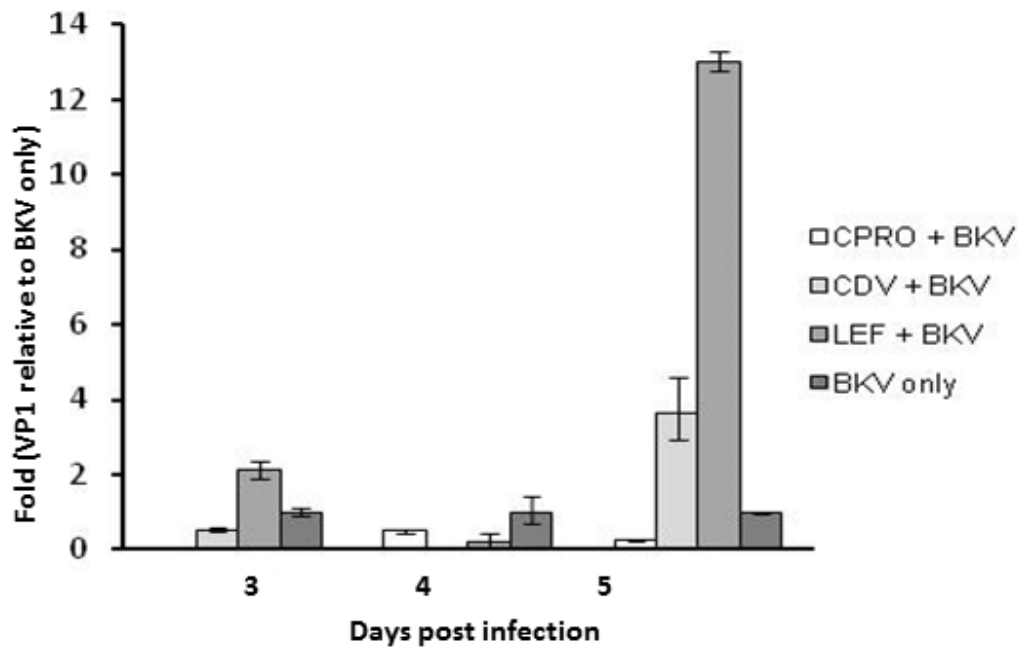
Figure 2B. Effect of drug treatment on late BK viral gene expression in Vero cells. Vero cells were infected with BKV for 24h then treated with drug as described in the materials and methods. At stated times post infection cells were collected, RNA isolated, cDNA generated and qRTPCR performed for VP1 viral transcripts. Gene expression values were normalized to the levels of β-actin transcripts, using $2^{-DDC(T)}$ method and are represented as the changes (n-fold) in VP1 transcript levels with the levels in non-drug treated (BKV only (-)) samples arbitrarily set to 1.

155
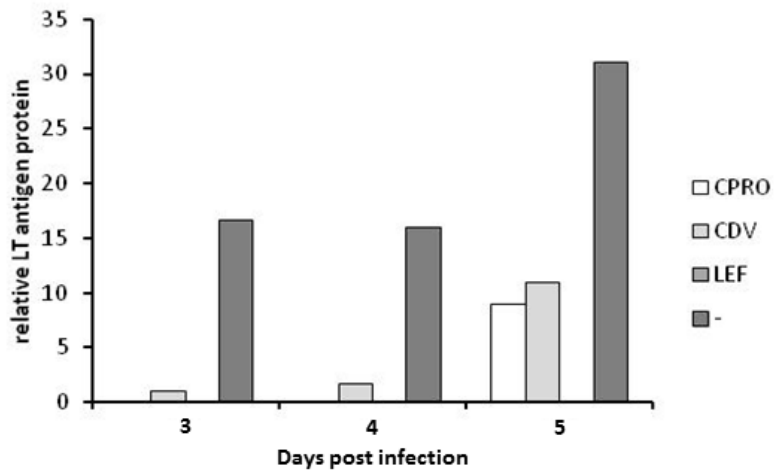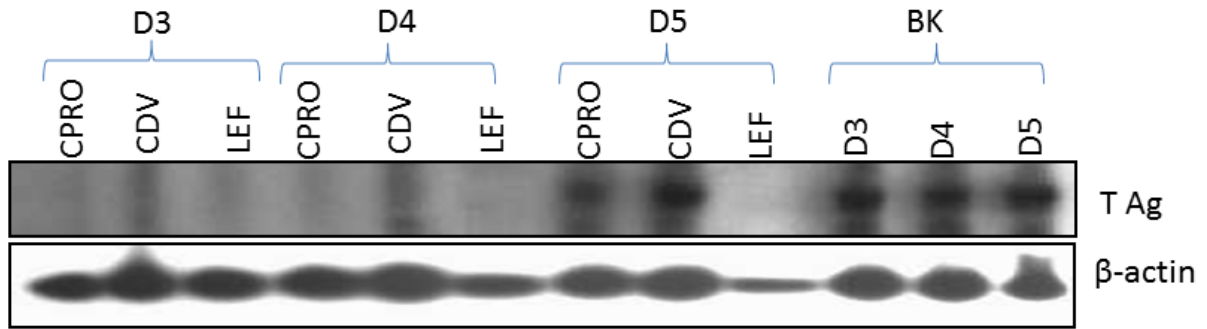
Figure 3A. Effect of drug treatment on BK protein expression in human salivary gland cells. At stated times post infection cell lysates were collected and used for immunoblotting as described in the materials and methods. Antibodies against T Ag (top panel) and β-actin (bottom panel) were used. Bottom panel shows relative L Tag protein expression compared to β-actin.
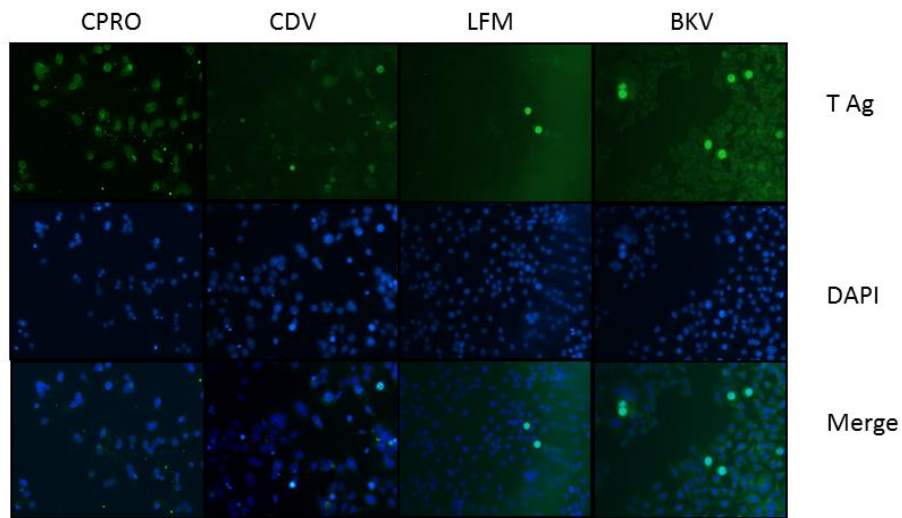
Figure 3B. Effect of drug treatment on BK protein expression in human salivary gland cells. At 4 days post infection cells were fixed and stained for T Ag (green). DAPI (blue) was used to stain the cell nuclei. Representative photograph of BKV T Ag and nuclear staining are shown for BKV-infected cells treated with and without drugs (20X magnification).
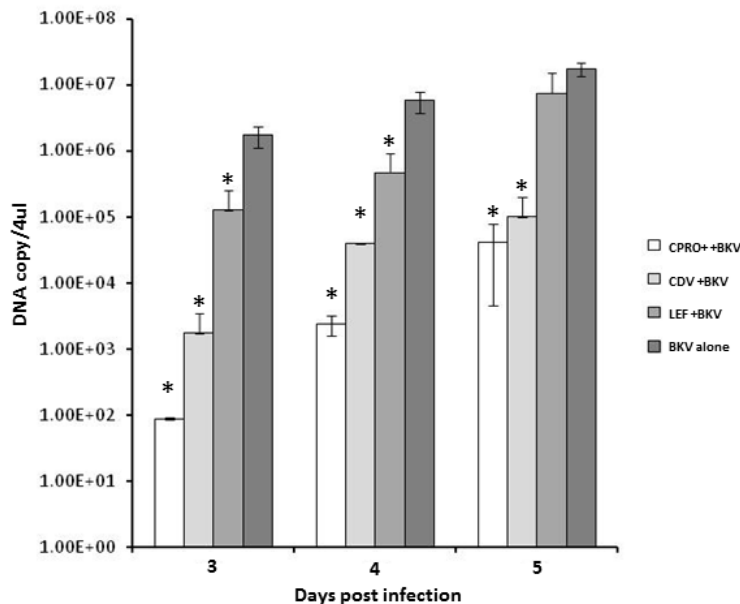
Figure 4. Effect of drug treatment on BKV genome replication in human salivary gland cells. HSG cells were infected with BKV and treated with drug as described in the materials and methods. At stated times post infection cells were collected, DNA isolated, and qrtPCR performed for T Ag DNA copy no. A standard curve (data not shown) was constructed using a

plasmid coding for BKV whole genome. The error bars represent the SD and the asterisk

denotes a p-value <0.05 as determined by the t-test.
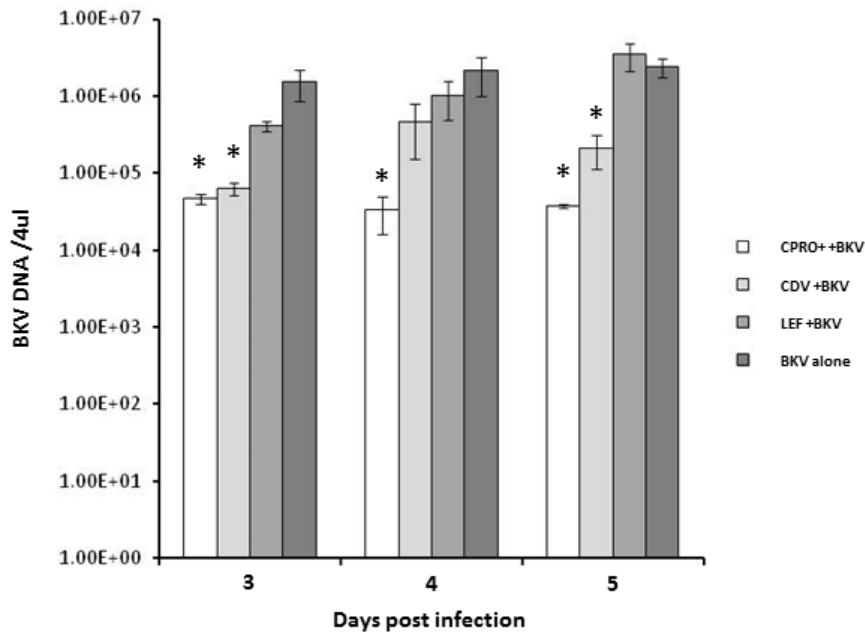
Figure 4 supplemental. Effect of drug treatment on BKV genome replication in human salivary gland cells. HSG cells were infected with BKV and treated with drug as described in the materials and methods. At stated times post infection cells were collected, DNA isolated, and qrtPCR performed for VP1 DNA copy no. A standard curve (data not shown) was constructed using a plasmid coding for BKV whole genome. The error bars represent the SD and the asterisk denotes a p-value <0.05 as determined by the t-test.
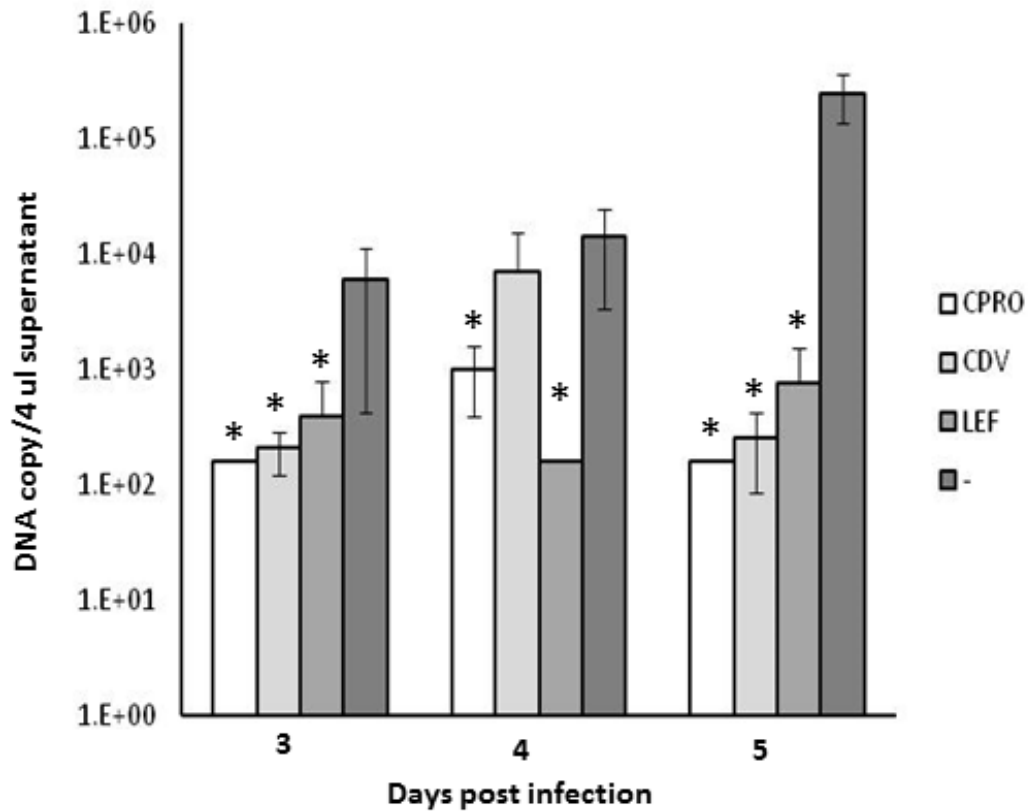
Figure 5A. Effect of drug treatment on infectious BK virus progeny release from human salivary gland cells. HSG cells were infected with BKV and treated with drug as described in the materials and methods. At stated times post infection supernatant was collected, Dnase-treated and qrtPCR performed for T Ag DNA copy no. A standard curve (data not shown) was constructed using a plasmid coding for BKV whole genome. The error bars represent the SD and the asterisk denotes a p-value <0.05 as determined by the t-test.
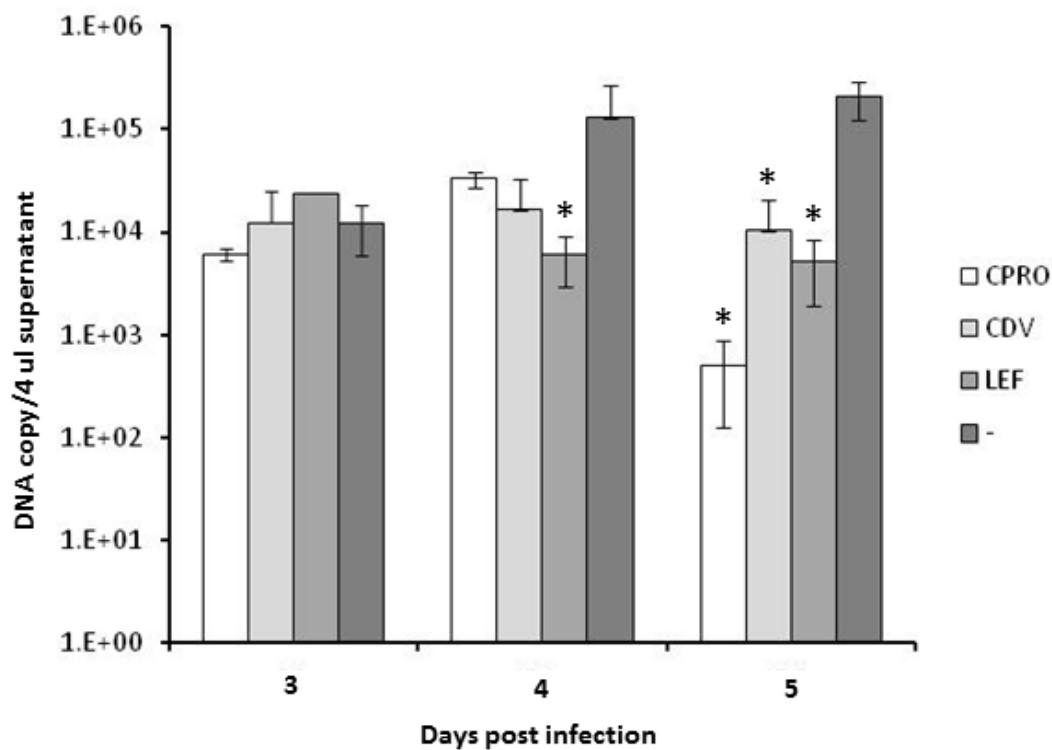
Figure 5A supplemental. Effect of drug treatment on infectious BK virus progeny release in human salivary gland cells.   HSG cells were infected with BKV and treated with drug as described in the materials and methods. At stated times post infection supernatant was collected, Dnase-treated and qrtPCR performed for VP1 DNA copy no. A standard curve (data not shown) was constructed using a plasmid coding for BKV whole genome. . The error bars represent the SD and the asterisk denotes a p-value <0.05 as determined by the t-test.
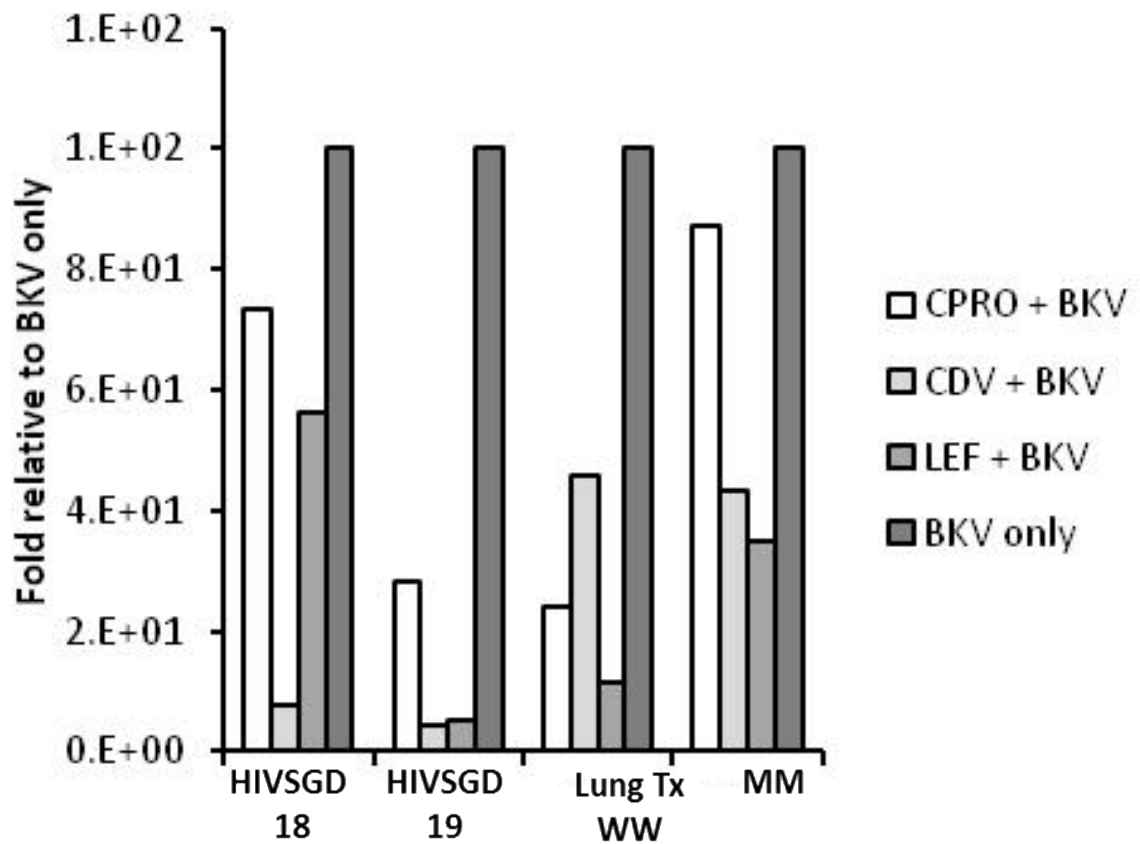
Figure 5B. Effect of drug treatment on patient-derived infectious BK virus progeny release in human salivary gland cells. HSG cells were infected with BKV and treated with drug as described in the materials and methods. At 5 days post infection supernatant was collected, Dnase-treated and qrtPCR performed for T Ag DNA copy no. A standard curve (data not shown) was constructed using a plasmid coding for BKV whole genome. Data is shown as fold relative to untreated, BKV-infected cells (BKV only), with BKV only set at 100%.
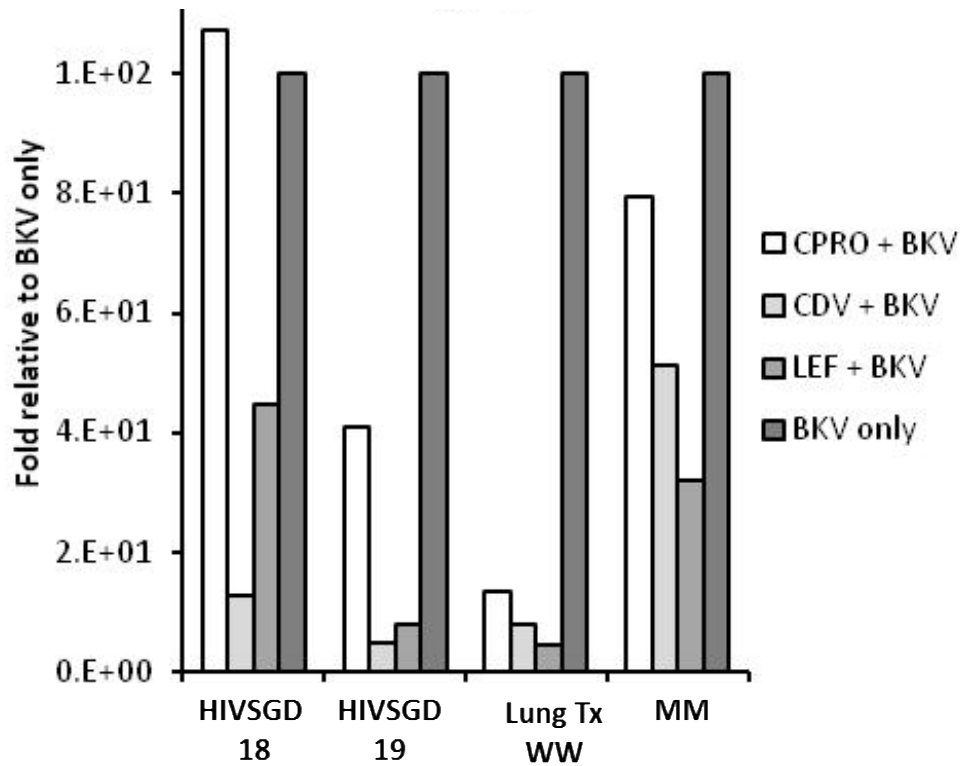
Figure 5B supplemental. Effect of drug treatment on patient-derived infectious BK virus progeny release in human salivary gland cells. HSG cells were infected with BKV and treated with drug as described in the materials and methods. At 5 days post infection supernatant was collected, Dnase-treated and qrtPCR performed for VP1 DNA copy no. A standard curve (data not shown) was constructed using a plasmid coding for BKV whole genome. Data is shown as fold relative to untreated, BKV-infected cells (BKV only), with BKV only set at 100%.
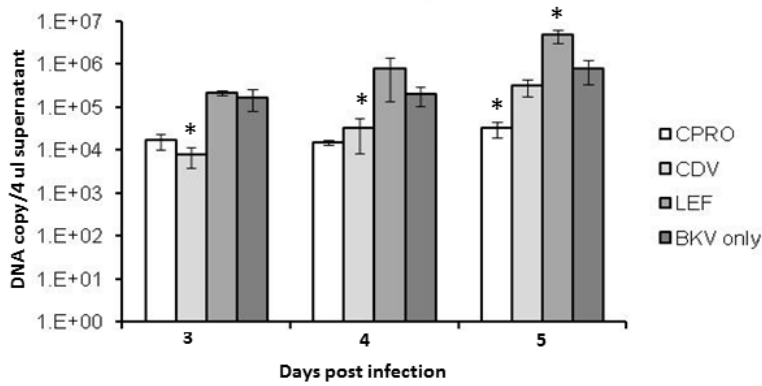
Figure 5C. Effect of drug treatment on infectious BK virus progeny release from Vero cells.

Vero cells were infected with BKV and treated with drug as described in the materials and methods. At stated times post infection supernatant was collected, Dnase-treated and qrtPCR performed for T Ag DNA copy no. A standard curve (data not shown) was constructed using a plasmid coding for BKV whole genome. The error bars represent the SD and the asterisk denotes a p-value <0.05 as determined by the t-test.
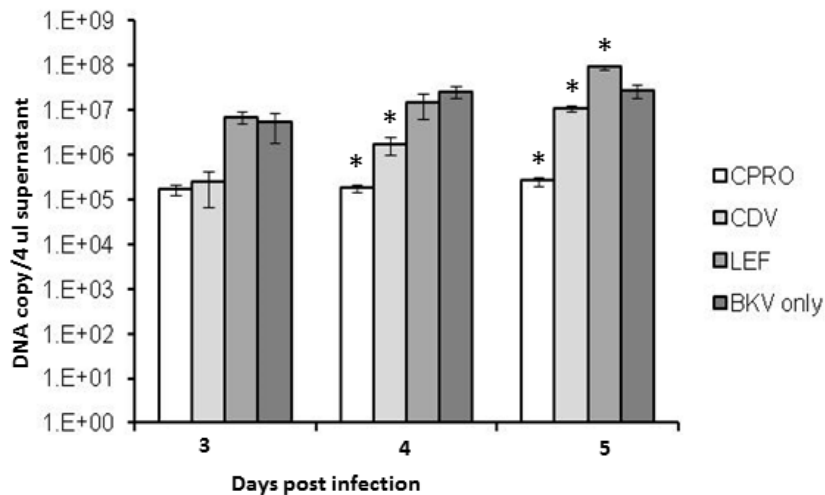
Figure 5C supplemental. Effect of drug treatment on infectious BK virus progeny release from Vero cells. Vero cells were infected with BKV and treated with drug as described in the materials and methods. At stated times post infection supernatant was collected, Dnase-treated

and qrtPCR performed for VP1DNA copy no. A standard curve (data not shown) was
constructed using a plasmid coding for BKV whole genome. The error bars represent the SD
and the asterisk denotes a p-value <0.05 as determined by the t-test.
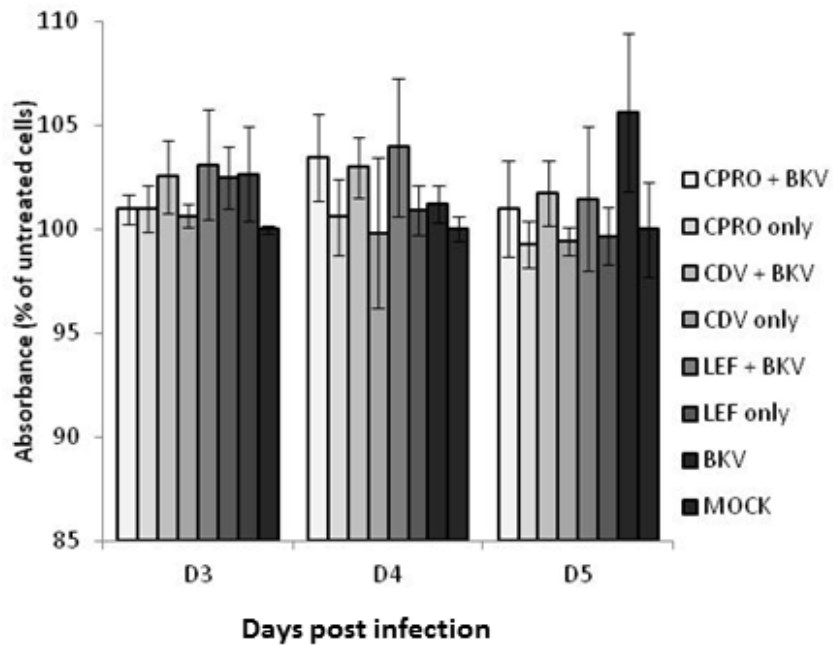
Figure 6A. Effect of drug treatment on total host cell DNA replication in BKV-infected and
uninfected human salivary gland cells. Cellular DNA replication was examined with BrdU
incorporation and metabolic activity as described in Materials and Methods. Medium with or
without drug was added 24hpi and absorbance measured at indicated time points. Absorbance for
untreated uninfected cells (mock) at each time point was set as 100%.
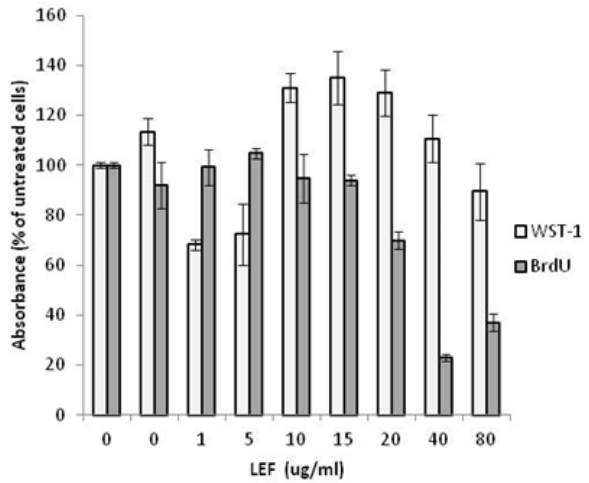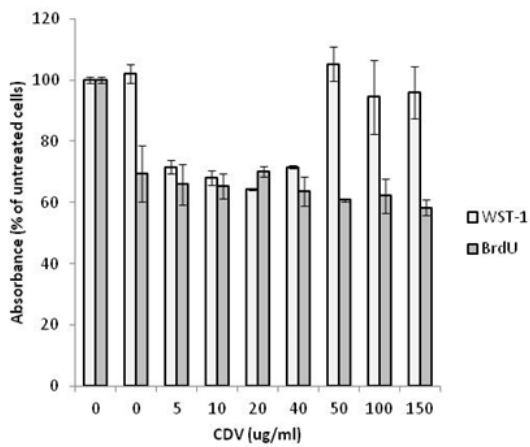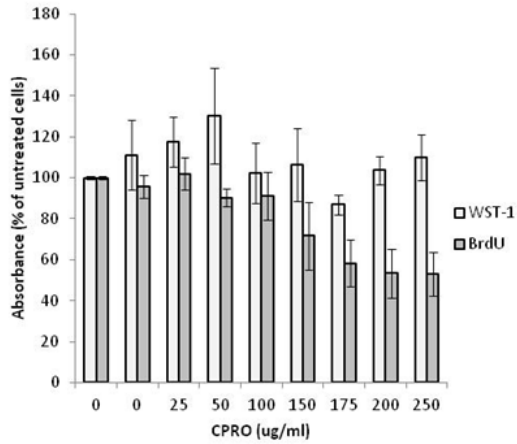
Figure 6B. Effect of drug treatment on metabolic activity in BKV-infected and uninfected human salivary gland cells. Medium with indicated drug concentrations was added 24hpi and absorbance measured at 72hpi. Absorbance for untreated uninfected cells was set as 100%.
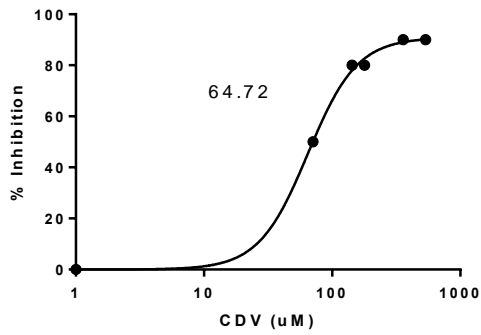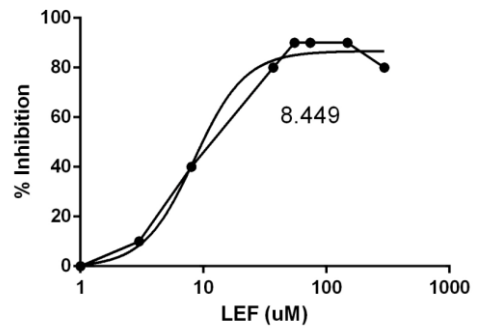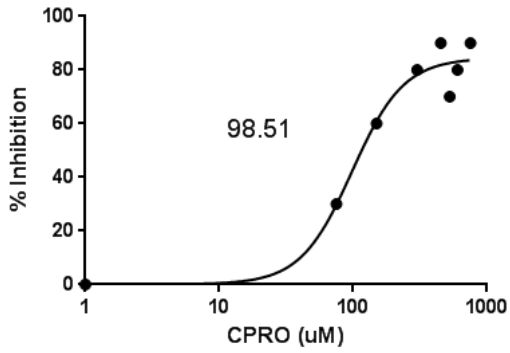
Figure 7A. Determination of EC50 values by curve fitting. The effect of increasing drug

concentration on BKV supernatant loads at 72 hpi was analyzed by curve fitting using GraphPad

Prism for EC50. The data display means of triplicate.
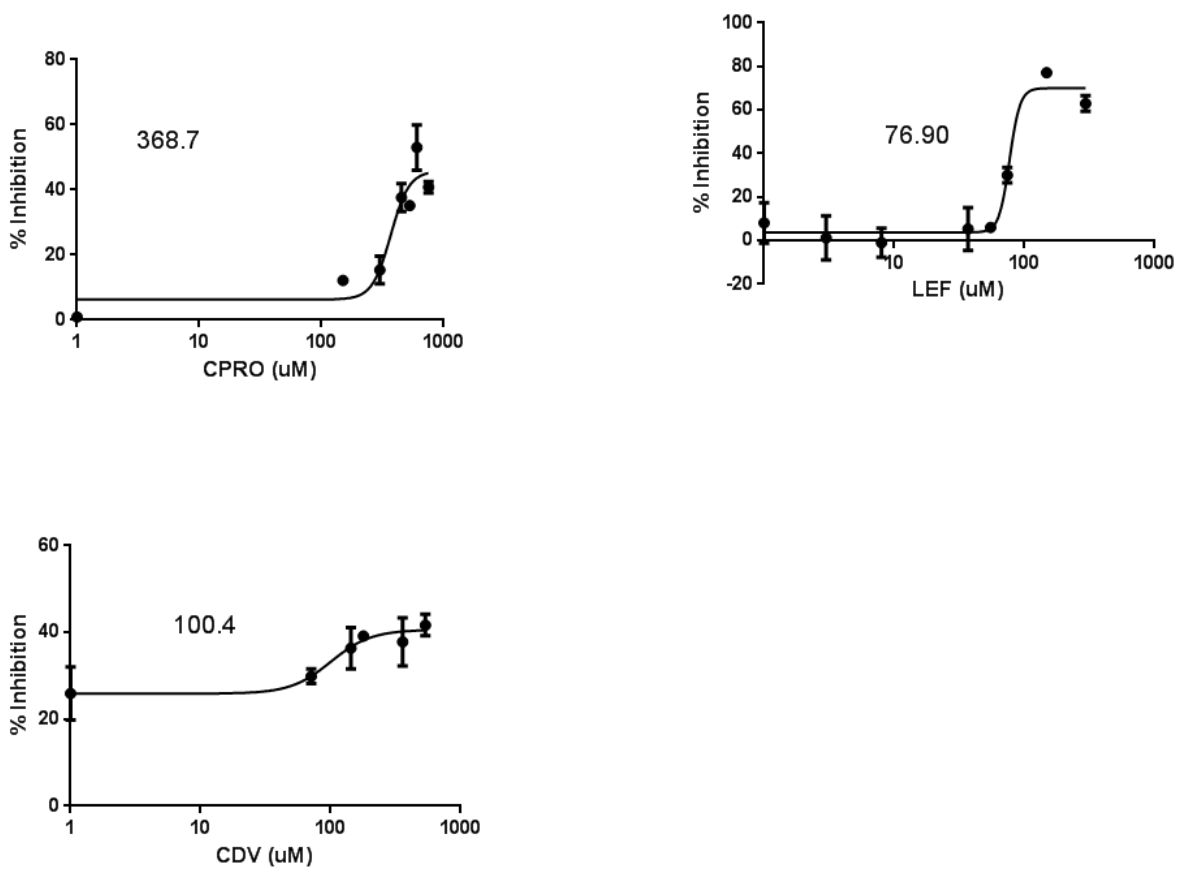
Figure 7B. Determination of CC50 values by curve fitting. The effect of increasing drug concentration on BrdU incorporation at 72 hpi was analyzed by curve fitting using GraphPad Prism for CC50. The data display means of triplicate

Discussion

HIV-SGD treatment thus far has been palliative due to the lack of an identified pharmacologic target. However, our group has recently shown that BK infection is associated with HIV-SGD (28, 29). All previous BKV anti-viral experiments have been performed in human or monkey kidney cells or lung fibroblasts (12, 34, 35). Based on our observation that BKV can also infect salivary gland cells and is associated with pathology both in vitro and in

vivo in humans (28, 29, 40, 41) we decided to test three antiviral drugs, CPRO, CDV and LEF on the BKV life cycle in salivary gland cells in vitro. The concentration of drugs used to treat cells were based on previous experiments performed by Bernhoff et al(14), Sharma et al(22)and Liacini et al(35). All of these drugs act by either inhibiting topoisomerase activity or are thought to disrupt DNA polymerases, effectively halting viral replication (42).

CPRO has been shown to inhibit BKV activity in vitro in kidney cells (43) and reduce BK viremia when used in combination with immunosuppression reduction in kidney transplant patients (16). CPRO inhibits type II topoisomerase activity during bacterial DNA replication and is thought to inhibit BKV T Ag viral helicase activity (20). Our data has shown that CPRO is able to inhibit BKV early and late gene expression in both salivary gland and monkey kidney cells (Fig 1, 2 and 3). As well as inhibit DNA replication (Fig 4) and progeny release in salivary gland cells and monkey kidney cells (Fig 5A, 5B). In addition, when BKV patient-derived clinical isolates were used to infect salivary gland cells, they were also inhibited by CPRO (Fig 5B). CPRO had minimal effect on metabolic activity and host cell DNA replication at the concentration used for these experiments over the three to five day time period tested (Fig 6A). However, we did observe a gradual decrease in host cell DNA replication when the concentration of drug was over 150ug/ml (Fig 6B). The EC50 and CC50 of CPRO in salivary gland cells were calculated at 98.51ug/ml and 368.7ug/ml, respectively (Figure 7A, 7B). The SI was calculated at 3.74. A low selectivity index, defined as the ratio of the 50% reduction in host cell replication value to the 50% virus inhibitory concentration value, suggests a modest anti-BKV effect.

CDV treatment is currently approved for CMV-induced retinitis in HIV infected patients (44) and has been used at low doses to treat transplant patients resulting in decreased BK viremia

and viruria (24). There are also reports however, of the deleterious effects of reduced renal function and increased viral load in cidofovir-treated BKVN patients (23). CDV inhibits CMV viral DNA polymerase activity, however it's mode of action against BKV is currently unknown. In vitro, CDV has been shown to inhibit BKV activity in human kidney and lung fibroblast cells (12, 14) but has never been tested in human salivary gland cells. Our data has shown that CDV inhibits BKV early gene expression but not late gene expression in human salivary gland cells (Fig 1A, 2A). However, in monkey kidney cells, early gene expression inhibition is inconsistent while late gene expression is inhibited up until 5dpi. CDV inhibited DNA replication (Fig 4) and progeny release in both salivary gland and monkey kidney cells (Fig 5), but were not as effective as CPRO. In addition, CDV inhibited two HIVSGD patient-derived viruses (HIVSGD 18 and 19) and the laboratory adapted strain (MM) more effectively than CPRO but not the urine derived archetype virus (lung transplant WW). CDV had minimal effect on metabolic activity and host cell DNA replication at the concentration used for these experiments over the three to five day time period tested (Fig 6). However, at 72hpi with increasing drug concentration we observed a seventy percent decrease in host cell DNA replication in the presence of viral infection with and without drug while cell metabolism decreased at lower drug concentrations (5- 40ug/ml) and increased at higher drug concentrations (50-150ug/ml) (Fig 6). The EC50 and CC50 of CDV in salivary gland cells were calculated at 64.72ug/ml and 100.4ug/ml, respectively. The SI was calculated at 1.55 suggesting a low anti-BKV effect. Previous work calculated the SI of CDV in human embryonic lung fibroblasts (WI-38) and human renal proximal tubular epithelial cells as 2.3 (12) and 4.9 respectively(45). Although CDV inhibited BKV replication in salivary gland cells, there are clinical limitations for its use due to its nephrotoxicity and limited oral bioavailability (23).

LEF is an anti-inflammatory drug approved to treat rheumatoid arthritis and other autoimmune conditions. LEF has been shown to inhibit pyrimidine synthesis, tyrosine kinase and dihydroorotate dyhydrogenase activity (12). Like CDV, there is conflicting data with regards to its activity against BKV in vitro (12, 13). In vivo studies have shown LEF activity against CMV and HSV and has been used in combination with immunosuppression reduction in treatment of BKVN (12, 26). LEF's antiviral activity against CMV has been shown via interference with viral assembly, specifically on the viral envelope (27), however BKV is a non-enveloped virus. At the level of transcription, our data showed that LEF inhibition was inconsistent over the three days tested in both salivary gland cells and in monkey kidney cells (Fig 1). It is possible that the observed variability in transcript levels in the presence of LEF may be due to drug toxicity. At the protein level, LEF consistently decreased T Ag expression, albeit beta actin levels were markedly lower with LEF treatment, suggesting cell toxicity. LEF appeared to be the least effective drug with regard to inhibiting BKV DNA replication (Fig 4) and progeny release in both Vero and salivary gland cells (Fig 5). LEF consistently inhibited patient-derived progeny release in salivary gland cells compared to the other drug types (Fig 5B). LEF had minimal effect on metabolic activity and host cell DNA replication at the concentration used for these experiments over the three to five day time period tested (Fig 6). However, at 72hpi we observed a decrease in host cell DNA replication at concentrations above 15ug/ml and an increase in cell metabolism at drug concentration between 10 and 40 ug/ml (Fig 6). The EC50 and CC50 of LEF in salivary gland cells were calculated at 8.449ug/ml and 76.9ug/ml, respectively. The SI was calculated at 9.1 suggesting a strong anti-BKV effect. Serum steady-state levels of the principal metabolite of LEF are 8.8, 18.0, and 63.0 µg/mL after 24 days of therapy with a 5, 10, or 25 mg daily dose, respectively (12)(Physicians Desk Reference, accessed at

http://www.micromedex.com), therefore the concentrations used in our experiments are in the clinically relevant range.

In conclusion, BKV genome replication in human salivary gland cells was decreased by all three drug types with CPRO being the most effective. The mechanism of these drugs against BKV are currently up for debate, however it is possible that BKV inhibition in salivary gland cells may be due to manipulation of a host intracellular signaling pathway that is altered by each drug that is important for BKV replication for example the Akt or mTOR pathway. With regards to patient treatment, CDV has been shown to be cytotoxic in kidney cells in vivo and is therefore not a favorable candidate for HIVSGD treatment in patients. Although LEF in our studies had a high SI in salivary gland cells, it was the most toxic based on the protein assay (Figure 3A). In kidney transplant patients however, LEF is used as an immunomodulatory agent to lower the incidence of organ rejection. Our data highlight the need for continued studies to discover more effective and less toxic drugs that can inhibit BKV replication in salivary gland cells. These studies are important because we have previously shown a causal relationship between BKV infection of the salivary gland and HIV-associated salivary gland disease (HIV-SGD)(29) which is AIDS defining in pediatric HIV infection and increasing in the adult HIV population(46). In addition, HIV-SGD is of particular interest because in 1-2% of patients malignant lymphomas have been described in association with glandular lesions making this disease a premalignant lesion(32, 33). Until better drugs become available and more in vitro and in vivo studies are performed, it would be reasonable to test CPRO in clinical trials to evaluate its efficacy in salivary gland disease in HIV patients.

REFERENCES

1. **Imperiale, M. J., and E. O. Major.** 2007. Polyomaviruses, p. 3091. *In* A. M. Field, D. M. Knipe, and P. M. Howley (ed.), Fields' Virology, 5th ed, vol. 2. Wolers Kluwer Health/Lippincott Williams & Wilkins, Philadelphia.

2. **Hirsch, H. H.** 2005. BK virus: opportunity makes a pathogen. Clin Infect Dis **41:**354-60.

3. **Hirsch, H. H., W. Knowles, M. Dickenmann, J. Passweg, T. Klimkait, M. J. Mihatsch, and J. Steiger.** 2002. Prospective study of polyomavirus type BK replication and nephropathy in renal-transplant recipients. N Engl J Med **347:**488-96.

4. **Kuypers, D. R.** 2012. Management of polyomavirus-associated nephropathy in renal transplant recipients. Nat Rev Nephrol **8:**390-402.

5. **Dugan, A. S., S. Eash, and W. J. Atwood.** 2006. Update on BK virus entry and intracellular trafficking. Transpl Infect Dis **8:**62-7.

6. **Hirsch, H. H., and J. Steiger.** 2003. Polyomavirus BK. Lancet Infect Dis **3:**611-23.

7. **Nickeleit, V., T. Klimkait, I. F. Binet, P. Dalquen, V. Del Zenero, G. Thiel, M. J. Mihatsch, and H. H. Hirsch.** 2000. Testing for polyomavirus type BK DNA in plasma to identify renal-allograft recipients with viral nephropathy. N Engl J Med **342:**1309-15.

8. **Ahsan, N., and K. V. Shah.** 2006. Polyomaviruses and human diseases. Adv Exp Med Biol **577:**1-18.

9. **Dropulic, L. K., and R. J. Jones.** 2008. Polyomavirus BK infection in blood and marrow transplant recipients. Bone Marrow Transplant **41:**11-8.

10. **Longhi, G., V. Pietropaolo, M. Mischitelli, C. Longhi, M. P. Conte, M. Marchetti, A. Tinari, P. Valenti, A. M. Degener, L. Seganti, and F. Superti.** 2006. Lactoferrin inhibits early steps of human BK polyomavirus infection. Antiviral Res **72:**145-52.

11.   **Rinaldo, C. H., R. Gosert, E. Bernhoff, S. Finstad, and H. H. Hirsch.** 2010. 1-O-hexadecyloxypropyl cidofovir (CMX001) effectively inhibits polyomavirus BK replication in primary human renal tubular epithelial cells. Antimicrob Agents Chemother **54:**4714-22.

12.   **Farasati, N. A., R. Shapiro, A. Vats, and P. Randhawa.** 2005. Effect of leflunomide and cidofovir on replication of BK virus in an in vitro culture system. Transplantation **79:**116-8.

13.   **Bernhoff, E., G. D. Tylden, L. J. Kjerpeseth, T. J. Gutteberg, H. H. Hirsch, and C. H. Rinaldo.** 2010. Leflunomide inhibition of BK virus replication in renal tubular epithelial cells. J Virol **84:**2150-6.

14.   **Bernhoff, E., T. J. Gutteberg, K. Sandvik, H. H. Hirsch, and C. H. Rinaldo.** 2008. Cidofovir inhibits polyomavirus BK replication in human renal tubular cells downstream of viral early gene expression. Am J Transplant **8:**1413-22.

15.   **Leung, A. Y., M. T. Chan, K. Y. Yuen, V. C. Cheng, K. H. Chan, C. L. Wong, R. Liang, A. K. Lie, and Y. L. Kwong.** 2005. Ciprofloxacin decreased polyoma BK virus load in patients who underwent allogeneic hematopoietic stem cell transplantation. Clin Infect Dis **40:**528-37.

16.   **Gabardi, S., S. S. Waikar, S. Martin, K. Roberts, J. Chen, L. Borgi, H. Sheashaa, C. Dyer, S. K. Malek, S. G. Tullius, N. Vadivel, M. Grafals, R. Abdi, N. Najafian, E. Milford, and A. Chandraker.** 2010. Evaluation of fluoroquinolones for the prevention of BK viremia after renal transplantation. Clin J Am Soc Nephrol **5:**1298-304.

17.   **Hasegawa, K., W. Motsuchi, S. Tanaka, and S. Dosako.** 1994. Inhibition with lactoferrin of in vitro infection with human herpes virus. Jpn J Med Sci Biol **47:**73-85.

18.   **Hara, K., M. Ikeda, S. Saito, S. Matsumoto, K. Numata, N. Kato, K. Tanaka, and H. Sekihara.** 2002. Lactoferrin inhibits hepatitis B virus infection in cultured human hepatocytes. Hepatol Res **24:**228.

19.   **Evers, D. L., X. Wang, S. M. Huong, K. A. Andreoni, and E. S. Huang.** 2005. Inhibition of human cytomegalovirus signaling and replication by the immunosuppressant FK778. Antiviral Res **65:**1-12.

20.   **Ali, S. H., A. Chandraker, and J. A. DeCaprio.** 2007. Inhibition of Simian virus 40 large T antigen helicase activity by fluoroquinolones. Antivir Ther **12:**1-6.

21.   **Rinaldo, C. H., and H. H. Hirsch.** 2007. Antivirals for the treatment of polyomavirus BK replication. Expert Rev Anti Infect Ther **5:**105-15.

22.   **Sharma, B. N., R. Li, E. Bernhoff, T. J. Gutteberg, and C. H. Rinaldo.** 2011. Fluoroquinolones inhibit human polyomavirus BK (BKV) replication in primary human kidney cells. Antiviral Res **92:**115-23.

23.   **Safrin, S., J. Cherrington, and H. S. Jaffe.** 1997. Clinical uses of cidofovir. Rev Med Virol **7:**145-156.

24.   **Savona, M. R., D. Newton, D. Frame, J. E. Levine, S. Mineishi, and D. R. Kaul.** 2007. Low-dose cidofovir treatment of BK virus-associated hemorrhagic cystitis in recipients of hematopoietic stem cell transplant. Bone Marrow Transplant **39:**783-7.

25.   **Gosert, R., C. H. Rinaldo, M. Wernli, E. O. Major, and H. H. Hirsch.** 2011. CMX001 (1-O-hexadecyloxypropyl-cidofovir) inhibits polyomavirus JC replication in human brain progenitor-derived astrocytes. Antimicrob Agents Chemother **55:**2129-36.

26.   **Josephson, M. A., D. Gillen, B. Javaid, P. Kadambi, S. Meehan, P. Foster, R. Harland, R. J. Thistlethwaite, M. Garfinkel, W. Atwood, J. Jordan, M. Sadhu, M. J. Millis, and J. Williams.** 2006. Treatment of renal allograft polyoma BK virus infection with leflunomide. Transplantation **81:**704-10.

27.   **Knight, D. A., A. Q. Hejmanowski, J. E. Dierksheide, J. W. Williams, A. S. Chong, and W. J. Waldman.** 2001. Inhibition of herpes simplex virus type 1 by the experimental immunosuppressive agent leflunomide. Transplantation **71:**170-4.

28.   **Jeffers, L. K., V. Madden, and J. Webster-Cyriaque.** 2009. BK virus has tropism for human salivary gland cells in vitro: implications for transmission. Virology **394:**183-93.

29.   **Jeffers, L., and J. Y. Webster-Cyriaque.** 2011. Viruses and salivary gland disease (SGD): lessons from HIV SGD. Adv Dent Res **23:**79-83.

30.   **Patton, L. L., and C. van der Horst.** 1999. Oral infections and other manifestations of HIV disease. Infect Dis Clin North Am **13:**879-900.

31.	**McArthur, C. P., A. Subtil-DeOliveira, D. Palmer, R. M. Fiorella, S. Gustafson, D. Tira, and R. N. Miranda.** 2000. Characteristics of salivary diffuse infiltrative lymphocytosis syndrome in West Africa. Arch Pathol Lab Med **124:**1773-9.

32.	**DiGiuseppe, J. A., R. L. Corio, and W. H. Westra.** 1996. Lymphoid infiltrates of the salivary glands: pathology, biology and clinical significance. Curr Opin Oncol **8:**232-7.

33.	**Ioachim, H. L., and J. R. Ryan.** 1988. Salivary gland lymphadenopathies associated with AIDS. Hum Pathol **19:**616-7.

34.	**Acott, P. D., P. A. O'Regan, S. H. Lee, and J. F. Crocker.** 2006. Utilization of vero cells for primary and chronic BK virus infection. Transplant Proc **38:**3502-5.

35.	**Liacini, A., M. E. Seamone, D. A. Muruve, and L. A. Tibbles.** 2010. Anti-BK virus mechanisms of sirolimus and leflunomide alone and in combination: toward a new therapy for BK virus infection. Transplantation **90:**1450-7.

36.	**Shirasuna, K., M. Sato, and T. Miyazaki.** 1981. A neoplastic epithelial duct cell line established from an irradiated human salivary gland. Cancer **48:**745-52.

37.	**Rollison, D. E., U. Utaipat, C. Ryschkewitsch, J. Hou, P. Goldthwaite, R. Daniel, K. J. Helzlsouer, P. C. Burger, K. V. Shah, and E. O. Major.** 2005. Investigation of human brain tumors for the presence of polyomavirus genome sequences by two independent laboratories. Int J Cancer **113:**769-74.

38.	**Ding, R., M. Medeiros, D. Dadhania, T. Muthukumar, D. Kracker, J. M. Kong, S. R. Epstein, V. K. Sharma, S. V. Seshan, B. Li, and M. Suthanthiran.** 2002. Noninvasive diagnosis of BK virus nephritis by measurement of messenger RNA for BK virus VP1 in urine. Transplantation **74:**987-94.

39.	**Li, R., B. N. Sharma, S. Linder, T. J. Gutteberg, H. H. Hirsch, and C. H. Rinaldo.** 2013. Characteristics of polyomavirus BK (BKPyV) infection in primary human urothelial cells. Virology **440:**41-50.

40.	**Robaina, T. F., G. S. Mendes, F. J. Benati, G. A. Pena, R. C. Silva, M. A. Montes, M. E. Janini, F. P. Camara, and N. Santos.** 2013. Shedding of polyomavirus in the saliva of immunocompetent individuals. J Med Virol **85:**144-8.

41. **Robaina, T. F., G. S. Mendes, F. J. Benati, G. A. Pena, R. C. Silva, M. A. Montes, R. Otero, G. F. Castro, F. P. Camara, and N. Santos.** 2013. Polyomavirus in Saliva of HIV-infected Children, Brazil. Emerg Infect Dis **19:**155-7.

42. **Bennett, S. M., N. M. Broekema, and M. J. Imperiale.** 2012. BK polyomavirus: emerging pathogen. Microbes Infect **14:**672-83.

43. **Portolani, M., P. Pietrosemoli, C. Cermelli, A. Mannini-Palenzona, M. P. Grossi, L. Paolini, and G. Barbanti-Brodano.** 1988. Suppression of BK virus replication and cytopathic effect by inhibitors of prokaryotic DNA gyrase. Antiviral Res **9:**205-18.

44. 1996. FDA approves cidofovir for treatment of CMV retinitis. Food and Drug Administration. J Int Assoc Physicians AIDS Care **2:**30.

45. **Topalis, D., I. Lebeau, M. Krecmerova, G. Andrei, and R. Snoeck.** 2011. Activities of different classes of acyclic nucleoside phosphonates against BK virus in primary human renal cells. Antimicrob Agents Chemother **55:**1961-7.

46. **Patton, L. L., R. McKaig, R. Strauss, D. Rogers, and J. J. Eron, Jr.** 2000. Changing prevalence of oral manifestations of human immuno-deficiency virus in the era of protease inhibitor therapy. Oral Surg Oral Med Oral Pathol Oral Radiol Endod **89:**299-304.

47. 2007. Fields' Virology. *In* P. M. H. David M. Knipe (ed.), 5th ed. Wolters Kluwer Health/Lippincott Williams & Wilkins, Philadelphia.

APPENDIX 2:
CORRELATION OF TRANSCRIPTION OF MALAT-1, A NOVEL NONCODING RNA, WITH DEREGULATED EXPRESSION OF TUMOR SUPPRESSOR p53 IN SMALL DNA TUMOR VIRUS MODELS[1]

Overview

Although metastasis-associated lung adenocarcinoma transcript (MALAT)-1 is known to be consistently upregulated in several epithelial malignancies, little is known about its function or regulation. We therefore examined the relationship between MALAT-1 expression and candidate modulators such as DNA tumor virus oncoproteins human papillomavirus (HPV)-16 E6 and E7, BK virus T antigen (BKVTAg), mouse polyoma virus middle T antigen (MPVmTAg) and tumor suppressor genes p53 and pRb. Using suppressive subtractive hybridization (SSH) and real-time reverse transcriptase polymerase chain reaction (RT-PCR) assays, MALAT-1 was shown to be increased in viral oncongene-expressing salivary gland biopsies from humans and mice. The results also indicated that MALAT-1 transcripts and promoter activity were increased in vitro when viral oncongene-expressing plasmids were introduced into different cell types. These same viral oncogenes in addition to increasing MALAT-1 transcription have also been shown to inhibit p53 and/or pRb function. In p53 mutant or inactive cell lines MALAT-1 was also shown to be highly upregulated. We hypothesize that there is a correlation between MALAT-1 over-expression and p53 deregulation. In conclusion, we show that disruption of p53, by both polyoma and papilloma oncoproteins appear to play an important role in the up-regulation of MALAT-1. MALAT-1 therefore might represent a biomarker for p53 deregulation within malignancies.

---

[1] This appendix previously appeared as an article in the Journal of Cancer Therapy. The original citation is as follows: Jeffers, LK *et al*. "Correlation of Transcription of MALAT-1, a Novel Noncoding RNA, with Deregulated Expression of Tumor Suppressor p53 in Small DNA Tumor Virus Models", Journal of Cancer Therapy, 2013, 4, 774-786.

Introduction

Metastasis-associated lung adenocarcinoma transcript-1 (MALAT-1) is a novel large, noncoding RNA. The MALAT-1 gene, also known as the α gene, is found on chromosome 11q13 and is well conserved among mammalian species (1). The MALAT-1 transcript is widely expressed in normal human and mouse tissue, has been shown to localize to the nucleus(2) and its 3' end can be processed to yield a tRNA-like cytoplasmic RNA(3). MALAT-1, has been shown to be a potentially generic marker for epithelial carcinomas(4-7)and is greatly up-regulated in lung adenocarcinoma metastasis(1) endometrial stromal sarcoma of the uterus(7), nonhepatic human carcinomas(5) and recently was reported to be overexpressed in placenta previa and to play a role in trophoblast invasion regulation (8). Up-regulation of MALAT-1 also has been shown to predict unfavorable outcomes of drug therapy in patients with osteosarcoma(4) and its 3' end is an important biological motif in the invasion and metastasis of colorectal cancer cells (9). These malignancies all have been associated with malfunction of p53(10, 11) a nuclear transcription factor that plays a role in cellular stress, including its accumulation during DNA damage and oncogene activation. P53 has been established as a key tumor suppressor, apoptosis inducer, and prognostic marker in cancer, with about 50% of human tumors encoding for a mutated p53 gene(12).

Several small DNA tumor viruses affect p53 function, including the polyomaviruses, the adenoviruses, and the papillomaviruses. These viruses play a role in the development of cancer in humans by encoding for proteins that interact with tumor suppressor genes p53 and pRb(13). Polyomavirus large T antigen, for example, binds to and inhibits p53 and pRb(14-16). The mouse polyoma virus middle T antigen (MPVmTAg) prevents p53-induced apoptosis through the phosphatidylinositol 3-kinase (PI3K) signal transduction pathway by way of PP2A

178

interactions(17). Adenovirus E1B(18) and high-risk human papillomavirus (HPV-16) E6(19) proteins both bind to and compromise p53 function, whereas HPV-16 E7 inhibits pRb function(20)

The genomes of small DNA tumor viruses have consistently been detected in certain malignancies. HPV is consistently detected in cervical cancer(21) and in a subset of oral cancers(22), whereas BK virus (BKV) DNA has been isolated in several human tumors, both integrated into the genome and episomally, including in bone, pancreatic islet cells, the kidney, the urinary tract, the prostate, and various brain tissues(23-29). In addition, overexpression of polyoma virus mTAg has been shown to cause salivary gland enlargement in mice and pathology similar to that observed in human salivary gland disease(30, 31).

We hypothesized that MALAT-1 expression is affected by dysregulation of tumor suppressor p53. We used viruses, viral gene products, and cell lines to test the modulation of a cloned MALAT-1 promoter and to determine the effect of p53 or p53 mutants on MALAT-1 expression. We also conducted in vivo testing of MALAT-1 expression in a transgenic mouse model of salivary gland disease (SGD) and in 4 subjects with HIV-associated SGD (HIVSGD).

Materials and Methods

Subjects, animals and cell culture

Minor salivary glands (MSG) were dissected from the lower lips of 4 HIV positive patients with SGD and from 4 healthy control subjects (with or without ranula) in IRB approved protocol at either the UNC University Hospital dental clinic or UCSF Oral AIDS Center. Biopsy samples were snap-frozen and kept in liquid nitrogen or formalin-fixed and embedded in paraffin until the RNA extraction procedure. Four MMTV/PyV-mT transgenic mice and 4 wild type mice parotid

samples were kindly donated from Dr. Lesley Ellies.

HSG cells are an epithelial cell line isolated by using tissue culture techniques from an irradiated human submandibular salivary gland which showed no neoplastic lesion(42). HSG cells were obtained as a gift from Dr. B. Baum (NIH) and cultured in McCoy's 5A medium (Sigma). African monkey kidney cells or Vero cells (American Type Culture Collection [ATCC]) were cultured in DMEM (Sigma). All cell types were grown in medium supplemented with 10% fetal bovine serum (FBS) (Sigma), and 1% penicillin-streptomycin (pen/strep)(Gibco) unless otherwise stated and maintained in a humidified 37^0C, 5%CO_2 chamber.

Suppression Subtractive Hybridization (SSH)

One to two μg of pooled biopsied salivary glands from HIV-SGD patients and pooled control (healthy persons) RNA was sent to Evrogen (Russian Republic) for SSH. In brief, SMART technology was used to synthesize cDNA, which was subsequently digested with RsaI in preparation for subtraction in both directions (HIV-SGD as driver/control as tester, and vice versa). Adaptors were ligated to the two cDNA populations, followed by two rounds of hybridization and amplification. The secondary PCR products from the two subtracted populations were then ligated into the pAL9 vector.

Sequencing of subtracted cDNA library

Two hundred and fifty positive clones from each of the subtractions were randomly selected and cultured in 1.5 mL LB-medium in duplicate 96-well plates at 37 °C overnight. Clones were selected by blue-white screening (Promega) and sequenced using a M13 forward promoter (-21) primer (5□-TGT AAA ACG ACG GCC AGT-3□) and BigDye 3.0 sequencing mix (Applied Biosystems) before analysis by capillary electrophoresis on an ABI 3700 genetic analyser (Applied Biosystems). The sequences of the inserts of differentially expressed genes

were identified using NCBI Blast search (blastn).

RNA extraction and cDNA synthesis

Total RNA was extracted from pooled MSGs of HIV-SGD patients, pooled MSGs of healthy controls, mouse parotid frozen tissues and Vero cells using RNeasy MiniKit (Qiagen,USA). Total RNA isolation from formalin fixed tissue using the Optimum FFPE RNA Isolation Kit (Ambion Diagnostics, INC) according to manufacturer's instructions. The RNA was suspended in nuclease-free water and quantitated by UV spectrophotometry, aliquoted and stored at -80°C. One μg total RNA from the HIV-SGD and control tissues, mice parotid tissue and Vero cells were reverse transcribed to cDNA using random primers and the SuperScript^{TM} II Reverse Transcriptase (RT) Kit (Invitrogen) as described by the manufacturer. Contaminating DNAs were removed by use of RQ1 DNase kit (Promega) as described by the manufacturer.

Northern Blot

Total RNA was isolated using TRizol (Invitrogen) as described by the manufacturer. Contaminating DNAs were removed by use of RQ1 DNase kit (Promega) as described by the manufacturer. 10 ug of RNA was subjected to electrophoresis and Northern blotting. MALAT-1 was hybridized with a ^{32}P-labeled oligonucleotide probe for MALAT-1

Semi-quantitative and quantitative real-time RT-PCR

Semi-quantitative RT-PCR was performed using previously published primers for T Ag(43)and Taq Polymerase (Qiagen, USA). The following program was used for amplification: 95˚C for 2 min (1x); 94˚C for 45 sec, 56˚C for 45 sec, 72˚C for 30 sec with 2 sec increase per cycle (35x), 72˚C for 10 min (1x). Amplified cDNA was electrophoresed on 2% agarose gel (Sigma).

Real time RT-PCR was performed with LightCycler 480 Syber Green I Master Mix in the

presence of transcribed cDNA and 0.25mM of gene specific primers. Experiments were performed in duplicate and β-actin was used as an internal control. Duplicate or triplicate Ct values were averaged, normalized to an average β-actin Ct value, and fold activation in healthy vs diseased tissue was calculated using the 2-ΔΔCt method. For Vero cells, gene expression values are presented as the changes (*n*-fold) in T Ag transcript levels, with the levels in non-transfected/mock samples arbitrarily set to 1.

Immunofluorescence/Immunohistochemistry

Frozen sections were cut from minor salivary glands (HIV-SGD and control glands) and from mouse parotid glands (transgenic and wild type) for immunofluorescent analysis. Tissue sections were fixed, blocked, then stained with either PAb416 (Genetex) antibody specific for SV40 T antigen or IgG isotype control. PAb416 has been shown to cross react with BKV Tag and is commonly used for BKV Tag detection. Both antibodies were incubated with fixed cells for 1 hr at 37^{0}C followed by a fluorescencein-conjugated anti-mouse (Sigma) antibody (1:20). Slides were overlaid with Vectashield (Vector Laboratories) then subjected to immunofluorescence microscopy.

Formalin fixed sections were deparaffinized, and washed. Slides were incubated in 3% hydrogen peroxide and blocked and incubated with PAb416 (Genetex). DAKO LSAB+ peroxidase kit (DAKO Corporation) was used according to manufacturer's specifications.

Plasmid cloning, transfection and infection

A 5.5 kb region upstream of MALAT-1 transcription site was amplified using primers 5'GGG<u>ACGCGT</u>AAAGAGGATTCTATCTAACAAGGA3' and 5'GGG<u>CTCGAG</u>GAAACGTGAAAACCCACTCT3' and inserted into pSeap2-Basic expression cloning vector (Clontech) using restriction sites MluI and XhoI. To determine MALAT-1

promoter activity, Vero cells were first infected with BKV as previously described(39) with 64

HAUs of virus for 24 h. At 24 h post infection (hpi), virus was removed from the culture media,

cells were washed with 1X PBS and replaced with fresh medium containing the MALAT-1

promoter plasmid and β-gal construct plus transfection reagent. At stated times post transfection

the cell monolayers or supernatant were collected for immunoblot assays, beta-galactosidase

enzyme assay (Promega) or secreted alkaline phophatase enzyme assay (Promega) according to

manufacturers instructions.

Immunoblotting

Total cell protein was extracted using 1% SDS lysis buffer (1% (w/v) SDS, 0.05M

Tris.Cl pH8, 1mM DTT). Protein concentrations were determined using the BioRad protein

assay, and equal amounts of protein were electrophoresed on a 10% Bis-Tris polyacrylamide

minigel (Invitrogen). PAb416 (1:200) (Genetex) in 5% non-fat dry milk in 0.1% Tween-20 PBS

(PBS-T) was used to detect T Ag expression and Actin (C-11)-R sc-1615-R (1:1000)(Santa Cruz

Biotechnology) in 1% BSA/TBS-T for actin expression. After washing in PBS-T/TBS-T, blots

were probed with a horseradish peroxidase-conjugated secondary antibody (1:10,000)

(Promega). Antibody complexes were detected using SuperSignal West Pico Chemiluminescent

substrate (Thermo scientific) and exposed to film (Kodak).

Beta galactosidase enzyme assay

β-Galactosidase Enzyme Assay System with Reporter Lysis Buffer (Promega) was

performed according to manufacturer's instructions. Briefly, cells were collected, centrifuged

and resuspended in1X lysis buffer and transferred in triplicate to 96 well plates. Diluted sample

was added to an equal volume of Assay 2X Buffer, which contained the substrate ONPG (o-

nitrophenyl-beta-D-galactopyranoside). Samples were incubated for 30 minutes, terminated by

addition of sodium carbonate, and the absorbance read at 420nm with a spectrophotometer.

Secreted alkaline phosphatase reporter gene assay, chemiluminescent

SEAP assay was performed according to manufacturer's instructions. Briefly, culture supernatant from transfected or mock (untreated) cells were collected at stated times post-transfection. Collected sample was diluted 1:4 in Dilution buffer, heated at 65^0C for 30 min then centrifuged at maximum speed to 30 s. Heat-treated samples were then transferred to a microplate (black or white), inactivated with Inactivation Buffer then treated with Substrate Reagent. Chemiluminescence was measured using a luminometer.

Statistical Analysis

One-way ANOVA tests were performed to determine statistically significant differences in MALAT-1 promoter activation and expression using Graph pad software.

miRNA Prediction

The entire MALAT-1 sequence was imported into an online program mfold (http://www.bioinfo.rpi.edu/applications/mfold) to predict the presence of micro RNAs within the genome.

Results

Differential gene expression in HIV-SGD by SSH

Differential gene expression in minor salivary glands from patients with HIV-SGD and healthy control subjects were examined with the use of SSH. Pooled RNA from four HIV-SGD positive subjects and from four HIV negative subjects was utilized to diminish individual variation. Two SSH libraries were constructed, disease (plus) and healthy library (minus). The minus library was enriched for genes whose expression was suppressed in HIV-SGD and the

plus library was enriched for genes whose expression was induced by disease development. 250 randomly selected clones were sequenced from the minus SSH library and 250 clones from the plus library; of those 232 and 208 contained cDNA inserts, respectively. The SSH library was automatically processed using a specifically created software tool. This processing included 3 basic steps: finding adaptor sequences on the 5' and 3' ends of a clone as markers and extracting a fragment from the clone, blasting the batch of fragments, clustering alignments and linking with unique gene identification. We were able to align 436 sequences with known or predicted human genes. Our total number of alignments reached 502 due to 57 chimeric clones which had 2 or three clones from different RNA's linked together during SSH. Of the 436 cDNAs 73 sequences were identified that did not match to any known or predicted mRNAs but aligned with the human genomic DNA and with EST databases. These were considered novel.

A non-redundant set of the genes was created which excluded highly expressed clones present in both disease and healthy genes in the plus library. There were 6 genes found more than once among sequenced SSH clones in each of the libraries (Table 1). It was shown previously that a number of cDNA fragments corresponding to a gene in the SSH library correlates with a degree of differential expression of the gene(32). Considering all of the differentially expressed clones detected by SSH analysis, major functional classes of transcriptionally regulated genes in minus library included signal transduction (9%), cell cycle(8%), immune/defense(8%), synthesis/ development/ differentiation (8%) and transport (8%). Transcriptionally regulated genes in the plus expression library included those involved in signal transduction (15%), synthesis/development/differentiation(13%), apoptosis(8%), metabolism(8%) and transport. The largest category of de-regulated genes were unknown, among these was the metastasis associated lung adenocarcinoma transcript-1 (MALAT-1).

185

<u>MALAT-1 transcript and promoter activity is deregulated in the absence of p53 expression, in vitro</u>

A reporter assay was developed to assess activation of MALAT-1's enhancer/promoter region. First, we examined the MALAT-1 enhancer/promoter region 5.5 kb upstream of the ATG start site by means of open-source software (PROMO 3.0; available at http://alggen.lsi.upc.es/cgi-bin/promo_v3/promo/promoinit.cgidirDB=TF_8.3)(33). This program identifies putative transcription factor binding sites in DNA sequences from the species (or group of species) of interest. The similarity between the sequence examined and the transcription binding site is > 98% (or dissimilarity is < 2%). Figure 1A shows the transcription sites found in the enhancer/promoter region of MALAT-1.We then quantified the MALAT-1– secreted embryonic alkaline phosphatase (SEAP) by chemiluminescent assay (Roche Diagnostic) and transiently cotransfected the reporter construct into p53-negative, sarcoma osteogenic (SAOS) cells with or without plasmids encoding wild-type p53 or p53 mutants R273H (a contact mutation), R175H (a structural mutation), H178Y, and L22QW23S(34-36). The first two mutants are considered hot-spot mutations; that is, they abolish the wild-type tumor suppression function of p53 (37, 38). The H178Y mutant has been shown to rescue the loss of function G245S phenotype when coexpressed in vitro. The L22QW23S mutant maintains its ability to bind to p53-specific DNA elements but lacks transactivation activity(34). Cotransfections were performed using p53 expression plasmids and MALAT-1 promoter in pSEAP vector and supernatant collected at 72 hours post transfection. Higher MALAT-1 expression levels were detected in cells that did not express p53 or that contained p53 mutations (Figure 1B). We also examined MALAT-1 expression profiles in cell lines containing p53 mutations (C33A, HSG),

those containing DNA tumor viruses that sequester p53 (CaSki, SiHa), p53-negative cells (SAOS), and cells containing wild-type p53 (OKF6-Tert). Only the cell types expressing wild-type p53 showed low MALAT-1 levels (Figure 1C). These differences were statistically significant ($P < 0.001$).

To further investigate the role of p53 in deregulating MALAT-1 expression, we over-expressed HPV16 oncogenes E6 and E7 which inhibit p53 and pRb respectively. Our results showed that over expression of HPV-16 E6 in oral keratinocytes significantly enhanced MALAT-1 expression while HPV-16 E7 did not. Coexpression of both E6 and E7 resulted in a net increase in MALAT-1 transcription (Figure 2A).

To confirm that viral oncogenes that inhibit p53 may play a role in MALAT-1 deregulation, we infected or transfected BK virus or viral genome into HSG or Vero cells. BKV T ag binds to and inhibits p53 and pRb function(16). Both human parotid salivary gland (HSG) and African monkey kidney (Vero) cells were used for in vitro studies because BKV has been shown to replicate in both cell types(39). MALAT-1 transcript levels were 1.6-fold higher in BKV-infected salivary gland cells versus uninfected/mock cells 4 days after infection (Figure 2B). MALAT-1 transcription was also consistently increased in Vero cells that overexpressed BKV whole genome compared to empty vector and nontransfected according to Northern blot testing (Figure 2B). Semi-quantitative real-time reverse transcriptase polymerase chain reaction (RT-PCR; Figure 2C), and quantitative real-time RT-PCR (Figure 2D) for MALAT-1 in T antigen transfected Vero cells also showed an increase in MALAT-1 transcripts. A 2.3 and 5.5 fold increase in MALAT-1 at 24 and 48 hours post transfection was detected by qRT-PCR in Vero cells.

To assess the correlation between p53 and T ag oncogene expression, we measured T ag and

p21 transcript levels in BKV infected Vero cells. T antigen is known to bind to and inhibit p53 activity, while p21 is a downstream effector of p53 and would be expected to decrease in the absence of p53 expression. The results as expected indicated that p21 transcripts were low with high levels of BKV T ag expression, and high with low levels of T ag expression (Figure 2E). To determine whether BKV T ag expression regulates MALAT-1 promoter activity, we transfected Vero cells with the MALAT-1 promoter followed by BKV infection. MALAT-1 promoter activity was up-regulated 7-fold at 72 hours post BKV infection in comparison to uninfected. BKV T ag expression within these cells was confirmed in the immunoblot assay (Figure 2F).

BKV T ag comprises of several transcription binding sites including p53 and pRb. To determine whether p53 or pRb plays a role in MALAT-1 regulation, we co-transfected both Vero (wild-type p53) and HSG (mutated p53) cells with either BKV T ag or BKV T ag pRb-binding mutant and the MALAT-1 promoter expression plasmid. The results showed that MALAT-1 promoter activity was increased compared to vector only in Vero cells regardless of T ag phenotype (Figure 2G). Whereas, in HSG cells containing mutant p53, neither wild-type TAg nor Rb further enhanced MALAT-1 transcription above vector alone (Figure 2H)

Next, we investigated MALAT-1 levels in an in vivo model of BK T antigen-expressing salivary gland premalignant lesion (HIVSGD). Among all of the differentially expressed clones detected by SSH analysis, the most common category of deregulated genes was the "unknown" category, which included MALAT-1 (Table 1). Quantitative real-time RT-PCR detected a 2.6-fold increase in MALAT-1 expression in pooled DNA analysis from patients with HIVSGD versus healthy controls (Figure 3A). Semi-quantitative real-time RT-PCR likewise detected up-regulation of MALAT-1 in individual DNA samples from four patients with SGD (A-D) versus four healthy controls (A-D) (Figure 3A).

Immunohistochemical analysis of salivary gland biopsy samples from three patients with HIVSGD detected BKV T ag protein within the tissues as well as in a BKV positive kidney control with BKV nephropathy (BKVN) (Figure 3B, top). In addition, p53 was colocalized with BKV T ag within biopsied salivary glands from the patients with SGD (representative figure, Figure 3B, bottom). Downstream effectors of p53 (p21, PIGP-1, and WIG-1) were consistently down-regulated in semi-quantitative (left) and quantitative real-time (right) RT-PCR, whereas ING-3, negatively regulated by p53 expression and T ag was overexpressed, in both pooled cDNA (data not shown) and individual samples from patients with HIVSGD compared with healthy controls (Figure 3C).

In the murine model of polyomavirus-associated SGD, semi-quantitative real-time RT-PCR detected greater amplification of MALAT-1 cDNA from four transgenic mice with SGD, whereas transcripts were consistently reduced in four wild-type mice (Figure 3D, middle). Immunofluorescence studies detected T ag within biopsied salivary glands of transgenic mice but not in the wild-type mice (Figure 3D, top). Both ING-3 and MALAT-1 were greatly upregulated in transgenic mice versus wild-type mice in quantitative real-time RT-PCR assay (Figure 3D, bottom).

Genes up-regulated in polyomavirus-associated salivary gland disease as assessed by suppressive subtractive hybridization

Gene	Description	Category	No. of clones
MALAT-1	metastasis-associated lung adenocarcinoma transcript 1 (noncoding RNA)	Unknown	4
PIGR	polymeric immunoglobulin receptor	Immunity	3
CYTB	Cytochrome B	Transport, Mitochondria	3
HLA-B	major histocompatibility complex, class I, B	Immunity	2
PIP	prolactin-induced protein	Immunity	2
RPLP0	ribosomal subunit protein L16	Protein synthesis	2

Table 1. Genes up-regulated in polyomavirus-associated salivary gland disease as assessed by suppressive subtractive hybridization.

Figure 1A.

Figure 1B.
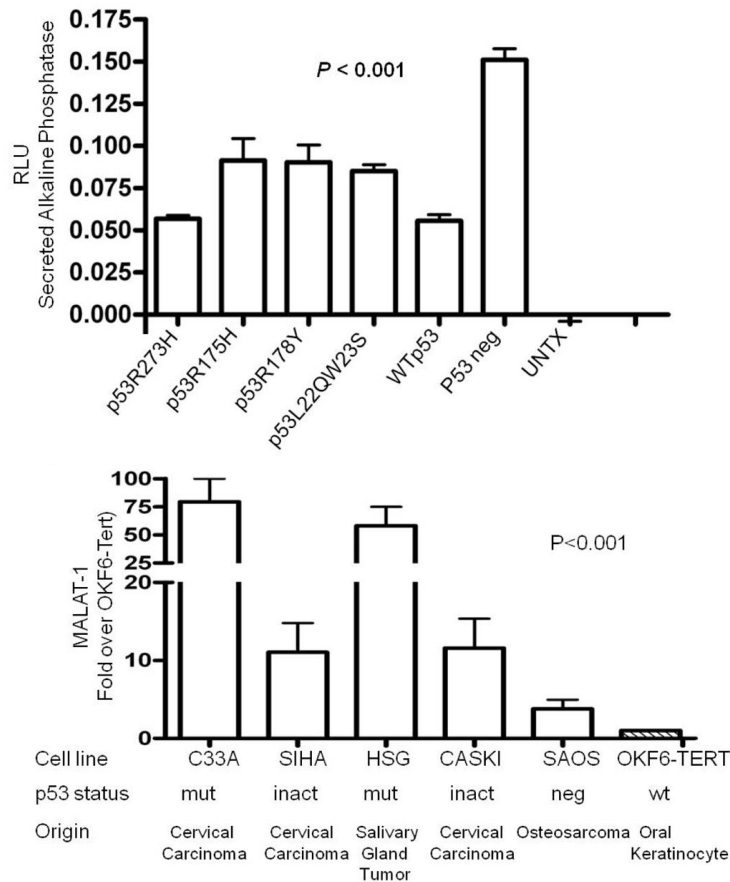
Figure 1. MALAT-1 promoter activity and transcript levels correlate with p53 activity. (a) Several consensus binding sites were detected upstream of the MALAT-1 start site, including five p53 binding sites (green), three T antigen binding sites (red), two TCF-2 binding sites (purple), and two E2F-1 binding sites (blue); (b) Representative data showing significantly increased MALAT-1 promoter activity in p53-deficient SAOS cells 72 hours after transfection with p53-expressing constructs. C. Representative levels of MALAT-1 expression in different cell types with or without p53 gene expression, presented as the change (n-fold) in MALAT-1 transcript levels (level in OKF6 cells arbitrarily set to 1).

Figure 2A.
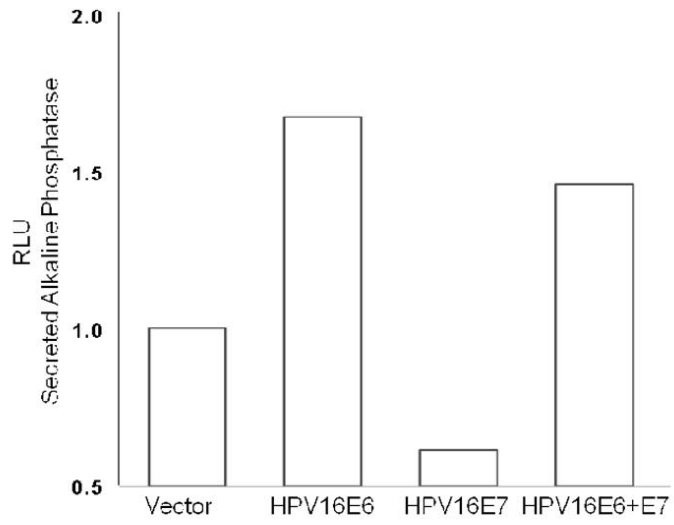
Figure 2B.
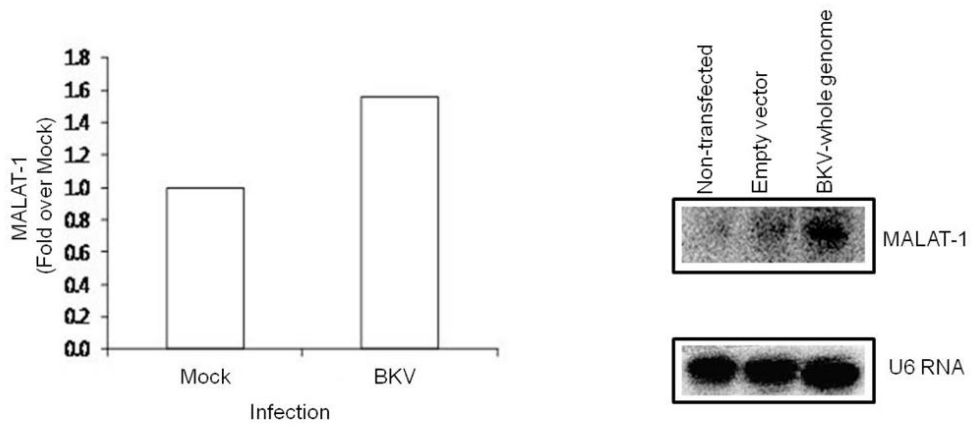
Figure 2C.
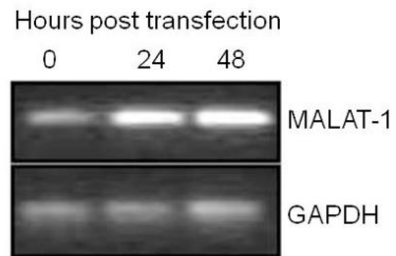
Figure 2D.
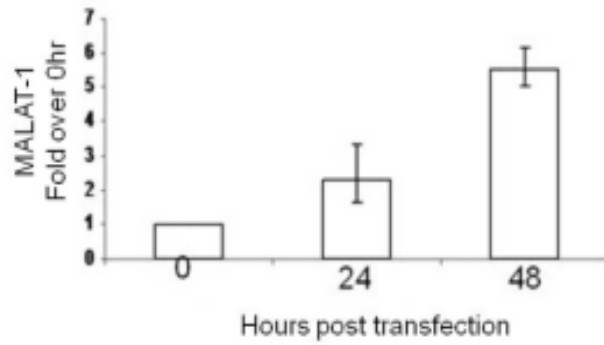
Figure 2E.
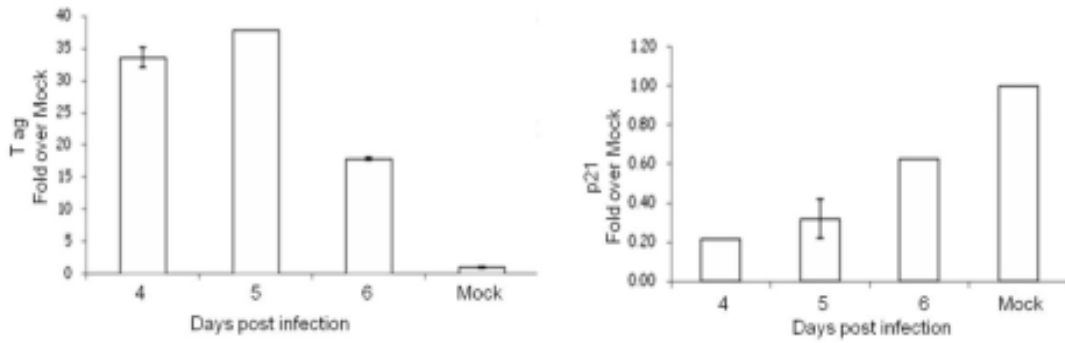
Figure 2F.
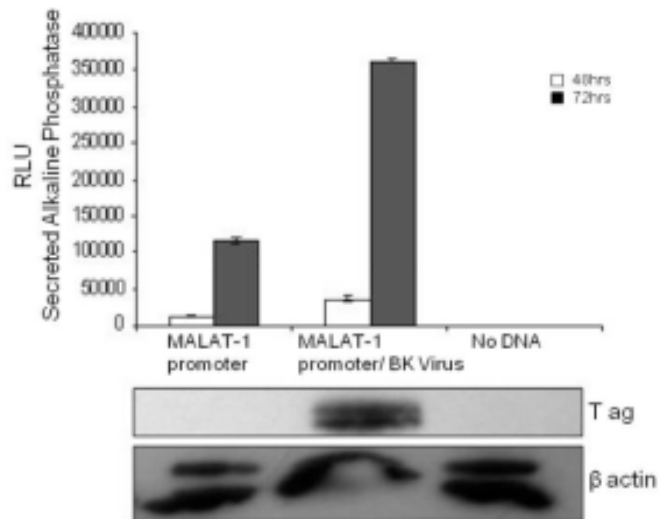
Figure 2G.
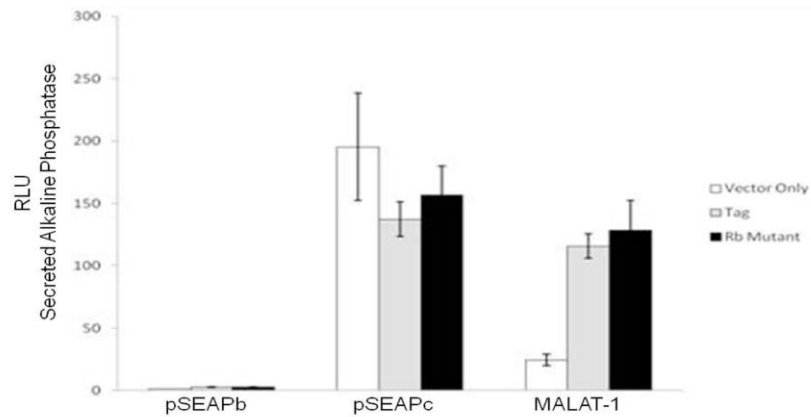
Figure 2H.
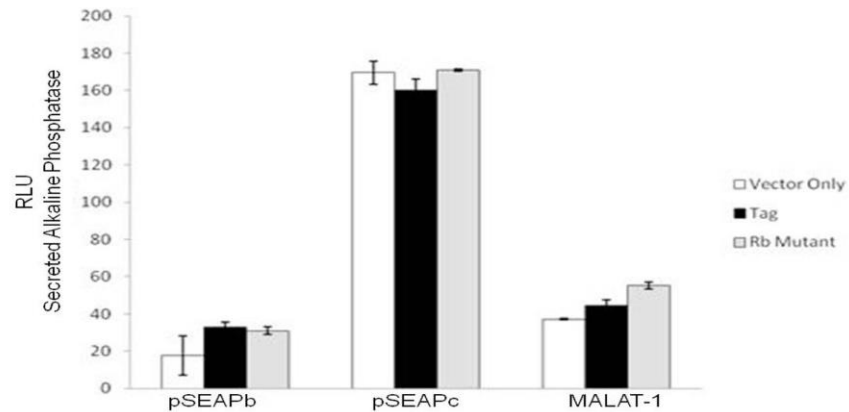
Figure 2. MALAT-1 promoter activity and transcript levels correlate with DNA tumor virus oncogene expression. (a) Representative data showing increased MALAT-1 promoter activity 48 hours after HPV16 E6 transfection and not with HPV16 E7. (b) Higher levels of MALAT-1 transcription, expressed as n-fold change in BK polyomavirus-infected human parotid gland (HSG) cells. Levels in mock samples were arbitrarily set to 1. Left. Northern blot showing a four-fold increase in MALAT-1 transcript levels in Vero cells transfected with BKV DNA. Right. (c) Semi-quantitative real-time RT-PCR shows amplified MALAT-1 cDNA bands from BKV-transfected Vero cells at stated times after transfection. (d) Quantitative real-time RT-PCR shows increased MALAT-1 transcript levels in BKV-transfected Vero cells at stated times

after transfection. Ex- pression values presented as the change (n-fold) in MALAT-1 transcript levels, with levels at time 0 arbitrarily set to 1. (e) Quantitative real-time RT-PCR showing BKV Tag and p21 transcript levels over stated times after BKV infection. (f) MALAT-1 promoter activity in BKV-infected and uninfected Vero cells at 48 and 72 hours after transfection. Top. BKV T ag protein (top) detected in Vero cells infected with BK virus and transfected with the MALAT-1 promoter plasmid. (g) BKV T ag up-regulated MALAT-1 promoter activity regardless of T ag pRb binding status in Vero cells containing wild-type p53 compare to positive and negative controls, pSEAPc and pSEAPb, respectively. (h) Neither wild-type BKV T ag nor T ag pRb binding mutant enhanced MALAT-1 transcript levels in human salivary gland cells containing mutant p53 expression.

Figure 3A.

Figure 3B.

HIV SGD

A   B   C   BKVN

HIV SGD

T ag   p53   merge
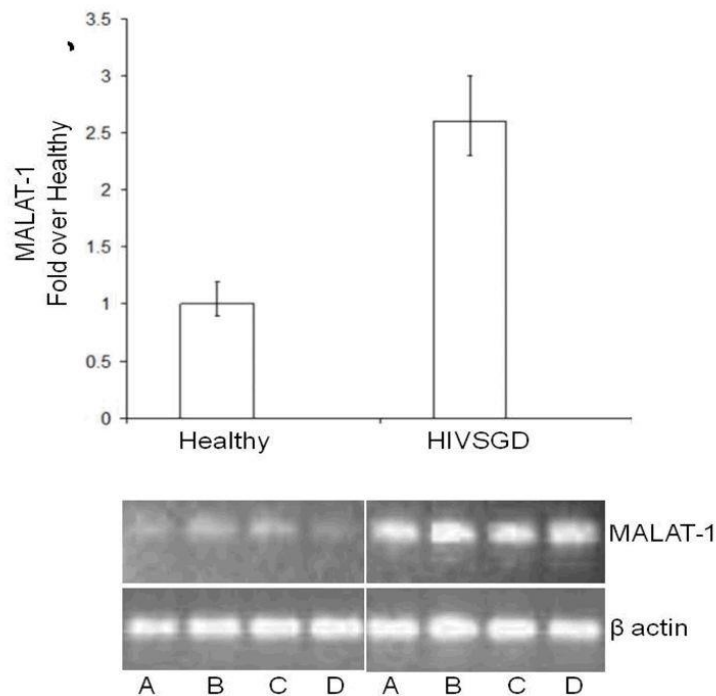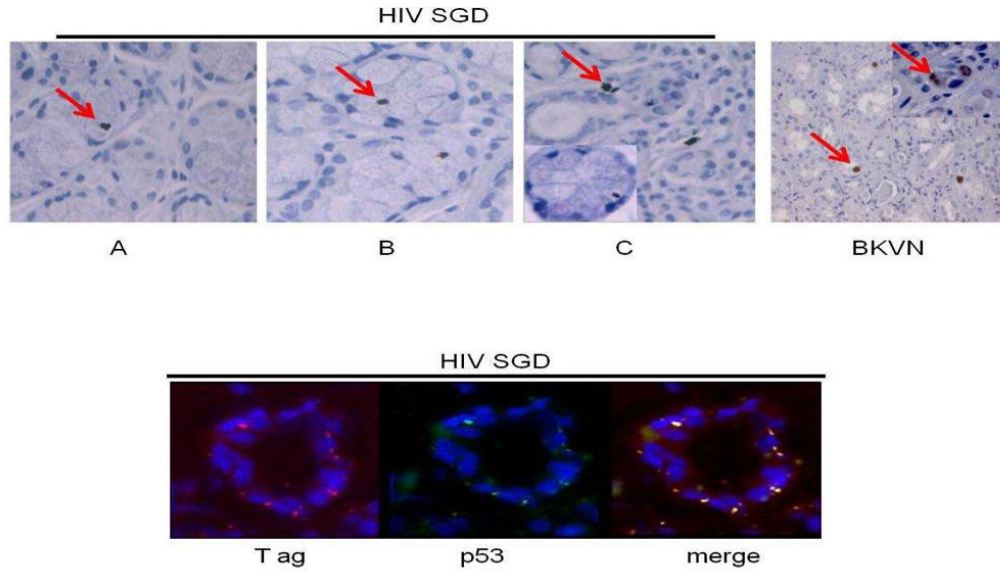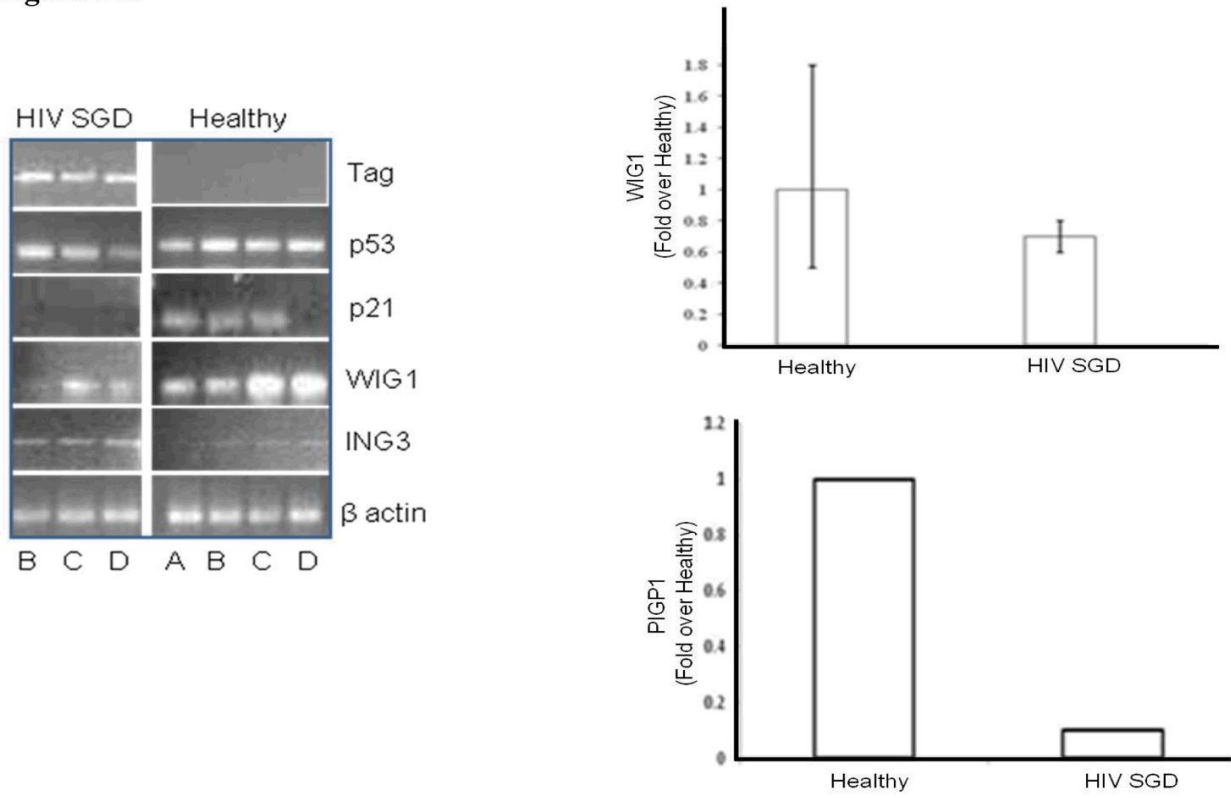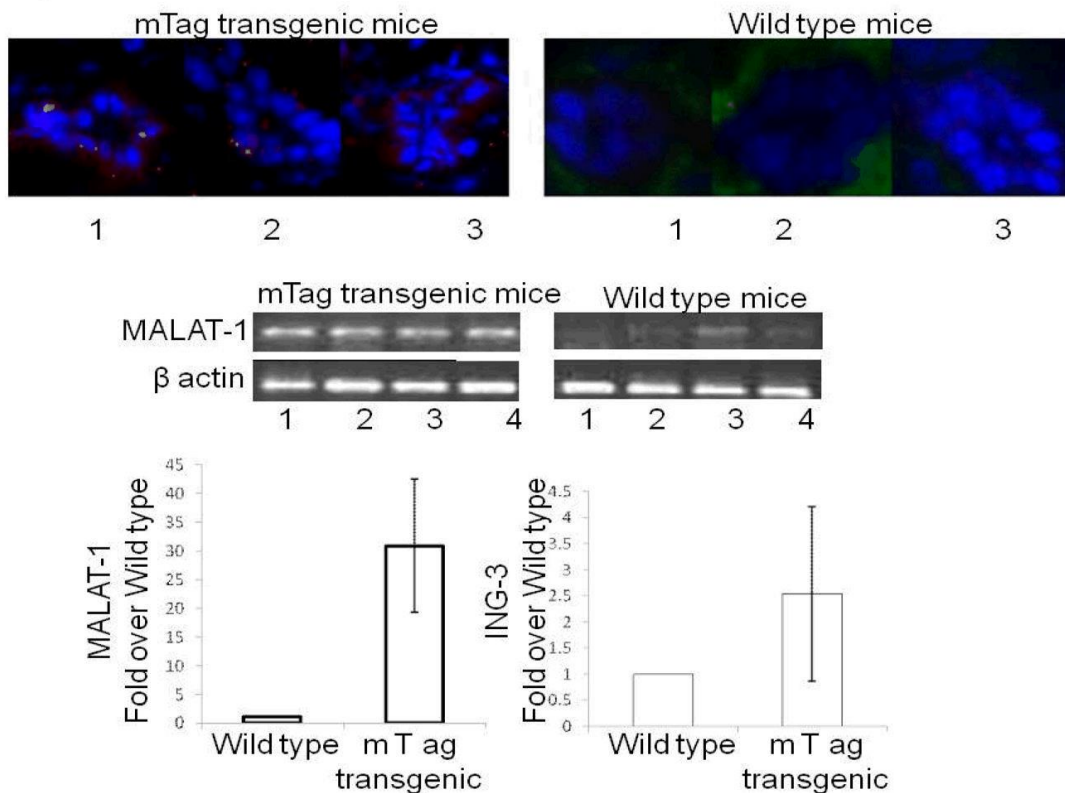
Figure 3C.

Figure 3D.

Figure 3. MALAT-1 transcript levels correlate with DNA tumor virus oncogene expression in vivo. (a) Quantitative real-time RT-PCR showing up-regulation of MALAT-1 in pooled DNA from four patients with HIV associated salivary gland disease (HIV SGD) compared with healthy control subjects, Top. Semi-quantitative real-time RT-PCR showing up-regulation of MALAT-1 in DNA from four patients with HIV SGD versus healthy control subjects, Bottom. (b) Nuclear BKVT ag (red arrows) detected via immunohistochemical analysis of representative biopsy samples from three patients with HIV-related SGD (Patient A 20×, B 40×, C 20× with inset at 40×) and in BKV-infected kidney cells from an individual with BKV neph- ropathy (positive control at 10×), Top. BKV T ag protein (red) and p53 protein (green) colocalized within salivary gland bi- opsy tissue from patients with HIV SGD (at 40× magnification). (c) Semi-quantitative (left) and quantitative real-time RT-PCR (right) showing detection of BKV T

ag in HIV SGD and not in healthy controls, down-regulation of p53-regulated genes p21, PIGP1 and WIG1 and up-regulation of ING3 in salivary gland tissue from patients with HIV SGD versus healthy controls. Healthy cDNA levels were arbitrarily set at 1. (d) BKV T ag protein (red) detected via immunofluorescence in three middle T ag-expressing transgenic mice with SGD (left) compared with wild-type mice without the disease (20× and 40× mag- nification) (right), Top. Semi-quantitative real-time RT-PCR showing up-regulation of MALAT-1 transcript levels in trans- genic mice salivary gland biopsies compared with wild-type mice, Middle. Quantitative real-time RT-PCR showing up-regulation of MALAT-1 and ING3 in transgenic mice with SGD versus wild-type mice. Wild-type cDNA levels arbitrarily set at 1, Bottom.

Human carcinomas	p53 status	MALAT-1 over-expressed
Endometrial Stromal Sarcoma[7]	P53 nuclear accumulation[44]	Yes
Hepatocellular Carcinoma[5]	P53 mutation[5]	Yes
Non Small Cell Lung Cancer[1]	P53 mutation[12]	Yes
HIV-Salivary Gland Disease (premalignant)	N/D	Yes
Osteosarcoma[4]	P53 mutation[45]	Yes
Breast[5]	P53 nuclear accumulation[46]	Yes
Pancreas[5]	P53 mutation[47]	Yes
Colon[5]	P53 mutation[48]	Yes
Late-Stage Prostate Cancer[5]	P53 mutation[49]	Yes
Cervical (CaSki cell line) [41]	HPV inhibits P53 activity[50]	Yes
Endometrial Stromal Sarcoma [7]	P53 nuclear accumulation[44]	Yes
Hepatocellular Carcinoma[5]	P53 mutation[5; 45]	Yes
Non Small Cell Lung Cancer[1]	P53 mutation[12]	Yes
HIV-Salivary Gland Disease (premalignant)	N/D	Yes
Osteosarcoma[4]	P53 mutation[46]	Yes
Breast[5]	P53 nuclear accumulation [47]	Yes
Pancreas [5]	P53 mutation[48]	Yes
Colon[5]	P53 mutation[49]	Yes
Late-Stage Prostate Cancer[5; 45]	P53 mutation[50; 51]	Yes
Cervical (CaSki cell line)[43]	HPV inhibits P53 activity[52]	Yes

Table 2. Correlation among cancers that express high MALAT1 transcripts, involve p53 deregulation and are associated with DNA tumor virus infection.
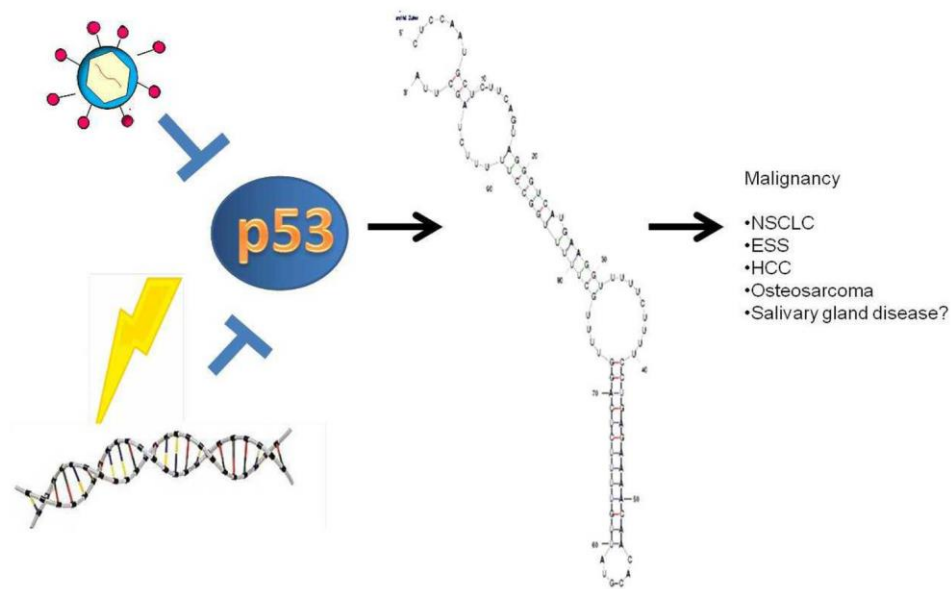
Figure 4. Model of MALAT-1 regulation including predicted miRNA at the 3' end of the MALAT-1 RNA.

Discussion

MALAT-1 is known to be up-regulated in several epithelial malignancies, including non-small cell lung tumors, stromal sarcomas, and nonhepatic carcinomas(4-7, 40). In this series of in vitro and in vivo experiments, we noted substantial MALAT-1 up-regulation in the presence of polyoma and papilloma oncoproteins that disrupt or negate p53 expression/function. In contrast, the pRb pathway did not appear to be critical to MALAT-1 regulation. Regardless of the mechanism of p53 deregulation—expression of frequently mutated p53 sites (Figure 1) or expression of tumorvirus oncoproteins targeting p53 (Figure 2 and 3)—MALAT-1 was consistently overexpressed. Thus MALAT-1 might represent a biomarker for p53 dysregulation within malignancies.

MALAT-1 expression in CaSki cells has been shown to be involved in cervical cancer cell growth, cell cycle progression, and invasion(41). CaSki cells harbor HPV-16, a small DNA

tumor virus that encodes for the E6 protein. This protein is known to form complexes with p53 and target it for degradation(41) . In contrast, the HPV-16 E7 protein is known to sequester pRb and inhibit its normal function in the cell cycle. The enhanced expression of MALAT-1 in the presence of HPV-16 E6, and its downregulation in the presence of HPV-16 E7, lend support to the hypothesis that p53, but not the pRb pathway, appears to be critical to MALAT-1 modulation (Figure 3).

In normal tissues, MALAT-1 is expressed in numerous cell types, with the highest relative expression found in the normal pancreas and lung (~2.0- and 1.6-fold relative increases in expression, respectively)(1). Its expression is also associated with epithelial cell malignancies such as non-small cell lung cancer(1) endometrial stromal sarcoma(7) and nonhepatic carcinomas(5). Of interest, all of these cancers are associated with p53 mutation (Table 2). However, normal salivary gland cells appear to express negligible MALAT-1(1). Our study shows, for the first time, that the presence of a polyoma virus (BKV) is linked to up-regulation of MALAT-1 in patients with HIVSGD. Interestingly, the perinuclear BKV Tag staining pattern in HIVSGD is very similar to that detected by the Imperiale group in prostate dysplasia(2, 3). Moreover, oncoprotein expression from three distinct DNA tumor viruses - HPV-16, BKV, and mouse polyoma virus -are capable of upregulating MALAT-1 potentially via p53 deregulation.

Interestingly, using an mRNA folding prediction program it appears that the 3' end of the MALAT-1 gene may encode a microRNA (miRNA) (Figure 4). miRNAs are single-stranded RNA molecules of 21-23 nucleotides in length, which regulate gene expression. miRNAs are encoded by genes from whose DNA they are transcribed but miRNA are not translated into protein, that is they are non-coding RNA; instead each primary transcript (a pri-miRNA) is processed into a short stem-loop structure called a pre-miRNA and finally into a functional

miRNA. Mature miRNA molecules are partially complementary to one or more messenger RNA (mRNA) molecules, and their main function is to down-regulate gene expression. Like known miRNAs, MALAT-1 is a non-coding transcript, folds into a short stem loop structure at the 3' end and is conserved across mammalian species. Modulation of MALAT-1 expression by p53, perhaps by miRNA regulation, is intriguing and opens the door toward understanding the regulation of this important malignancy-associated gene. Investigation of MALAT-1 as a miRNA is currently being explored and potential targets in SGD will be determined. In the meantime, MALAT-1 might represent a biomarker for p53 deregulation within malignancies.

REFERENCES

1.   **Ji, P., S. Diederichs, W. Wang, S. Boing, R. Metzger, P. M. Schneider, N. Tidow, B. Brandt, H. Buerger, E. Bulk, M. Thomas, W. E. Berdel, H. Serve, and C. Muller-Tidow.** 2003. MALAT-1, a novel noncoding RNA, and thymosin beta4 predict metastasis and survival in early-stage non-small cell lung cancer. Oncogene **22:**8031-41.

2.   **Hutchinson, J. N., A. W. Ensminger, C. M. Clemson, C. R. Lynch, J. B. Lawrence, and A. Chess.** 2007. A screen for nuclear transcripts identifies two linked noncoding RNAs associated with SC35 splicing domains. BMC Genomics **8:**39.

3.   **Wilusz, J. E., S. M. Freier, and D. L. Spector.** 2008. 3' end processing of a long nuclear-retained noncoding RNA yields a tRNA-like cytoplasmic RNA. Cell **135:**919-32.

4.   **Fellenberg, J., L. Bernd, G. Delling, D. Witte, and A. Zahlten-Hinguranage.** 2007. Prognostic significance of drug-regulated genes in high-grade osteosarcoma. Mod Pathol **20:**1085-94.

5.   **Lin, R., S. Maeda, C. Liu, M. Karin, and T. S. Edgington.** 2007. A large noncoding RNA is a marker for murine hepatocellular carcinomas and a spectrum of human carcinomas. Oncogene **26:**851-8.

6.   **Perez, D. S., T. R. Hoage, J. R. Pritchett, A. L. Ducharme-Smith, M. L. Halling, S. C. Ganapathiraju, P. S. Streng, and D. I. Smith.** 2008. Long, abundantly expressed non-coding transcripts are altered in cancer. Hum Mol Genet **17:**642-55.

7.   **Yamada, K., J. Kano, H. Tsunoda, H. Yoshikawa, C. Okubo, T. Ishiyama, and M. Noguchi.** 2006. Phenotypic characterization of endometrial stromal sarcoma of the uterus. Cancer Sci **97:**106-12.

8.   **Tseng, J. J., Y. T. Hsieh, S. L. Hsu, and M. M. Chou.** 2009. Metastasis associated lung adenocarcinoma transcript 1 is up-regulated in placenta previa increta/percreta and strongly associated with trophoblast-like cell invasion in vitro. Mol Hum Reprod **15:**725-31.

9.   **Xu, C., M. Yang, J. Tian, X. Wang, and Z. Li.** 2011. MALAT-1: a long non-coding RNA and its important 3' end functional motif in colorectal cancer metastasis. Int J Oncol **39:**169-75.

10.   **Breuer, R. H., P. E. Postmus, and E. F. Smit.** 2005. Molecular pathology of non-small-cell lung cancer. Respiration **72:**313-30.

11.   **Liu, F. S., M. F. Kohler, J. R. Marks, R. C. Bast, Jr., J. Boyd, and A. Berchuck.** 1994. Mutation and overexpression of the p53 tumor suppressor gene frequently occurs in uterine and ovarian sarcomas. Obstet Gynecol **83:**118-24.

12.   **Soussi, T.** 2007. p53 alterations in human cancer: more questions than answers. Oncogene **26:**2145-56.

13.   **Howley, P. M., and D. M. Livingston.** 2009. Small DNA tumor viruses: large contributors to biomedical sciences. Virology **384:**256-9.

14.   **Lane, D. P., and L. V. Crawford.** 1979. T antigen is bound to a host protein in SV40-transformed cells. Nature **278:**261-3.

15.   **Saenz Robles, M. T., and J. M. Pipas.** 2009. T antigen transgenic mouse models. Semin Cancer Biol **19:**229-35.

16.   **Shivakumar, C. V., and G. C. Das.** 1996. Interaction of human polyomavirus BK with the tumor-suppressor protein p53. Oncogene **13:**323-32.

17.   **Qian, W., and K. G. Wiman.** 2000. Polyoma virus middle T and small t antigens cooperate to antagonize p53-induced cell cycle arrest and apoptosis. Cell Growth Differ **11:**31-9.

18.   **Sarnow, P., C. A. Sullivan, and A. J. Levine.** 1982. A monoclonal antibody detecting the adenovirus type 5-E1b-58Kd tumor antigen: characterization of the E1b-58Kd tumor antigen in adenovirus-infected and -transformed cells. Virology **120:**510-7.

19.   **Werness, B. A., A. J. Levine, and P. M. Howley.** 1990. Association of human papillomavirus types 16 and 18 E6 proteins with p53. Science **248:**76-9.

20.   **Sdek, P., Z. Y. Zhang, J. Cao, H. Y. Pan, W. T. Chen, and J. W. Zheng.** 2006. Alteration of cell-cycle regulatory proteins in human oral epithelial cells immortalized by HPV16 E6 and E7. Int J Oral Maxillofac Surg **35:**653-7.

21.   **Lowy, D. R., R. Kirnbauer, and J. T. Schiller.** 1994. Genital human papillomavirus infection. Proc Natl Acad Sci U S A **91:**2436-40.

22.   **Rautava, J., and S. Syrjanen.** 2011. Human papillomavirus infections in the oral mucosa. J Am Dent Assoc **142:**905-14.

23.   **Caputo, A., A. Corallini, M. P. Grossi, L. Carra, P. G. Balboni, M. Negrini, G. Milanesi, G. Federspil, and G. Barbanti-Brodano.** 1983. Episomal DNA of a BK virus variant in a human insulinoma. J Med Virol **12:**37-49.

24.   **Corallini, A., M. Pagnani, P. Viadana, E. Silini, M. Mottes, G. Milanesi, G. Gerna, R. Vettor, G. Trapella, V. Silvani, and et al.** 1987. Association of BK virus with human brain tumors and tumors of pancreatic islets. Int J Cancer **39:**60-7.

25.   **Das, D., R. B. Shah, and M. J. Imperiale.** 2004. Detection and expression of human BK virus sequences in neoplastic prostate tissues. Oncogene **23:**7031-46.

26.   **Dorries, K., G. Loeber, and J. Meixensberger.** 1987. Association of polyomaviruses JC, SV40, and BK with human brain tumors. Virology **160:**268-70.

27.   **Flaegstad, T., P. A. Andresen, J. I. Johnsen, S. K. Asomani, G. E. Jorgensen, S. Vignarajan, A. Kjuul, P. Kogner, and T. Traavik.** 1999. A possible contributory role of BK virus infection in neuroblastoma development. Cancer Res **59:**1160-3.

28.   **Negrini, M., P. Rimessi, C. Mantovani, S. Sabbioni, A. Corallini, M. A. Gerosa, and G. Barbanti-Brodano.** 1990. Characterization of BK virus variants rescued from human tumours and tumour cell lines. J Gen Virol **71 (Pt 11):**2731-6.

29.   **Monini, P., L. de Lellis, A. Rotola, D. Di Luca, T. Ravaioli, B. Bigoni, and E. Cassai.** 1995. Chimeric BK virus DNA episomes in a papillary urothelial bladder carcinoma. Intervirology **38:**304-8.

30. **Imperiale, M. J., and E. O. Major.** 2007. Polyomaviruses, p. 3091. *In* A. M. Field, D. M. Knipe, and P. M. Howley (ed.), Fields' Virology, 5th ed, vol. 2. Wolers Kluwer Health/Lippincott Williams & Wilkins, Philadelphia.

31. **Maglione, J. E., D. Moghanaki, L. J. Young, C. K. Manner, L. G. Ellies, S. O. Joseph, B. Nicholson, R. D. Cardiff, and C. L. MacLeod.** 2001. Transgenic Polyoma middle-T mice model premalignant mammary disease. Cancer Res **61:**8298-305.

32. **Diatchenko, L., Y. F. Lau, A. P. Campbell, A. Chenchik, F. Moqadam, B. Huang, S. Lukyanov, K. Lukyanov, N. Gurskaya, E. D. Sverdlov, and P. D. Siebert.** 1996. Suppression subtractive hybridization: a method for generating differentially regulated or tissue-specific cDNA probes and libraries. Proc Natl Acad Sci U S A **93:**6025-30.

33. **Farre, D., R. Roset, M. Huerta, J. E. Adsuara, L. Rosello, M. M. Alba, and X. Messeguer.** 2003. Identification of patterns in biological sequences at the ALGGEN server: PROMO and MALGEN. Nucleic Acids Res **31:**3651-3.

34. **Lin, J., J. Chen, B. Elenbaas, and A. J. Levine.** 1994. Several hydrophobic amino acids in the p53 amino-terminal domain are required for transcriptional activation, binding to mdm-2 and the adenovirus 5 E1B 55-kD protein. Genes Dev **8:**1235-46.

35. **Lozano, G.** 2007. The oncogenic roles of p53 mutants in mouse models. Curr Opin Genet Dev **17:**66-70.

36. **Otsuka, K., S. Kato, Y. Kakudo, S. Mashiko, H. Shibata, and C. Ishioka.** 2007. The screening of the second-site suppressor mutations of the common p53 mutants. Int J Cancer **121:**559-66.

37. **Hainaut, P., and M. Hollstein.** 2000. p53 and human cancer: the first ten thousand mutations. Adv Cancer Res **77:**81-137.

38. **Sigal, A., and V. Rotter.** 2000. Oncogenic mutations of the p53 tumor suppressor: the demons of the guardian of the genome. Cancer Res **60:**6788-93.

39. **Jeffers, L. K., V. Madden, and J. Webster-Cyriaque.** 2009. BK virus has tropism for human salivary gland cells in vitro: implications for transmission. Virology **394:**183-93.

40.   **Sun, Y., J. Wu, S. H. Wu, A. Thakur, A. Bollig, Y. Huang, and D. J. Liao.** 2009. Expression profile of microRNAs in c-Myc induced mouse mammary tumors. Breast Cancer Res Treat **118:**185-96.

41.   **Guo, F., Y. Li, Y. Liu, J. Wang, and G. Li.** 2010. Inhibition of metastasis-associated lung adenocarcinoma transcript 1 in CaSki human cervical cancer cells suppresses cell proliferation and invasion. Acta Biochim Biophys Sin (Shanghai) **42:**224-9.

42.   **Shirasuna, K., M. Sato, and T. Miyazaki.** 1981. A neoplastic epithelial duct cell line established from an irradiated human salivary gland. Cancer **48:**745-52.

43.   **Rollison, D. E., U. Utaipat, C. Ryschkewitsch, J. Hou, P. Goldthwaite, R. Daniel, K. J. Helzlsouer, P. C. Burger, K. V. Shah, and E. O. Major.** 2005. Investigation of human brain tumors for the presence of polyomavirus genome sequences by two independent laboratories. Int J Cancer **113:**769-74.

44.   **Nordal, R. R., G. B. Kristensen, A. E. Stenwig, C. G. Trope, and J. M. Nesland.** 1998. Immunohistochemical analysis of p53 protein in uterine sarcomas. Gynecol Oncol **70:**45-8.

45.   **Overholtzer, M., P. H. Rao, R. Favis, X. Y. Lu, M. B. Elowitz, F. Barany, M. Ladanyi, R. Gorlick, and A. J. Levine.** 2003. The presence of p53 mutations in human osteosarcomas correlates with high levels of genomic instability. Proc Natl Acad Sci U S A **100:**11547-52.

46.   **Thor, A. D., D. H. Moore, II, S. M. Edgerton, E. S. Kawasaki, E. Reihsaus, H. T. Lynch, J. N. Marcus, L. Schwartz, L. C. Chen, B. H. Mayall, and et al.** 1992. Accumulation of p53 tumor suppressor gene protein: an independent marker of prognosis in breast cancers. J Natl Cancer Inst **84:**845-55.

47.   **Morton, J. P., P. Timpson, S. A. Karim, R. A. Ridgway, D. Athineos, B. Doyle, N. B. Jamieson, K. A. Oien, A. M. Lowy, V. G. Brunton, M. C. Frame, T. R. Evans, and O. J. Sansom.** 2010. Mutant p53 drives metastasis and overcomes growth arrest/senescence in pancreatic cancer. Proc Natl Acad Sci U S A **107:**246-51.

48.   **Iacopetta, B.** 2003. TP53 mutation in colorectal cancer. Hum Mutat **21:**271-6.

49.   **Aprikian, A. G., A. S. Sarkis, W. R. Fair, Z. F. Zhang, Z. Fuks, and C. Cordon-Cardo.** 1994. Immunohistochemical determination of p53 protein nuclear accumulation in prostatic adenocarcinoma. J Urol **151:**1276-80.

50.   **Scheffner, M., B. A. Werness, J. M. Huibregtse, A. J. Levine, and P. M. Howley.** 1990. The E6 oncoprotein encoded by human papillomavirus types 16 and 18 promotes the degradation of p53. Cell **63:**1129-36.